EXPANSION AND AUTOMATION OF ITERATIVE CROSS-COUPLING: TOTAL SYNTHESIS OF SYNECHOXANTHIN AND DEVELOPMENT OF A SMALL MOLECULE SYNTHESIZER

BY

SEIKO FUJII SISCO

DISSERTATION

Submitted in partial fulfillment of the requirements
for the degree of Doctor of Philosophy in Chemistry
in the Graduate College of the
University of Illinois at Urbana-Champaign, 2014

Urbana, Illinois

Doctoral Committee:

Professor Martin D. Burke, Chair
Professor James A. Imlay
Professor John A. Katzenellenbogen
Professor Wilfred A. van der Donk

ABSTRACT

Small molecules perform an extraordinary range of important functions. Major advances have been achieved in the laboratory synthesis of small molecules, yet most synthetic efforts are specialized for each target, making synthesis a complex and time-intensive process reserved for specialists. Instead, a general and automated synthesis strategy could provide the broader scientific community rapid access to small molecules for functional studies. To achieve this goal, this dissertation describes the advances toward expanding and automating the iterative cross-coupling (ICC) strategy with *N*-methyliminodiacetic acid (MIDA) boronate building blocks, an analogous approach to how Nature makes small molecules by iterative assembly of bifunctional building blocks.

With the ultimate goal of understanding and optimizing the promising antilipoperoxidant activity of carotenoid natural products, the first total synthesis of synechoxanthin was accomplished. The synthesis was enabled by the development of a new methodology for small molecule synthesis termed reversed-polarity iterative cross-coupling (RP-ICC), in which the polarity of the building blocks is reversed to match the preferred polarity for Suzuki-Miyaura cross-coupling. This strategy expanded the scope and flexibility of ICC by increasing the number of building blocks that can be utilized in the same platform. With an efficient method to access this small molecule, the antilipoperoxidant activity of synechoxanthin was investigated in a chemically-defined liposome system. Preliminary studies indicated that synechoxanthin is an antilipoperoxidant with similar activity to the carotenoid gold standard astaxanthin.

To further simplify and generalize the synthesis of small molecules, the ICC strategy was automated through the development of a small molecule synthesizer. Key to this advance was the discovery that MIDA boronates can be purified via a novel type of catch-and-release chromatography. Many different types of small molecules, including materials, pharmaceuticals, and a range of complex natural products and their derivatives were prepared via the fully automated iterative assembly of MIDA boronate building blocks. Contemporaneously with the development of the synthesizer, the ICC platform was expanded to include C-N and Csp^3-Csp^2 bond formations. Collectively, these advances seek to establish the foundation for a general and automated platform for small molecule synthesis to ultimately help shift the rate-limiting step in small molecule science from synthesis to functional studies.

To my family and Scott

ACKNOWLEDGEMENTS

I wish to first thank my advisor Professor Marty Burke for the tremendous support and guidance I have received throughout my graduate school career. Marty taught me the importance of selecting problems based on potential impact, and the rewards of solving these problems by hypothesis-driven research. His enthusiasm helped me overcome setbacks and his constructive feedbacks have instilled in me the confidence to succeed. I would also like to acknowledge my wonderful thesis committee: Professor James Imlay, Professor John Katzenellenbogen, and Professor Wilfred van der Donk. They challenged my views, provided encouragement, and supported my aspirations throughout each stage of my graduate career. They have continuously held me to the highest levels of scholarship, and I am a much better scientist because of their efforts.

The completion of this degree would not have been possible without the support and contributions from all members of the Burke Group. In particular, I would like to extend my sincere thanks to the members of Team Machine: Eric Gillis, Steven Ballmer, Junqi Li, Gregory Morehouse, Andrea Palazzolo, Jonathan Lehmann, and Michael Schmidt. I am lucky to have learned from an extraordinary group of talented individuals on a daily basis and experienced the rewards of achieving an ambitious goal together. I also enjoyed working with Hannah Haley and would like to thank her for stimulating ideas and providing many insights. I would also like to thank Hannah, Andrea, and Bowei Hu for being great labmates and creating a friendly work environment. I was fortunate to serve as a mentor to many talented undergraduate students who played a crucial role in moving the projects forward: Stephanie Chang, Matthew Clark, Hannah Lant, and Scott Patennaude. Witnessing their development into independent scientists was one of the most rewarding experiences I had as a graduate student. Many past members of the group were an invaluable resource: Eric Gillis, Dan Palacios, Kaitlyn Gray, Suk Joong Lee, Pulin Wang, Brandon Wilcock, Eric Woerly, Brice Uno, and Steven Ballmer must be acknowledged for their willingness to answer any questions I had. I would also like to thank Arjun Palyam, Tom Anderson, and Justin Struble for their kindness, mentorship, and friendship throughout the years. I must acknowledge Ian Dailey and Dave Knapp for not only establishing what has been known to be the Best Bay Ever, but also for all of the help and scientific input they have given me. I feel very lucky to have worked next to Ian; his positive energy helped keep our bay a

happy and productive place to work. I am forever thankful for his continued mentorship and friendship.

My graduate experience would not have been the same without an amazing group of friends. I am lucky to have joined the department as a part of a great class and experienced the highs and the lows of graduate school with them. Thank you to Preston May, Carl Liskey, and Iulia Strambeanu for all their friendship, and Shauna Paradine, Karen Morrison, Claire Knezevic, and Jenna Klubnick for the occasional G0 lunches. I would also like to thank Stephen Davis for the daily greetings and fun conversations. I am especially thankful to have met my partner-in-crime, Jenna. I could not have gotten through the first few years of graduate school without her friendship and will forever cherish the late nights and some of the silly things we did as first years, which include making multiple flow charts. I would like to thank Erin Davis for making my second year of graduate school a fun and memorable experience. Many thanks go out to Tommy Osberger + Thy and Matt Endo + Qi for the fun weekend get-togethers and for simply being awesome. Thanks to my zumba buddies Tommy, Jenna, Tom, and Yi (I would say that mueve la colita is still my favorite!) for helping me get through the stressful times. I would also like to thank the members of the Moore Group for being so friendly and welcoming. I am also truly grateful to Junqi for being such a sincere friend and being my confidant throughout this journey.

I must thank the wonderful group of professionals that helped improve my graduate school experience: Stacy Olson, Susan Lighty, Becky Duffield, Krista Smith, and Ellen Wang Althaus were always there to lend an ear. I am forever grateful to have met and worked with Patricia Simpson. She has been a great mentor outside of lab, encouraged me to pursue my dreams, and helped me discover the transferrable skills I have developed as a graduate student.

I would also like to thank Professor Jeffrey Bode for providing me with an opportunity to conduct research in his group as an undergraduate student, and extending his support and encouragement throughout the last seven years. I also want to thank the Chemistry Department at Smith College for not only instilling my excitement for Chemistry, but for their continual support even after I had graduated. Thank you especially to Professor Kevin Shea for believing in my abilities and supporting me throughout these years, in addition to being an amazing advisor and friend.

A big, big thank you to my parents and my brother for their love and supporting my aspirations in all the ways they possibly could, even though we are miles apart from one another. I am also lucky to have a wonderful family in Ohio and I am so thankful for their warmth, support, and love over the last four years. Finally, I cannot express in words how grateful I am to have met my husband Scott and for his unwavering support and unconditional love.

I was fortunate to be the recipient of numerous awards while at Illinois, including the University of Illinois Graduate Fellowship (Block Grant), Procter & Gamble Fellowship, the Pines Travel Award, the Fuson Travel Award, and the Best Poster Award at the Allerton Conference. I would like to acknowledge BASF for donating astaxanthin. I also gratefully acknowledge Sigma-Aldrich, the NSF, NIH, HHMI, Bristol-Myers Squibb, and Professor Martin Burke for funding.

TABLE OF CONTENTS

CHAPTER 1
INTRODUCTION

Small molecules perform an extraordinary range of important functions in science, medicine, and technology. Small molecules include, but are not limited to: materials components, pharmaceuticals, natural products, and biological probes (Figure 1-1). In fact, more than 238,000 natural products have been isolated to date,[1] yet many of their functions are still unknown because of limited access to these isolates from its natural source. If the ultimate goal is to understand and optimize the function of these small molecules for the study of biological systems, for application as drugs, and/or role as materials, small molecule science can be represented in three distinct stages: target identification, synthesis, and functional studies. Functional discovery studies require rapid access to a range of different small molecules and derivatives. However, there are two major challenges that limit small molecule access. First, perhaps due to the diversity present in small molecules, target-oriented synthesis is highly complex and specific. This fact alone has significantly limited the access of small molecules to the general scientific community because of the prerequisite knowledge and training needed to be a synthetic chemist. Second, laboratory synthesis is inevitably a labor- and time-intensive process. Due to these reasons, synthesis can take months to even years and represents the slow step in small molecule science. Thus, a unified, ideal synthesis platform capable of rapidly accessing a wide range of different small molecules for functional discoveries must address both of these challenges. This can be achieved by the development of a general synthesis strategy to be used across different classes of small molecules and minimization of the labor- and time-intensive nature of synthesis by automation of this general strategy.

This chapter will provide background on the advent of general and automated synthesis platforms for biomolecules that have enabled functional studies of these molecules. These advances as well as the inherent modularity that is present in small molecules became the inspiration for the development of a similarly general and automated synthesis platform for small molecules. Toward this goal, iterative cross-coupling (ICC) of MIDA boronate building blocks show promise as a general strategy to construct many different types of small molecules in an automated fashion. Background for the work described in subsequent Chapters, specifically the expansion of the MIDA boronate platform to complete a total synthesis of the carotenoid natural

product synechoxanthin (Chapter 2) and the development of a small molecule synthesizer (Chapter 3), will be summarized in this introductory Chapter. Such advances have the potential to broaden the access of small molecules and help shift the rate-limiting step in small molecule science from synthesizing these molecules to understanding their functional potential.

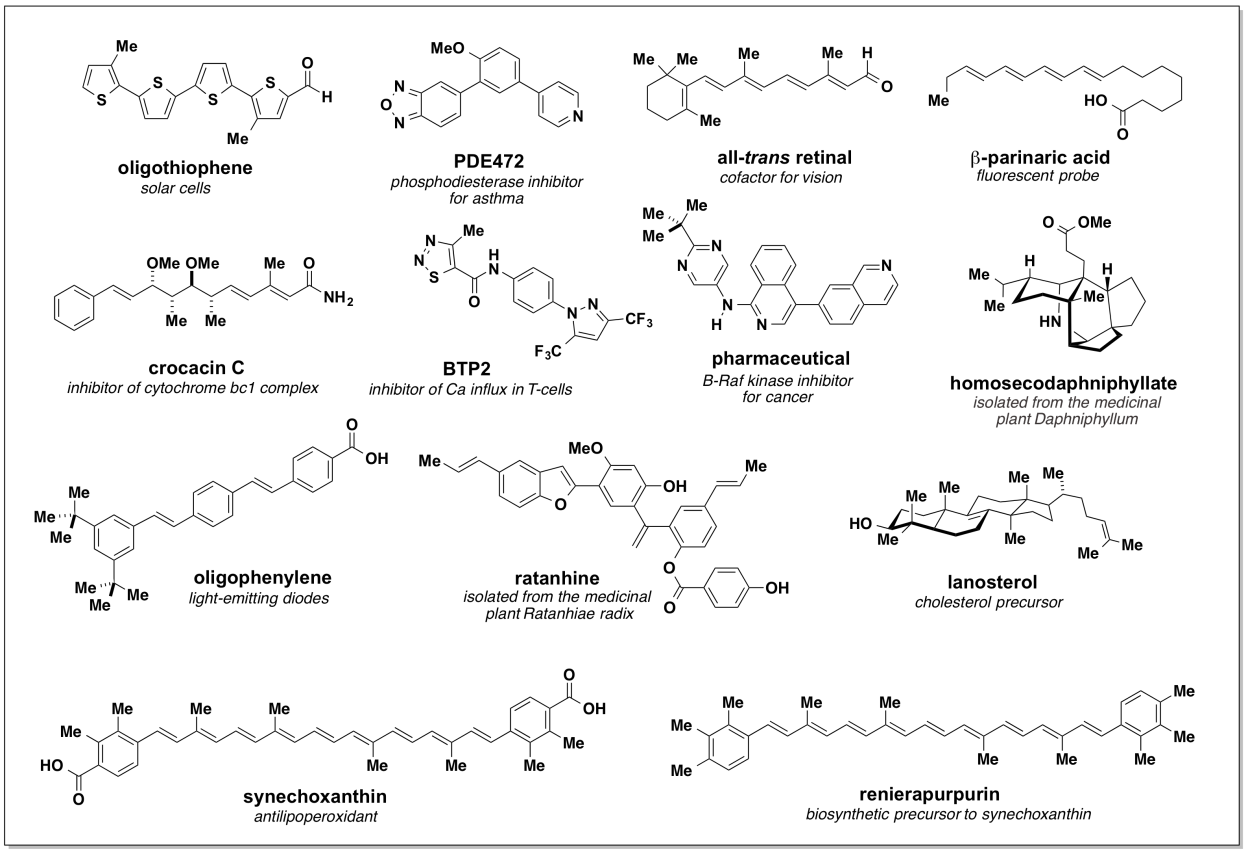

Figure 1-1. Small molecules are structurally and functionally diverse class of compounds.

1-1 GENERAL AND AUTOMATED SYNTHESIS OF BIOMOLECULES FACILITATES FUNCTIONAL STUDIES

In contrast to small molecules, many biomolecules including peptides, oligonucleotides, and oligosaccharides are now routinely prepared via strategies that are general and automated. These synthesis platforms have enabled practical approaches toward understanding the structure-function relationships that underlie the remarkable functional properties of proteins, DNA, and carbohydrates.

Nature's common strategy of iterative coupling of bifunctional building blocks has been translated into the laboratory synthesis of these biomolecules. Even though at first glance these

molecules are structurally complex, biomolecules are inherently modular; their linear sequence is made from small monomer units that are joined together in an iterative fashion.[2] For example, polypeptides are made from amino acid building blocks, oligonucleotides from nucleosides, and oligosaccharides from individual sugar units (Figure 1-2).

Mirroring the simple way Nature makes these complex biomolecules, all of these platforms iteratively employ one type of reaction to assemble common sets of readily accessible units. These processes involve a bifunctional building block where one end is protected, but the other is capable of coupling to a growing oligomer attached to a solid support. Following the key bond formation, the protecting group is deprotected to allow another iteration of this same process in a highly controlled manner. The key to the efficiency of these processes is the simple, yet effective solid-phase purification technique, which allows the growing oligomer, linked to a solid support, to be purified from excess reagents by washing and filtering. As stated above, due to the inherent modularity in the constitution of these biomolecules, they contain common functional groups for attachment to a solid support, which make this purification technique generally applicable to the entire class of molecules, despite other structural differences.

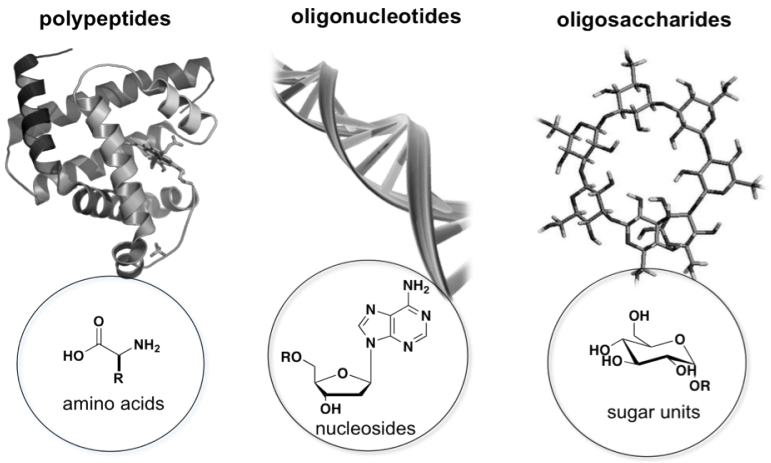

Figure 1-2. Polypeptides, oligonucleotides, and oligosaccharides are inherently modular and all are biosynthetically derived from the iterative coupling of bifunctional building blocks.

1-1-1 GENERAL AND AUTOMATED PEPTIDE SYNTHESIS

The pioneering example of a general synthesis platform is demonstrated by the solid phase peptide synthesis (SPPS) strategy conceptualized by Bruce Merrifield in 1963.[3] Before SPPS, assembling amino acids together to form even small peptide chains was a laborious procedure. SPPS revolutionized peptide synthesis by providing a general strategy for this class of

biomolecules. Specifically, SPPS is enabled by the use of an amino acid bifunctional building block that is orthogonally protected at the N-terminus, frequently as the fluorenylmethoxycarbonyl (Fmoc) or tert-butyloxycarbonyl (Boc) derivative, to prevent random oligomerization during the coupling event (Scheme 1-1). The C-terminus of a growing polypeptide chain is covalently linked to a polystyrene solid support through the presence of a common functional group, in this case, a carboxylic acid. After each C-N bond formation event, a deprotection sequence reveals a free N-terminus capable of undergoing another C-N bond formation. Once the construction process is completed, the peptide can be released from the support. This approach is flexible and modular since any protected amino acid can be introduced during the coupling reactions.

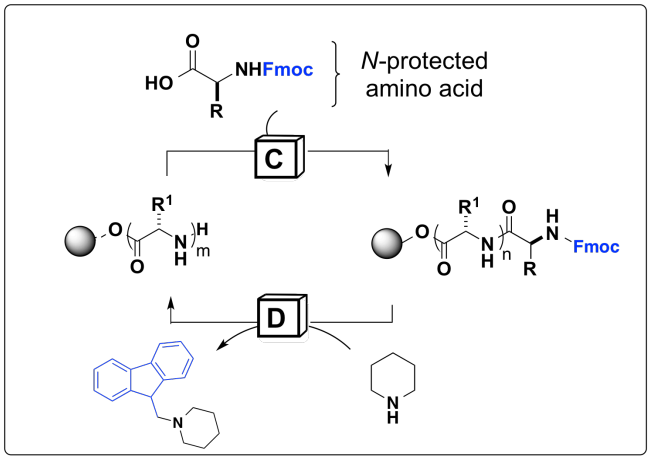

Scheme 1-1. General and automated synthesis strategy for peptides. Growing oligomer (m = n + 1) is attached to a soild support for simple purification. [C] = coupling, [D] = deprotection.

Only two years after the development of SPPS, this general strategy was transformed into an automated platform and successfully applied to synthesize bradykinin, a polypeptide consisting of 9 amino acids.[4] Less than 20 years later, fully automated peptide synthesizers became available as commercial units, extending the power of synthesis to non-specialists.[5] This impact was further exemplified in the automated synthesis of interleukin-3 (IL-3), a protein of 140 amino acids, which had been a difficult protein to isolate, thus its functional studies had been hindered by the lack of its availability.[6] Enabled by the modular approach, analogues of IL-3 were prepared by systematically modifying the primary structure of the protein, i.e. by changing the amino acid building blocks incorporated into the iterative sequence. Efficient access to IL-3

and its analogs led to the understanding that the protein's tertiary structure is required for its activity. This work established the applicability of peptide synthesizers to study large peptides and demonstrated to the scientific community the power of such a rapid, fully-automated, readily-accessible, and reproducible synthesis platform in understanding functions of biological significance.

Several decades later, a variety of linear peptides can now be synthesized using one synthesis platform demonstrating a high level of generality making automation highly practical. Cyclic peptides can also be efficiently synthesized simply by folding linear peptides that have been synthesized in an automated fashion. The combination of a general and automated synthesis platform has had a profound effect on accelerating the ease in which peptides can be accessed thereby facilitating functional studies especially in the areas of molecular biology and biotechnology.

1-1-2 GENERAL AND AUTOMATED OLIGONUCLEOTIDE SYNTHESIS

The above pioneering work and fundamental concepts of SPPS have been applied to the automated synthesis of oligonucleotides by Ogilvie and co-workers[7] as well as Caruthers and co-workers.[8] In automated oligonucleotide synthesis, an O-protected nucleotide serves as a bifunctional building block to prevent random oligomerization during the coupling event (Scheme 1-2). Deprotection of the dimethoxytrityl (DMT) protecting group using dichloroacetic acid reveals a free hydroxyl group capable for a subsequent cycle of coupling and deprotection. Similarly to SPPS, the key to the success and generality of this platform is the use of a solid-support, where the growing oligomer can be purified by simple wash and filtration.

Before the development of such a common and automated platform, it would have taken a highly trained and skilled chemist three months of person time to synthesize a 12-unit DNA,[7] but now DNA synthesis can be conducted in a matter of hours by non-specialists with no previous experience in nucleotide synthesis. Furthermore, as a testament to the DNA synthesizer's impact on the scientific community, DNA fragments are now commercially available and can be purchased on-demand.[9] The significant decrease in person time required to access such biomolecules has had tremendous impact on facilitating the functional understanding and applications of genes in synthetic biology as well as other areas of science.

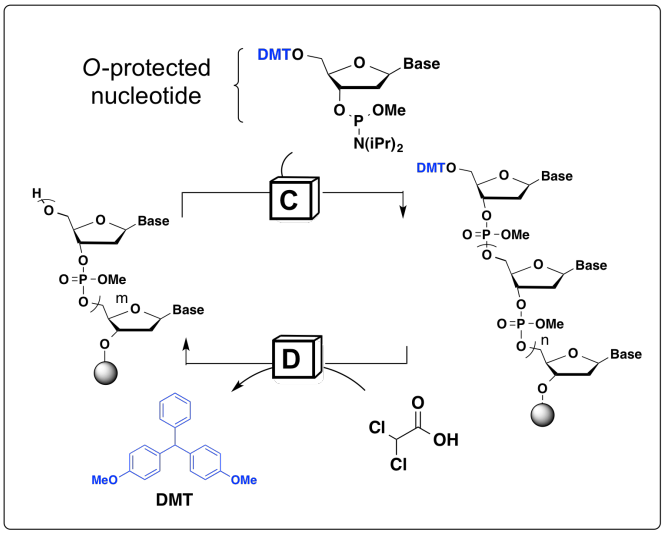

Scheme 1-2. General and automated synthesis of oligonucleotides. Growing oligomer (m = n + 1) is attached to a soild support for simple purification. [C] = coupling, [D] = deprotection.

1-1-3 GENERAL AND AUTOMATED OLIGOSACCHARIDE SYNTHESIS

Recently, Seeberger and co-workers advanced the synthesis of oligosaccharides by developing a fully automated platform (Scheme 1-3). [10] Similarly to peptides and oligonucleotides, oligosaccharide synthesis involve a saccharide bifunctional building block that is orthogonally protected as the levulinoyl (Lev) ester in the presence of other protecting groups such as benzyl ethers and pivaloyl esters. This protecting group can be selectively cleaved by addition of hydrazine to the reaction mixture to allow another iteration. The growing oligomer undergoes the same facile solid-phase purification process as the other biomolecule automated platforms that helps turn over the cycle. Since its invention in 2001, this automated synthesis platform for oligosaccharides has been optimized and expanded.[11] Similar to how the automated peptide and oligonucleotide synthesis platforms impacted the scientific community, this platform already shows promise to accelerate the understanding of oligosaccharide function in biology and drug discovery.[12]

Although synthesis of some specialty building blocks and the optimization of reaction conditions for more challenging couplings are sometimes necessary, all three of these platforms have dramatically increased the efficiency with which these compounds can be prepared, and extended the access of these biomolecules to non-specialists. As a result, the focus of research has shifted from synthesis of these biomolecules to identification of targets and understanding

function. This leads us to question whether a similar type of transformation in small molecule science would be possible by a general and automated synthesis platform.

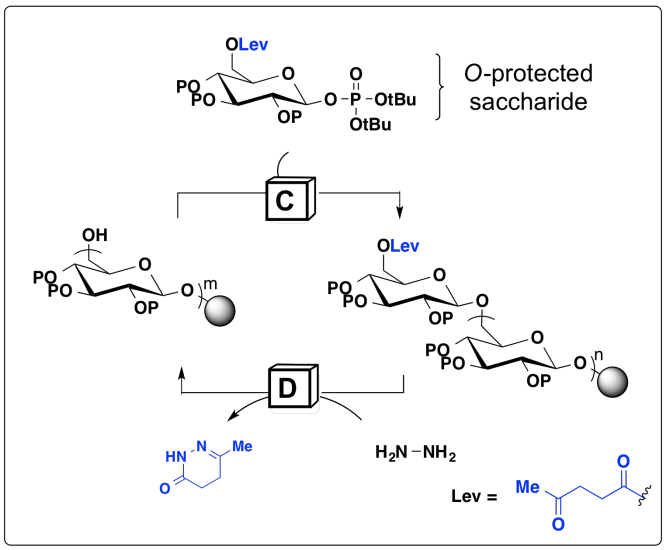

Scheme 1-3. General and automated synthesis of oligosaccharides. Growing oligomer (m = n + 1) is attached to a soild support for simple purification. [C] = coupling, [D] = deprotection.

1-2 CHALLENGES IN DEVELOPING A GENERAL AND AUTOMATED SMALL MOLECULE SYNTHESIS PLATFORM

The key to the efficiency and practicality of automated peptide, oligonucleotide, and oligosaccharide syntheses is the general solid-phase purification of intermediates. Solid-phase synthesis strategy has also been applied to the synthesis of small molecules with the goal of achieving a general strategy amenable for automation. The first report of solid-phase small molecule synthesis was by Clifford Leznoff in 1976, which was accomplished by attachment of a solid support to a diol functionality that was present in a specific class of insect pheromones.[13] Since then, the hydroxyl groups present in certain small molecules have attracted interest in expanding the field of solid-phase organic synthesis,[14] but the applicability of this approach has been hindered by the customized conditions used to link each type of small molecule and the fact that only a portion of small molecules contain this functional group for attachment to a solid support.

To overcome the challenge of applying solid-supported methods to small molecule synthesis, recent advances have focused on addressing the labor- and time-intensive nature of the synthesis process through automating the process in solution-phase. For example, the Takahashi

group has focused their efforts to access complex natural products,[15] including (±) baccatin III, a taxol precursor, via automation of solution-phase synthesis. They reasoned that if synthesis of key intermediates can be accomplished using an automated synthesizer, this will provide the researcher with greater time to focus on the more challenging and down-stream steps of the synthesis (Scheme 1-3). With this goal, they showed that solution-phase automated synthesizers Sol-capa and ChemKonzert[16] was capable of constructing the A and C rings of (±) baccatin III through formation of three C-C bonds, 10 oxidations and reductions, 16 protection and deprotection steps, and 7 other functional group manipulations on 100 mg - 300 g scale (Scheme 1-4). Subsequently, the B-ring was synthesized in a semi-automated fashion, which afforded the key intermediate. From this point forward, one PhD student carried out the post-automated synthesis to (±) baccatin III in 12 steps.[17] While this example demonstrated how automated synthesizers could minimize the burden of repetitive, routine operations that are inevitable in organic chemistry research, this multi-step synthetic sequence had to be manually interrupted to execute custom purifications for each intermediate.

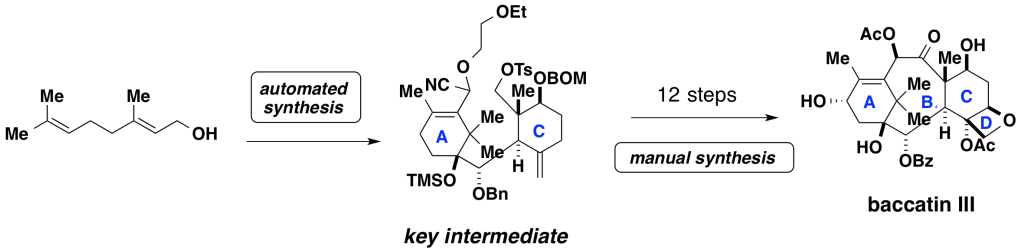

Scheme 1-4. Takahashi group's strategy to automate the synthesis of key intermediates toward total synthesis of taxol derivative, (±) baccatin III.

In efforts to make automated systems more practical, continuous flow multi-step synthesis methods have recently been developed.[18] Compared to traditional multi-step synthesis where each reaction requires purification and isolation of intermediates, one-flow multi-step synthesis does not require purification of intermediates. Specifically, the Ley group has pioneered the use of immobilized reagents, catalysts, and scavengers to facilitate organic synthesis and has applied this concept to flow multi-step processes for the synthesis of natural products and pharmaceutical compounds.[19] The first multi-step natural product synthesis using flow chemistry was accomplished in 2006, which impressively required no manual interventions and purifications of intermediates in the 7-step route toward oxomaritidine in 40% overall yield

(Scheme 1-5). This complex alkaloid was synthesized in 6 h to afford 20 mg of the target small molecule. If conducted in manual batch mode, this synthesis would have taken 4 days of person time.[20]

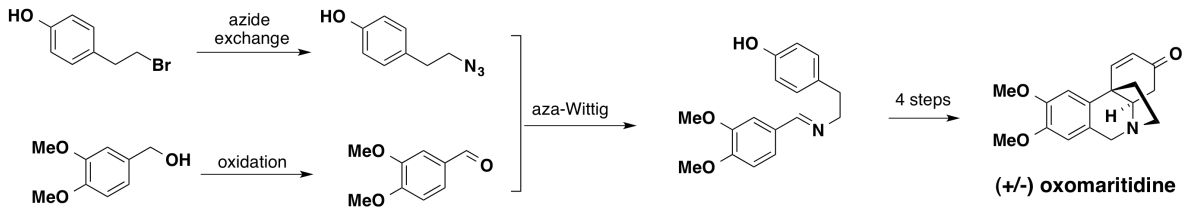

Scheme 1-5. Multi-step flow synthesis of (±) oxamaritidine via the use of immobilized reagents, catalysts, scavengers, and catch-and-release agents.

The same multi-step flow strategy was applied to the synthesis of Gleevec®, a drug marketed by Novartis for the treatment of chronic leukemia, and its structural derivatives.[21] Employing a sulfonic acid-functionalized silica (QuadraSil-SA, SS-SA) for catch-and-release purification helped address the problematic precipitation that occurred during the reaction, and afforded this drug in 32% yield (>95% purity) over a 3-step procedure with minimal manual interventions (Scheme 1-6). However, this catch-and-release purification strategy did not fully translate to all of the Gleevec® derivatives. As shown in Scheme 1-6, the nitrogen of the R^2 group must remain basic enough to allow the product to be captured on the SS-SA resin for purification. This example demonstrated some of the advantages of flow chemistry employing immobilized reagents, namely minimized manual handling of intermediates and increased efficiency, but the purification technology limits the type of small molecules to only those containing basic nitrogen atoms.

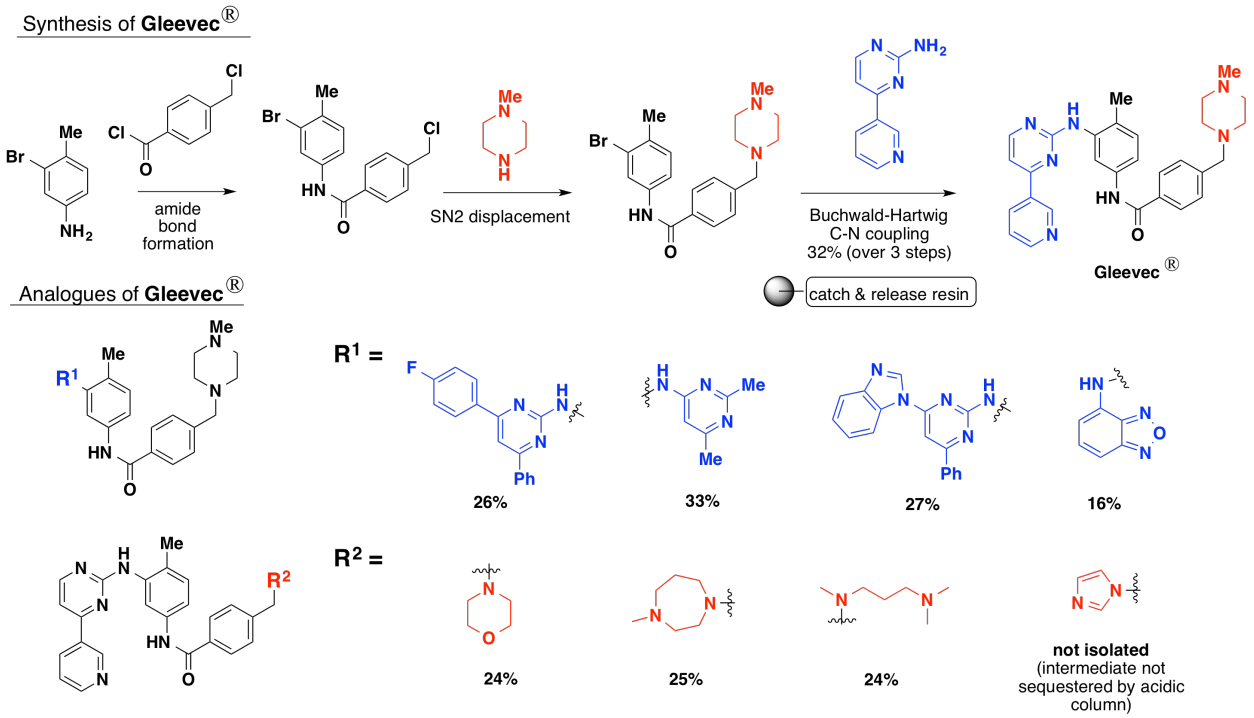

Scheme 1-6. Synthesis of Gleevec® and its analogues via three-step flow synthesis.

Developments in methods to automate small molecule synthesis have been impressive,[22] yet the main disadvantage that all of these advances have in common is their customized approaches toward each small molecule target that require a high degree of specialist expertise for planning, execution, and optimization for each small molecule target. Automating a customized approach only reduces person-time required for that target alone, and does not represent a general synthesis platform.

1-3 SMALL MOLECULES ARE DIVERSE YET INHERENTLY MODULAR

Due to the target-oriented nature of synthesis, most efforts have focused on optimizing the automation of a specific set of reactions to enable the preparation of a single product. However, perhaps it is not beyond our imagination to envision a platform where only one strategy and a few reactions can be used to build most small molecules. This will certainly lend itself well to automation, and serve as a platform on which to build. The success of automated biomolecule synthesis can be attributed to the modular structure. In fact, many natural products are inherently modular because they are biosynthesized via iterative assembly of common building blocks in the same way peptides, oligonucleotides, and oligosaccharides are made. For

example, polyketide natural products are constructed from malonyl-CoA and methylmalonyl-CoA units,[23] polyterpenes from isopentyl and dimethylallyl pyrophosphates,[24] and fatty acids from malonyl-CoA[25] (Figure 1-3). Other classes of small molecules such as nonribosomal peptides come from amino acids[26] and polyphenylpropanoids are derived from shikimic acid[27]. Even many typologically complex macrocyclic and polycyclic natural products are biosynthetically derived from relatively simple and modular linear precursors that are cyclized into the final framework.[28] Furthermore, reoccurring motifs are found across many materials, pharmaceuticals, and biological probes that represent oligomers of aryl or heteroaryl fragments (Figure 1-1).

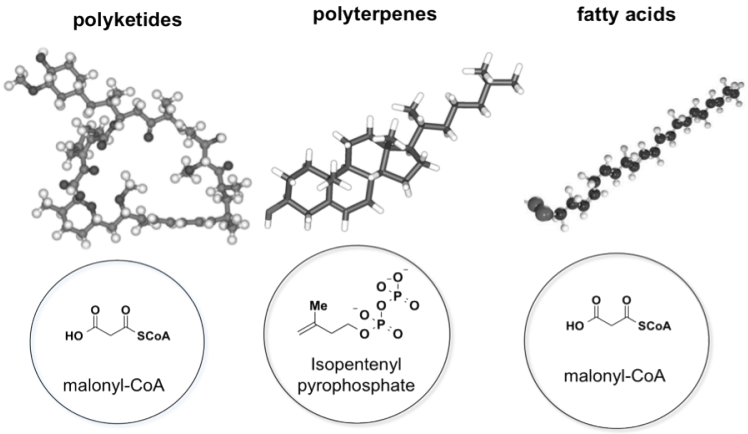

Figure 1-3. Modularity in natural products.

Nature has shown us a simple solution to a complex problem. The question becomes whether we can learn from Nature and apply this approach in the laboratory. As a step in this direction, Moore and co-workers have developed a simple and general synthesis strategy for conjugated oligomers via the iterative assembly of phenylacetylene building blocks.[29] Analogous to how peptides are made, phenylacetylene bifunctional building block protected at one end with a trimethylsilyl (TMS) group and an aryl iodide at the other is coupled to a growing oligomer containing a free alkyne orthogonally linked to a solid support through a triazene linker. After C-C bond formation using Pd-catalyzed Sonogashira coupling, addition of TBAF conveniently transforms the TMS protecting group to its corresponding free alkyne for another iteration of cross-coupling (Scheme 1-7). This method was initially developed as a solution-phase process and further developed into a solid-supported synthesis strategy, which simplified workup and purification by allowing filtration and washing of insoluble intermediates.[30] This method was

successfully applied to the iterative synthesis of a wide range of linear phenylacetylene oligomers and macrocycles, which helped dramatically advance the understanding of functional properties of these polymeric materials.[31]

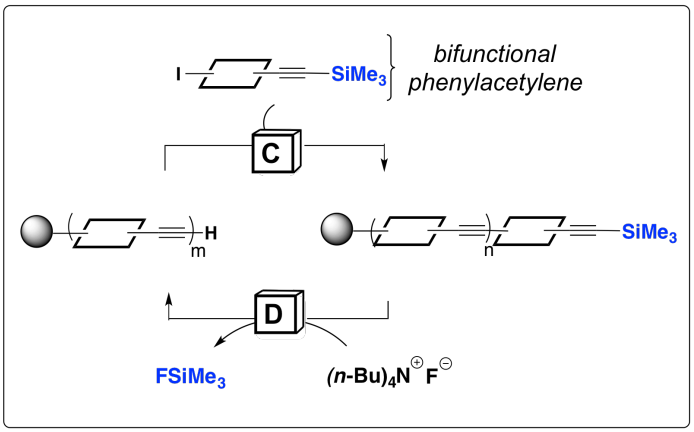

Scheme 1-7. Solid-phase synthesis strategy for conjugated oligomers that involves iterative assembly of bifunctional phenylacetylene building blocks. The rectangle represents an aryl functional group. Growing oligomer (m = n + 1) is attached to a soild support for simple purification. [C] = cross-coupling, [D] = deprotection.

1-4 BUILDING BLOCK APPROACH TO SMALL MOLECULE SYNTHESIS: ITERATIVE CROSS-COUPLING (ICC) STRATEGY ENABLED BY MIDA BORONATES

A building block approach for conjugated oligomer synthesis inspired the development of a general synthesis strategy for small molecules, with the goal of ultimately transforming this strategy into an automated platform. Harnessing the inherent modularity present in a wide range of small molecules, we questioned whether we could access most small molecules, including materials, pharmaceuticals, and natural products, via a single bond-forming reaction. Since all small molecules contain carbon atoms in their backbones, a flexible and modular strategy for making small molecules would incorporate a general way to form such C-C bonds in a controlled, iterative fashion (Figure 1-4).

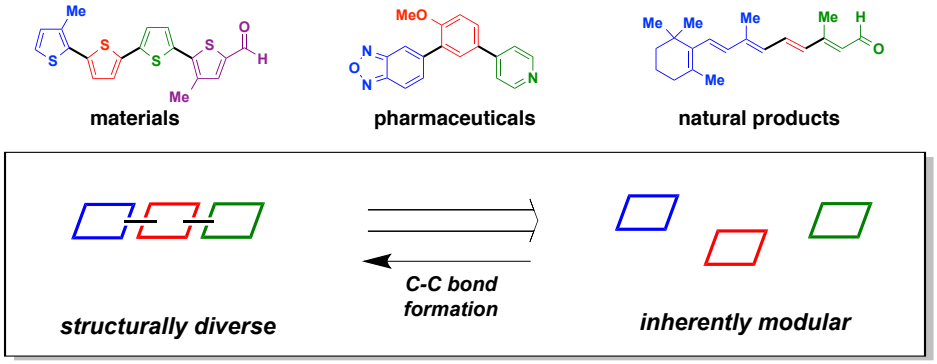

Figure 1-4. Small molecules, including materials, pharmaceuticals, and natural products, are modular in their constitution and can be viewed as a collection of building blocks connected by C-C bonds.

As a step in this direction, Dr. Eric Gillis developed a synthesis strategy analogous to peptide synthesis termed iterative cross-coupling (ICC) (Scheme 1-8).[32] In this ICC approach, small molecules are viewed as a collection of building blocks connected by C-C bonds. The Suzuki-Miyaura cross-coupling, a metal-mediated coupling reaction between a boronic acid or boronic ester to a halide or pseudohalide, was selected to form such bonds for its generality and functional group compatibility.[22] In Suzuki-Miyaura cross-coupling, it is hypothesized that a vacant and Lewis acidic boron p-orbital is required for transmetalation of a boronic acid[33] to the reactive Pd-OR complexes which have been postulated as the reactive intermediates during transmetalation.[34] In order to reversibly attenuate the reactivity of the boronic acid and prevent random oligomerization for successful iteration, methods to decrease the Lewis acidity of the boron p-orbital was investigated by surveying various trivalent heteroatomic ligands capable of lone pair electron donation and rehybridization of the boron atom from sp^2 to sp^3. Through this exploration, it was discovered that *N*-methyliminodiacetic acid (MIDA) can reversibly attenuate the reactivity of a boronic acid, similar to the way a Fmoc group protects an amine. This enables iterative C–C bond formation between a free boronic acid and the halide terminus of a MIDA protected haloboronic acid building block using Suzuki-Miyaura cross-coupling.

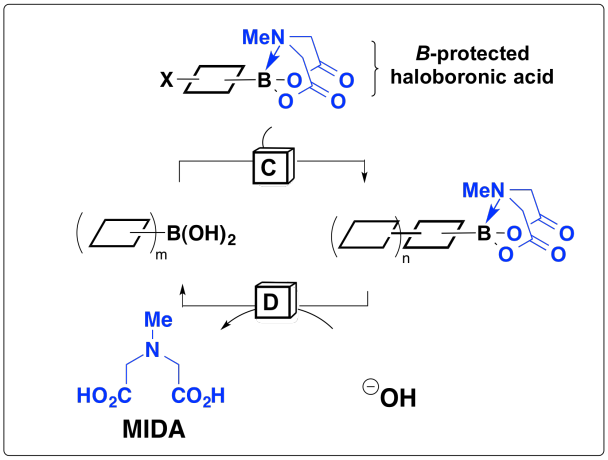

Scheme 1-8. Iterative cross-coupling (ICC) strategy for making small molecules. The rectangle represents building blocks containing a wide range of functional groups including: aryl, heteroaryl, vinyl, acetyl, and alkyl motifs. Growing oligomer is represented as (m = n + 1). [C] = Suzuki-Miyaura cross-coupling, [D] = deprotection to boronic acid (1 N aqueous NaOH/THF, 23 ^{o}C, 10 min).

This strategy is general and can be used to protect a wide range of haloboronic acid building blocks with aryl, heteroaryl, alkynyl, alkenyl, and alkyl moieties. Moreover, the MIDA boronate functional group is inert to anhydrous cross-coupling conditions, yet can be readily hydrolyzed under mild aqueous conditions compatible with many other functional groups to generate the corresponding free boronic acid or boronic ester. Advances have been made to control the release of boronic acid slowly over the course of the reaction (K_3PO_4 in 5:1 dioxane/water at 60 ^{o}C) in order to avoid the isolation of unstable boronic acids before and during the cross-coupling event.[35] Moreover, MIDA boronates are shelf-stable building blocks that can be readily accessed via many different methods (Scheme 1-9).[36] In addition, the MIDA ligand is nontoxic, biodegradable[37], and commercially available, therefore MIDA boronates can be synthesized conveniently and inexpensively on large scale from the commodity chemical iminodiacetic acid. Encompassing all of these advantageous features, more than 160 MIDA boronates are already commercially available to date, making this technology readily accessible to the scientific community. In addition to these MIDA boronates, thousands of commercially available boronic acids and halides serve as MIDA boronate precursors (Scheme 1-9) and constitute a formidable pool of off-the-shelf building blocks that are readily available for ICC.

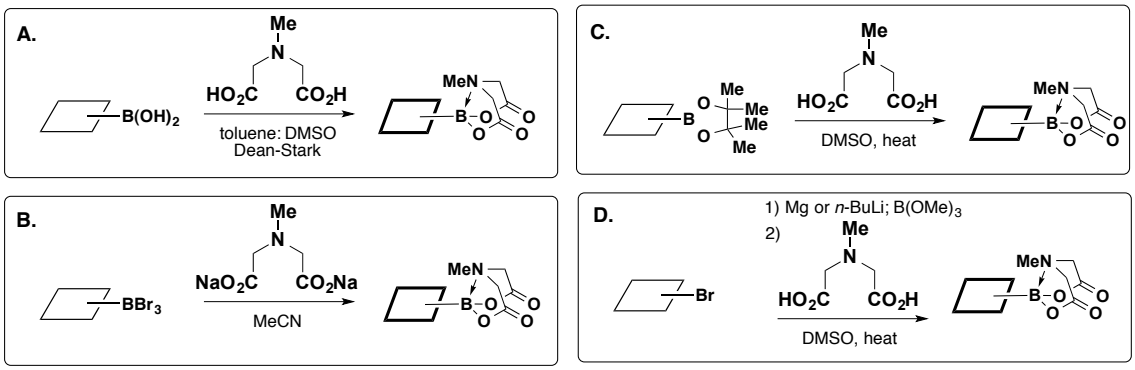

Scheme 1-9. Examples of known methods for the synthesis of MIDA boronate building blocks. A. Condensation of MIDA boronates to boronic acids under Dean-Stark conditions. **B.** The use of haloborane and disodium salt of MIDA. **C.** Transesterification of boronic esters to MIDA boronates. **D.** Trapping of the Grignard or lithium reagent with trimethyl borate followed by transligation with MIDA affords corresponding MIDA boronates.

1-5 SMALL MOLECULE SYNTHESIS VIA ICC

Employing this ICC approach, small molecules are first retrosynthesized into building blocks, via disconnections at C-C bonds, where all but the last building block contains a MIDA boronate motif. With the exception of the first and last building blocks, all others are bifunctional haloboronic acid building blocks where the boronic acid is protected as MIDA, and the halide terminus is available for coupling. With building blocks in hand, the first step in ICC begins with deprotection of the unreactive Bsp^3 MIDA boronate to the corresponding reactive Bsp^2 boronic acid. This boronic acid can be coupled to the halide terminus of a bifunctional MIDA boronate building block, and the resulting MIDA boronate-containing product can be purified by standard silica gel chromatography to be ready for another cycle. These bifunctional building blocks are assembled in an iterative fashion similar to how peptides and other biomolecules are now synthesized in an automated fashion (Scheme 1-10).

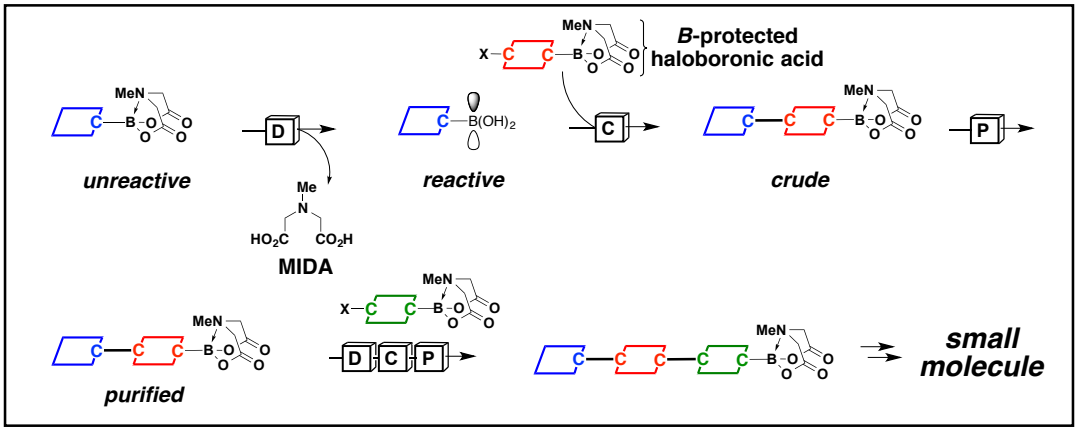

Scheme 1-10. ICC strategy for the synthesis of small molecules.

Since its initial report in 2007, MIDA boronate building blocks have been used in the manual synthesis of many different types of small molecules including natural products [ratanhine,[32a] crocacin C,[38] all-*trans*-retinal,[39] β-parinaric acid,[39] peridinin,[36a] (-)-myxalamide A[40], methyl (5*Z*, 8*Z*, 10*E*, 12*E*, 14*Z*)-eicosapentaenoate,[41] and synechoxanthin (further discussed in Chapter 2)[42]] and natural product derivatives [C35-deoxy amphotericin B[43], the polyene core of vacidin A[44]] (Figure 1-5). As shown in Figure 1-5, wide range of different types of building blocks have been incorporated into ICC, majority of them consisting of aryl, heteroaryl, and vinyl fragments.

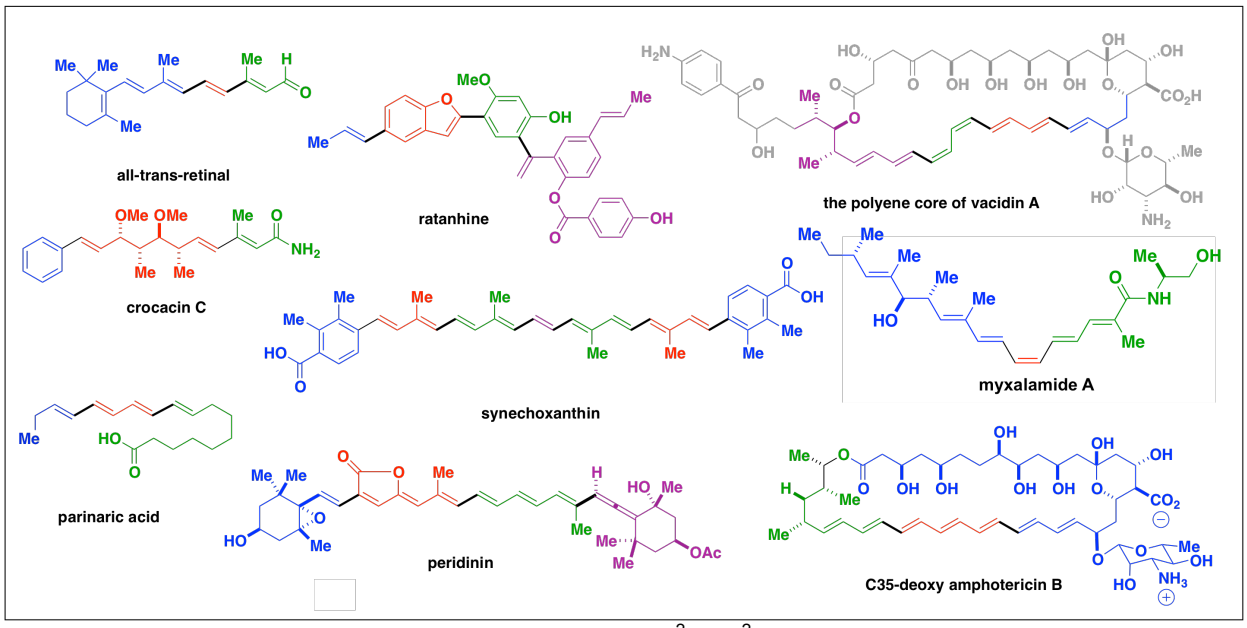

Figure 1-5. Small molecules synthesized via ICC via Csp^2-Csp^2 bond formations.

As illustrated in Figure 1-5, polyene motifs are prevalent across many different types of natural product classes. In fact, many of these repeating polyene units are modular; for example, the tri-substitued olefin motif is present in all-*trans* retinal, synechoxanthin, and peridinin. To further explore the potential for a systematized and modular building-block approach to small molecule synthesis, Dr. Eric Woerly and Jahnabi Roy questioned how many building blocks it would take to access most natural products of a single class. Specifically, they asked: if restricting the bond-forming reactions to only the Suzuki-Miyaura reaction, how many bifunctional MIDA boronate building blocks would be required to make most polyene natural product motifs?

They addressed this question by devising an algorithm for systematically retrosynthesizing polyene core motifs into bifunctional building blocks. A polyene motif was defined as three or more carbon-carbon double bonds in conjugation, none of which are contained in a <12-membered ring. This analysis returned 2,839 compounds, or 1.2% of all known natural products as polyene natural products. Further analysis showed that polyene motifs found in >75% of all polyene natural products isolated to date represent all major biosynthetic classes (polyterpenes, polyketides, hybrid peptide/polyketides, fatty acids, and polyphenylpropanoids), and can be prepared using only 12 MIDA boronate building blocks (Figure 1-6). Assembly of these building blocks was performed under a general set of cross-coupling and deprotection conditions.[45] Furthermore, these building blocks and general conditions were applied to the first total synthesis of several polyene natural products such as α-parinaric acid.

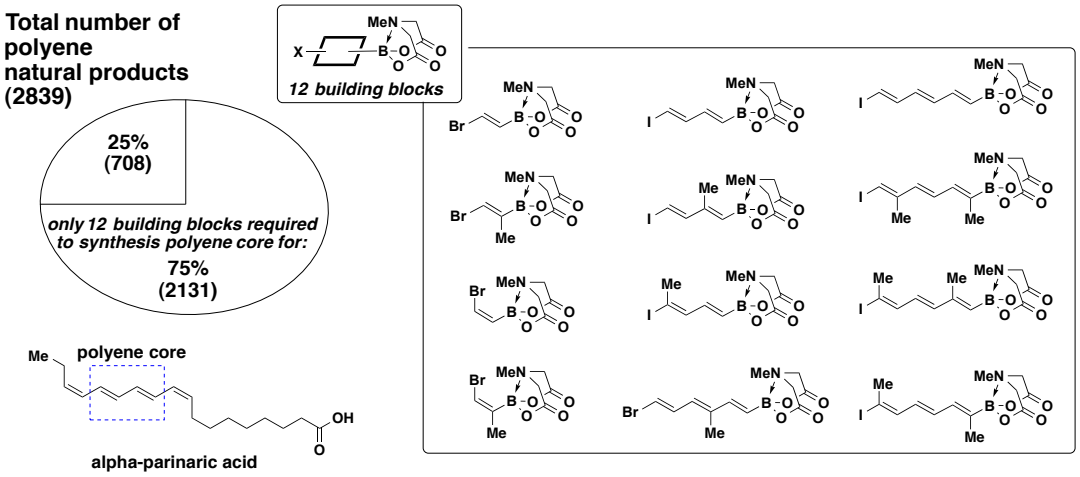

Figure 1-6. Synthesis of >75% polyene natural product motifs using just 12 building blocks and 1 reaction.

This example further illustrates the diversity of natural products, but more importantly it demonstrates the modularity as well. Even though there are over 238,000 natural products isolated and characterized to date, it is encouraging to know that there is a bounded number of building blocks needed to access a large portion of a certain structural class of natural products. While polyene natural products only represent 1.2% of all natural products, it is possible to envision the same concept would translate to other small molecule classes due to the modular nature. Furthermore, if this general strategy can be automated, it will greatly simplify the synthesis process by eliminating the need to isolate intermediates, minimizing person time spent on synthesis, and elevating the access of these molecules to specialists as well as non-specialists. Chapter 3 will build on this recent advance and address challenges that are associated with translating the ICC platform into a synthesizer capable of automatically coupling together MIDA boronate building blocks.

1-6 RECENT ADVANCES IN THE MIDA BORONATE TECHNOLOGY

It is intriguing to consider how many building blocks would be required to access most of the structural motifs found in small molecules by applying this concept to other classes of small molecule natural products, pharmaceuticals, and materials. The polyene example demonstrates that this may be attainable. This concept seeks to promote a systematic approach that has the potential to enable the efficient, flexible, and even fully automated access to many classes of small molecules. In order for this general strategy to be realized, current limitations of the ICC platform must be addressed.

First, increasing the diversity of building blocks available for coupling and developing general and robust methods to couple them would increase the generality and flexibility of this strategy. In the ICC approach, starting building blocks have been limited to boronic acid or boronic esters capable of coupling to the halide terminus of a bifunctional MIDA boronate building block. Chapter 2 will cover the development of a reversed-polarity ICC approach that complements the established ICC approach, with an emphasis on increasing the flexibility in which small molecules are constructed by expansion of building blocks that can be utilized in a single synthetic platform.

Second, initial reports applying the ICC strategy to the synthesis of small molecules mostly consisted of forming Csp^2-Csp^2 bonds with aryl, heteroaryl, or vinyl MIDA boronate

building blocks (Figure 1-5). Many small molecules not only contain C-C, but C-heteroatom bonds (such as O, N, S) in their backbones. Due to the masked reactivity of MIDA boronates and its broad tolerance to many different types of reaction conditions and reagents, the ICC platform can be expanded to include increased variety of building blocks that can undergo different reactions beyond Suzuki cross-coupling.[46]

Additionally, progress has been made in the area of developing efficient ways to synthesize heterocycles incorporating MIDA boronates, because of the importance of these structures in drug targets and natural products.[47] For example, Hamann and co-workers have demonstrated that MIDA boronate-functionalized isoxazoles and triazoles can be prepared through cycloaddition reactions (Scheme 1-11A).[48] Also, Toste and co-workers have prepared heterocyclic MIDA boronates through a tandem gold-catalyzed cycloisomerization reaction followed by Suzuki-Miyaura cross-coupling from substituted alkynyl MIDA boronates (Scheme 1-11B).[49]

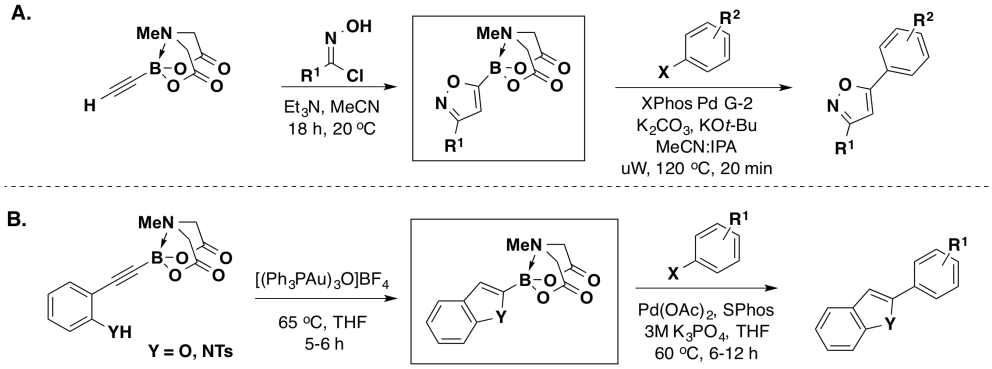

Scheme 1-11. A. Isoxazole synthesis via MIDA boronate chemistry. **B.** Benzofuran and indole synthesis via MIDA boronate building blocks.

In addition, palladium-catalyzed bond formations of MIDA boronates with heteroatoms and challenging heterocycles have recently shown promise.[50] Natural products and pharmaceutical agents have been prepared via C-N bond formations using MIDA chemistry.[51] One recent example by Hamman and co-workers demonstrates a method to couple a wide range of aliphatic and aromatic amines to haloarene MIDA boronates via Buchwald-Hartwing cross-coupling to form N-Csp^2 bonds. Employing this method, histamine H3 antagonist was synthesized in 63% yield via a two-step, one-pot cross-coupling sequence via N-C/C-C bond formations via formation of an enolized MIDA boronate in situ (Scheme 1-12).[52]

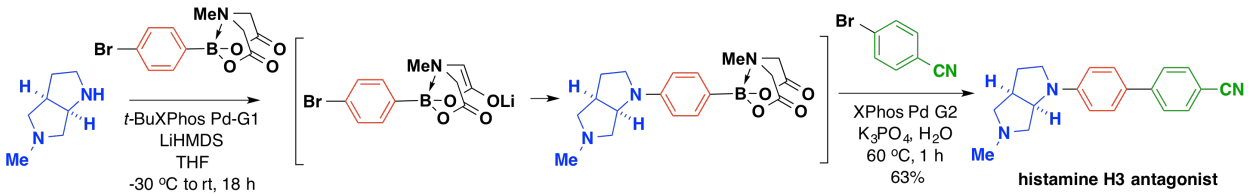

Scheme 1-12. Synthesis of histamine H3 antagonist via N-C followed by C-C bond formations through an enolized MIDA boronate intermediate.

Finally, it would be advantageous to apply MIDA boronates to cross-coupling of Csp^3-hybridized building blocks. However, this field of synthetic chemistry has many challenges and unsolved problems. Cyclic natural products, such as steroids, are biosynthesized via cyclization of linear precursors that contain increased levels of saturation in their backbones due to the presence of Csp^3-hybridized atoms that allow predisposed flexibility for cyclization. If we wanted to use the same strategy Nature uses to make even these complex architectures, we need efficient ways to make such Csp^3-Csp^3 or Csp^3-Csp^2 bonds. While significant advances have been made to couple Csp^3 atoms, the scope of Suzuki-Miyaura cross-coupling methods are still limited to a particular set of substrates or conditions that are not compatible with a wide range of functional groups (Scheme 1-13).[53] The challenges with unstable boronic acid resurface again as B-alkyl boronic acids are known to be susceptible to protodeborylation and β-hydride elimination.

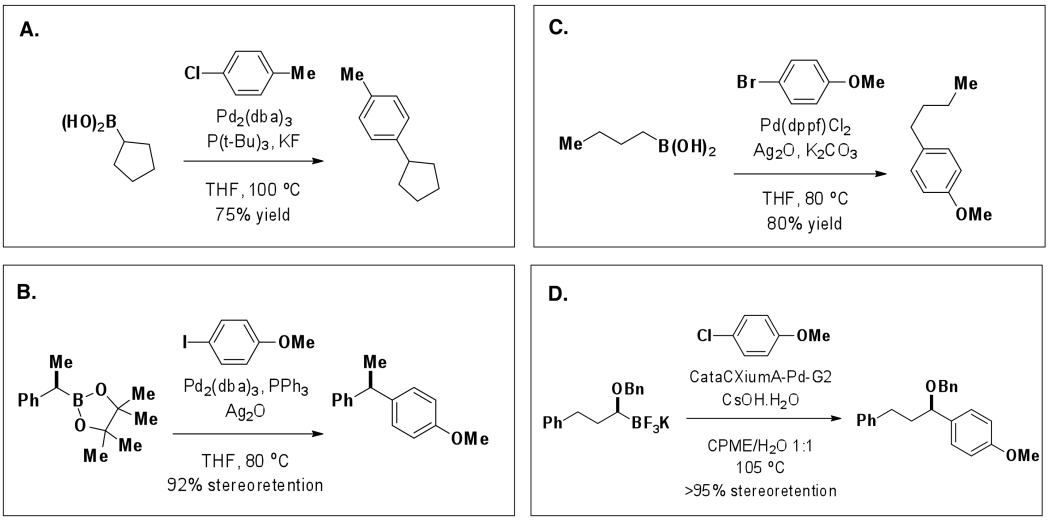

Scheme 1-13. Recent advances in Suzuki-Miyaura cross-coupling of Csp^3-hybrized atoms utilizing alkyl boronates.

Recently, two reports in the literature have utilized MIDA boronates as precursors for Csp^3 cross-coupling. Junqi Li has pioneered the development of iterative Csp^3 coupling via a chiral PIDA (pinene-derived iminodiacetic acid) boronate bifunctional building block.[54] Specifically, glucagon receptor antagonist under evaluation for treatment of type-II diabetes was synthesized in a stereocontrolled manner by iterative Csp^3-Csp^2 Negishi cross-coupling followed by Csp^3-Csp^2 Suzuki-Miyaura cross-coupling (Scheme 1-14). Furthermore, Yudin and co-workers developed a direct method to couple B-alkyl MIDA boronates and alkyl bromides (Scheme 1-15).[55] Collectively, these results show that new methods can be incorporated with the ICC platform. Chapter 3 describes our latest efforts to address the latter two challenges by building on these recent advances to achieve a small molecule synthesis platform that can synthesize a wide range of small molecules.

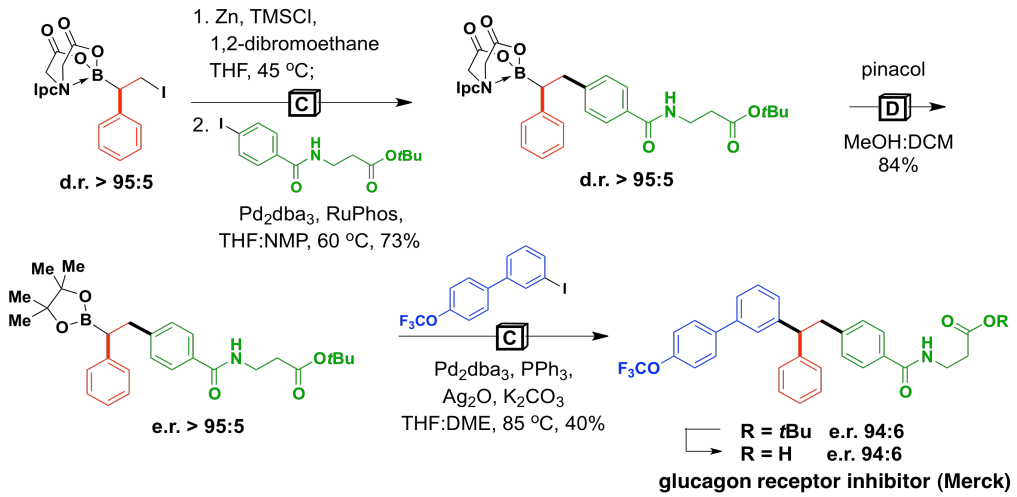

Scheme 1-14. Synthesis of glucagon receptor inhibitor via Csp^3-Csp^2 Negishi cross-coupling followed by Csp^3-Csp^2 Suzuki-Miyaura cross-coupling enabled by the bifunctional PIDA boronate building block.

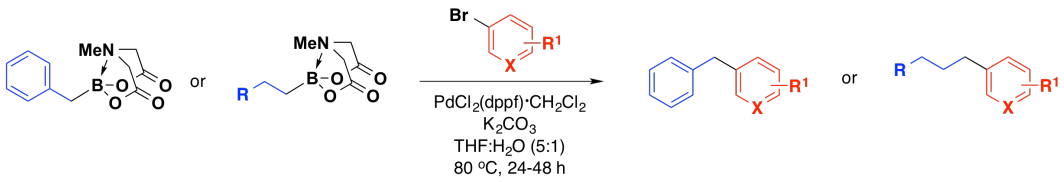

Scheme 1-15. Csp^3-Csp^2 Suzuki-Miyaura cross-coupling with alkyl MIDA boronates.

1-7 THE PROSPECT OF A GENERAL APPROACH TO SMALL MOLECULE SYNTHESIS

Over the last century, impressive number of advances has been made in the development of synthetic methods that nearly any small molecule can now be made by a specialist with enough time and effort.[56] Several perspectives have been written on the topic of an ideal synthesis and have focused on the aspects of atom-economy,[57] step-economy,[58] and redox economy.[56] These concepts translate well for a process-level synthesis of a small molecule with already known functional interest. The collective limitation to these concepts is that it focuses on one small molecule synthesis pathway. While one synthetic path may be ideal to make one small molecule, these concepts may require much time and effort to be translated to another target, which does not enable rapid and systematized access to many different small molecules using one general strategy.

Small molecules represent 85% of new drug approvals in 2013.[59] The increased demands for small but diverse libraries in the drug discovery process within the past decade have led to a demand for automated synthesis platforms.[60] In this context, a remote-controlled medicinal chemistry lab was built at Eli Lilly & Co. that is capable of running more than 60 different types of reactions. The senior director of discovery research and technology at Eli Lilly was recently quoted in C&EN stating, "We measure the value of automation not by the number of compounds it turns out but by the diversity of the compounds."[61]

Developing a general strategy to synthesize most small molecules is an ambitious goal, yet the establishment of this automated synthesis lab suggests that this goal might be achievable. Of the total 16,349 reactions run in this remote chemistry lab from late 2008 through 2011, amide coupling and Suzuki-Miyaura cross-coupling were the two most popular methods employed, totalling ~6500 reactions. In addition, another ~4500 reactions represent chemistry that has been shown to be compatible with the MIDA boronate technology. In fact, the ICC strategy could potentially incorporate close to 70% of the total number of procedures employed by the remote-controlled synthesis lab at Eli Lilly, suggesting the possibility that a range of different small molecules can be accessed through one common strategy. Expansion and automation of the ICC strategy with the MIDA boronate platform could simplify the synthesis process and provide access to small molecule targets relevant not only to the pharmaceutical industry, but many other sectors of the scientific community such as biotechnology and functional materials.

1-8 REFERENCES

[1] http://dnp.chemnetbase.com/

[2] (a) Garret, R. H.; Grisham, C. M. Biochemistry; Saunders College Publishing: Fort Worth, TX, 1995. (b) Voet, D.; Voet, J. G. Biochemistry 3rd Edition; Wiley Publishing: Hoboken, NJ, 2004.

[3] Merrifield, R. B. *J. Am. Chem. Soc.* **1963**, *85*, 2149-2154.

[4] (a) Merrifield, R. B. *Science* **1965**, *150*, 178-185. (b) Merrifield, R. B.; Stewart, J. M. *Nature* **1965**, *207*, 522-523.

[5] Andrews, R. P. *Nature* **1986**, *319*, 429-430.

[6] Clark-Lewis, I.; Aebersold, R.; Ziltener, H.; Schrader, J. W.; Hood, L. E.; Kent, S. B. H. *Science* **1986**, *231*, 134-139.

[7] Alvarado-Urbina, G.; Sathe, G. M.; Liu, W.; Gillen, M. F.; Duck, P. D.; Bender, R.; Ogilvie, K. K. *Science* **1981**, *214*, 270-274.

[8] Caruthers, M. H. *Science* **1985**, *230*, 282-285.

[9] Hunkapiller, M.; Kent, S. Caruthers, M.; Dreyer, W.; Firca, J.; Giffin, C.; Horvath, S.; Hunkapiller, T.; Tempst, P.; Hood, L. *Nature* **1984**, *310*, 105-111.

[10] Plante, O. J.; Palmacci, E. R.; Seeberger, P. H. *Science* **2001**, *291*, 1523-1527.

[11] Seeberger, P. H. *Chem. Soc. Rev.* **2008**, *37*, 19-28.

[12] Seeberger, P. H.; Werz, D. B. *Nature Rev. Drug Discov.* **2005**, *4*, 751-763.

[13] Leznoff, C.C.; Fyles, T. M. *J. Chem. Soc. Chem. Comms.* **1976**, 251-252.

[14] Nam, N-H.; Sardari, S.; Parang, K. *J. Comb. Chem.* **2003***, 5,* 479-546.

[15] Fuse, S.; Machida, K.; Takahashi, T. *New Strategies in Chemical Synthesis and Catalysis,* Chapter 2, Pignataro, B. ed. Wiley-VCH, 2012. (b) Tanaka, Y.; Fuse, S.; Tanaka, H.; Doi, T.; Takahashi, T. *Org. Process Res. Dev.* **2009**, *13*, 1111-1121. (c) Fuse, S.; Okada, K.; Iijima, Y.; Munakata, A.; Machida, K.; Takahashi, T.; Takagi, M.; Shin-ya, K.; Doi, T. *Org. Biomol. Chem.* **2011**, *9*, 3825.

[16] This synthesizer is capable of executing standard processes of a typical reaction procedure including: solvent addition, reagent addition, reaction cooling, heating, stirring, precipitation, aqueous work-up, drying, and purification via Combi-Flash. Manual supplementation of the following procedures complete all tasks required for synthesis: reagent addition, reaction set-up,

and evaporation of solvent after each run. Machida, K.; Hirose, Y.; Fuse, S.; Sugawara, T.; Takahashi, T. *Chem. Pharm. Bull.* **2010**, *58*, 87-93.

[17] Doi, T.; Fuse, S.; Miyamoto, S.; Nakai, K.; Sasuga, D.; Takahashi, T. *Chem. Asian. J.* **2006**, *1*, 370-383.

[18] Flow reactors are most suited for fast and exothermic reactions due to enhanced mass and heat transfer, excellent mixing, and safer use of hazardous reagents: Wedd, D.; Jamison, T. F. *Chem. Soc.* **2010**, *1*, 675-680.

[19] Myers, R. M.; Roper, K. A.; Baxendale, I. R.; Ley, S. V. *Modern Tools for the Synthesis of Complex Bioactive Molecules,* Chapter 11, Cossy, J. & Arseniyadis, S. eds. Wiley, 2012.

[20] Bazendale, I. R.; Deeley, J.; Griffiths-Jones, C. M.; Ley, S. V.; Saaby, S.; Tranmer, G. K. *Chem. Comm.* **2006**, 2566-2568.

[21] Ley, S. V. *Org. Biomol. Chem.* **2013**, *11*, 1822-1839.

[22] Cross-coupling reactions have been recently introduced into flow systems: Noël, T.; Buchwald, S. L. *Chem. Soc. Rev.* **2011**, *40*, 5010-5029.

[23] (a) Birch, A. J. *Science* **1967**, *156*, 202-206. (b) Staunton, J.; Weissman, K. J. *Nat. Prod. Rep.* **2001**, *18*, 380-416.

[24] Newsholme, E. A.; Leech, A. R. Biochemistry for the Medical Sciences; Wiley, 1983.

[25] (a) Brownsey, R. W.; Denton, R. M. in Boyer, P. D.; Krebs, E. G. The Enzymes 3rd Edition; Academic Press, 1987, vol. 18, p. 123-146. (b) Wakil, S. J. *Biochemistry* **1989**, *28*, 4523-4530.

[26] Sieber, S. A.; Marahiel, M. A. *Chem. Rev.* **2005**, *105*, 715-738.

[27] Dewick, P. M. ed. *Medicinal Natural Products,* p. 121-164, John Wiley & Sons, West Sussex, England, 2002.

[28] (a) Fischbach, M. A.; Walsh, C. T. *Chem. Rev.* **2006**, *106*, 3468-3496. (b) Heathcock, C. H. *Proc. Natl. Acad. Sci. U.S.A.* **1996**, *93*, 14323-14327. (c) Yoder, R. A.; Johnston, J. N. *Chem. Rev.* **2005**, *105*, 4730-4756.

[29] (a) Zhang, J.; Moore, J. S.; Xu, Z.; Aguirre, R. A. *J. Am. Chem. Soc.* **1992**, *114*, 2273-2274. (b) Moore, J. S.; Weinstein, E. J.; Wu, Z. *Teterahedron Lett.* **1991**, *32*, 2465-2466.

[30] Nelson, J. C.; Young, J. K.; Moore, J. S. *J. Org. Chem.* **1996**, *61*, 10841-10842.

[31] Zhang, J.; Moore, J. S. *J. Am. Chem. Soc.*, **1996**, *116*, 2655–2656.

[32] (a) Gillis, E. P.; Burke, M. D. *J. Am. Chem. Soc.* **2007**, *129*, 6716-6717. (b) Gillis, E. P.; Burke,

M. D. *Aldrichimica Acta* **2009**, *42*, 17-27; Suginome and co-workers reported the use of iterative cross-coupling reactions for the preparation of oligoarenes based on 1,8-diaminonapthalene: (c) Noguchi, H.; Hojo, K.; Suginome, M. *J. Am. Chem. Soc.* **2007**, *127*, 758-759; (d) Noguchi, H.; Shioda, T.; Chou, C. M.; Suginome, M. *Org. Lett.* **2008**, *10*, 377-380.

[33] (a) Matos, K.; Soderquist, J. A. *J. Org. Chem.* **1998**, *63*, 461. (b) Miyaura, N. *J. Organomet. Chem.* **2002**, *653*, 54-57. (c) Braga, A. A. C.; Morgon, N. H.; Ujaque, G.; Maseras, F. *J. Am. Chem. Soc.* **2005**, *127*, 9298.

[34] (a) Carrow, B. P.; Hartwig, J. F. *J. Am. Chem. Soc.* **2011**, *133*, 2116-2119. (b) Amatore, C.; Jutand, A.; Le Duc, G. *Chem. Eur. J.* **2011**, *17*, 2492-2503.

[35] Knapp, D. M.; Gillis, E. P.; Burke, M. D. *J. Am. Chem. Soc.* **2009**, *131*, 6961-6963.

[36] (a) Ballmer, S. G.; Gillis, E. P.; Burke, M. D. *Org. Syn.* **2009**, *86*, 344-359. (b) Uno, B. E.; Gillis, E. P.; Burke, M. D. *Tetrahedron* **2009**, *65*, 3130-3138. (c) Woerly, E. M.; Cherney, A. H.; Davis, E. K.; Burke, M. D. *J. Am. Chem. Soc.* **2010**, *132*, 6941-6943. (d) Dick, G. R.; Knapp, D. M.; Gillis, E. P.; Burke, M. D. *Org. Lett.* **2010**, *12*, 2314-2317. (e) Grillo, A. S.; Woerly, E. M.; Burke, M. D. *Org. Syn.* submitted.

[37] Warren, C. B.; Malec, E. J. *Science* **1972**, *176*, 277.

[38] Gillis, E. P.; Burke, M. D. *J. Am. Chem. Soc.* **2008**, *130*, 14084-14085.

[39] Lee, S. J.; Gray, K. C.; Paek, J. S.; Burke, M. D. *J. Am. Chem. Soc.* **2008**, *130*, 466-468.

[40] Fujita, K.; Matsui, R.; Suzuki, T.; Kobayashi, S. *Angew. Chem. Int. Ed.* **2012**, *51*, 7271-7274.

[41] Mohamed, Y. M. A.; Hansen, T. V. *Tetrahedon Lett.* **2011**, *52*, 1057- 1059.

[42] Fujii, S.; Chang, S. Y.; Burke, M. D. *Angew. Chem. Int. Ed.* **2011**, *50*, 7862-7864.

[43] Gray, K. C.; Palacios, D. S.; Dailey, I.; Endo, M. M.; Uno, B. E.; Wilcock, B. C.; Burke, M. D. *Proc. Natl. Acad. Sci. U.S.A.* **2012**, *109*, 2234-2239.

[44] Lee, S. J.; Anderson, T. M.; Burke, M. D. *Angew. Chem. Int. Ed.* **2010**, *49*, 1-6.

[45] Woerly, E. M.; Roy, J. R.; Burke, M. D. *Nature Chem.* **2014**, *in press*.

[46] Recent examples of coupling boronic acids with building blocks other than halides: (a) Barluenga, J.; Tomás,-Gamasa, M.; Aznar, F.; Valés, C. *Nat. Chem.* **2009**, *1*, 494-499. (b) DeBergh, J. R.; Niljianskul, N.; Buchwald, S. L. *J. Am. Chem. Soc.* **2013**, *135*, 10638-10641. (c) Qiao, J. X.; Lam, P. Y. S. *Synthesis*, **2011**, 829-856. (d) Quach, T. D.; Batey, R. A. *Org. Lett.* **2003**, *5*, 1381-1384.

[47] Wang, H.; Grohmann, C.; Nimphius, C.; Glorius, F. *J. Am. Chem. Soc.* **2012**, *134*, 19592-19595.

[48] Grob, J. E.; Nunez, J.; Dechantsreiter, M. A.; Hamann, L. G. *J. Org. Chem.* **2011**, *76*, 4930-4940.

[49] Chan, J. M. W.; Amarante, G. W.; Toste, F. D. *Tetrahedron* **2011**, *67*, 4306-4312.

[50] (a) Dick, G. R.; Woerly, E. M.; Burke, M. D. *Angew. Chem. Int. Ed.* **2012**, *51*, 2667-2672. (b) Bagutski, V.; Grosso, A. D.; Carrillo, J. A.; Cade, I. A.; Helm, M. D.; Lawson, J. R.; Singleton, P. J.; Solomon, S. A.; Marcelli, T.; Ingleson, M. J. *J. Am. Chem. Soc.* **2013**, *135*, 474−487.

[51] Brak, K.; Ellman, J. A. *Org. Lett.* **2010**, *12*, 2004-2007.

[52] Grob, J. E.; Dechantsreiter, M. A.; Tichkule, R. B.; Connolly, M. K.; Honda, A.; Tomlinson, R. C.; Hamann, L. G. *Org. Lett.* **2012**, *14*, 5578-5581.

[53] (a) Imao, D.; Glasspoole, B. W.; Laberge, V. S.; Crudden, C. M. *J. Am. Chem. Soc.* **2009**, *131*, 5024-5025. (b) Awano, T.; Ohmura, T.; Suginome, M. *J. Am. Chem. Soc.* **2011**, *133*, 20738–20741. (c) Wilsily, A.; Tramutola, F.; Owston, N. A.; Fu, G. C. *J. Am. Chem. Soc.* **2012**, *134*, 5794−5797. (d) Molander, G. A.; Wisniewski, S. R. *J. Am. Chem. Soc.* **2012**, *134*, 16856-16868.

[54] Li, J.; Burke, M. D. *J. Am. Chem. Soc.* **2011**, *133*, 13774-13777.

[55] St. Denis, J. D.; Scully, C. C. G.; Lee, F.; Yudin, A. K. *Org. Lett.* **2014**, *16*, 1338-1341.

[56] Gaich, T.; Baran, P. S. *J. Org. Chem.* **2010**, *75*, 4657-4673.

[57] Trost, B. M. *Science* **1991**, *254*, 1471-1477.

[58] Wender, P. A.; Verma, V. A.; Paxton, T. J.; Pillow, T. H. *Acc. Chem. Res.* **2008**, *41*, 40-49.

[59] Jarvis, L. M. The Year in New Drugs, *C&EN*, p. 10-13, January, 27, 2014.

[60] Hoeprich Jr., P. D. *Nature Biotech.* **1996**, *14*, 1312-1313.

[61] (a) Thayer, A. M. Hands-Off Chemistry, *C&EN*, p. 12-17, November, 26, 2012. (b) Godfrey, G. A.; Masquelin, T.; Hemmerle, H. *Drug Discov. Today* **2013**, *18*, 795-802.

CHAPTER 2
TOTAL SYNTHESIS OF SYNECHOXANTHIN VIA REVERSED-POLARITY ITERATIVE CROSS-COUPLING

ABSTRACT

Deficiencies of human proteins that protect cells from lipid peroxidation have been linked to many prevalent diseases, including atherosclerosis, neurodegenerative disorders, and cancer. Remarkably, some species of bacteria have the ability to thrive in environments of extreme oxidative stress, which has been attributed to the presence of specialized carotenoids in their membranes. These natural products might therefore serve as valuable prototypes for understanding and optimizing the capacity for small molecules to serve as antilipoperoxidants in human cells. In this vein, a structurally unique aromatic dicarboxylate carotenoid, synechoxanthin, was isolated in 2008 from the exceptionally reactive oxygen species (ROS)-resistant cyanobacterium *Synechococcus*. With the ultimate goal of understanding and optimizing the promising antioxidant activity of this natural product, we herein report its first total synthesis. This synthesis was achieved using only one reaction iteratively to assemble three simple and readily accessible building blocks in a completely stereocontrolled fashion. This route was enabled by a novel Reversed-Polarity Iterative Cross-Coupling (RP-ICC) strategy, in which the polarity of the bifunctional building blocks is reversed to match the preferred polarity for Suzuki-Miyaura cross-coupling. Moreover, a final one-pot two-directional double cross-coupling sequence enabled rapid assembly of the C_2-symmetric carotenoid core. This convergent approach also enabled a total synthesis of renierapurpurin, a biosynthetic precursor to synechoxanthin. With synechoxanthin in hand, the antilipoperoxidant activity of synechoxanthin was evaluated in comparison to β-carotene and the carotenoid gold standard astaxanthin. Synechoxanthin demonstrated equally effective antilipoperoxidant activity compared to astaxanthin in an *in vitro* chemically defined liposome system. This preliminary result demonstrates the potential for synechoxanthin to serve as an antilipoperoxidant and as a probe to interrogate the still poorly understood mechanism of lipid peroxidation. The efficient, completely stereocontrolled, and inherently flexible nature of this building block-based pathway has opened the door to systematic studies of the antioxidant functions of synechoxanthin and its derivatives.

Stephanie Y. Chang contributed to the total synthesis of synechoxanthin, specifically by assisting with the synthesis and characterization of building blocks **2.17**, **2.32**, and **2.26**. Hannah M. S. Haley contributed to the optimization of the chemically-defined TBARS assay, originally developed by Dr. Eric M. Woerly, and control experiments with β-carotene and astaxanthin, in addition to completing the total synthesis of renierapurpurin.

Portions of this chapter are adapted from Fujii, S.; Chang, S. Y.; Burke, M. D. *Angew*. *Chem*. *Int*. *Ed*. **2011**, *50*, 7862-7864.

2-1 CAROTENOID NATURAL PRODUCTS ARE PROMISING ANTILIPOPEROXIDANTS

Lipid peroxidation is a naturally occurring physiological process that plays an important role in aerobic metabolism.[1] However, lipids containing polyunsaturated fatty acids (PUFAs) are primary targets for attack by reactive oxygen species (ROS), and this autooxidation process can cause or exacerbate diseases of inflammation.[2] Although the underlying connection between lipid peroxidation and the development of human diseases is still not well understood, it is known that lipid peroxidation affords several toxic electrophiles that can alkylate DNA or proteins.[3] Fortunately, there are a number of proteins in the body that protect humans from the deleterious effects of lipid peroxidation.[4] As further evidence indicating the importance of attenuating lipid peroxidation, deficiencies of such proteins have been linked to the molecular pathophysiology of many prevalent diseases such as atherosclerosis,[5] cancer,[6] rheumatoid arthritis,[7] and may also contribute to an accelerated aging process.[8] Given the deleterious impact these diseases have on human health, the potential health benefit of small molecule antilipoperoxidants is exceptional. Small molecules that can safely and effectively replicate this antilipoperoxidant function can, in theory, serve as substitutes for these missing or dysfunctional proteins, thereby operating as prostheses on a molecular scale.

In recent years, carotenoid natural products have received tremendous attention as one of the most promising classes of small molecule antilipoperoxidants.[9] Carotenoids are tetraterpenoid molecules that are naturally produced in chloroplasts and chromoplasts of plants and photosynthetic organisms such as plants, protists, bacteria, and fungi. The highly conjugated polyene core of a carotenoid is mainly responsible for the bright colors present in many fruits, vegetables, and fish. Among these carotenoid natural products, β-carotene (**2.1**, Figure 2-1) is perhaps one of the most well studied, yet *in vitro* as well as *in vivo* studies demonstrate that its antioxidant activity remain unclear and controversial.[10] In fact, one clinical trial was interrupted because the study showed that large doses of β-carotene in combination with vitamin A increased the incidence of lung cancer in smokers by 28%.[11] In contrast, astaxanthin (**2.2**, Figure 2-1) is considered the "gold standard" antilipoperoxidant,[12] and is available as a dietary supplement, generating $200 million in sales per year.[13] In addition, an astaxanthin derivative has shown promise as a cardioprotective agent in preclinical trials for the treatment of ischemia and reperfusion injuries[14] and atherosclerosis.[15]

However, due to the proposed stoichiometric reactivity of typical carotenoids through free radical scavenging,[16] the protective capability of astaxanthin is inherently limited.[17] Free radical scavenging is initially effective because carotenoids can react in a stoichiometric fashion with ROS and thereby eliminate these potential peroxidants from the lipid membrane.[18] Eventally, however, the carotenoid is consumed to form breakdown products that may even promote lipoperoxidation.[19] In fact, it has been shown that high molar ratios of astaxanthin (>5% of total lipid content) are generally required to achieve substantial antilipoperoxidant activity in an *in vitro* assay.[17]

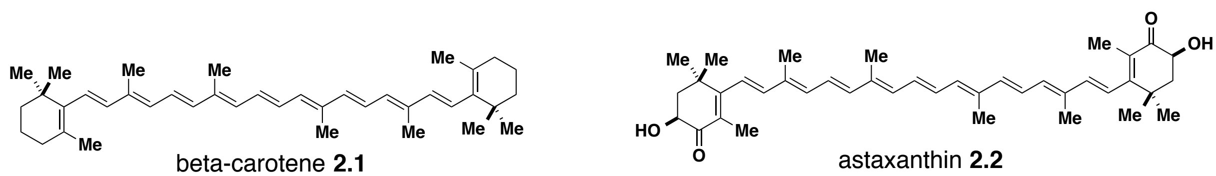

beta-carotene **2.1** astaxanthin **2.2**

Figure 2-1. Carotenoid natural products β-carotene and astaxanthin.

Alternate mechanisms for antilipoperoxidation such as catalytic ROS quenching[20] or modulation of membrane dynamics[21] have been proposed. These mechanisms have an advantage over stoichiometric antilipoperoxidation of carotenoids because it does not result in the consumption of the carotenoid. However, the lack of direct evidence regarding these mechanisms and limited access to non-commerial carotenoids have precluded the rational optimization of the antilipoperoxidant activity of common carotenoids, including astaxanthin.

2-2 AROMATIC CAROTENOIDS SHOW PROMISE AS ANTILIPOPEROXIDANTS

These studies suggest that one possible approach to increase the antilipoperoxidant activity and lifetime of a carotenoid would be to diminish the stoichiometric reactivity of the carotenoid toward reactions with electrophilic oxidants by increasing its stability. Thus, in order to guide our search for small molecules that possess exceptional stability yet maintain the capacity for antilipoperoxidant activity via catalytic quenching, we became intrigued by atypical carotenoids with aromatic functionality.

Carotenoids with aromatic termini have shown exceptional stability, such as isorenieratene (**2.3**, Fig 2-2), which was found intact in carbonates of the 1.6 billion year old Barney Creek Formation in Australia.[22] In addition, 3,3'-dihydroxyisorenieratene (3,3'-DHIR) (**2.4**, Fig 2-2),

also an aromatic carotenoid, was shown to have superior antilipoperoxidant activity compared to non-aromatic carotenoids.[23] A recent study showed that both of these aromatic carotenoids prevented UV-induced DNA damage in human skin fibroblast cells and showed reduced levels of lipid peroxidation in a liposome-based assay.[24] Although it has been demonstrated that aromatic polyenes have increased chemical stability over their non-aryl-substituted counterparts in solution-phase experiments,[25] the stabilizing effect of an aromatic terminus on the overall reactivity of the carotenoid has not yet been directly tested in a lipoperoxidation assay.

In addition to the aromatic functionality of some carotenoids, we also questioned whether polarity has an effect on antilipoperoxidant activity of the carotenoid. A leading model suggests that non-polar carotenoids align perpendicular to the bilayer normal, thus disrupting the membrane alignment and promoting lipoperoxidation.[26] In contrast, polar carotenoids are predicted to favor a parallel alignment in the lipid bilayer, thereby stabilizing the membrane and decreasing its permeability to ROS.[26] With this logic, 3,3'-DHIR shows promise as an exceptional antilipoperoxidant. However, 3,3'-DHIR has been shown to oxidize to the quinone leading to the destruction of the carotenoid in a cumene hydroperoxide inhibition assay.[23] Thus, although these studies are promising, they suggest that an ideal carotenoid antilipoperoxidant would possess polar termini that cannot be further oxidized.

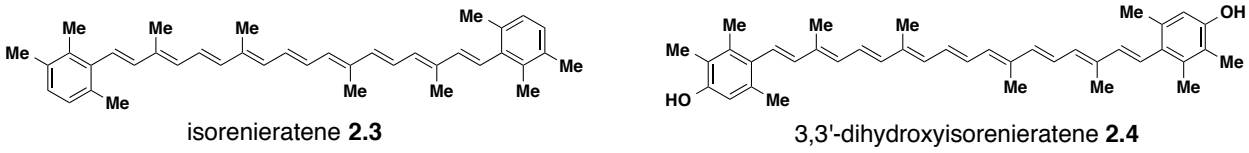

isorenieratene **2.3** 3,3'-dihydroxyisorenieratene **2.4**

Figure 2-2. Apolar aromatic carotenoid natural products isorenieratene and 3,3'-dihydroxyisorenieratene.

2-3 SYNECHOXANTHIN: A CAROTENOID NATURAL PRODUCT PRODUCED IN AN ORGANISM THAT THRIVES IN ENVIRONMENTS OF HIGH OXIDATIVE STRESS

We therefore turned our attention to carotenoids produced by organisms that thrive in environments of extreme oxidative stress[27] that ideally possess aromatic termini with polar functional group appendages that cannot be easily oxidized. We hypothesized that these natural products might serve as valuable prototypes for understanding and optimizing the capacity for small molecules to serve as powerful antilipoperoxidants in human cells.

In this vein, a structurally unique aromatic dicarboxylate carotenoid, synechoxanthin (**2.6**, Scheme 2-1), was isolated in 2008 from the exceptionally ROS-resistant cyanobacterium *Synechococcus* sp. strain PCC 7002.[28] This strain of cyanobacteria is known to be remarkably tolerant to light-intense environments,[29] and a higher level of synechoxanthin was isolated from this strain compared to other cyanobacteria. We were intrigued by the unique chemical features of synechoxanthin, specifically its aromatic termini and biscarboxylic acid appendages. Specifically, we hypothesized that the carboxylic acid appendages might perform the dual functions of 1) reinforcing parallel alignment of synechoxanthin to the bilayer normal and 2) decreasing the nucleophilicity of the polyene toward stoichiometric reactions with electrophillic oxidants. In fact, studies have shown that electron-withdrawing groups in close proximity to the double bond decreases the reactivity of the olefin toward peroxy acids.[30]

Moreover, a recent study reported that knocking out synechoxanthin via genetic manipulation of the cyanobacterial biosynthetic machinery diminished the ROS resistance, indicating that this natural product may help protect the cyanobacterium from oxidative stress.[31] Furthermore, it was recently reported that a series of enzyme-mediated modifications of the terminal rings of β-carotene transform this typical carotenoid into synechoxanthin (Scheme 2-1).[32] It is proposed that the *cru*E gene encodes β-ring desaturase/methyltransferase enzymes to afford renierapurpurin (**2.5**), and the *cru*H gene is involved in the initial oxidation of renierapurpurin at the C-18 and C-18' positions.[32] This proposed biosynthesis outlines a unique transformation from an apolar non-aromatic carotenoid, to renierapurpurin, an apolar aromatic carotenoid, to synechoxanthin, a polar aromatic carotenoid (Scheme 2-1). As described earlier in this Chapter, the antiliperoxidant activity of β-carotene has been controversial, and the antilipoperoxidant activities of the latter two carotenoids have not been systematically investigated to date. Thus, these carotenoids serve as excellent probes to interrogate the impact of these tailoring enzyme modifications on carotenoid antilipoperoxidant activities.

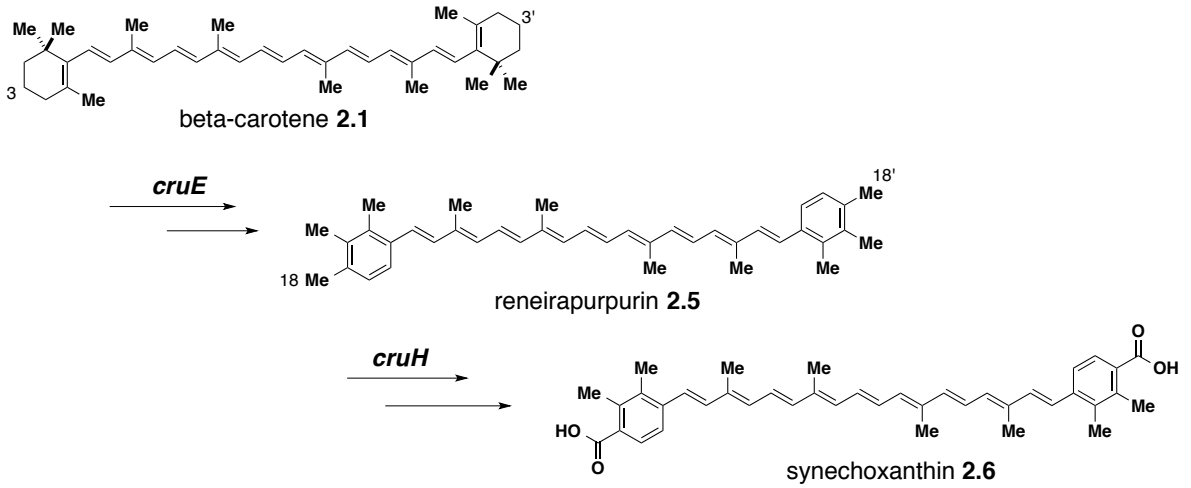

Scheme 2-1. Proposed biosynthetic pathway from β-carotene to synechoxanthin.

2-4 TOTAL SYNTHESIS OF C_2-SYMMETRIC CAROTENOIDS

In order to systematically compare the antilipoperoxidant activity of synechoxanthin to its biosynthetic precursors as well as to the gold standard astaxanthin, we sought for an efficient and modular approach to access synechoxanthin. In general, isolation of carotenoids from natural sources is inefficient, and does not readily allow derivatization for systematic testing of the above hypotheses. Perhaps due to these reasons, the biological function of synechoxanthin has been minimally explored to date. Obviating the challenges associated with isolating synechoxanthin from the producing organism, we sought to gain access via a fully stereocontrolled total synthesis.

The highly complex nonaene framework found in synechoxanthin and many other C_2-symmetric carotenoids represents a substantial structural and stereochemical challenge. One of the most commonly employed strategies to access this motif involves carbonyl condensation reactions. For example, retrosynthesis of the polyene core via a double Wittig olefination to a C_{10}-trienedialdehyde and two C_{15}-polyenylphosphonate salts is a common method (Scheme **2-2**).[33]

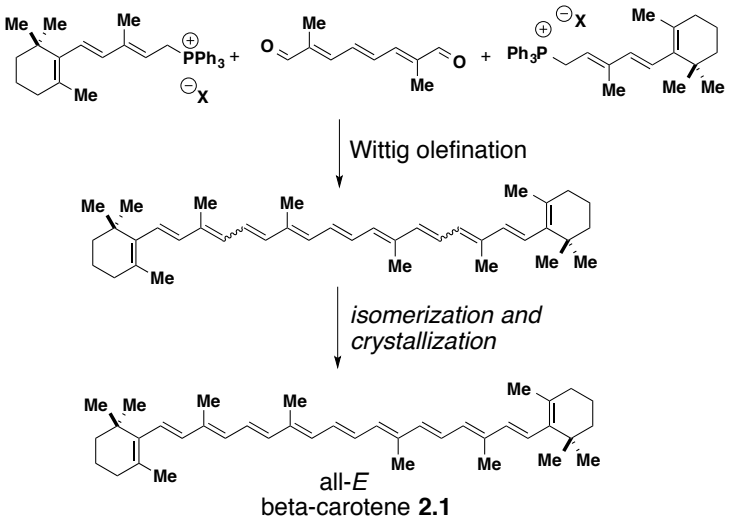

Scheme 2-2. Commonly employed double Wittig olefination approach toward C_2-symmetric carotenoids.

Two advantages of this route include the utilization of carotenoid symmetry in which only two building blocks are required, and high yields that are achieved on the key Wittig olefination step. However, one of the main challenges of this approach is the lack of stereocontrol, which results in a mixture of *cis* and *trans* isomers that must be thermally isomerized followed by tedious and carotenoid-specific crystallizations to form the all-*E* isomer.[33] In some cases, unprotected polar functional groups are not compatible with this approach; thus a different protecting group strategy may be needed for each polar carotenoid. Although this strategy has been extensively applied to the industrial synthesis of several C_2-symmetric carotenoids, this approach is not ideal when the goal is to prepare many polar derivatives as single stereoisomers.[33]

Another convergent approach that has been applied to the synthesis of C_2-symmetric carotenoids is through a homodimerization reaction. McMurry carbonyl coupling has been used to synthesize β-carotene and isorenieratene (Scheme 2-3).[34] In addition, olefin metathesis has been employed in the construction of several carotenoids, including β-carotene, zeaxanthin, and violaxanthin (Scheme 2-3).[35] These methods offer the advantage of only requiring one functionalized fragment that can be transformed to the target in one step. However, since a stereoselective bond-forming reaction is used, carefully optimized conditions are necessary, especially for the olefin metathesis method, to avoid the formation of several side products resulting from competitive metathesis side reactions.[35]

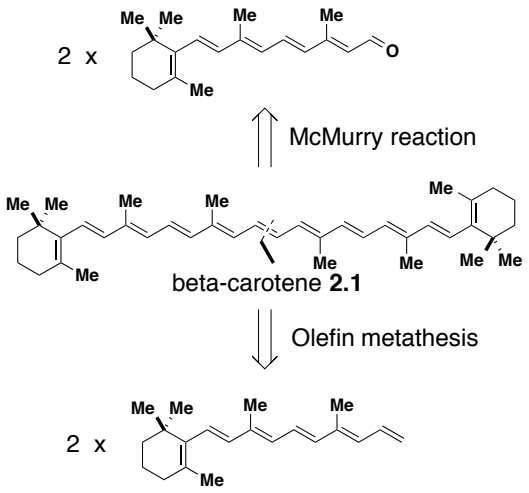

Scheme 2-3. Homodimerization approach toward C_2-symmetric carotenoids.

Recently, palladium-catalyzed cross-coupling reactions have received much attention for their utility in constructing polyenes because the key C-C bonds can be constructed in a stereospecific manner. Several notable examples include the iterative carbometalation/metal-exchange/Negishi approach and the two-fold Stille method.[36] Negishi and co-workers have reported the synthesis of both symmetrical and unsymmetrical carotenoids, β-carotene and γ-carotene, using the former method.[37] Specifically, dienyne **2.8**, a bifunctional building block containing a vinyl bromide and a protected alkyne, is coupled to an organozinc intermediate (that is synthesized from **2.7**) using a stereospecific palladium-catalyzed cross-coupling reaction. Removal of the alkyne protecting group reveals a terminal alkyne **2.9**, regenerating the functionality needed for another carboalumination/cross-coupling cycle (Scheme 2-4).[37] (*E*)-1-bromo-2-iodoethene (**2.10**) was used as a key two-carbon synthon to couple the organozinc reagents to complete the synthesis of β-carotene in 41% overall yield. While this method provided all-*E* carotenoids without the need for cystallizations or isomerizations, the functional group compatibility of the carboalumination reaction has limited the application of this method to apolar carotenoids.[37]

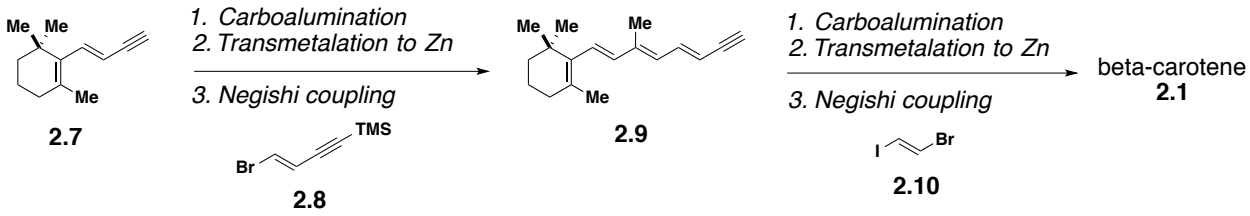

Scheme 2-4. Synthesis of β-carotene by an iterative carbometalation/metal exchange/Negishi reaction.

The two-fold Stille coupling approach, developed by de Lera and co-workers, was applied to the synthesis of β-carotene and zeaxanthin (Scheme 2-5).[38] This methodology provides an efficient preparation of these carotenoids by constructing the polyene core using a double Stille coupling to a central pentenyl bisstannane building block **2.11**. However, the synthesis of **2.11** utilized a Julia olefination reaction and resulted in a mixture of isomers.[38] As a result, this strategy does not provide a completely stereocontrolled synthesis of these carotenoids.

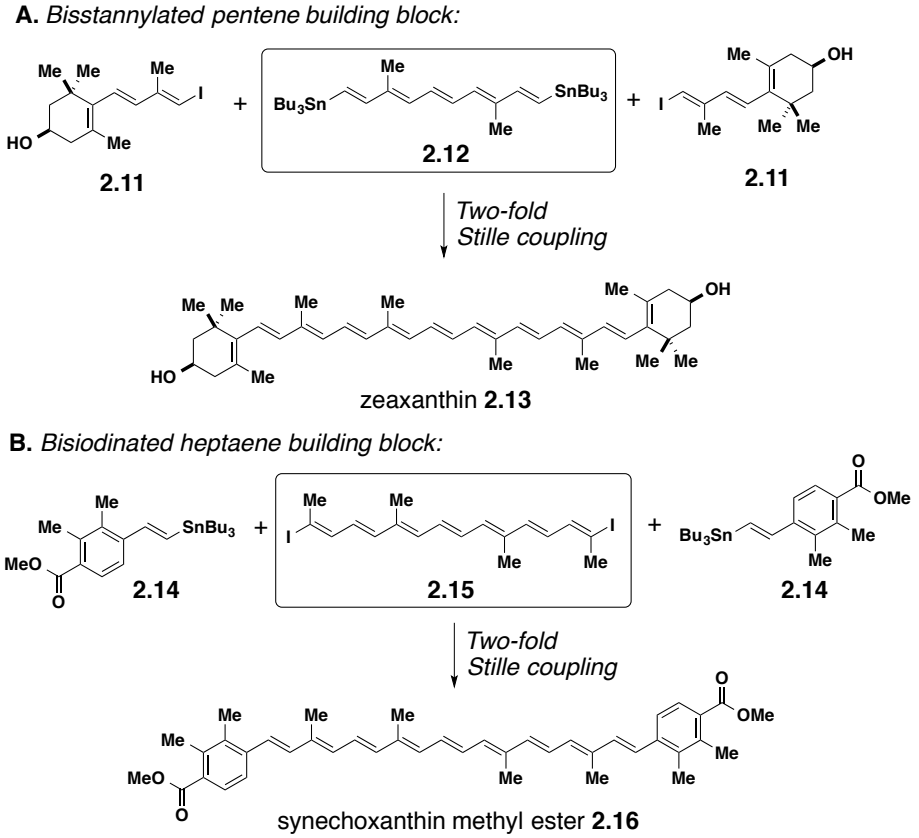

Scheme 2-5. Two-fold Stille coupling approach toward the synthesis of zeaxanthin and synechoxanthin methyl ester.

As an extension to this approach, de Lera and co-workers recently employed a C_{18} diiodoheptaene **2.15** to synthesize several C_2-symmetric carotenoids, including β-carotene, lycopene, and synechoxanthin methyl ester either through Suzuki-Miyaura or Stille cross-coupling reactions (Scheme 2-5).[39] For example, synechoxanthin methyl ester **2.16** was synthesized in 79% from vinyl stannane **2.14** and diiodoheptaene **2.15** via a two-fold Stille coupling. The advantage of this approach is the rapid construction of the carotenoid skeleton utilizing a common polyene core. For this reason, this strategy is most beneficial for accessing carotenoids that have greater than nine conjugated double bonds. However, this comes with a major limitation in that key building block **2.15** readily isomerizes to the di-*cis*-isomer upon exposure to light or heat, making it an unstable fragment incompatible for long-term storage.

2-5 RETROSYNTHESIS OF SYNECHOXANTHIN VIA ITERATIVE CROSS-COUPLING

In contrast to these common methods, the use of only stereospecific cross-coupling reactions to assemble stable, stereochemically defined polyene building blocks represents a very attractive alternative. Ideally, these building blocks would be readily accessible, non-toxic, and very stable to long-term storage. We thus aimed to synthesize carotenoid natural products using an efficient, modular, and flexible synthetic strategy using only stable building blocks and stereospecific reactions to construct the polyene core. Iterative cross-coupling (ICC)[40] introduced in Chapter 1 offers an attractive, alternate approach towards the construction of small molecules in this manner. In this ICC approach, polar functional groups are tolerated, modularity and flexibility for derivatization are introduced, and the issue of stereocontrol is addressed by the stereospecific Suzuki-Miyaura cross-coupling of bifunctional haloboronic acid building blocks protected as the corresponding *N*-methyliminodiacetic acid (MIDA) boronate esters.[41] Because these building blocks contain preinstalled functionality and stereochemistry required in the target molecule, this approach requires no post-coupling modifications aside from global deprotections. Prior to this work, ICC has enabled the construction of many polyene-containing small molecules including the following: one-half of the polyene macrolide amphotericin B,[25] all *trans*-retinal,[25] β-paranaric acid,[42] and the polyene core of vacidin A.[43] Furthermore, a total synthesis of carotenoid natural product (-)-peridinin was achieved in a fully stereocontrolled manner via ICC one year prior to the completion of this work.[44]

Taking advantage of the C_2-symmetry of synechoxanthin, we envisioned this natural product could be synthesized using a convergent building block approach and the ICC methodology. Synechoxanthin was retrosynthesized in a manner that would be maximally amenable to derivative synthesis (Scheme 2-6). One retrosynthesis suggested that synechoxanthin can come from three different building blocks that can be assembled via an "outside-in" or an "inside-out" approach (Scheme 2-6). A method that allows assembly of the polyene core later in the route, i.e. the outside-in approach, is attractive because this avoids the need to purify, isolate, and carry forward the sensitive polyene functionality through multiple reactions.[45] The longest polyene intermediate formed via this outside-in strategy would be a tetraene, which is less susceptible to decomposition or isomerization than the longest polyene intermediate that would be formed via an inside-out approach (Scheme 2-6).[45]

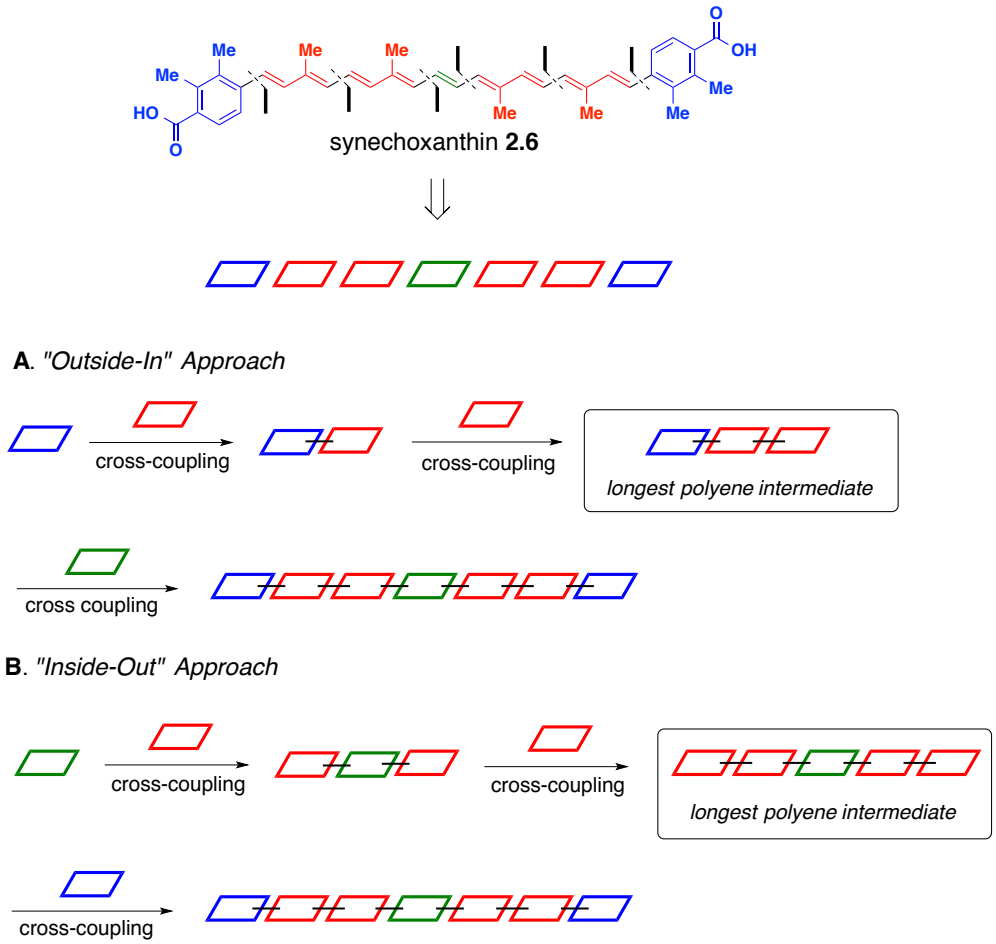

Scheme 2-6. A. "Outside-in" approach toward the synthesis of C_2-symmertric small molecules. **B.** "Inside-out" approach toward the synthesis of C_2-symmertric small molecules.

Guided by this established ICC strategy, we applied only Suzuki-Miyaura transforms to retrosynthesize synechoxanthin into three readily accessible building blocks (**2.17, 2.18**, and **2.10**) having all of the required functionality preinstalled in the correct oxidation states and with the desired stereochemical relationships (Scheme 2-7). In the final step, we anticipated a convergent two-directional Suzuki-Miyaura coupling with lynchpin building block **2.10** to complete the assembly of the polyene core.

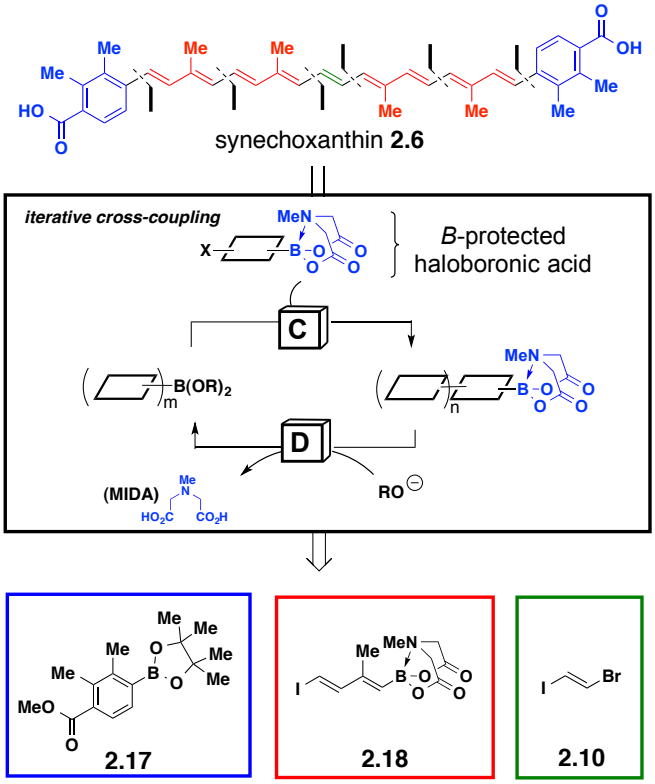

Scheme 2-7. Retrosynthetic analysis of synechoxanthin via ICC (m = n + 1). [C] = coupling, [D] = deprotection.

The synthesis of building block **2.17** commenced with electrophilic aromatic substitution on commercially available phenol **2.19** using *N*-bromosuccinimide to afford aryl bromide **2.20** (Scheme 2-8).[46] MOM protection of phenol **2.20** afforded aryl bromide **2.21** in 85% yield. Aryl bromide **2.21** was then lithiated and trapped with carbon dioxide to afford benzoic acid **2.22** in moderate yield. Benzoic acid **2.22** was protected as the methyl ester, and the MOM group was deprotected in one pot to afford benzoate **2.23** in 89% yield. Methylation of the acid facilitated the purification and handling of subsequent intermediates, and later allowed a direct comparison

of synechoxanthin methyl ester **2.16** to the structural data reported in the literature. Notably, these reactions required minimal to no purifications and were scalable on gram scale. Triflation of benzoate **2.23** afforded aryl triflate **2.24** in 89% yield. Finally, Miyaura borylation of **2.24** using bispinacolatodiboron achieved the synthesis of building block **2.17** in 90% yield (Scheme 2-8).

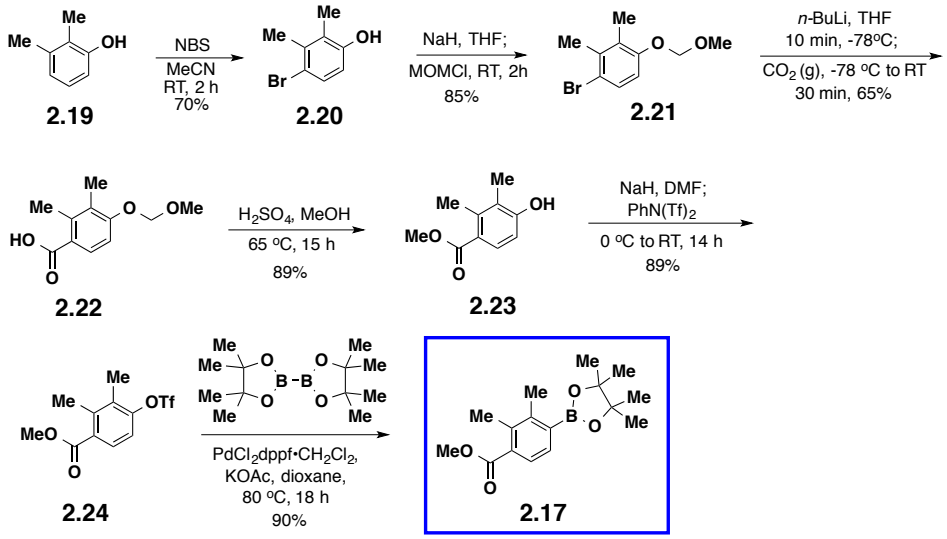

Scheme 2-8. Synthesis of building block **2.17**.

Synthesis of bifunctional building block **2.18** was accomplished by applying the methodology recently developed in our laboratories for the metal-selective coupling of bismetalated olefin **2.27**.[23] First, vinyl stannane **2.25** underwent highly regio- and stereocontrolled iododestannylation to afford vinyl iodide **2.26** in 75% yield. The *trans* relationship of the iodine to the MIDA boronate was confirmed by X-ray crystallography (Scheme 2-9). Vinyl iodide **2.26** was coupled to **2.27** under standard Stille coupling conditions to afford dienyl germane **2.28** in 86% yield. Iododegermylation of **2.28** afforded building block **2.18** in 83% yield.

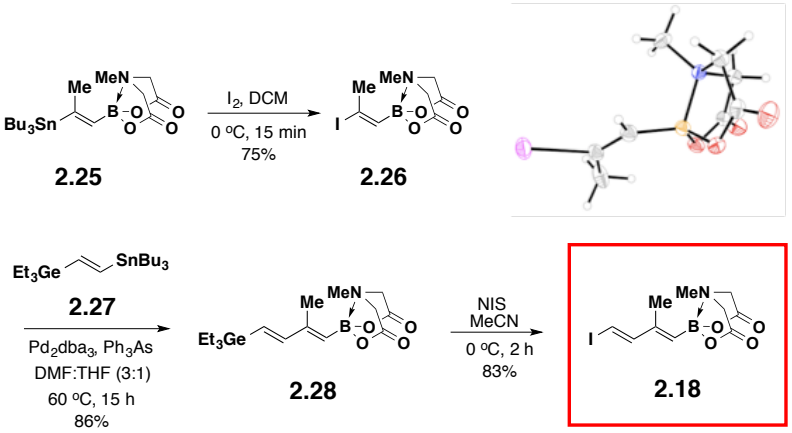

Scheme 2-9. Synthesis of building block **2.18**.

With the first two building blocks in hand, we targeted the synthesis of tetraenyl MIDA boronate **2.31**. Suzuki-Miyaura cross-coupling of **2.17** with halodienyl MIDA boronate **2.18** produced dienyl MIDA boronate **2.29** in 60% yield as a single stereoisomer under optimized conditions (Scheme 2-10). Subsequent transesterification of MIDA boronate **2.29** with pinacol[44] revealed the sp^2-hybridized pinacol boronic ester **2.30** in 92% yield. Pinacol boronic ester **2.30** was subsequently coupled to another equivalent of bifunctional building block **2.18** to provide the key tetraene MIDA boronate **2.31** in a modest 50% yield, but again with complete stereocontrol. In addition to providing very modular and completely stereocontrolled access to key intermediate **2.31**, this route revealed that polyenyl MIDA boronates **2.18**, **2.29**, **2.30** and **2.31** are crystalline solids that are fully compatible with silica gel chromatography and long-term storage. However, the overall yield of **2.31** over this three-step sequence was only 28%, despite extensive optimization of these conditions. We therefore sought to retain the highly favorable features of this ICC-based pathway, but gain more efficient access to this key tetraenyl MIDA boronate intermediate.

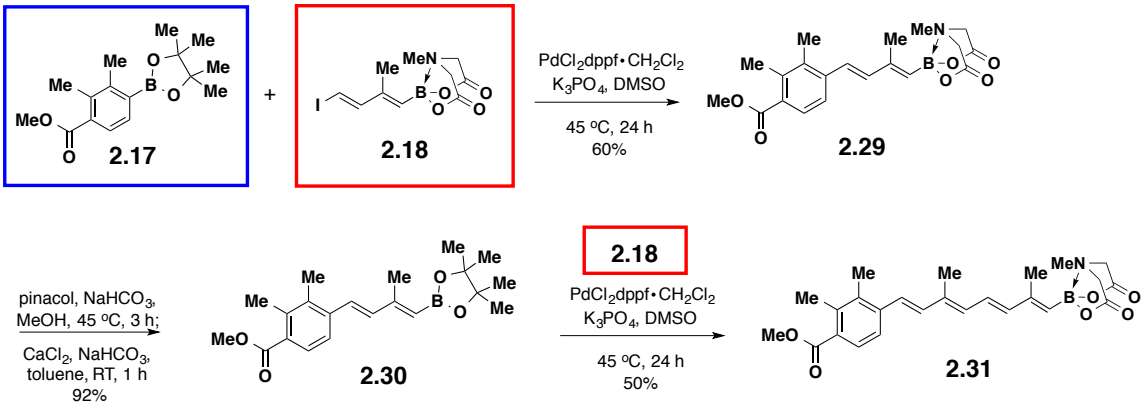

Scheme 2-10. Synthesis of tetraene MIDA boronate intermediate **2.31**.

2-6 RETROSYNTHESIS OF SYNECHOXANTHIN VIA RP-ICC

We hypothesized that these modest yields observed in the ICC pathway may be attributable to a polarity mismatch between the building blocks and the inherent polarity preference for Suzuki-Miyaura cross-coupling.[47] In cross-coupling, the organoboron species generally serves as the nucleophile and the halide represents the electrophile (Scheme 2-11A).[48] Therefore, electron-donating functional groups that enhance the nucleophilicity of the organoboron species and electron-withdrawing functional groups that enhance the electrophilicity of the halide both increase the reactivity between the two coupling partners. In fact, Monteiro and co-workers conducted competitive Suzuki-Miyaura cross-coupling experiments surveying a variety of aryl halides with electronically different *para*-substituents and observed that electron-withdrawing substituents on the aryl halide increase the rate of oxidative addition through a Hammett analysis ($\rho = 2.3$).[49] On the other hand, electron-donating *para*-substituents on the arylboronic acid was correlated to the increase in the rate of the reaction with bromobenzene ($\rho = -0.68$).[49]

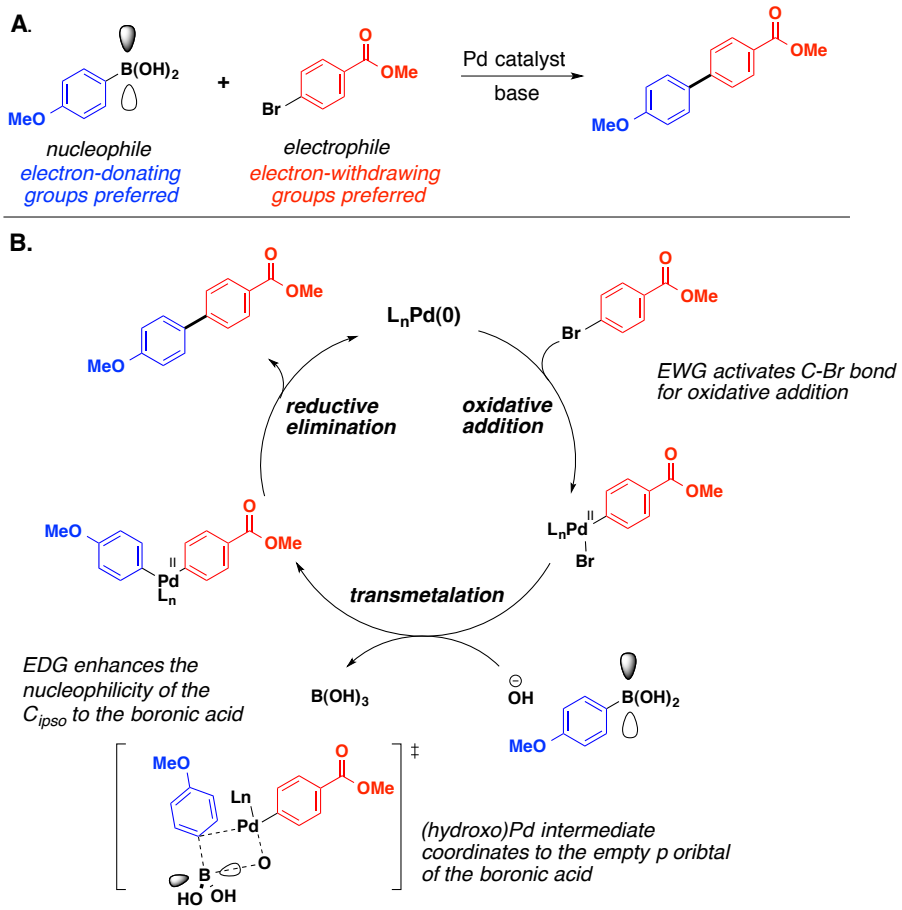

Scheme 2-11. A. Electronic preference in Suzuki-Miyaura cross-coupling. **B.** Example catalytic cycle of Suzuki-Miyaura cross-coupling. EDG = electron-donating group, EWG = electron-withdrawing group.

In the case for building blocks retrosynthesized for synechoxanthin via ICC (Scheme 2-7), due to conjugation with the electron-withdrawing methyl ester substituent at the *para*-position of the aryl ring, **2.17** and **2.30** represent electron-deficient boronic esters that are poor cross-coupling substrates in Suzuki-Miyaura cross-coupling.[50] Specifically, electron-poor arylboronic acids are less nucleophilic and undergo transmetalation at a slower rate than electron-neutral and -rich arylboronic acids, and are more susceptible to base and metal-catalyzed protodeboronation[51] and homocoupling (Scheme 2-11B).[52] In contrast, aryl halides and alkenyl halides with proximal electron-withdrawing groups are more activated toward oxidative addition than those with donating groups, making electron-deficient halides superior substrates, often cross-coupling under milder conditions and/or in higher yields than their electron-neutral and -rich counterparts (Scheme 2-11B).[53]

In this vein, we were interested in probing whether the MIDA boronate functional group serves as an electron-donor or an electron-acceptor. To test this, we performed a simple NMR experiment surveying a range of monosubstituted benzenes along with phenyl MIDA boronate to determine the chemical shift at the para position, since ^{13}C chemical shifts at the *para* position of mono-substituted benzenes have been correlated with chemical reactivity parameters.[54] The following ^{13}C chemical shifts suggested that the MIDA boronate group is neither electron-withdrawing or donating (Figure 2-3).

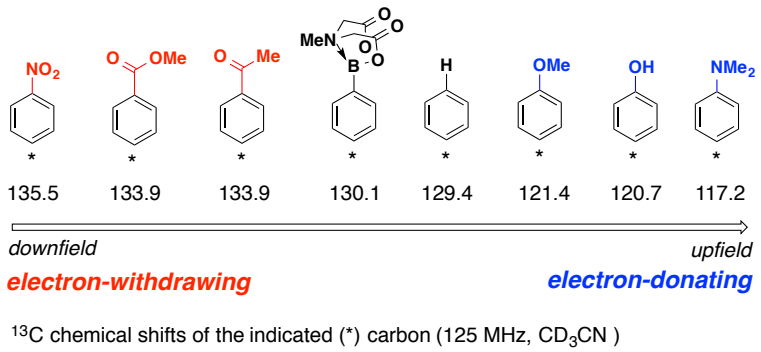

^{13}C chemical shifts of the indicated (*) carbon (125 MHz, CD_3CN)

Figure 2-3. ^{13}C chemical shifts suggest that the MIDA boronate functional group is neither electron-withdrawing or donating.

Stimulated by this logic, the inherent electronic preference in Suzuki-Miyaura cross-coupling guided us to alternatively start with an activated organohalide. This switch in polarity required us to also reverse the polarity of the bifunctional building block employed in the ICC sequence. This retrosynthesis led to the following three building blocks: **2.32**, **2.33**, and **2.10** (Scheme 2-12). The next challenge focused on the synthesis of a new type of bifunctional building block, **2.33**, containing a nucleophilic boron terminus and a protected electrophilic halide. However, it was important to first determine the feasibility of this approach on whether the MIDA protecting group can be deprotected under mild conditions to reveal the masked iodide.

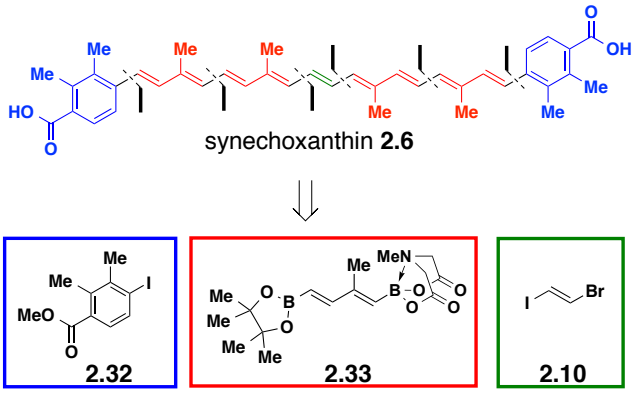

Scheme 2-12. Retrosynthesis of synechoxanthin via polarity reversal of building blocks.

Mild and general methods for halide masking are scarce, but several notable approaches have been developed for iterative synthesis. Moore and co-workers discovered that 1-aryl-3,3-dialkyltriazenes can be employed as a masking group for aryl iodides in the iterative assembly of phenylacetylene oligomers (Scheme 2-13).[55] Oligomer assembly is accomplished using Sonogashira cross-coupling to form Csp^2-Csp bonds. Addition of methyl iodide conveniently transforms the diethyltriazene (N_3Et_2) protecting group to its corresponding iodide for another iteration of Sonogashira cross-coupling (Scheme 2-13).[56]

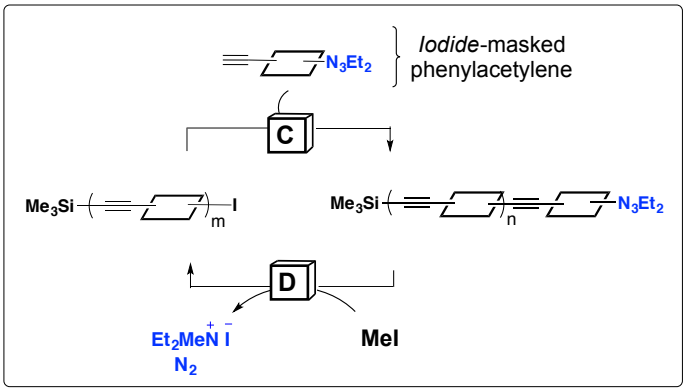

Scheme 2-13. A strategy for the iterative synthesis of phenylacetylene oligomers (m = n + 1) using diethyltriazene protecting group for aryl iodides. [C] = coupling, [D] = deprotection.

In the context of iterative polyene synthesis, Dr. Suk Joong Lee developed a novel strategy for making iodopolyenyl MIDA boronate building blocks by employing triethylgermane ($GeEt_3$) as a protecting group for vinyl iodides (Scheme 2-14).[43] This approach involves a metal-selective

Stille coupling of the bifunctional building block to afford polyenylgermanium intermediates followed by iododegermylation to reveal another polyenyl iodide for a subsequent Stille cross-coupling cycle. [43]

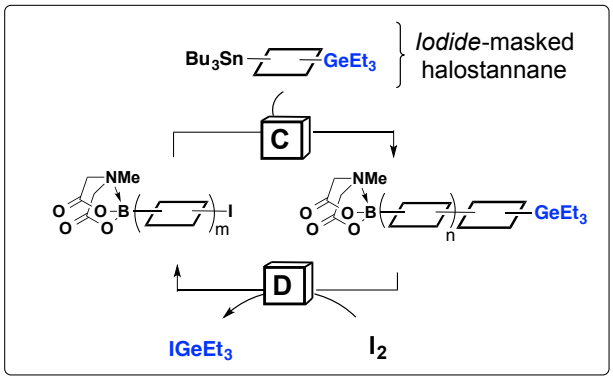

Scheme 2-14. A metal-selective cross-coupling cycle for polyene synthesis (m = n + 1) employing triethylgermane as an iodide protecting group. [C] = coupling, [D] = deprotection.

One example from the literature that was particularly relevant to this work was the report by H. C. Brown and co-workers in which nucleophilic vinylboronic acids were transformed into electrophilic iodides with retention of stereochemistry upon treatment with base and iodine (Scheme 2-15A).[57] Given that MIDA boronates can be hydrolyzed to boronic acids under similar basic conditions, we sought to employ the direct transformation of a MIDA boronate into a halide in one step.

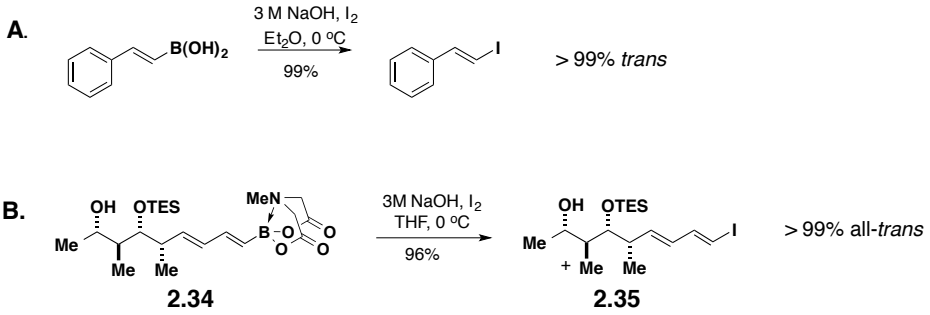

Scheme 2-15. A. Report by H. C. Brown and co-workers showed the transformation of vinyl boronic acids to vinyl iodides can be achieved in one-step. **B.** Dr. Kaitlyn Gray showed that a dienyl MIDA boronate **2.34** can also undergo a one-step transformation to its corresponding dienyl iodide with complete retention of stereochemistry.

In fact, Dr. Kaitlyn Gray showed that vinyl MIDA boronate **2.34** can undergo a one-step, one-pot transformation to its corresponding vinyl iodide **2.35** with retention of stereochemistry using 3M NaOH and I_2 during the synthesis towards the western half of amphotericin B (Scheme 2-15B).[58] Encouraged by this preliminary result, we predicted that the transformation of MIDA boronate **2.33** into a halide intermediate can be readily achieved in a single-pot operation upon treatment with base and iodine.

The capacity of the MIDA boronate to serve as a masked iodide enabled the development of a novel ICC platform termed Reversed-Polarity (RP)-ICC, where an optimal set of building blocks that match the inherent electronic preference present in the target molecule can be used to construct complex small molecules (Scheme 2-16). Specifically, a boron selective Suzuki-Miyaura cross-coupling forms a Csp^2-Csp^2 bond between a halide and a bifunctional building block containing a nucleophilic boron terminus and a masked halide. Although the polarity of the building blocks in RP-ICC are reversed from the original ICC strategy, this approach affords the same MIDA boronate intermediate that would be accessed via the original ICC approach, allowing incorporation of this strategy into the same synthesis platform. Addition of base and iodine reveals another dienyl iodide capable for a subsequent Suzuki-Miyaura cross-coupling.

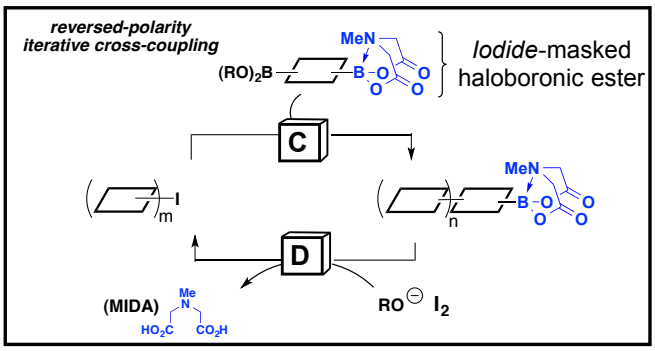

Scheme 2-16. RP-ICC strategy for small molecule synthesis (m = n + 1) employing a bifunctional building block that contains a nucleophilic boronate terminus and a halide terminus masked as the MIDA boronate. [C] = coupling, [D] = deprotection.

Complementary to the original ICC approach where the MIDA boronate masks a reactive boronic acid or a pinacol boronic ester, both nucleophilic reagents, this approach utilizes the MIDA boronate as a halide surrogate, an electrophilic reagent, introducing exceptional flexibility

in synthesis design and providing an opportunity to mix and match appropriate strategies depending on the target small molecule. Furthermore, this strategy expands the scope of ICC to include a larger variety of building blocks. As demonstrated further in section 2-8 and Chapter 3, this strategy can also be beneficial when certain starting materials are more easily accessible than others, not limiting this strategy to be used only to match the inherent electronic preference present in target molecules.

2-7 TOTAL SYNTHESIS OF SYNECHOXANTHIN VIA RP-ICC

The capacity to carry MIDA boronates through multiple chemical transformations[59] enabled facile preparation of key building block **2.33** (Scheme 2-17). Transesterification[44] of MIDA boronate **2.36**[60] afforded bismetalated bifunctional building block **2.37** in quantitative yield. Vinyl iodide **2.26** underwent Stille coupling with stannane **2.37** to achieve the synthesis of **2.33** in 80% yield. ^{11}B NMR analysis was consistent with distinct hybridization states of the two terminal boron atoms (sp^2 and sp^3) in **2.33**, which was confirmed unambiguously via single crystal X-ray analysis (Scheme 2-17). Building block **2.33** proved to be a remarkably stable, crystalline solid that has been stored under air, ambient temperature, and light on the bench top for more than a year without any noticeable decomposition analyzed via a bench-top stability test.[61] This building block, along with vinyl iodide **2.26** are now commercially available from Sigma Aldrich.

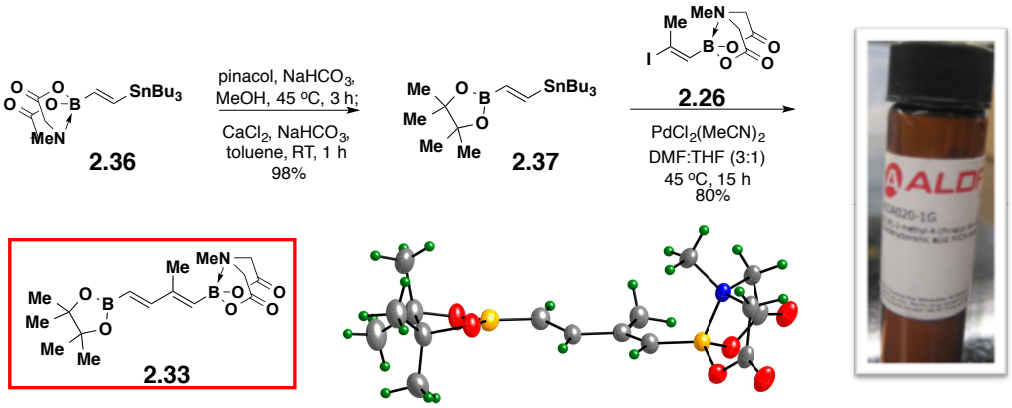

Scheme 2-17. Synthesis of **2.33**, a building block that consists of a nucleophilic Bsp^2 pinacol boronic ester terminus and Bsp^3 MIDA boronate terminus as a masked halide.

Building block **2.32**, now an activated electron-deficient halide, was synthesized in two

steps from aryl triflate intermediate **2.24** synthesized in the previous ICC synthesis pathway (Scheme 2-8). Miyaura borylation of **2.24** afforded neopentylglycol boronic ester **2.38** in 66% yield, and this boronic ester was converted to its corresponding iodide in one-step using choloramine-T and NaI in 76% yield (Scheme 2-18).[62] Building block **2.10** was synthesized in one step using known literature conditions (Scheme 2-19).[63]

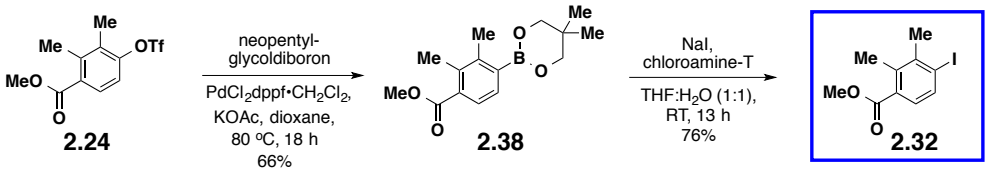

Scheme 2-18. Synthesis of building block **2.32**.

Scheme 2-19. Synthesis of building block **2.10** according to literature procedure.

With this RP-ICC strategy and necessary building blocks in hand, we targeted the iterative Suzuki-Miyaura cross-coupling of the novel bifunctional building block **2.33**. Key to the execution of this plan was the predicted capacity to selectively couple the Bsp^2-hybridized pinacol ester terminus of bisborylated diene **2.33** in the presence of the alternatively Bsp^3-hybridized MIDA boronate unit.[64] Subsequent halodeborylation at the MIDA boronate terminus was anticipated to regenerate a new electron-deficient iodide intermediate, which could undergo another Bsp^2-selective coupling with **2.33** to efficiently build the required tetraene motif **2.31**. As planned, all the cross-couplings required for this pathway involve activated, electron-deficient iodide intermediates.

As expected, Suzuki-Miyaura cross-coupling of activated, electron-deficient aryl iodide **2.32** with the Bsp^2-hybridized terminus of bisborylated building block **2.33** afforded **2.29** in 70% yield as a single stereoisomer (Scheme 2-20). MIDA boronate **2.29** was then halodeborylated in a single-pot operation using NaOMe and I_2 to afford **2.39** in quantitative yield and with complete

retention of stereochemistry, thereby unmasking a new electron-deficient halide for a second iteration of Suzuki-Miyaura cross-coupling. Activated dienyl iodide **2.39** was coupled with another equivalent of **2.33** to afford stereochemically pure tetraenyl MIDA boronate **2.31** in 65% yield. Over this three-step sequence under the same exact cross-coupling conditions, key intermediate **2.31** was synthesized in 45% via the RP-ICC strategy compared to only 28% using the original ICC approach, highlighting the advantage of this strategy.

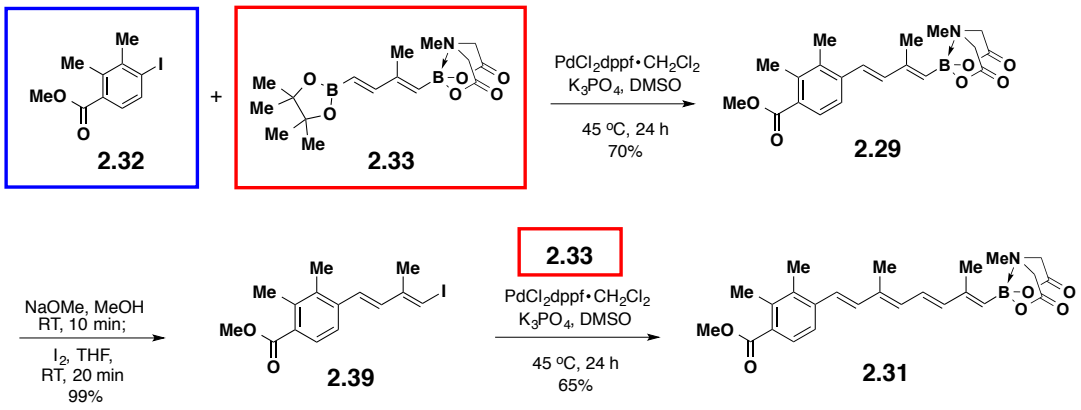

Scheme 2-20. Synthesis of tetraenyl MIDA boronate **2.31** via RP-ICC.

Finally, harnessing the capacity of the versatile MIDA boronate motif to also represent a masked boronic acid which can be released and coupled in situ and thereby obviate the isolation of unstable intermediates,[45] a highly convergent and stereospecific assembly of the complete polyene framework of **2.16** was achieved (Scheme 2-21). Although (*trans*)-1-bromo-2-iodoethylene, **2.10**, has been utilized extensively as a versatile two-carbon synthon in the synthesis of polyene frameworks,[65] to the best of our knowledge, this type of two-directional, one-pot Suzuki-Miyaura coupling represents an unprecedented transformation. The goal for this final coupling was to enable fast-release of the potentially unstable tetraenyl boronic acid from the stable MIDA boronate building block.[61] Specifically, an in situ MIDA boronate hydrolysis followed by two-directional double cross-coupling sequence between two equivalents of **2.31** and electronically activated **2.10** yielded synechoxanthin bismethylester **2.16** with complete stereoretention in an overall very efficient one-pot operation (Scheme 2-21). To the best of our knowledge, **2.16** represented the longest contiguous polyene prepared at the time of the synthesis using Suzuki-Miyaura cross-coupling.

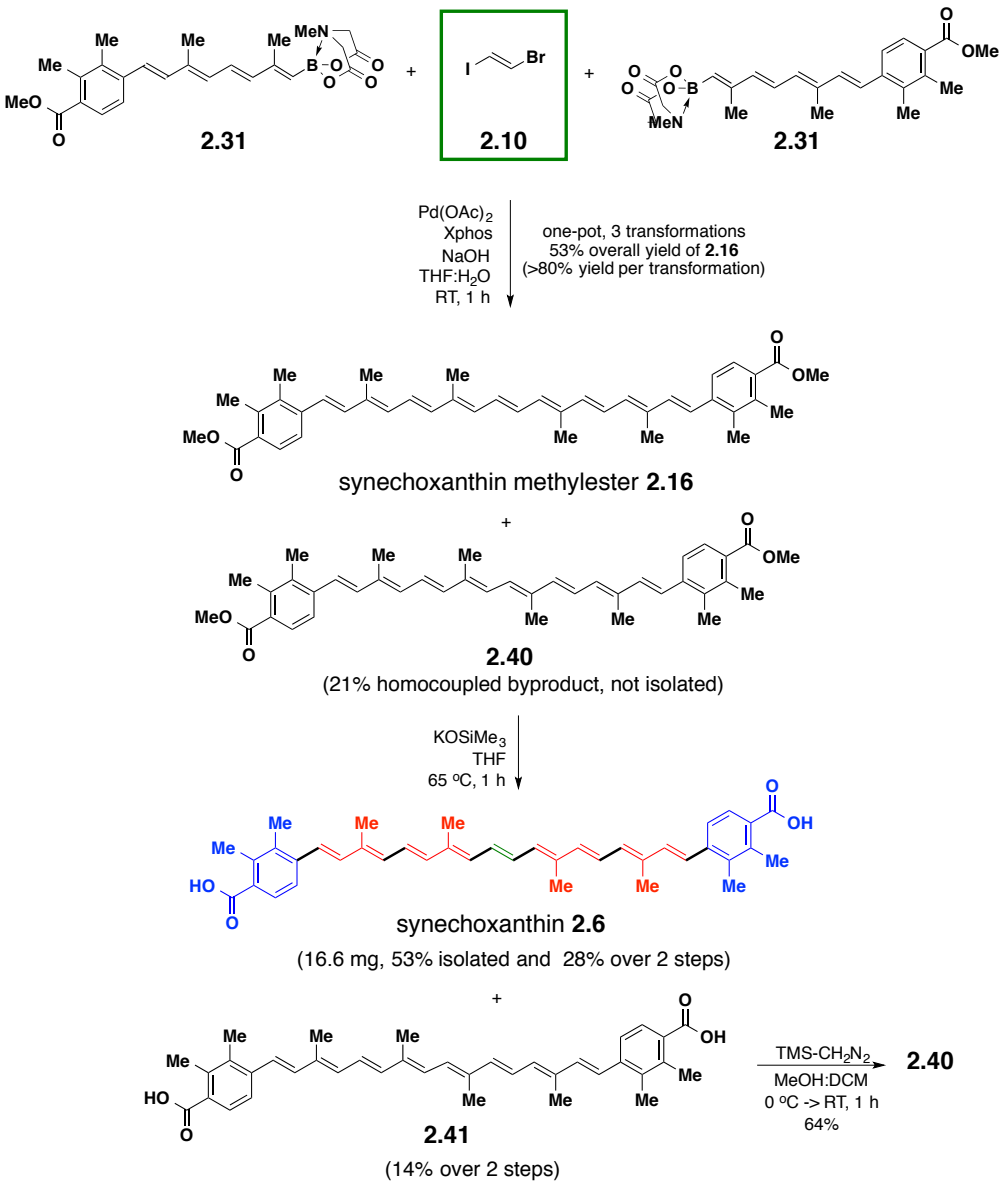

Scheme 2-21. Convergent assembly of synechoxanthin methylester **2.16** followed by global deprotection completed the first total synthesis of synechoxanthin **2.6**.

One final challenge that surfaced during this final C-C bond formation was the identification of byproduct **2.40** resulting from an unproductive homocoupling of two polyenyl boronic acids **2.31**, which could not be separated from **2.16** by silica gel chromatography or reverse-phase HPLC purification (both C-18 and C-8 columns were investigated). We anticipated that carrying forward this mixture to the global deprotection might result in a better separation of the two products. After surveying a variety of methylester deprotection conditions, $KOSiMe_3$ provided clean and rapid conversion to the anhydrous acid salts of synechoxanthin **2.6**

and its octaene derivative **2.41** (Scheme 2-21).[66] Encouragingly, HPLC purification in NH_4OAc buffer achieved a clean separation of these two polyenes to afford **2.6** in 28% over two steps (or 53% in the deprotection step). To confirm that the byproduct produced in the previous step was indeed **2.40**, octaene **2.41** was subjected to methylation using TMS-diazomethane, which unambiguously afforded **2.40** in 64% yield and the characterization of this product matched that of **2.40** (Scheme 2-21). This concluded, to the best of our knowledge, the first total synthesis of synechoxanthin **2.6**. In one run, >15 mg of synechoxanthin was synthesized, providing a roadmap to study the antilipoperoxidant activity of this unique natural product.

2-8 TOTAL SYNTHESIS OF RENIERAPURPURIN

The current route to synechoxanthin allows modification of the core and/or the terminal rings for derivative synthesis simply by substituting modified building blocks into the synthetic pathway. As discussed earlier in this Chapter, in order to understand the impact of the tailoring enzyme modifications on β-carotene to afford synechoxanthin (Scheme 2-1),[28] we next targeted the preparation of the apolar intermediate renierapurpurin **2.5**. This was accomplished by replacing building block **2.32** with building block **2.42**, which now contains a methyl group instead of a methyl ester at the *para* position (Scheme 2-22). The reason for choosing the first building block as a halide instead of a boronic ester was governed by the quick accessibility of this building block, which was synthesized in one step using a literature procedure.[67]

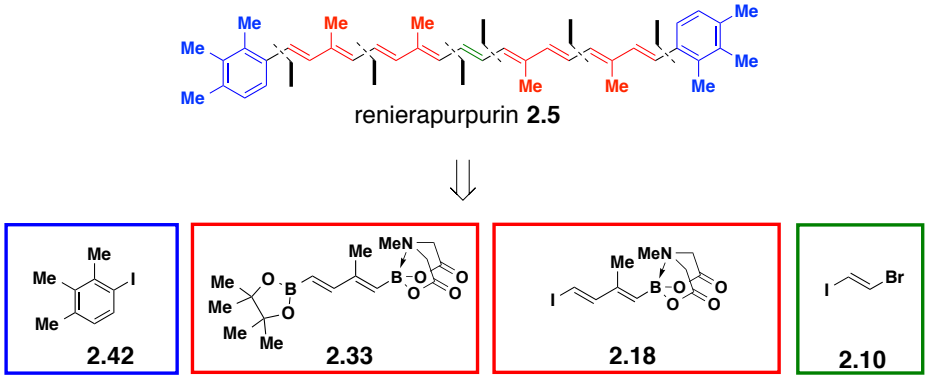

Scheme 2-22. Retrosynthesis of renierapurpurin **2.5** via both RP-ICC and ICC where only the terminal building block **2.42** required development.

The synthesis commenced with the coupling of the capping aryl iodide **2.42** to the reactive pinacol boronic ester terminus of building block **2.33**, which encouragingly afforded dienyl MIDA boronate **2.43** in 70% yield (Scheme 2-23). Mirroring the synthesis of synechoxanthin, halodeborylation of MIDA boronate **2.43** was attempted to unmask a new electrophilic halide for a second iteration of Suzuki-Miyaura cross-coupling to **2.33**. Unexpectedly, exposure of **2.43** to I_2 and base (NaOH or NaOMe) consistently resulted in an inseparable mixture of byproducts. Fortunately, because this retrosynthesis is flexible, we turned our attention to converting MIDA boronate **2.43** to a pinacol boronic ester to form intermediate **2.44** (Scheme 2-23). Simply switching the bifunctional building block to **2.18**, pinacol boronic ester **2.44** was coupled to the halide terminus of **2.18** to afford tetraenyl MIDA boronate **2.45** as a single stereoisomer in an unoptimized 39% yield. The final bidirectional coupling proceeded with the in situ release of two equivalents of boronic acid derived from tetraenyl MIDA boronate **2.45** and double cross-coupling with **2.10** to afford renierapurpurin **2.5** in ~20% semi-purified yield as confirmed by ^{1}H NMR and HRMS.[68]

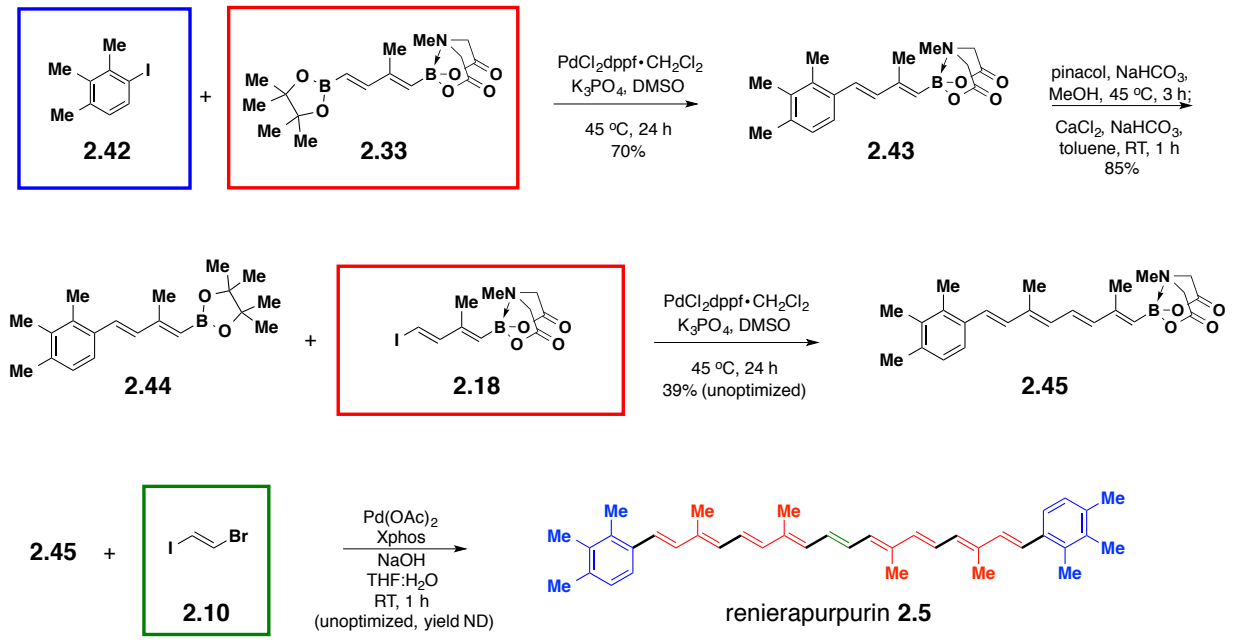

Scheme 2-23. Total synthesis of renierapurpurin **2.5** via incorporating both RP-ICC and ICC strategies.

2-9 SYNECHOXANTHIN IS AN ANTILIPOPEROXIDANT IN A LIPOSOME-BASED TBARS ASSAY

We aimed to compare the antilipoperoxidant activity of these carotenoid natural products first in an *in vitro* antilipoperoxidation assay by replicating the lipoperoxidation process in large unilamellar vesicles (LUVs).[69] Pre-existing lipid hydroperoxides, when exposed to either Cu[70] or Fe[71] salts, are broken down to generate LOO•. Following this initiation event, radical chain propagation can proceed, leading to the progressive formation of malondialdehyde (MDA). The thiobarbituric acid reactive substances (TBARS) assay[72] is a well-established method for monitoring lipid peroxidation by quantification of this reactive byproduct formed as a result of lipoperoxidation. One molecule of MDA reacts with two molecules of TBA to produce a TBA-MDA adduct that can be detected at 535 nm (Figure 2-4).[73]

To monitor lipoperoxidation in a controlled-manner, Dr. Eric Woerly developed a LUV-based lipid peroxidation assay system comprised completely of synthetic lipid components [POPC (16:0-18:1, 75 mol%) and PUFA (18:0-20:4, 25 mol%)] that retains biological relevance.[74] For this assay, carotenoids are dissolved in an organic solvent, such as THF, and incorporated into the LUV solution via external addition, followed by size exclusion chromatography to remove unincorporated carotenoids and non-LUV liposomes.

In this assay, carotenoid-incorporated liposome solutions were incubated under air at 37 ^{o}C in the presence of a $CuCl_2$ initiator and absorbance was measured via HPLC coupled to ultraviolet-visible (UV-Vis) spectrometry. Preliminary studies in our laboratory have demonstrated this method to be reproducible, but control experiments had to be pursued to validate several parameters before applying this method to test the antilipoperoxidant activity of synechoxanthin. After confirming the optimal heating time to produce the MDA-TBA adduct, and determining that the number of size-exclusion columns do not affect the percent incorporation of carotenoids,[75] we started by probing the antilipoperoxidant activity of well-studied carotenoids astaxanthin and β-carotene.

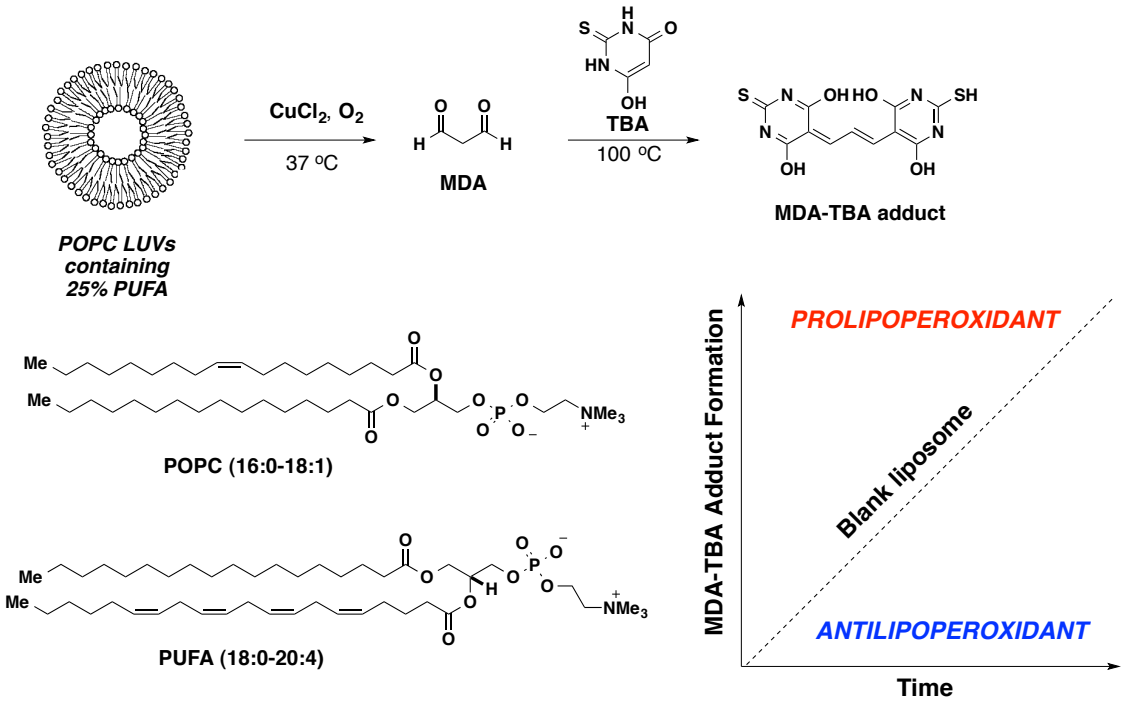

Figure 2-4. TBARS assay with a chemically-defined liposome system.

Based on the key structural features of these carotenoids and previous findings, we expected to observe increased levels of MDA formation in the presence of β-carotene compared to the control with no carotenoids added. In contrast, we expected to observe significantly decreased levels of MDA formation in the presence of the gold standard astaxanthin. Consistent with our hypothesis, we reproducibly found that β-carotene is a prolipoperoxidant and astaxanthin is an antilipoperoxidant under these assay conditions (Figure 2-5).

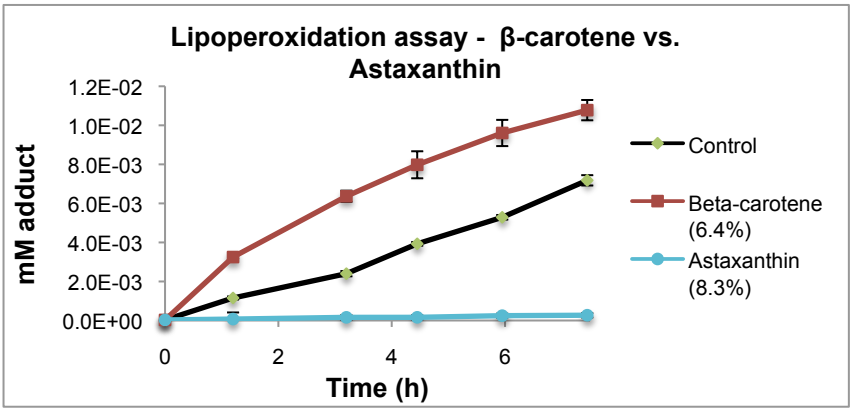

Figure 2-5. TBA-MDA adduct formation over time was evaluated with β-carotene- and astaxanthin-incorporated liposomes. Each sample was run in triplicate (plotted as average ± 1 standard deviation).

With established benchmarks for carotenoid prolipoperoxidant and antilipoperoxidant activities, the antilipoperoxidant activity of synechoxanthin was investigated in a liposome system. In this assay, we expected to observe decreased levels of MDA formation in the presence of synechoxanthin compared to the control. However, initial attempts to incorporate synechoxanthin into liposomes were complicated by the insolubility of this natural product in common organic solvents such as THF and MeOH, which hindered carotenoid addition to liposomes via external addition. Dissolving synechoxanthin (2-3 mg) in DMSO (3 mL) at 30 ^{o}C still afforded undissolved synechoanthin as an aggregate, and adding large amounts of DMSO (>1 mL) to the lipid film led to disruption of the lipid membrane.

This led us to investigate alternate solvent systems that will allow sufficient solubility of synechoxanthin so that the external addition protocol can be pursued. We hypothesized that the unique polar appendages and the hydrophobic polyene core of synechoxanthin was contributing to the insolubility of this natural product in both organic solvents as well as aqueous media, favoring aggregation through π-stacking, hydrogen-bonding, and/or the hydrophobic effect. We thus tested pH dependence of buffers used as well as the addition of acids and bases to DMSO. Employing octaene **2.41** as a control, we saw no effect with surveying pH of the buffer, but we were encouraged to see that addition of 5% Et_3N in DMSO (v/v) visibly increased the solubility of this polyene.

With this solvent system, we discovered that octaene **2.41**, a derivative of synechoxanthin, is an antilipoperoxidant under this assay condition, with equal potency compared to astaxanthin over the course of 10 hours.[76] Encouraged by this result, the antilipoperoxidant activity of synechoxanthin was evaluated under the same assay conditions. Encouragingly, supporting our hypothesis, we discovered that synechoxanthin indeed functions as an antilipoperoxidant in this lipoperoxidation assay and protects lipids from oxidation at similar levels compared to the gold standard astaxanthin (Figure 2-6).

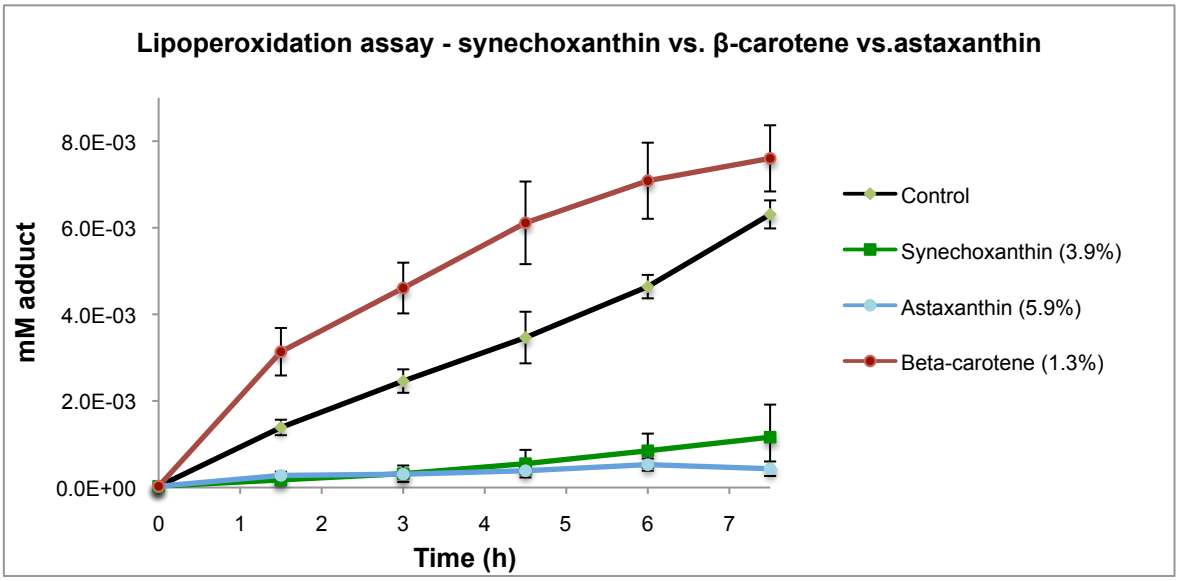

Figure 2-6. Antilipoperoxidant activity of synechoxanthin was evaluated against β-carotene and astaxanthin. DMSO + 5% Et_3N control had no effect compared to the blank liposome. Each sample was run in triplicate (plotted as average ±1 standard deviation).

2-10 SUMMARY AND CONCLUSIONS

Stimulated by the potential for carotenoid natural products to serve as antilipoperoxidants, an efficient, modular, and flexible synthetic approach was developed to access small molecules. Through this process, a novel RP-ICC strategy was developed, substantially expanding the scope of ICC by introducing new types of building blocks into the same platform. This RP-ICC strategy was key to the completion of the first total synthesis of synechoxanthin, as well as its biosynthetic precursor renierapurpurin, in a convergent and flexible manner. Although the RP-ICC strategy was developed in the context of the synechoxanthin total synthesis, further expansion of this strategy beyond polyene natural products can be envisioned by incorporating MIDA boronates as halide or pseudo-halide masks for aryl and alkyl building blocks.

Enabled by the efficient access to synechoxanthin, preliminary *in vitro* liposome studies indicate that synechoxanthin is an antilipoperoxidant. This encouraging data serves as a starting point to systematically investigate the antilipoperoxidant activity of other carotenoid natural products including renierapurpurin. It would also be informative to probe the effect of various carotenoid lengths on the antilipoperoxidant activity, given that an octaene derivative demonstrated similar antilipoperoxidant activity compared to synechoxanthin. Moreover, because this building block-based synthesis is highly amenable for derivative synthesis, it stands

to enable rationally guided systematic dissection of the structure/function relationships that underlie the very promising activities of carotenoid natural products.

2-11 REFERENCES

[1] Meerson, F. Z.; Kagan, V. E.; Kozov, Yu. P.; Belkina, L. M.; Arkhipenko, Yu. V. *Basic Res. Cardiol.* **1982**, *77*, 465-485.

[2] Berliner, J. A.; Watson, A. D. *N. Eng. J. Med.* **2005**, *353*, 9-11.

[3] Williams, M. V.; Wishnok, J. S.; Tannenbaum, S. R. *Chem. Res. Toxicol.* **2007**, *20*, 767-775.

[4] Holm, J. P.; Bhakat, P.; Jegerschold, C.; Gyobu, N.; Mitsuoka, K.; Fujitoshi, Y.; Morgenstern, R.; Herbert, H. *J. Mol. Biol.* **2006**, *360*, 934-945.

[5] (a) de Waart, F. G.; Kok, F. J.; Smilde, T. J.; Hijmans, A.; Wollersheim, H.; Stalenhoef, A. F. H. *Atherosclerosis* **2001**, *158*, 227-231. (b) Lewis, P.; Stefanovic, N.; Pete, J.; Calkin, A. C.; Giunti, S.; Thallas-Bonke, V.; Jandeleit-Dahn, K. A.; Allen, T. J.; Cooper, M. E.; de Haan, J. B. *Circulation* **2007**, *115*, 2178–2187.

[6] Saadat, M. *Cancer Sci.* **2006**, *97*, 505-509.

[7] Seven, A.; Güzel, S.; Aslan, M.; Hamuryudan, V. *Clin. Biochem.* **2008**, *41*, 538-543.

[8] Hulbert, A. J.; Pamplona, R.; Buffenstein, R.; Buttemer, W. A. *Physiol. Rev.* **2007**, *87*, 1175-1213.

[9] Krinsky, N. I.; Johnson, E. J. *Mol. Aspects Med.* **2005**, *26*, 459-516.

[10] (a) Bosio, G. N.; Breitenbach, T.; Parisi, J.; Reigosa, M.; Blaikie, F. H.; Pedersen, B. W.; Silva, E. F. F.; Mártire, D. O.; Ogilby, P. R. *J. Am. Chem. Soc.* **2013**, *135*, 272-279. (b) Druesne-Pecollo, N.; Latino-Martel, P.; Norat, T.; Barrandon, E.; Bertrais, S.; Galan, P.; Hercberg, S. *Int. J. Cancer* **2010**, *127*, 172-184. (c) Jeon, Y.-J.; Myung, S.-K.; Lee, E.-H.; Kim, Y.; Chang, Y. J.; Ju, W.; Cho, H.-J.; Seo, H. G.; Huh, B. Y. *Nutr. Cancer* **2011**, *63*, 1196-1207.

[11] Heinonen, O. P.; Albanes, D. *N. Engl. J. Med.* **1994**, *330*, 1029-1035.

[12] (a) Shen, H.; Kuo, C.; Chou, J.; Delvolve, A.; Jackson, S. N.; Post, J.; Woods, A.; Hoffer, B. J.; Wang, Y.; Harvey, B. K. *FASEB J.* **2009**, *23*, 1958-1968. (b) Fassett, R. G.; Coombes, J. S. *Mar. Drugs* **2011**, *9*, 447-475. (c) Hussein, G.; Sankawa, U.; Goto, H.; Matsumoto, K.; Watanabe, H., *J. Nat. Prod.* **2006,** *69*, 443-449. (d) Miki, W. *Pure Appl. Chem.* **1991**, *63*, 141-146.

[13] www.astafactor.com

[14] (a) Lauver, D. A.; Lockwood, S. F.; Lucchesi, B. R. *J. Pharm. Exp. Ther.* **2005,** *314*, 686-692. (b) Gross, G. J.; Hazen, S. L.; Lockwood, S. F. *Mol. Cell. Biochem.* **2006,** *283*, 23-30. (c) Gross, G. J.; Lockwood, S. F. *Life Sci.* **2004,** *75*, 215-224. (d) Gross, G. J.; Lockwood, S. F. *Mol. Cell. Biochem.* **2005,** *272*, 221-227.

[15] Ryu, S. K.; King, T. J.; Fujioka, K.; Pattison, J.; Pashkow, F. J.; Tsimikas, S. *Atherosclerosis* **2012,** *222*, 99-105.

[16] (a) Burton, G. W.; Ingold, K. U. *Science* **1984**, *224*, 569-573. (b) Krinsky, N. I. *Pure and Appl. Chem.* **1979**, *51*, 649-660. (c) Liebler, D. C. *Ann. N. Y. Acad. Sci.* **1993**, *691*, 20-31. (d) Burton, G. W. *J. Nutr.* **1989**, *119*, 109-111.

[17] Rengel, D.; Díes-Navajas, A.; Serna-Rico, P.; Veiga, P.; Muga, A.; Milicua, J. C. G. *Biochim. Biophys. Acta.* **2000**, *1463*, 179-187.

[18] Liebler, D. C. *Ann. N Y Acad. Sci.* **1993**, *691*, 20-31.

[19] El-Agamey, A.; Lowe, G. M.; McGarvey, D. J.; Mortensen, A.; Phillip, D. M.; Truscott, T. G.; Young, A. J. *Arch. Biochem. Biophys.* **2004**, *430*, 37-48.

[20] Hirayama, O.; Nakamura, K.; Hayama, S.; Kobayashi, Y. *Lipids* **1994**, *29*, 149-150.

[21] (a) Schafer, F.; Wang, H. P.; Kelley, E. E.; Cueno, K. L.; Martin, S. M.; Buettner, G. R. *Biol. Chem.* **2002**, *383*, 671-681. (b) Wisniewska, A.; Subczynski, W. K.; *Biochim. Biophys. Acta.* **1998**, *1368*, 235-246.

[22] Brocks, J. J.; Schaeffer, P. *Geochimica et Cosmochimica Acta* **2008**, *72*, 1396-1414.

[23] Martin, H-D.; Kock, S.; Scherrers, R.; Lutter, K.; Wagener, T.; Hundsdörfer, C.; Frixel, S.; Schaper, K.; Ernst, H.; Schrader, W.; Görner, H.; Stahl, E. *Angew. Chem. Int. Ed.* **2008**, *47*, 1-5.

[24] Wagener, S.; Völker, T.; De Spirt, S.; Ernst, H.; Stahl, W. *Free Radical Biol. Med.* **2012**, 53, 457-463.

[25] (a) Bachilo, S. M.; Spangler, C. W.; Gilbro, T. *Chem. Phys. Lett.* **1998**, *283*, 235-242. (b) Drenth, W.; Wiebenga, E. H. *Acta Cryst.* **1955**, *8*, 755.

[26] Gabrielska, J.; Gruszecki, W. I. *Biochim. Biophys. Acta.* **1996**, *1285*, 167-174.

[27] (a) Mohamed, H. E.; van de Meene, A. M. L.; Roberson, R. W.; Vermaas, W. F. J. *J. Bacteriol.* **2005**, *187*, 6883-6892. (b) Anwar, M.; Khan, T. H.; Prebble, J.; Zagalsky, P. F. *Nature*

1977, *270*, 538-540. (c) Rohmer, M.; Bouvier, P.; Ourisson, G. *Proc. Natl. Acad. Sci. USA* **1979**, *76*, 847-851.

[28] Graham, J. E.; Lecomte, J. T.; Bryant, D. A. *J. Nat. Prod.* **2008**, *71*, 1647-1650.

[29] Nomura, C. T.; Sakamoto, T.; Bryant, D. A. *Arch. Microbiol.* **2006**, *185*, 471-479.

[30] Swern, D. *J. Am. Chem. Soc.* **1947**, *69*, 1692-1698.

[31] Xhu, Y.; Graham, J. E.; Ludwig, M.; Xiong, W.; Alvey, R. M.; Shen, G.; Bryant, D. A. *Arch. Biochem. Biophys.* **2010**, *504*, 86-99.

[32] Graham, J. E.; Bryant, D. A. *J. Bacteriol.* **2008**, *190*, 7966-7974.

[33] Ernst, H. *Pure. Appl. Chem.* **2002**, *74*, 2213-2226.

[34] (a) McMurry, J. E.; Fleming, M. P. *J. Am. Chem. Soc.* **1974**, *96*, 4708-4709. (b) Ishida, A.; Mukaiyama, T. *Chem. Lett.* **1976**, 1127-1130.

[35] (a) Fontán, N.; Domínguez, M.; Alvarez, R.; de Lera, A. R. *Eur. J. Org. Chem.* **2011**, *33*, 6704-6712. (b) Kajikawa, T.; Iguchi, N.; Katsumura, S. *Org. Biomol. Chem.* **2009**, *7*, 4586-4589. (c) Fontán, N.; Alvarez, R.; de Lera, A. R. *J. Nat. Prod.* **2012**, *75*, 975-979.

[36] Álvarez, R.; Vaz, B.; Gronemeyer, H.; de Lera, Á. R. *Chem. Rev.* **2014**, *114*, 1-125.

[37] Negishi, E.; Alimardanov, A.; Xu, C. *Org. Lett.* **2000**, *2*, 65-67.

[38] Vaz, B.; Alvarez, R.; de Lera, A. R. *J. Org. Chem.* **2002**, 67, 5040-5043.

[39] Fontán, N.; Vaz, B.; Álvarez, R.; de Lera, Á. R. *Chem. Commun.* **2013**, *49*, 2694-2696.

[40] Gillis, E. P.; Burke, M. D. *J. Am. Chem. Soc.* **2007**, *129*, 6716-6717.

[41] For recent reviews on iterative cross-coupling, see: (a) Wang, C.; Glorius, F. *Angew. Chem. Int. Ed.* **2009**, *48*, 5240-5244. (b) Tobisu, M.; Chatani, N. *Angew. Chem. Int. Ed.* **2009**, *48*, 3565-3568. (c) E. P. Gillis, M. D. Burke, *Aldrichimica Acta* **2009**, *42*, 17-27.

[42] Lee, S. J.; Gray, K. C.; Peak, J. S.; Burke, M. D. *J. Am. Chem. Soc*. **2008**, *130*, 466-468.

[43] Lee, S. J.; Anderson, T. M.; Burke, M. D. *Angew. Chem. Int. Ed.* **2010**, *49*, 1-6.

[44] Woerly, E. M.; Cherney, A. H.; Davis, E. K.; Burke, M. D. *J. Am. Chem. Soc.* **2010**, *132*, 6941-6943.

[45] Polyenylboronic acids are notoriously unstable: (a) Roush, W. R.; Brown, B. B. *J. Am. Chem. Soc.* **1993**, *115*, 2268-2278. (b) Torrado, A.; Iglesias, B.; López, S.; de Lera, A. R. *Tetrahedron* **1995**, *51*, 2435-2454.

[46] Kaiser, F.; Schwink, L.; Velder, J.; Schmalz, H-G. *Tetrahedron* **2003**, *59*, 3201-3217.

[47] For an example of polarity reversal leading to improved yields in silicon-based cross-coupling, see: (a) Denmark, S. E.; Liu, J. H-C.; Muhuhi, J. M. *J. Am. Chem. Soc.* **2009**, *131*, 14188-14189. (b) Denmark, S. E.; Liu, J. H-C.; Muhuhi, J. M. *J. Org. Chem.* **2011**, *76*, 201-215.

[48] Miyaura, N.; Suzuki, A. *Chem. Rev.* **1995**, *95*, 2457-2483.

[49] Zim, D.; Nobre, S. M.; Monteiro, A. L. *J. Mol. Catal. A: Chem.* **2008**, *287*, 16-23.

[50] (a) Kinzel, T; Zhang, Y.; Buchwald, S. L. *J. Am. Chem. Soc.* **2010**, *132*, 14073-14075. (b) Barder, T. E.; Walker, S. D.; Martinelli, J. R.; Buchwald, S. L. *J. Am. Chem. Soc.* **2005**, *127*, 4685-4696.

[51] (a) Kuivila, H. G.; Reuwer, J. F.; Mangravite, J. A. *Can. J. Chem.* **1963**, *41*, 3081-3090. (b) Kuivila, H. G.; Reuwer, J. F.; Mangravite, J. A. *J. Am. Chem. Soc.* **1964**, *86*, 2666-2670.

[52] Wong, M. S.; Zhang, X. L. *Tetrahedron Lett.* **2001**, *42*, 4087-4089

[53] (a) Zim, D.; Monteiro, A. L.; Dupont, J. *Tetrahedron Lett.* **2000**, *41*, 8199-8202. (b) LeBlond, C. R.; Andrews, A. T.; Sun, Y.; Sowa, Jr. J. R. *Org. Lett.* **2001**, *3*, 1555-1557.

[54] Spiesecke, H.; Schneider, W. G. *J. Chem. Phys.* **1961**, *35*, 731-738.

[55] Moore, J. S.; Weinstein, E. J.; Wu, Z. *Teterahedron Lett.* **1991**, *32*, 2465-2466.

[56] Zhang, J.; Moore, J. S.; Xu, Z.; Aguirre, R. A. *J. Am. Chem. Soc.* **1992**, *114*, 2273-2274.

[57] (a) Brown, H. C.; Hamaoka, T.; Ravindran, N. *J. Am. Chem. Soc.* **1973**, *95*, 5786-5788. (b) Brown, H. C.; Hamaoka, T.; Ravindran, N. *J. Am. Chem. Soc.* **1973**, *95*, 6456-6457.

[58] Gray, K. C. Semisynthesis of Amphotericin B and Its Derivatives via Iterative Cross-Coupling. PhD. Dissertation, University of Illinois at Urbana-Champaign, 2011.

[59] Gillis, E. P.; Burke, M. D. *J. Am. Chem. Soc.* **2008**, *130*, 14084-14085.

[60] Struble, J. R.; Lee, S. J.; Burke, M. D. *Tetrahedron* **2010**, *66*, 4710-4718.

[61] Knapp, D. M.; Gillis, E. P.; Burke, M. D. *J. Am. Chem. Soc.* **2009**, *131*, 6961-6963.

[62] Thompson, A. L. S.; Kabalka, G. W.; Akula, M. R.; Huffman, J. W. *Synthesis* **2005**, *4*, 547-550.

[63] Negishi, E.; Alimardanov, A.; Xu, C. *Org. Lett.* **2000**, *2*, 65-67.

[64] For other examples of selective functionalization of bisborylated building blocks, see: (a) Desurmont, G.; Klein, R.; Uhlenbrock, S.; Laloë, E.; Deloux, L.; Giolando, D. M.; Kim, Y. W.; Pereira, S.; Srebnik, M. *Organometallics* **1996**, *15*, 3323-3328. (b) Ishiyama, T.; Miyaura, N. *J.*

Organomet. Chem. **2000**, *611*, 392-402. (c) Ref. 42 (d) Noguchi, H.; Shioda, T.; Chou, C-M.; Suginome, M. *Org. Lett.* **2008**, *10*, 377-380.

[65] (a) Zeng, F.; Negishi, E. *Org. Lett.* **2001**, *5*, 719-722. (b) Ghasemi, H.; Antunes, L. M.; Organ, M. G. *Org. Lett.* **2004**, *17*, 2913-2916.

[66] Laganis, E. D.; Chenard, B. L. *Tetrahedron Lett.* **1984**, *25*, 5831-5834.

[67] Stavber, S.; Kralj, P.; Zupan, M. *Synlett* **2002**, *4*, 598 - 600.

[68] Limited characterization data has been reported for renierapurpurin: (a) Yamaguchi, M. *Bull. Chem. Soc. Jpn.* **1960**, *33*, 1560-1562. (b) Cooper, R D. G.; Davis, J. B.; Weedon, B. C. L. *J. Chem. Soc.* **1963**, 5720-5723.

[69] Rengel, D.; Diez-Navajas, A.; Serna- Rico, A.; Veiga, P.; Muga, A.; Milicua, J. C. *Biochem. Biophys. Acta* **2000**, *1463*, 179-187.

[70] (a) Jones, C. M.; Burkitt, M. J. *J. Am. Chem. Soc.* **2003**, *125*, 6946-6954. (b) Pinchuk, I.; Schnitzer, E.; Lichtenberg, D. *Biochim. Biophys. Acta* **1998**, *1389*, 155-172. (c) Patel, R. P.; Svistunenko, D.; Wilson, M. T.; Darley-Usmar, V. M. *Biochem. J.* **1997**, *322*, 425-433.

[71] Tang, L.; Zhang, Y.; Qian, Z.; Shen, X. *Biochem. J.* **2000**, *352*, 27-36.

[72] Janero, D. R. *Free Radical Biol. Med.* **1998**, *9*, 515-540.

[73] (a) Esterbauer, H.; Cheeseman, K. H. *Methods Enzym.* **1990**, *186*, 407-421. (b) Yu, L. W.; Latriano, L.; Duncan, S.; Hartwick, R. A.; Witz, G. Anal. *Biochem.* **1986**, *156*, 326-333.

[74] Woerly, E. W. Total Synthesis and Study of the Antilipoperoxidant Peridinin, Synthesis of Versatile MIDA Boronate Building Blocks, and a General Strategy for the Synthesis of Polyenes. PhD. Dissertation, University of Illinois at Urbana-Champaign, 2013.

[75] See Experimental Section Figure 2-8.

[76] See Experimental Section Figure 2-7.

CHAPTER 2
EXPERIMENTAL SECTION

Materials. Commercial reagents were purchased from Sigma-Aldrich, TCI America, Alfa Aesar, Strem Chemicals Inc. or Fisher Scientific and used without further purification unless otherwise noted. Solvents were purified via passage through packed columns as described by Pangborn and coworkers[1] (THF, Et_2O, CH_3CN, CH_2Cl_2: dry neutral alumina; hexane, benzene, and toluene: dry neutral alumina and Q5 reactant; DMSO, DMF: activated molecular sieves). All water was deionized prior to use. The following compounds were prepared by their literature methods: **2.20**[2], **2.10**[3], and **2.42**[4]. The following compounds were prepared as previously described: 1-triethylgermanium-2-tributyltin ethylene **2.27**[5], MIDA boronate **2.36**[6], and vinyl stannane **2.25**.[7]

General Experimental Procedures. All reactions were performed in flame- or oven (125 °C)-dried glassware equipped with a stir bar under an atmosphere of dry argon unless otherwise stated. Organic solutions were concentrated via rotary evaporation under reduced pressure with a bath temperature of 30-40 °C. Reactions were monitored by analytical thin layer chromatography (TLC) on Merck silica gel 60 F254 plates (0.25 mm) using the indicated solvent system. Compounds were visualized by exposure to UV light (254 nm) or potassium permanganate ($KMnO_4$) followed by brief heating with a Varitemp heat gun. MIDA boronates are compatible with standard silica gel chromatography, including standard loading techniques. Column chromatography was performed using standard methods[8] or on a Teledyne- Isco CombiFlash Rf purification system using Merck silica gel grade 9385 60Å (230-400 mesh). For loading, compounds were adsorbed onto non acid-washed Celite *in vacuo* from an acetone solution. Specifically, for a 1 g mixture of crude material the sample is dissolved in reagent grade acetone (25 to 50 mL) and to the flask is added Celite 545 Filter Aid (5 to 15 g). The mixture is then concentrated *in vacuo* to afford a powder, which is then loaded on top of a silica gel column. Flash column chromatography was performed as described by Still and coworkers[1] using Merck silica gel 60 (230-400 mesh). RP-HPLC purification was performed on Agilent 1100 series HPLC system equipped with a Sunfire™ C_{18} 5 micron 10 x 250 mm column (Waters Corp. Milford, MA) with indicated eluent, flow rate, and wavelength.

Structural Analysis. ^{1}H NMR spectra were recorded at 23 °C using one of the following instruments: Varian Unity Inova 500 (500 MHz), Varian VXR 500 (500 MHz), and Varian Unity Inova 500NB (500 MHz). Chemical shifts are reported in parts per million (ppm) downfield from tetramethylsilane and referenced to residual protium in the NMR solvent ($CDCl_3$, δ = 7.26; acetone-d_6, δ = 2.04; CD_2Cl_2, δ = 5.32, center line). When solvent mixtures were used, spectra were referenced to an internal standard of tetramethylsilane (δ = 0.00). Spectral data are presented as follows: chemical shift, multiplicity (s = singlet, d = doublet, t = triplet, q = quartet, quint = quintet, sext = sextet, m = multiplet, b = broad), coupling constant (*J*), and integration. ^{13}C NMR spectra were recorded at 23 °C using one of the following instruments: Varian Unity Inova 500 (500 MHz), Varian VXR 500 (500 MHz), or Varian Unity Inova 600 (600 MHz). Chemical shifts are reported in parts per million (ppm) downfield from tetramethylsilane and referenced to carbon resonances in the NMR solvent ($CDCl_3$, δ = 77.0; acetone-d_6, δ = 29.8; CD_2Cl_2, δ = 53.8; DMSO-d_6, δ = 49.0; CD_3CN, δ = 118.2, center line) or to added tetramethylsilane (δ = 0.00). Many of the carbon bearing boron substituents were not observed (quadrupole relaxation). ^{11}B NMR were recorded at 23 °C on a Varian Unity Inova 400 instrument and referenced to an external standard of $BF_3 \bullet Et_2O$. High-resolution mass spectra (HRMS) were performed by Furong Sun, Elizabeth Eves, and Dr. Haijun Yao at the University of Illinois School of Chemical Sciences Mass Spectrometry Laboratory. Data are reported in the form of m/z. Infrared spectra were collected from a thin film on NaCl plates on a Mattson Galaxy Series FT-IR 5000 spectrometer. Absorption maxima ($\#_{max}$) are reported in wavenumbers (cm^{-1}). X-ray crystallographic analysis was carried out by Dr. Danielle Gray at the University of Illinois George L. Clark X-Ray facility.

I. TOTAL SYNTHESIS OF SYNECHOXANTHIN

Synthesis of Building Block **2.17**

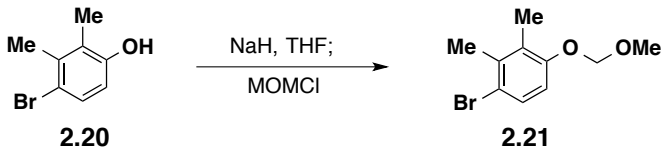

2.20 **2.21**

Aryl bromide 2.21. A 500 mL round bottom flask was charged with NaH (60 wt% in mineral oil, 2.911 g, 72.8 mmol, 1.22 equiv.) and THF (200 mL, 0.24 M) and the reaction mixture was cooled to 0 ^{o}C for 30 min. A 100 mL pear-shaped flask was charged with **2.20** (12 g, 59.7 mmol, 1.0 equiv.) and THF (50 mL x 2) to afford a clear, pale yellow solution. The solution containing **2.20** was transferred dropwise via cannula into the reaction flask over 20 min at 0 ^{o}C while vigorous H_2 evolution was observed. The reaction mixture was warmed to 23 ^{o}C over 30 min. The reaction mixture was cooled again to 0 ^{o}C and MOMCl (6.0 mL, 79.4 mmol, 1.33 equiv.) was added dropwise to the reaction mixture over 10 min. The reaction mixture was warmed to 23 ^{o}C with stirring over 2 h under positive Ar pressure. After 2 h, saturated aqueous NH_4Cl (500 mL) was added to the reaction mixture. The resulting biphasic mixture was transferred to a 2-L separatory funnel, rinsing with diethyl ether (500 mL) for quantitative transfer. The layers were separated and the aqueous layer was extracted with diethyl ether (500 mL). The combined organic layers were washed with 1M aqueous NaOH (2 x 200 mL), H_2O (200 mL), and brine (200 mL), dried over $MgSO_4$, filtered through a plug of Celite and silica gel, and concentrated *in vacuo* to afford **2.21** as a clear yellow oil (12.37 g, 85%).

TLC (hexanes:EtOAc 3:1)

R_f = 0.64, stained by $KMnO_4$

^{1}H-NMR (500 MHz, $CDCl_3$)

δ 7.32 (d, *J* = 9.0 Hz, 1H), 6.82 (d, *J* = 9.0 Hz, 1H), 5.16 (s, 2H), 3.47 (s, 3H), 2.37 (s, 3H), 2.24 (s, 3H).

^{13}C-NMR (125 MHz, $CDCl_3$)

δ 154.3, 137.2, 129.8, 128.0, 117.7, 113.3, 94.8, 56.0, 20.0, 13.1

HRMS (EI+)

Calculated for $C_{10}H_{13}O_2Br$: 244.00989

Found: 244.00851

IR (thin film, cm^{-1})

2992, 2927, 2854, 2825, 2073, 1641, 1573, 1461, 1403, 1382, 1307, 1253, 1205, 1157.08, 1099, 1066, 1002, 923, 892, 802.

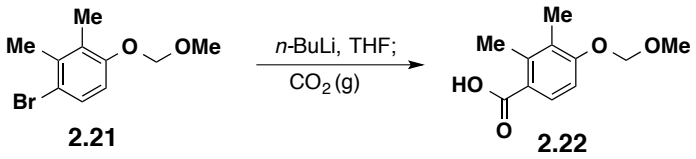

Benzoic acid 2.22. A 100 mL round bottom flask was charged with **2.21** (4.27 g, 17.4 mmol, 1.0 equiv). THF (58 mL, 0.3M) was added to afford a clear, pale yellow solution and the reaction mixture was cooled to -78 ^{o}C over 10 min. *n*-BuLi (2.5M, 7.45 mL, 18.63 mmol) was added dropwise to the reaction mixture, which was stirred for 10 min at -78 ^{o}C. CO_2 (g) was bubbled through the reaction mixture at -78 ^{o}C for 10 min while the reaction mixture turned from pale yellow to bright red, then back to pale yellow over 10 min. The reaction mixture was warmed to 23 ^{o}C over 30 min. The crude mixture was quenched by the addition of 1M HCl (50 mL) and transferred to a separatory funnel, diluting with EtOAc (50 mL). The layers were separated and the aqueous layer was extracted with EtOAc (50 mL). The combined organic layers were dried over $MgSO_4$, filtered, and concentrated *in vacuo*. The crude solid was washed with hexanes, filtered, and concentrated *in vacuo* to afford **2.22** as a pale pink solid (2.37 g, 65%).

TLC (hexanes:EtOAc 3:1)

R_f = 0.19, stained by $KMnO_4$

^{1}H-NMR (500 MHz, $CDCl_3$)

δ 7.87 (d, *J* = 9.0 Hz, 1H), 6.97 (d, *J* = 8.5 Hz, 1H), 5.26 (s, 2H), 3.49 (s, 3H), 2.58 (s, 3H), 2.23 (s, 3H).

^{13}C-NMR (125 MHz, $CDCl_3$)

δ 173.4, 158.4, 141.4, 130.5, 127.0, 122.5, 110.5, 94.2, 56.2, 17.2, 12.0

HRMS (ESI+)

Calculated for $C_{11}H_{14}O_4Na$: 233.0790

Found: 233.0793

IR (thin film, cm^{-1})

3438, 3330, 3060, 2962, 2923, 2865, 2854, 2362, 1681, 1579, 1479, 1432, 1384, 1257.36, 1189, 1174, 1151, 1097, 1066, 1027, 914.

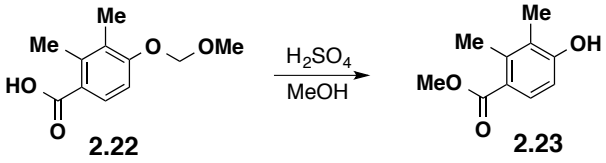

Methyl Benzoate 2.23. A 100 mL round bottom flask was charged with benzoic acid **2.22** (2.49 g, 11.86 mmol, 1.0 equiv.), H_2SO_4 (1.0 mL, 1.0 equiv.) and MeOH (40 mL, 0.3 M). The flask was fitted with a reflux condenser and a gas inlet needle and flushed with N_2. The reaction mixture was refluxed in an oil bath for 13 h. The reaction mixture turned clear brown. After 13 h, the reaction mixture was cooled to 23 ^{o}C and concentrated *in vacuo*. The crude mixture was dissolved in diethyl ether (50 mL) and neutralized with K_2CO_3, dried over $MgSO_4$, filtered through a plug of silica gel, and concentrated *in vacuo* to afford **2.23** as an off-white solid (1.91g, 89%).

TLC (hexanes:EtOAc 5:1)

R_f = 0.23, stained by $KMnO_4$

^{1}H-NMR (500 MHz, $CDCl_3$)

δ 7.64 (d, *J* = 8.5 Hz, 1H), 6.64 (d, *J* = 8.5 Hz, 1H), 5.02 (s, 1H), 3.85 (s, 3H), 2.52 (s, 3H), 2.20 (s, 3H).

^{13}C-NMR (125 MHz, $CDCl_3$)

δ 168.6, 156.4, 140.9, 129.4, 123.7, 123.2, 112, 51.7, 17.1, 11.7

HRMS (ESI+)

Calculated for $C_{10}H_{13}O_3$:	180.0865
Found:	180.0872

IR (thin film, cm^{-1})

3467, 3419, 3037, 2996, 2948, 2117, 1650, 1581, 1490, 1446, 1432, 1373, 1340, 1278, 1191, 1174, 1147, 1072.

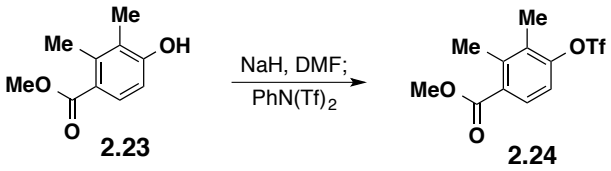

Triflate 2.24. A 50 mL round bottom flask was charged with NaH (60 wt% in mineral oil, 231 mg, 5.78 mmol, 1.0 equiv.) and DMF (7.0 mL) and cooled to 0 ^{o}C. A 50-mL pear flask was charged with **2.23** (1.042 g, 5.78 mmol, 1.0 equiv) and DMF (12 mL) to afford a clear yellow solution. The solution containing **2.23** was added dropwise to the reaction flask at 0 ^{o}C. The reaction mixture turned greenish grey. The reaction mixture was warmed to 23 ^{o}C and stirred for 30 min. After 30 min, the reaction flask was once again cooled to 0 ^{o}C and $NPhTf_2$ (2.065 g, 5.78 mmol, 1.0 equiv.) was added in small portions. The reaction mixture was slowly warmed to 23 ^{o}C overnight with stirring. After 12 h, the yellow/brown reaction mixture was diluted with saturated aqueous NH_4Cl (60 mL) while stirring. The mixture was transferred to a separatory funnel, rinsing with diethyl ether (60 mL). The aqueous layer was extracted with ether (60 mL x 2). The combined organic layers were washed with water to remove residual DMF. The organic layer was dried over $MgSO_4$, filtered, and concentrated *in vacuo* to afford a yellow oil. The crude

material was adsorbed onto Celite from an acetone solution and purified by MPLC (Hexanes → Hexanes: EtOAc 4:1) to afford **2.24** as a clear, yellow oil (1.65 g, 89% yield).

TLC (hexanes:EtOAc 5:1)

R_f = 0.56, stained by $KMnO_4$

^{1}H-NMR (500 MHz, $CDCl_3$)

δ 7.69 (d, *J* =8.5 Hz, 1H), 7.16 (d, *J* = 8.5 Hz, 1H), 3.91 (s, 3H), 2.52 (s, 3H), 2.33 (s, 3H).

^{13}C-NMR (125 MHz, $CDCl_3$)

δ 167.7, 150.0, 141.3, 131.1, 131.0, 128.9, 119.8, 118.4, 52.3, 17.3, 13.4

HRMS (ESI+)

Calculated for $C_{11}H_{12}O_5SF_3$: 313.0358

Found: 313.0361

IR (thin film, cm^{-1})

3033, 3014, 2956, 2881, 2352, 2090, 1725, 1643, 1585, 1477, 1425, 1297, 1253, 1224.58, 1160, 1141, 1060, 1031, 931.

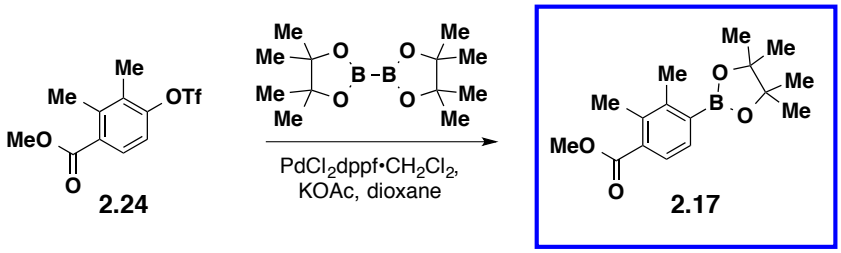

Building block 2.17. In a glovebox, to a 20 mL vial charged with triflate **2.24** (252 mg, 0.81 mmol, 1.0 equiv.) was added bispinacolatodiboron (307 mg, 1.21 mmol. 1.5 equiv.), $PdCl_2dppf•CH_2Cl_2$ (33 mg, 0.041 mmol, 5 mol%), and KOAc (238.5 mg, 2.43 mmol, 3.0 equiv.) were added followed by dioxane (4 mL, 0.2 M). The vial was sealed with a PTFE-lined cap under Ar, removed from the glovebox, placed in an 80 ^{o}C aluminum heat block and maintained

at that that temperature with stirring for 18 h. After 18 h, the reaction mixture was cooled to 23 ^{o}C and diluted with EtOAc and filtered through a plug of silica gel and concentrated *in vacuo*. The crude mixture was adsorbed onto Celite from an acetone solution and purified via normal phase MPLC (Hexanes → 1:4 EtOAc:Hexanes) and the collected fractions were concentrated *in vacuo* to afford pinacol boronic ester **2.17** as a white solid (200.5 mg, 90% yield).

TLC (hexanes:EtOAc 1:1)

R_f = 0.84, stained by $KMnO_4$

^{1}H-NMR (500 MHz, $CDCl_3$)

δ 7.59 (d, *J* = 8.0 Hz, 1H), 7.52 (d, *J* = 8.0 Hz, 1H), 3.88 (s, 3H), 2.51 (s, 3H), 2.42 (s, 3H), 1.36 (s, 12H).

^{13}C-NMR (125 MHz, $CDCl_3$)

δ 169.4, 144.1, 136.7, 133.2, 132.4, 125.9, 83.8, 51.9, 24.8, 19.0, 16.8

^{11}B-NMR (128 MHz, acetone-d_6)

δ 31.4

HRMS (ESI+)

Calculated for $C_{16}H_{24}BO_4$: 291.1768

Found: 291.1768

IR (thin film, cm^{-1})

2992, 2979, 2956, 2103, 1724, 1641, 1483, 1438, 1375, 1353, 1282, 1247, 1145, 1056, 1027, 964, 898, 856, 782, 732

Synthesis of Building Block **2.18**

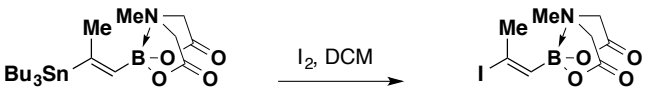

2.25 **2.26**

Vinyl iodide 2.26. A 100 mL round bottom flask was charged with stannane **2.25** (1.5 g, 3.0 mmol, 1 equiv.) and topped with a septum and a gas inlet needle. Dichloromethane (6 mL) was added to afford a pale yellow solution, and the flask was cooled to 0 ^{o}C. A 50 mL pear-shaped flask was charged with I_2 (822 mg, 3.24 mmol, 1.05 equiv.) and dichloromethane (29 mL). The I_2 solution was added dropwise to the reaction flask over the course of 1 h and stirred at 0 ^{o}C for an additional 15 min. The reaction mixture was quenched by the addition of saturated $Na_2S_2O_3$ solution (20 mL) and stirred at 10 ^{o}C until the reaction mixture became clear. The mixture was transferred to a separatory funnel, rinsing with EtOAc (70 mL) and brine (30 mL). The aqueous layer was extracted with EtOAc (3 x 50 mL) and the combined organic layers were dried over $MgSO_4$, filtered, and concentrated *in vacuo* to afford a white solid. The crude material was adsorbed onto Celite from an acetone solution and purified by SiO_2 chromatography (Et_2O → Et_2O:MeCN 10:1 → 7:1 → 5:1) to yield **2.26** as a white solid (725 mg, 75%).

TLC (Et_2O:MeCN 4:1)

R_f = 0.4, stained by $KMnO_4$

^{1}H-NMR (500 MHz, acetone-d_6)

δ 6.22 (s, 1H), 4.25 (d, *J* = 17.0 Hz, 2H), 4.11 (d, *J* = 17.0 Hz, 2H), 3.12 (s, 3H), 2.61 (s, 3H).

^{13}C-NMR (125 MHz, acetone-d_6)

δ 168.6, 110.9, 62.5, 47.2, 33.2

^{11}B-NMR (128 MHz, acetone-d_6)

δ 9.58

HRMS (EI+)

Calculated for $C_8H_{11}BINO_4$: 321.98625

Found: 321.98653

IR (thin film, cm^{-1})

3008, 2972, 2951, 2916, 1757, 1620, 1466, 1450, 1429, 1340, 1290, 1124, 1090, 1066, 1001, 964, 887

X-ray quality crystals were grown by layering pentane on top of a solution of **2.26** in acetone.

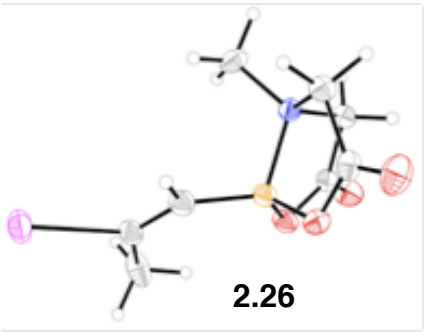

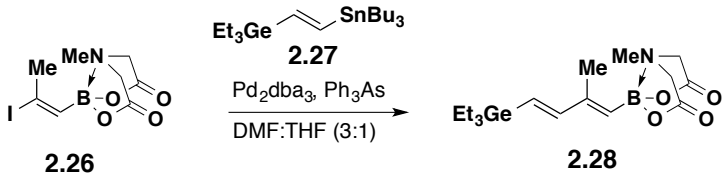

Dieneyl germane 2.28. In a glovebox, to a 7 mL vial charged with 1-triethylgermanium-2-tributyltin ethylene **2.27** (443 mg, 0.93 mmol, 1.5 equiv.) and vinyl iodide **2.26** (200 mg, 0.62 mmol, 1.0 equiv.) was added Pd_2dba_3 (14 mg, 0.016 mmol, 2.5 mol%), Ph_3As (9.5 mg, 0.03 mmol, 9.5 mol%), DMF (9.3 mL, 0.05M) and THF (3 mL). The vial was sealed with a PTFE-lined cap, removed from the glove box, and placed in a 60 ^oC aluminum heat block and maintained at that temperature with stirring for 15 h. The reaction was cooled to 23 ^oC and transferred to a separatory funnel. EtOAc (20 mL) and brine (20 mL) were added, and the layers were separated. The aqueous phase was extracted with EtOAc (3 x 20 mL), dried over $MgSO_4$, filtered, and concentrated *in vacuo*. The resulting brown oil was adsorbed onto Celite from an acetone solution and purified by silica gel chromatography (1:1 petroleum ether:EtOAc → EtOAc → 9:1 EtOAc:MeCN) to afford dienyl germane **2.28** as a white solid (204.5 mg, 86%).

TLC (EtOAc)

R_f = 0.38, stained by $KMnO_4$

^{1}H-NMR (500 MHz, acetone-d_6)

δ 6.61 (d, *J* = 18.5 Hz, 1H), 6.04 (d, *J* = 19.0 Hz, 1H), 5.42 (s, 1H), 4.21 (d, *J* = 17.0 Hz, 2H), 4.05 (d, *J* = 17.0 Hz, 2H), 3.03 (s, 3H), 1.92 (s, 3H), 1.03 (t, 9H), 0.88 (q, 6H).

^{13}C-NMR (125 MHz, acetone-d_6)

δ 169.1, 152.0, 149.5, 126.5, 62.6, 47.2, 15.1, 9.36, 5.06

^{11}B-NMR (128 MHz, acetone-d_6)

δ 10.9

HRMS (ESI+)

Calculated for $C_{16}H_{29}BNO_4Ge$:	384.1401
Found:	384.1404

IR (thin film, cm^{-1})

2954, 2871, 2088, 1741, 1648, 1456, 1338, 1292, 1128, 1022, 985, 885, 848, 819.

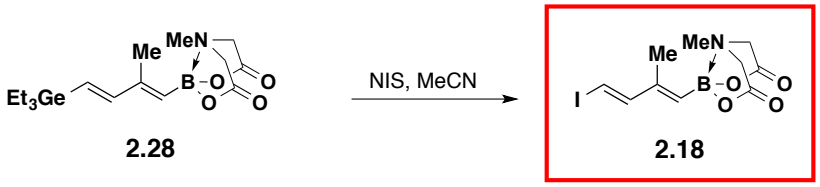

2.28 **2.18**

Building Block 2.18. A 250 mL round bottom flask was charged with dienyl germane **2.28** (1.41 g, 3.7 mmol, 1.0 equiv.) and topped with a septum and gas inlet needle. MeCN (70 mL) was added to afford a clear solution and the flask was cooled to 0 °C in an ice bath. A 100 mL pear-shaped flask was charged with *N*-iodo succinimide (NIS) (2.49 g, 11.1 mmol, 3.0 equiv.) followed by MeCN (60 mL). The NIS solution was added dropwise to the reaction mixture at 0 °C over 30 min. The resulting reaction mixture was stirred at 0 °C for 2 h. The reaction mixture was quenched with saturated $Na_2S_2O_3$ solution (100 mL) and the mixture was transferred to a

separatory funnel and diluted with EtOAc (100 mL). The layers were separated and the aqueous phase was extracted with EtOAc (2 x 100 mL). The combined organic layers were dried over $MgSO_4$, filtered, and concentrated *in vacuo*. The resulting yellow solid was adsorbed onto Celite from an acetone solution and purified by silica gel chromatography (1:1 petroleum ether:EtOAc → EtOAc) to afford dienyl iodide **2.18** as a white solid (1.07 g, 83%).

TLC (EtOAc)

R_f = 0.38, stained by $KMnO_4$

^{1}H-NMR (500 MHz, acetone-d_6)

δ 7.16 (d, *J* = 14.5 Hz, 1H), 6.56 (d, *J* = 15.0 Hz, 1H), 5.42 (s, 1H), 4.24 (d, *J* = 17.0 Hz, 2H), 4.05 (d, *J* = 17.0 Hz, 2H), 3.04 (s, 3H), 1.92 (s, 3H).

^{13}C-NMR (125 MHz, acetone-d_6)

δ 168.7, 152.8, 148.3, 77.6, 62.2, 46.9, 14.8

^{11}B-NMR (128 MHz, acetone-d_6)

δ 10.5

HRMS (ESI+)

Calculated for $C_{10}H_{14}BNO_4I$: 350.0061

Found: 350.0066

IR (thin film, cm^{-1})

3066, 3007, 2956, 2923, 2360, 1770, 1711, 1606, 1452, 1338, 1294, 1184, 1128, 1026, 991.

Synthesis of MIDA boronate **2.31** via Original ICC Pathway

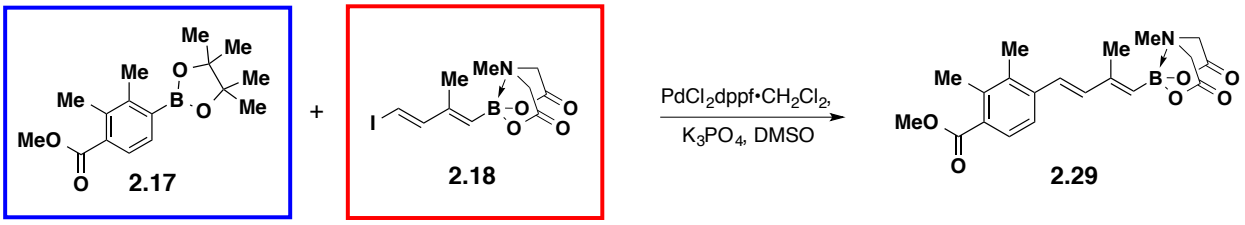

MIDA boronate 2.29. In a glovebox, to a 20 mL vial charged with **2.17** (205.9 mg, 0.75 mmol, 1.3 equiv.) and **2.18** (200.2 mg, 0.57 mmol, 1.0 equiv.) was added $PdCl_2dppf•CH_2Cl_2$ (23 mg, 0.03 mmol, 5 mol%), finely ground anhydrous K_3PO_4 (731 mg, 3.4 mmol, 6.0 equiv.), and DMSO (9 mL). The vial was sealed with a PTFE-lined cap and removed from the glove box. The vial was placed in a 45 °C aluminum heat block and maintained at that temperature with stirring for 24 h. The reaction was cooled to 23 °C and transferred to a separatory funnel, diluting with EtOAc (20 mL). The organic layer was washed with brine:H_2O (1:1, 2 x 40 mL) to remove DMSO, dried over $MgSO_4$, filtered, and concentrated *in vacuo* to afford a yellow solid. The crude material was adsorbed onto Celite from an acetone solution and purified by SiO_2 chromatography (hexanes:EtOAc 1:1 → EtOAc) to afford **2.29** as a pale yellow solid (140 mg, 60%).

TLC (EtOAc)

R_f = 0.39, stained by $KMnO_4$

^{1}H-NMR (500 MHz, acetone-d_6)

δ 7.55 (d, *J* = 8.0 Hz, 1H), 7.41 (d, *J* = 8.0 Hz, 1H), 6.94 (d, *J* = 16.0 Hz, 1H), 6.82 (d, *J* = 15.5 Hz, 1H), 5.62, (s, 1H), 4.24 (d, *J* = 17.0 Hz, 2H), 4.07 (d, *J* = 17.0 Hz, 2H), 3.83 (s, 3H), 3.01 (s, 3H), 2.45 (s, 3H), 2.33 (s, 3H), 2.10 (s, 3H).

^{13}C-NMR (125 MHz, acetone-d_6)

δ 169.3, 169.0, 148.5, 141.0, 140.4, 138.3, 136.4, 128.0, 126.6, 123.8, 117.5, 62.4, 52.1, 47.1, 17.2, 15.8, 15.6

^{11}B-NMR (128 MHz, acetone-d_6)

δ 10.9

HRMS (ESI+)

Calculated for $C_{20}H_{25}BNO_6$: 386.1775

Found: 386.1779

IR (thin film, cm^{-1})

3220, 3178, 3139, 3006, 2964, 2927, 2127, 1760, 1710, 1637, 1600, 1448, 1286, 1245, 1151, 983, 889.

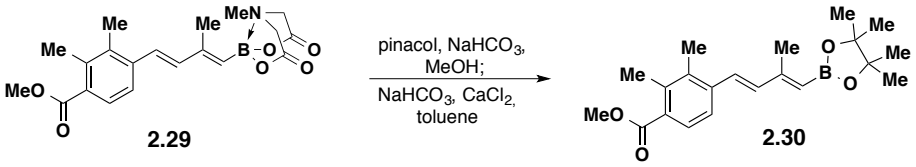

Pinacol boronic ester 2.30. A 20 mL vial was charged with MIDA boronate **2.29** (145 mg, 0.376 mmol, 1.0 equiv.), pinacol (88.9 mg, 0.752 mmol, 2.0 equiv.), and solid $NaHCO_3$ (158 mg, 1.88 mmol, 5.0 equiv.). The vial was flushed with N_2 and MeOH (1.9 mL) was added. The reaction mixture was placed in a 45 ^oC aluminum heat block and stirred at that temperature for 3 h. The reaction mixture was cooled to 23 ^oC and filtered through a pad of Celite, rinsing with Et_2O. The collected solution was concentrated *in vacuo* and the resulting residue was azeotroped with toluene to afford a yellow oil. To remove residual pinacol, finely ground $CaCl_2$ (584 mg, 5.26 mmol, 14.0 equiv.), solid $NaHCO_3$ (158 mg, 0.75 mmol, 5.0 equiv), and toluene (12.5 mL, 0.03M) were added to the crude material. The resulting suspension was stirred at 23 ^oC for 1 h and filtered through a pad of Celite, rinsing with Et_2O. The collected solution was concentrated *in vacuo* to afford **2.30** as a yellow solid (124 mg, 92%).

TLC (EtOAc)

R_f = 0.88, stained by $KMnO_4$

^{1}H-NMR (500 MHz, acetone-d_6)

δ 7.63 (d, J = 8.0 Hz, 1H), 7.44 (d, J = 8.0 Hz, 1H), 7.08 (d, J = 16 Hz, 1H), 6.83 (d, J = 15.5 Hz, 1H), 5.49 (s, 1H), 3.84 (s, 3H), 2.44 (s, 3H), 2.33 (s, 3H), 2.24 (s, 3H), 1.27 (s, 12H).

^{13}C-NMR (125 MHz, acetone-d_6)

δ 169.1, 155.8, 140.3, 138.8, 138.2, 136.6, 131.3, 129.4, 127.9, 123.9, 83.5, 52.0, 25.0, 17.1, 16.6, 15.7

^{11}B-NMR (128 MHz, acetone-d_6)

δ 30.1

HRMS (ESI+)

Calculated for $C_{21}H_{29}BO_4Na$: 379.2057

Found: 379.2055

IR (thin film, cm^{-1})

2974, 2931, 2852, 2360, 2330, 1722, 1599, 1437, 1363, 1437, 1363, 1286, 1242, 1144, 968.

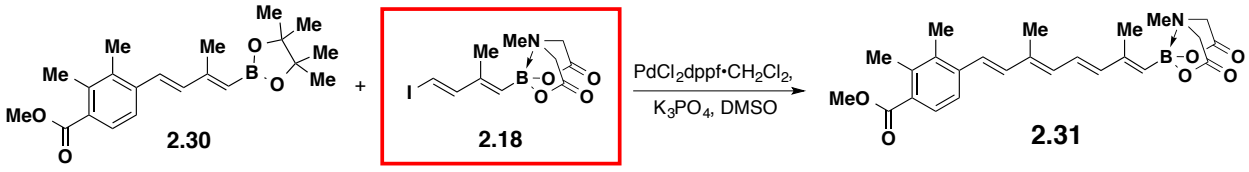

Tetraenyl MIDA boronate 2.31. In a glovebox, to a 7 mL vial charged with **2.30** (123.7 mg, 0.35 mmol, 1.3 equiv.) and **2.18** (93.2 mg, 0.27 mmol, 1.0 equiv.) was added $PdCl_2dppf•CH_2Cl_2$ (10.9 mg, 0.014 mmol, 5 mol%), finely ground anhydrous K_3PO_4 (340 mg, 1.60 mmol, 6.0 equiv.), and DMSO (3.8 mL). The vial was sealed with a PTFE-lined cap and removed from the glove box. The vial was placed in a 45 ^{o}C aluminum heat block and maintained at that temperature with stirring for 24 h. The reaction was cooled to 23 ^{o}C and transferred to a separatory funnel, diluting with EtOAc (20 mL). The organic layer was washed with brine:H_2O (1:1, 2 x 40 mL) to remove DMSO, dried over $MgSO_4$, filtered, and concentrated *in vacuo* to

afford a yellow-orange solid. The crude material was adsorbed onto Celite from an acetone solution and purified by SiO_2 chromatography (hexanes:EtOAc 1:1 → EtOAc) to afford **2.31** as a yellow solid (60.2 mg, 50%).

TLC (EtOAc)

R_f = 0.39, stained by $KMnO_4$

^{1}H-NMR (500 MHz, acetone-d_6)

δ 7.56 (d, *J* = 8.5 Hz, 1H), 7.46 (d, *J* = 8.5 Hz, 1H), 6.96 (d, *J* = 15.5 Hz, 1H), 6.90 (d, *J* = 16.0 Hz, 1H), 6.75, (dd, *J* = 15.0 Hz, 11.0 Hz, 1H), 6.46 (d, *J* = 14.5 Hz, 1H), 6.40 (d, *J* = 12.0 Hz, 1H), 5.49 (s, 1H), 4.22 (d, *J* = 17.0 Hz, 2H), 4.05 (d, *J* = 17.0 Hz, 2H), 3.83 (s, 3H), 3.04 (s, 3H) 2.45 (s, 3H), 2.34 (s, 3H), 2.08 (s, 3H), 2.03 (s, 3H).

^{13}C-NMR (125 MHz, acetone-d_6)

δ 168.7, 168.3, 148.4, 141.6, 140.4, 137.8, 137.2, 136.2, 135.5, 133.8, 130.2, 127.4, 125.5, 125.0, 122.9, 61.8, 51.4, 46.5, 16.7, 15.2, 15.0, 12.3

^{11}B-NMR (128 MHz, acetone-d_6)

δ 11.1

HRMS (ESI+)

Calculated for $C_{25}H_{31}BNO_6$: 452.2244

Found: 452.2263

IR (thin film, cm^{-1})

3012, 2962, 2595, 2098, 1760, 1710, 1643, 1450, 1340, 1288, 1243, 1189, 1151, 1093, 1066, 1024, 985, 964, 889.

Synthesis of Building Block **2.32**

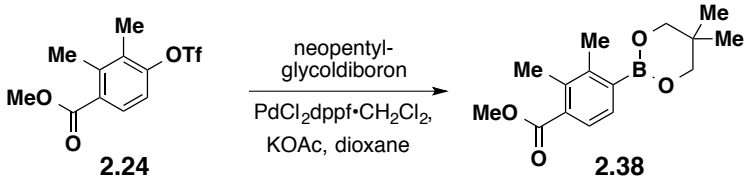

Neopentyl glycol boronic ester 2.38. In a glove box, to a 40 mL vial charged with **2.24** (949 mg, 3.04 mmol, 1.0 equiv.) was added neopentylglycolatodiboron (1.03 g, 4.56 mmol. 1.5 equiv.), $PdCl_2dppf•CH_2Cl_2$ (124 mg, 0.15 mmol, 5 mol%), and KOAc (895 mg, 9.11 mmol, 3.0 equiv.), followed by dioxane (15 mL, 0.2 M). The vial was sealed with a PTFE-lined cap under Ar and removed from the glovebox. The vial was placed in an 80 ^oC aluminum heat block and maintained at that temperature with stirring for 18 h. After 18 h, the reaction mixture was cooled to 23 ^oC and diluted with EtOAc and filtered through a plug of silica gel. The crude mixture was adsorbed onto Celite from an acetone solution and purified by MPLC (Hexanes→ 1:4 EtOAc:Hexanes) and the collected fractions were concentrated *in vacuo* to afford neopentyl glycol boronic ester **2.38** as a white solid (555 mg, 66% yield).

TLC (hexanes:EtOAc 4:1)

$R_f = 0.68$, stained by $KMnO_4$

^{1}H-NMR (500 MHz, $CDCl_3$)

δ 7.52 (s, 2H), 3.88 (s, 3H), 3.79 (s, 4H), 2.47 (s, 3H), 2.43 (s, 3H), 1.05 (s, 6H).

^{13}C-NMR (125 MHz, $CDCl_3$)

δ 169.6, 142.9, 136.7, 132.4, 131.3, 126.0, 72.4, 51.9, 31.6, 21.9, 19.1, 16.8

^{11}B-NMR (128 MHz, acetone-d_6)

δ 27.8

HRMS (EI+)

Calculated for $C_{15}H_{21}O_4B$: 276.15330

Found: 276.15268

IR (thin film, cm^{-1})

3531, 3419, 2956, 2893, 1724, 1556, 1479, 1419, 1377, 1317, 1284, 1155, 1078, 1074.

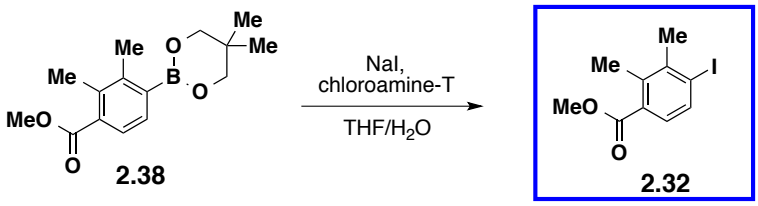

Building block 2.32. A 20 mL vial was charged with neopentylglycol boronic ester **2.38** (555 mg, 2.01 mmol, 1.0 equiv.) and THF:H_2O (1:1, 0.8 mL, 2.5 M) to afford a pale yellow solution and the vial was cooled to 0 ^oC. A solution of NaI (1.63 g, 2.51 mmol, 1.25 equiv.) in H_2O (2.5 mL) was added dropwise to the reaction vial followed by chloroamine-T (915 mg, 4.02 mmol, 2.0 equiv.) in THF:H_2O (1:1, 8.04 mL, 0.5 M). The reaction mixture was stirred under N_2 at 0 ^oC and warmed to 23 ^oC over 13 h. The reaction mixture turned from dark purple to orange over the course of the reaction. The mixture was quenched with saturated $Na_2S_2O_3$ solution (5 mL) and transferred to a separatory funnel, rinsing with diethyl ether (40 mL) and H_2O (40 mL). The layers were separated and the aqueous layer was extracted with diethyl ether (2 x 40 mL). The combined organic layers were dried over $MgSO_4$, filtered, and concentrated *in vacuo*. The resulting solid was adsorbed onto Celite from an acetone solution and purified by SiO_2 chromatography (100:1 petroleum ether:EtOAc) to afford **2.32** as a pale yellow solid (445 mg, 76%).

TLC (hexanes:EtOAc 4:1)

R_f = 0.63, stained by $KMnO_4$

^{1}H-NMR (500 MHz, acetone-d_6)

δ 7.75 (d, *J* = 8.5 Hz, 1H), 7.23 (d, *J* = 8.5 Hz, 1H), 3.84 (s, 3H), 2.47 (s, 3H), 2.45 (s, 3H).

^{13}C-NMR (125 MHz, acetone-d_6)

δ 168.7, 141.4, 138.7, 137.3, 132.5, 129.2, 106.9, 52.3, 26.0, 18.6

HRMS (EI+)

Calculated for $C_{10}H_{11}O_2I$: 289.98041

Found: 289.98135

IR (thin film, cm^{-1})

3347, 3261, 2926, 2357, 2341, 1722, 1567, 1527, 1433, 1398, 1230, 1248, 1159, 1097, 1051, 903, 816, 766, 669.

Synthesis of Building Block **2.33**

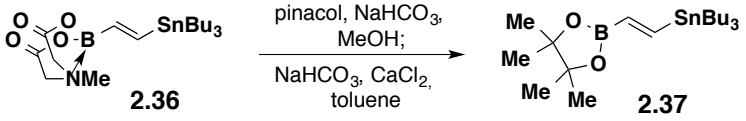

Pinacol boronic ester 2.37. A 500 mL round bottom flask was charged with MIDA boronate **2.36** (17.2 g, 36.4 mmol, 1.0 equiv.), pinacol (8.61 g, 72.9 mmol, 2,0 equiv), solid $NaHCO_3$ (15.3 g, 182.2 mmol, 5.0 equiv), and MeOH (180 mL). The reaction flask was topped with a septum and a gas inlet needle and flushed with N_2. The reaction mixture was placed in a 45 ^oC oil bath and maintained at that temperature with stirring for 3 h. The reaction mixture was cooled to 23 ^oC and filtered through a pad of Celite, rinsing with Et_2O. The collected solution was concentrated *in vacuo* in a 500 mL round bottom flask. The resulting residue was azeotroped with toluene to afford a clear oil. To remove residual pinacol, finely ground $CaCl_2$ (40.0 g, 364.4 mmol, 10 equiv.), solid $NaHCO_3$ (15.3 g, 182.2 mmol, 5.0 equiv), and toluene (200 mL) were added to the flask containing the crude material. The resulting suspension was stirred at 23 ^oC for 1 h and filtered through a pad of silica gel, rinsing with Et_2O. The collected solution was concentrated *in vacuo* to afford **2.37** as a clear oil (15.8 g, 98%).

TLC (hexanes)

R_f = 0.38, stained by $KMnO_4$

^{1}H-NMR (500 MHz, acetone-d_6)

δ 7.52 (d, *J* = 22.0 Hz, 1H), 6.28 (d, *J* = 22.0 Hz, 1H), 1.54 (quint, *J* = 7.5 Hz, 6H), 1.33 (sext, *J* = 7.5 Hz, 6H), 1.23 (s, 12 H), 0.95 (t, *J* = 7.5 Hz, 6H), 0.89 (t, *J* = 7.5 Hz, 9 H).

^{13}C-NMR (125 MHz, acetone-d_6)

δ 159.1, 83.7, 27.9, 25.2, 13.9, 11.9, 9.9

^{11}B-NMR (128 MHz, acetone-d_6)

δ 28.0

HRMS (ESI+)

Calculated for $C_{20}H_{41}BO_2SnNa$:	467.2119
Found:	467.2108

IR (thin film, cm^{-1})

3205, 2977, 2958, 2927, 2871, 2854, 2362, 2341, 2100, 1641, 1573, 1369, 1328, 1265, 1145, 1018, 970, 848.

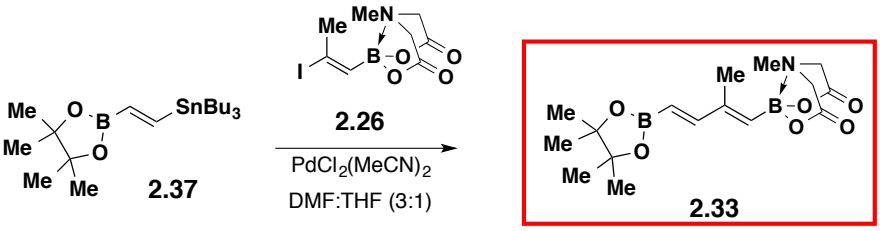

Building block 2.33. In a glovebox, to a 20 mL vial charged with stannane **2.37** (280.5 mg, 0.63 mmol, 1.3 equiv.) and iodide **2.26** (157 mg, 0.49 mmol, 1.0 equiv) was added *trans*-bis(acetonitrile)palladium dichloride (6.3 mg, 0.024 mmol, 5 mol%), DMF (7 mL) and THF (2.4 mL). The vial was sealed with a PTFE-lined cap and removed from the glovebox. The vial was placed in a 45 ^{o}C aluminum heat block and maintained at that temperature with stirring for 15 h. The reaction mixture was transferred into a separatory funnel containing brine (50 mL), rinsing with EtOAc (20 mL), and the layers were separated. The aqueous layer was extracted with EtOAc (2 x 30 mL). The combined organic layers were washed with brine:H_2O (1:1, 50 mL),

dried over $MgSO_4$, filtered, and concentrated *in vacuo* to afford an off-white solid. The crude material was adsorbed onto Celite from an acetone solution and purified by SiO_2 chromatography (hexanes:EtOAc 1:1 → EtOAc) to afford **2.33** as a white solid (135 mg, 80%).

TLC (EtOAc)

R_f = 0.33, stained by $KMnO_4$

^{1}H-NMR (500 MHz, acetone-d_6)

δ 7.06 (d, *J* = 18.5 Hz, 1H), 5.64 (s, 1H), 5.54 (d, *J* = 18.0 Hz, 1H), 4.26 (d, *J* = 16.5 Hz, 2H), 4.09 (d, *J* = 17.0 Hz, 2H), 3.08 (s, 3H), 1.97 (s, 3H), 1.27 (s, 12H).

^{13}C-NMR (125 MHz, acetone-d_6)

δ 168.9, 157.3, 149.1, 83.7, 62.4, 47.1, 25.1, 14.8

^{11}B-NMR (128 MHz, acetone-d_6)

δ 30.3, 10.7

HRMS (ESI+)

Calculated for $C_{16}H_{25}B_2NO_6Na$:	372.1766
Found:	372.1777

IR (thin film, cm^{-1})

2977, 2929, 2871, 2732, 2142.54, 1754, 1710, 1596, 1454, 1336, 1186, 1143, 995, 890, 850, 728, 651.

X-ray quality crystals were grown by layering ether on top of a solution of **2.33** in MeCN.

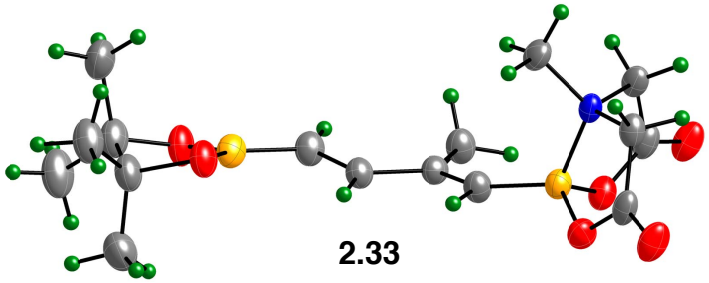

2.33

Synthesis of MIDA boronate **2.31** via RP-ICC

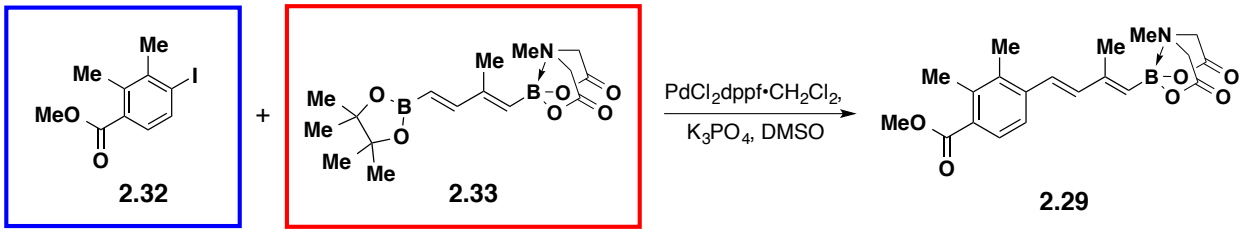

Dienyl MIDA boronate 2.29. In a glovebox, to a 20 mL vial charged with **2.32** (240 mg, 0.83 mmol, 1.3 equiv.) and **2.33** (222.3 mg, 0.637 mmol, 1.0 equiv.) was added $PdCl_2dppf•CH_2Cl_2$ (26 mg, 0.032 mmol, 5 mol%), finely ground anhydrous K_3PO_4 (811 mg, 3.8 mmol, 6.0 equiv.), and DMSO (9 mL). The vial was sealed with a PTFE-lined cap and removed from the glove box. The vial was placed in a 45 ^oC aluminum heat block and maintained at that temperature with stirring for 24 h. The reaction was cooled to 23 ^oC and transferred to a separatory funnel, diluting with EtOAc (20 mL). The organic layer was washed with brine:H_2O (1:1, 2 x 40 mL) to remove DMSO, dried over $MgSO_4$, filtered, and concentrated *in vacuo* to afford a yellow solid. The crude material was adsorbed onto Celite from an acetone solution and purified by SiO_2 chromatography (hexanes:EtOAc 1:1 → EtOAc) to afford **2.29** as a pale yellow solid (171 mg, 70%).

For characterization data, see section: Synthesis of MIDA boronate **2.31** via Original ICC Pathway.

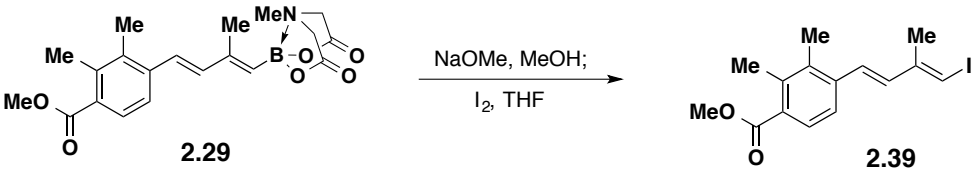

Dienyl iodide 2.39. In a glovebox, a 7 mL vial was charged with NaOMe (67.9 mg, 1.26 mmol, 5.0 equiv.). The vial was sealed with a PTFE-lined septum cap and removed from the glove box, and MeOH (2.0 mL) and THF (1.0 mL) were added to afford a clear solution. A separate 7 mL vial was charged with I_2 (192 mg, 0.756 mmol, 3.0 equiv) and THF (3.8 mL, 0.2M with respect to I_2). A 20 mL vial was charged with **2.29** (96.9 mg, 0.252 mmol, 1.0 equiv.) and THF (2.0 mL). The NaOMe solution was added dropwise to the reaction vial over 5 min. The reaction mixture

was vigorously stirred at 23 ^{o}C. TLC analysis indicated complete deprotection of the MIDA boronate to the boronic acid in 10 min. The I_2 solution was dropwise added to the vigorous stirring mixture and the resulting dark purple mixture was stirred at 23 ^{o}C for 20 min. The reaction mixture was quenched with pH7 phosphate buffer (20 mL) and transferred to a separatory funnel, rinsing with EtOAc (20 mL) and the layers were separated. The organic layer was washed with saturated $Na_2S_2O_3$ (2 x 20 mL) and the aqueous layer was back-extracted with EtOAc (10 mL). The combined organic layers were dried over $MgSO_4$, filtered, and concentrated *in vacuo* to afford **2.39** as a yellow solid (89 mg, 99%).

TLC (EtOAc)

R_f = 0.90, stained by $KMnO_4$

^{1}H-NMR (500 MHz, acetone-d_6)

δ 7.55 (d, *J* = 8.0 Hz, 1H), 7.42 (d, *J* = 8.0 Hz, 1H), 7.06 (d, *J* = 16.0 Hz, 1H), 6.94 (d, *J* = 15.5 Hz, 1H), 6.77, (s, 1H), 3.83 (s, 3H), 2.44 (s, 3H), 2.32 (s, 3H), 2.13 (s, 3H).

^{13}C-NMR (125 MHz, acetone-d_6)

δ 169.2, 146.3, 140.3, 138.4, 136.5, 133.6, 131.3, 128.0, 127.9, 123.7, 86.2, 52.1, 20.2, 17.2, 15.9

HRMS (ESI+)

Calculated for $C_{15}H_{18}O_2I$:	357.0352
Found:	357.0345

IR (thin film, cm^{-1})

3216, 3116, 2950, 2360, 2341, 1718, 1643, 1592, 1432, 1407, 1380, 1282, 1243, 1207, 1187, 1147, 1066, 1037, 960.

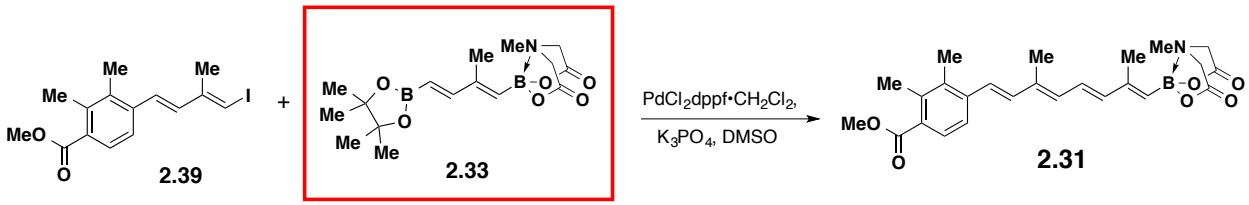

MIDA boronate 2.31. In a glovebox, to a 7 mL vial charged with **2.39** (125.4 mg, 0.35 mmol, 1.3 equiv.) and **2.33** (94.5 mg, 0.27 mmol, 1.0 equiv.) was added $PdCl_2dppf•CH_2Cl_2$ (11.1 mg, 0.014 mmol, 5 mol%), finely ground anhydrous K_3PO_4 (345 mg, 1.62 mmol, 6.0 equiv.), and DMSO (3.9 mL). The vial was sealed with a PTFE-lined cap and removed from the glove box. The vial was placed in a 45 °C aluminum heat block and maintained at that temperature with stirring for 24 h. The reaction was cooled to 23 °C and transferred to a separatory funnel, diluting with EtOAc (20 mL). The organic layer was washed with brine:H_2O (1:1, 2 x 40 mL) to remove DMSO, dried over $MgSO_4$, filtered, and concentrated *in vacuo* to afford a yellow-orange solid. The crude material was adsorbed onto Celite from an acetone solution and purified by SiO_2 chromatography (hexanes:EtOAc 1:1 → EtOAc) to afford **2.31** as a yellow solid (78.9 mg, 65%).

For characterization data, see section: Synthesis of MIDA boronate **2.31** via Original ICC Pathway.

Total Synthesis of Synechoxanthin **2.6**

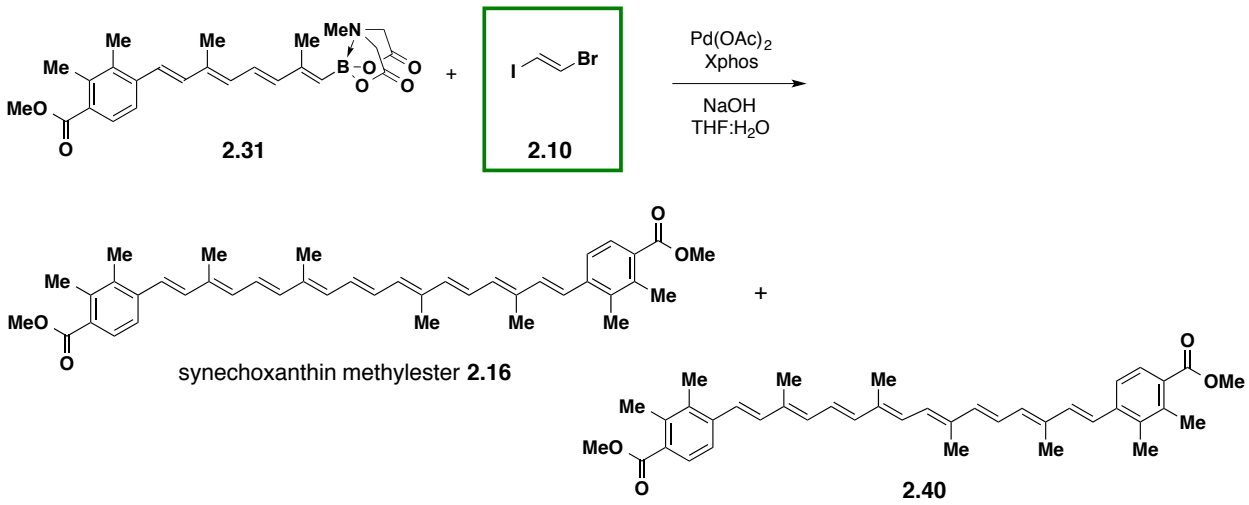

Synechoxanthin dimethyl ester 2.16.

Preparation of stock solutions. In a glovebox, a 7 mL vial was added XPhos and THF (8.6 mg/mL) to afford a clear solution. To another 7 mL vial was added $Pd(OAc)_2$ and THF (2.2 mg/mL) to afford a pale yellow-orange solution. To a separate 7 mL vial was added **2.10**[4] and THF (21.1 mg/mL).

The freshly prepared stock solutions were used in the following reaction:

In a glovebox, to a 7 mL vial charged with MIDA boronate **2.31** (100 mg, 0.22 mmol, 2.2 equiv.) was added solid NaOH (56 mg, 1.4 mmol, 14.0 equiv.) and THF (0.56 mL). The stock solution of **2.10** in THF (1.11 mL) was added to the reaction vial followed by the XPhos stock solution (0.56 mL, which contains 4.7 mg, 0.01 mmol, 10 mol%) and the $Pd(OAc)_2$ stock solution (0.56 mL, which contains 1.2 mg, 0.005 mmol, 5 mol%). The vial was sealed with a PTFE-lined septum cap, removed from the glovebox, and stirred at 23 °C for 5 min. Degassed DI H_2O (0.66 mL, 0.15 M) was added dropwise. The solution was stirred in a subdued light environment at 23 °C for 1 h. The reaction mixture was quenched with pH 7 phosphate buffer (10 mL) and transferred to a separatory funnel, rinsing with Et_2O (10 mL). The layers were separated and the aqueous layer was extracted with Et_2O (2 x 10 mL), dried over $MgSO_4$, filtered, and concentrated *in vacuo* to afford a bright orange-red solid. The resulting residue was adsorbed onto Celite from an acetone solution and purified by SiO_2 chromatography (hexanes:EtOAc 20:1 → 10:1) to afford a mixture of synechoxanthin dimethyl ester **2.16** as a red solid (32.6 mg, 53%) and byproduct **2.40** (13.1 mg, 21%). Due to difficulty in separating **2.40** from **2.16**, the semi-purified mixture was carried forward to the deprotection step.

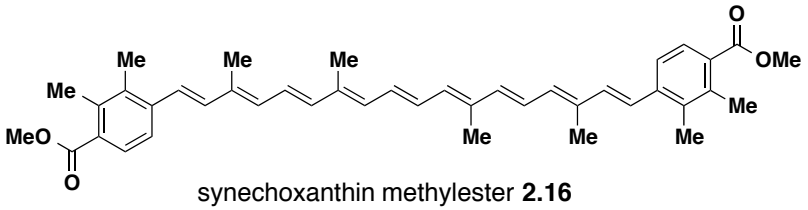

synechoxanthin methylester **2.16**

TLC (hexanes:EtOAc 4:1)

R_f = 0.57, visualized by visible light (orange)

^{1}H-NMR (500 MHz, CD_2Cl_2)

δ 7.57 (d, *J* = 8.5 Hz, 2H), 7.40 (d, *J* =8.5 Hz, 2H), 6.89 (d, *J* = 16.0 Hz, 2H), 6.83 (d, *J* = 16.0 Hz, 2H), 6.73-6.69 (m, 4H), 6.47 (d, *J* =15.0 Hz, 2H), 6.39 (d, *J* =11.5 Hz, 2H), 6.33 (d, *J* =10.0 Hz, 2H), 3.86 (s, 6H) 2.47 (s, 6H), 2.34 (s, 6H), 2.09 (s, 6H), 2.01 (s, 6H).

^{13}C-NMR (125 MHz, CD_2Cl_2)

169.3, 140.5, 139.0, 138.2, 137.2, 137.2, 136.2, 135.8, 134.3, 133.6, 130.8, 130.1, 127.6, 125.7, 125.4, 122.9, 52.2, 17.4, 15.9, 13.1, 12.9

HRMS (ESI+)

Calculated for $C_{42}H_{49}O_4$:	617.3631
Found:	617.3625

IR (thin film, cm^{-1})

3280, 3174, 3066, 2960, 2237, 1643 (broad), 1413

^{13}C NMR data for synechoxanthin dimethyl ester δ_C/ppm

Natural synechoxanthin dimethyl ester **2.16** (literature reference, 600 MHz, CD_2Cl_2)[9]	Synthetic synechoxanthin dimethyl ester **2.16** (500 MHz, CD_2Cl_2)
169.3	169.3
140.7	140.5
139.2	139.0
138.2	138.2
137.2	137.2
137.2	137.2
136.4	136.2
135.7	135.8
134.3	134.3
133.7	133.6
130.9	130.8
130.1	130.1
127.6	127.6
125.7	125.7
125.4	125.4
123.0	122.9
52.2	52.2
17.5	17.4
16.0	15.9
13.2	13.1
13.1	12.9

^{1}H NMR data for synechoxanthin dimethyl ester δ_H/ppm

Natural synechoxanthin dimethyl ester **2.16** (literature reference,[9] 600 MHz, CD_2Cl_2)	Synthetic synechoxanthin dimethylester **2.16** (500 MHz, CD_2Cl_2)
7.57	7.57
7.40	7.40
6.89	6.89
6.83	6.83
6.73	6.73-6.69
6.69	6.73-6.69
6.47	6.47
6.39	6.39
6.33	6.33
3.86	3.86
2.47	2.47
2.33	2.34
2.08	2.09
2.01	2.01

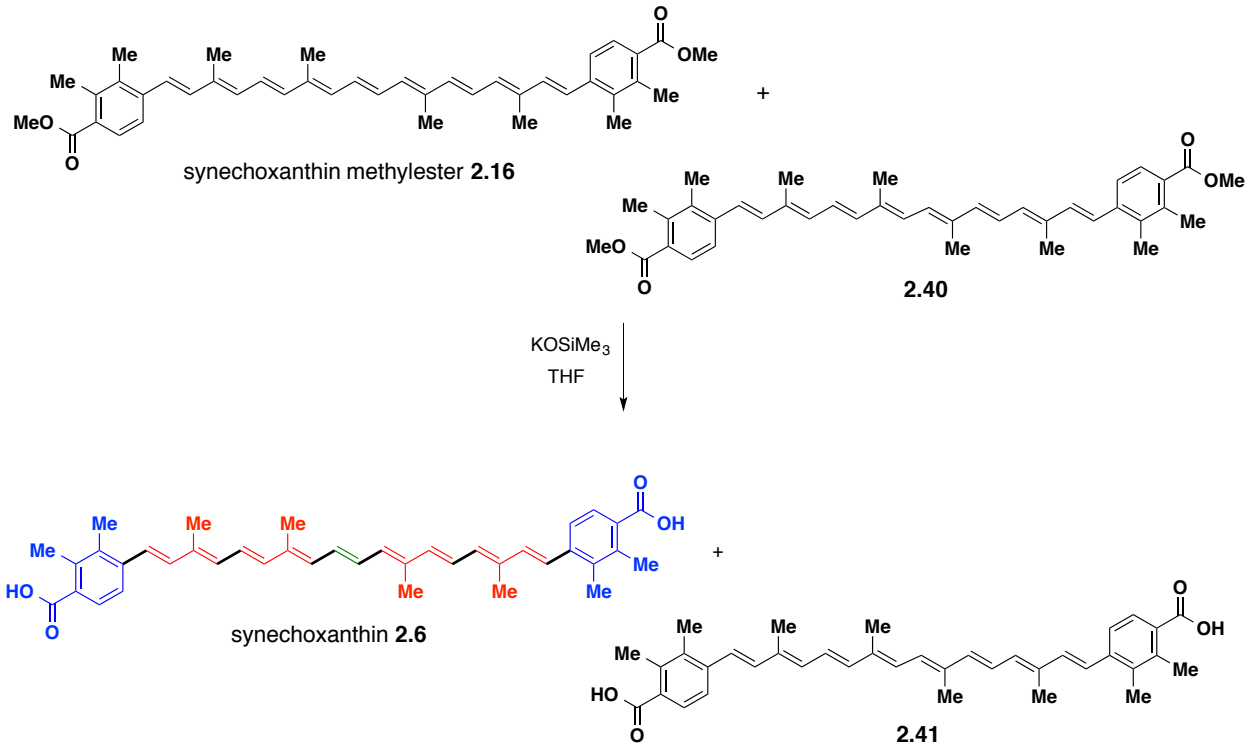

Synechoxanthin (2.6). In a glovebox, to a 20 mL vial charged with a mixture of synechoxanthin dimethyl ester **2.16** and octaene **2.40** (45.7 mg, 0.073 mmol, 1.0 equiv.) was added $KOSiMe_3$ (43 mg, 1.46 mmol, 20 equiv.) and THF (7.3 mL, 0.01 M). The vial was sealed with a PTFE-lined cap and removed from the glove box. The vial was placed in a 65 °C aluminum heat block and maintained at that temperature with stirring for 1 h. The reaction mixture was cooled to 23 °C and concentrated *in vacuo* to afford a bright red solid. The crude material was filtered through a small pad of celite with MeOH and DMSO and purified by preparatory HPLC (70% MeOH in 25 mM NH_4OAc buffer → 95% MeOH in 25 mM NH_4OAc buffer) to afford **2.41** as a bright red solid (7.6 mg, 14% over 2 steps) and synechoxanthin (**2.6**) as a bright red solid (16.6 mg, 53%, 28% over steps).

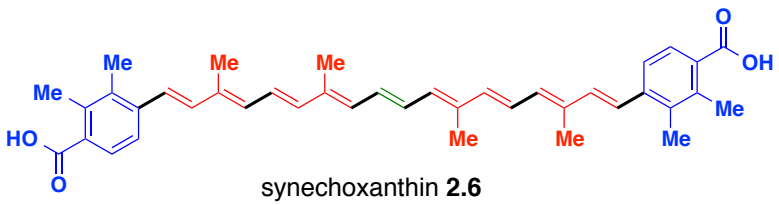

TLC (hexanes:EtOAc:AcOH 4:1:0.5)

R_f = 0.43, visualized by visible light (orange)

HPLC

tR = 10.2 min; flow rate = 25 mL/min, gradient of 70% → 95% MeOH in 25 mM NH_4OAc buffer over 10 min followed by 95% MeOH in 25 mM NH_4OAc buffer over 10 min. Detect at λ= 478 nm.

^{1}H-NMR (500 MHz, CD_3OD:DMSO-d_6, 1:1)

δ 7.37 (d, *J* = 8.0 Hz, 2H), 7.28 (d, *J* = 7.5 Hz, 2H), 6.91 (d, *J* = 16.0 Hz, 2H), 6.84 (d, *J* = 16.0 Hz, 2H), 6.78-6.73 (m, 4H), 6.49 (d, *J* = 15.0 Hz, 2H), 6.49 (d, *J* = 11.5 Hz, 2H), 6.39 (d, *J* = 8.0 Hz, 2H), 2.37 (s, 6H), 2.30 (s, 6H), 2.07 (s, 6H), 2.00 (s, 6H). The proton signal for the carboxylic acid (2H) was not observed.

^{13}C-NMR (150 MHz, DMSO-d_6)

δ 16.9, 15.3, 12.7, 12.5 (partial assignment due to low solubility of **1** in DMSO)

HRMS (ESI+)

Calculated for $C_{40}H_{44}O_4Na$: 611.3137

Found: 611.3130

IR (thin film, cm^{-1})

3461, 3419, 3365, 3234, 3089, 2919, 2360, 2132, 1751, 1644, 1047, 1025, 991.

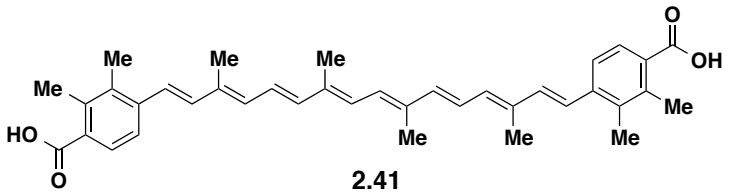

2.41

TLC (hexanes:EtOAc:AcOH 4:1:0.5)

R_f = 0.43, visualized by visible light (orange)

HPLC

tR = 9.4 min; flow rate = 25 mL/min, gradient of 70% → 95% MeOH in 25 mM NH_4OAc buffer over 10 min followed by 95% MeOH in 25 mM NH_4OAc buffer over 10 min. Detect at λ= 478 nm.

^{1}H-NMR (500 MHz, CD_3OD: DMSO-d_6, 1:1)

δ 7.37 (d, *J* = 8.0 Hz, 2H), 7.27 (d, *J* = 8.0 Hz, 2H), 6.91 (d, *J* = 15.5 Hz, 2H), 6.85 (d, *J* = 15.5 Hz, 2H), 6.79-6.74 (m, 2H), 6.60 (s, 2H), 6.57 (d, *J* = 15.0 Hz, 2H), 6.43 (d, *J* = 11.0 Hz, 2H), 2.38 (s, 6H), 2.29 (s, 6H), 2.07 (s, 6H), 2.01 (s, 6H). The proton signal for the carboxylic acid (2H) was not observed.

HRMS (ESI+)

Calculated for $C_{38}H_{42}O_4Na$:	585.2981
Found:	585.2979

In order to verify the structure of byproduct **SI-9**, **SI-10** was subjected to methylation:

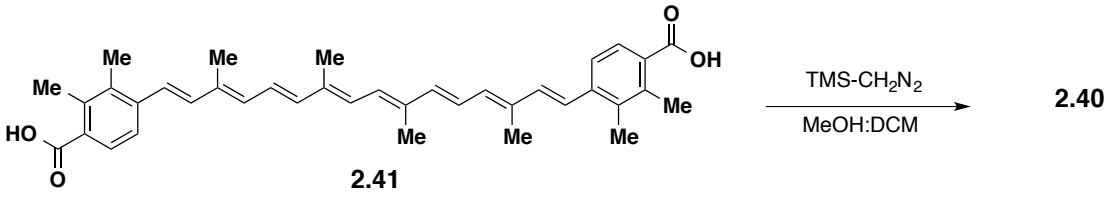

Octaene 2.40. A 1.5-mL vial was charged with **2.41** (3 mg, 0.005 mmol, 1.0 equiv.) and flushed with N_2. MeOH:DCM (1:1. 0.5 mL) was added and the reaction vial was cooled to 0 ^oC. TMS-diazomethane (2.0 M in ether, 0.2 mL) was added dropwise and stirred at 0 ^oC for 30 min. The reaction was warmed to 23 ^oC for 1 h. The reaction was quenched by the addition of a few drops of acetic acid and the mixture was concentrated *in vacuo* to afford a bright red solid. The crude material was dissolved in dichloromethane and filtered through a plug of Celite and silica gel and concentrated *in vacuo* to afford **2.40** as a bright red solid (2 mg, 64%).

TLC (hexanes:EtOAc 4:1)

R_f = 0.57, visualized by visible light (orange)

^{1}H-NMR (500 MHz, CD_2Cl_2)

δ 7.57 (d, *J* = 8.5 Hz, 2H), 7.40 (d, *J* =8.0 Hz, 2H), 6.89 (d, *J* = 16.0 Hz, 2H), 6.84 (d, *J* = 15.5 Hz, 2H), 6.74 (dd, *J* = 15.0 Hz, *J* = 11.5 Hz, 2H), 6.55 (s, 2H), 6.53 (d, *J* =15.0 Hz, 2H), 6.40 (d, *J* =11.5 Hz, 2H), 3.86 (s, 6H) 2.47 (s, 6H), 2.33 (s, 6H), 2.09 (s, 6H), 2.03 (s, 6H).

^{13}C-NMR (125 MHz, CD_2Cl_2)

169.3, 140.6, 139.5, 138.3, 137.5, 137.2, 136.2, 135.8, 134.3, 130.1, 129.4, 127.6, 125.7, 125.3, 122.9, 52.1, 17.4, 15.9, 13.1, 12.9

HRMS (ESI+)

Calculated for $C_{40}H_{46}O_4Na$: 613.3294

Found: 613.3291

IR (thin film, cm^{-1})

2920, 2848, 2364, 2341, 1714, 1589, 1554, 1431, 1236, 1146, 957.

II. TOTAL SYNTHESIS OF RENIERAPURPURIN

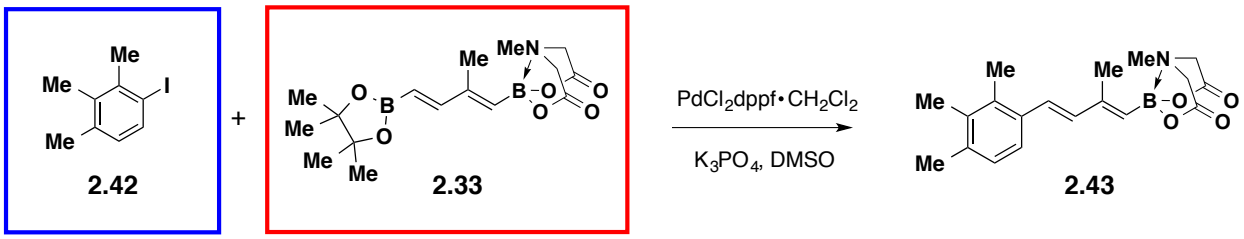

MIDA boronate 2.43. In a glovebox, to a flame-dried 20 mL vial charged with aryl iodide **2.42** (150 mg, 0.610 mmol, 1.2 equiv.) and bisborylated diene **2.33** (177 mg, 0.508 mmol, 1.0 equiv.) was added $PdCl_2$(dppf)•DCM (20.7 mg, 0.0254 mmol, 5 mol%), finely ground anhydrous K_3PO_4 (647 mg, 3.05 mmol, 6.0 equiv.) and DMSO (4 mL). The vial was sealed with a PTFE-lined cap and removed from the glove box. The vial was stirred at 45 °C in an aluminum heat block for 24

h and was then cooled to 23 °C. The reaction was transferred to a separatory funnel, diluting with 10 mL EtOAc. The organic layer was washed with brine:H_2O (1:1, 2 x 20 mL) to remove DMSO, dried over $MgSO_4$, filtered, and concentrated *in vacuo* to afford an orange oil. The crude material was adsorbed onto Celite from an acetone solution and purified by SiO_2 flash chromatography (petroleum hexanes:EtOAc 1:1 → EtOAc) to afford MIDA boronate **2.43** as a light orange solid (121 mg, 70%).

TLC (EtOAc)

R_f = 0.57, visualized by UV and stained by $KMnO_4$

^{1}H-NMR (500 MHz, acetone-d_6)

δ 7.23 (d, *J* = 7.9Hz, 1H), 6.95 (d, *J* = 8.1, 1H), 6.90 (d, *J* = 15.9, 1H), 6.69 (d, *J* = 15.9, 1H), 5.51 (s, 1H), 4.22 (d, *J* = 17.0, 2H), 4.06 (d, *J* = 16.9, 2H), 3.06 (s, 3H), 2.27 (s, 3H), 2.24 (s, 3H), 2.17 (s, 3H), 2.07 (s, 3H).

HRMS (ES+)

Calculated for $C_{19}H_{25}BNO_4$: 342.1877

Found: 342.1878

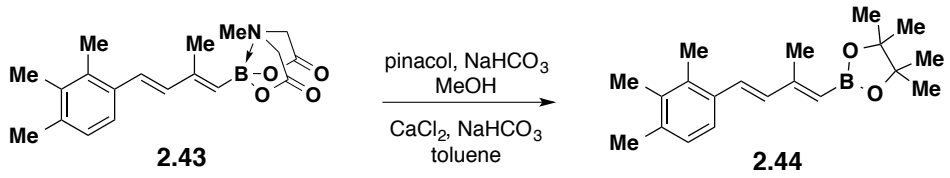

Pinacol boronic ester 2.44. To a 7 mL vial equipped with a stirbar was added MIDA boronate **2.43** (59.6 mg, 0.175 mmol, 1.0 equiv.), pinacol (41.3 mg, 0.349 mmol, 2.0 equiv.), and solid $NaHCO_3$ (73.4 mg, 0.874 mmol, 5.0 equiv.). The vial was sealed with a PTFE- lined cap, flushed with nitrogen, and MeOH (0.9 mL) was added via syringe to afford a cloudy light orange solution. The vial was stirred at 45 °C in an aluminum heat block for 3 h and was then cooled to 23 °C. The reaction mixture was filtered through a pad of Celite, rinsing with Et_2O, and the solution concentrated *in vacuo* in a 50 mL round bottom flask. To remove residual pinacol, finely ground $CaCl_2$ (271 mg, 2.45 mmol, 14 equiv.), solid $NaHCO_3$ (73.4 mg, 0.874 mmol, 5.0 equiv.), and toluene (5.8 mL) were added to the flask containing the crude material. The

resulting cloudy suspension was stirred at 23 °C for 1 h and filtered through a pad of Celite, rinsing with Et_2O, and concentrated *in vacuo* to afford an orange oil. The crude material was adsorbed onto Celite from an acetone solution and purified by SiO_2 flash chromatography (hexanes:EtOAc 9:1) to afford aryl pinacol boronic ester **2.44** as a light orange solid (46.4 mg, 85%).

TLC (hexanes:EtOAc 9:1)

R_f = 0.25, visualized by UV and stained by $KMnO_4$

^{1}H-NMR (500 MHz, acetone-d_6)

δ 7.26 (d, *J* = 8.0Hz, 1H), 7.05 (d, *J* = 15.9, 1H), 6.97 (d, *J* = 7.8, 1H), 6.71 (d, *J* = 15.8, 1H), 5.40 (s, 1H), 2.28 (s, 3H), 2.25 (s, 3H), 2.23 (s, 3H), 2.18 (s, 3H), 1.26 (s, 12H).

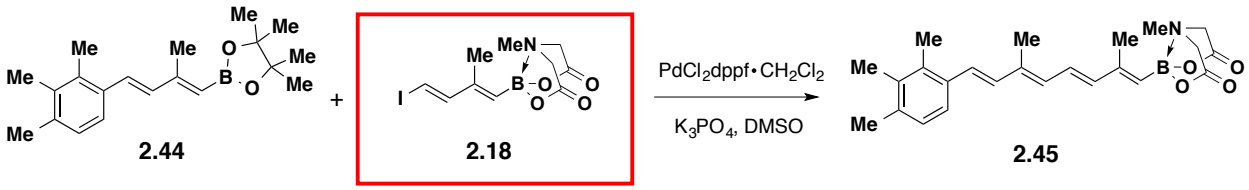

Tetraenyl MIDA boronate 2.45. In a glovebox, to a flame-dried 20 mL vial equipped with a stirbar and charged with pinacol boronic ester **2.44** (322 mg, 1.03 mmol, 1.2 equiv.) and dienyl iodide **2.18** (300 mg, 0.860 mmol, 1.0 equiv.) was added $PdCl_2$(dppf)•DCM (35.1 mg, 0.0430 mmol, 5 mol%), finely ground anhydrous K_3PO_4 (1.10 g, 5.16 mmol, 6.0 equiv.) and DMSO (5.8 mL). The vial was sealed with a PTFE- lined cap and removed from the glove box. The vial was stirred at 45 °C in an aluminum heat block for 24 h and was then cooled to 23 °C. The reaction was transferred to a separatory funnel, diluting with 15 mL EtOAc. The organic layer was washed with brine:H_2O (1:1, 2 x 30 mL) to remove DMSO. The aqueous phase was extracted with EtOAc (1 x 15 mL). The combined organic layers were dried over $MgSO_4$, filtered, and concentrated *in vacuo* to afford an orange oil. The crude material was adsorbed onto Celite from an acetone solution and purified by SiO_2 flash chromatography (hexanes:EtOAc 1:1 → EtOAc) to afford tetraenyl MIDA boronate **2.45** as an orange solid (137 mg, 39%).

TLC (EtOAc)

R_f = 0.26, visualized by UV (λ = 365 nm)

^{1}H-NMR (500 MHz, acetone- d_6)

δ 7.27(d, J = 8.0Hz, 1H), 6.96 (d, J = 7.9Hz, 1H), 6.93 (d, J = 15.7Hz, 1H), 6.75 (d, J = 16.1 Hz, 1H), 6.42 (d, J = 15.3 Hz, 1H), 6.32 (d, J = 11.3 Hz, 1H), 5.46 (s, 1H), 4.21 (d, J = 16.9 Hz, 2H), 4.04 (d, J =17.0 Hz, 2H), 3.03 (s, 3H), 2.28 (s, 3H), 2.24 (s, 3H), 2.17 (s, 3H), 2.06 (s, 3H), 2.02 (s, 3H).

HRMS (ES+)

Calculated for $C_{24}H_{31}BNO_4$:	408.2346
Found:	408.2352

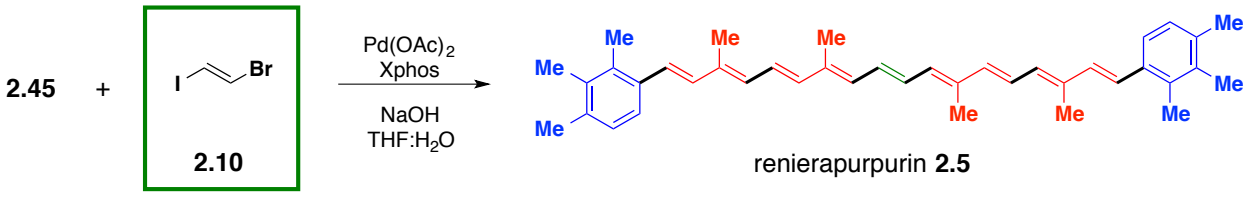

Renierapurpurin (2.5).

Preparation of stock solutions. In a glovebox, to a 7 mL vial was added XPhos and THF (4.3 mg/mL) to afford a clear solution. To a second 7 mL vial was added $Pd(OAc)_2$ and THF (1.1 mg/mL) to afford a pale yellow-orange solution. To a separate 7 mL vial was added **2.10** and THF (21.0 mg/mL).

The freshly prepared stock solutions were used in the following reaction: In a glovebox, to a 7 mL vial equipped with stirbar and charged with tetraenyl MIDA boronate **2.45** (19.7 mg, 0.0484 mmol, 2.2 equiv.) was added finely ground solid NaOH (12 mg, 0.307 mmol, 14.0 equiv.). The stock solution of **2.10** in THF (0.244 mL, containing 5.12 mg, 0.0220 mmol, 1.0 equiv.) was added to the reaction vial followed by the XPhos stock solution (0.244 mL, containing 1.05 mg, 0.00220 mmol, 10 mol%) and the $Pd(OAc)_2$ stock solution (0.244 mL, containing 0.268 mg, 0.00110 mmol, 5 mol%). The vial was sealed with a PTFE-lined septum cap, removed from the glovebox, and stirred at 23 °C for 5 min. Degassed DI H_2O (0.147 mL, 0.15 M) was added dropwise. The solution was stirred in a subdued light environment at 23 °C for 1 h. The reaction mixture was quenched with pH 7 phosphate buffer (10 mL) and transferred to a separatory

funnel with Et_2O (10 mL). The layers were separated and the aqueous layer was extracted with Et_2O (2 x 10 mL), dried over $MgSO_4$, filtered, and concentrated *in vacuo* to afford a dark red solid. The resulting residue was adsorbed onto Celite from an acetone solution and purified by SiO_2 chromatography (hexanes) to afford **2.5** (isolated yield not yet obtained, semi-purified yield containing homocoupled byproduct is ~20% in this unoptimized condition).

TLC (hexanes:EtOAc 10:1)

R_f = 0.89, visualized by visible light (orange)

^{1}H-NMR (500 MHz, CD_2Cl_2)

δ 7.25(d, *J* = 8.0Hz, 1H), 6.97 (d, *J* = 8.5Hz, 1H), 6.89 (d, *J* = 15.5, 1H), 2.30 (s, 3H), 2.28 (s, 3H), 2.21 (s, 3H), 2.07 (s, 3H). All peaks not assigned.

HRMS (ES+)

Calculated for $C_{40}H_{48}$:	528.3756
Found:	528.3763

III. LIPOPEROXIDATION ASSAY

Materials. 1-palmitoyl-2-oleoyl-sn-glycero-3-phosphocholine (16:0-18:1 PC, POPC) was obtained as a 25 mg/mL solution in $CHCl_3$ from Avanti Polar Lipids (catalog number 850457C), and 1-stearoyl-2-arachidonoyl-sn-glycero-3-phosphocholine (18:0-20:4 PC, PUFA) was obtained as a 10 mg/mL solution in $CHCl_3$ from Avanti Polar Lipids (catalog number 850469C) and were stored at -20 ^oC under an atmosphere of dry nitrogen and used within 1.5 months. Prior to preparing the lipid film, the solution was warmed to ambient temperature to prevent condensation from contaminating the solution. Astaxanthin was a generous donation from BASF. Synechoxanthin was synthesized as above and was HPLC purified to >95% prior to use. β-carotene was purchased from Sigma Aldrich.

General Liposome Preparation

Preparation of lipid films: To separate 12 x 75 mm test tubes was added 150 μL POPC solution and 125 μL PUFA solution via Hamilton syringe. The solvent was removed under a gentle stream of nitrogen and the resulting lipid film was stored under high vacuum for a minimum of 12 h prior to use to remove any residual solvent.

Preparation of LUVs: The lipid film was hydrated with 300 μL 150 mM KCl/0.5 mM HEPES pH 7.4 aqueous buffer (K buffer) and vortexed vigorously for 1 minute (until the film no longer coated the sides of the test tube) to form a suspension of multilamellar vesicles (MLVs). The resulting lipid suspension was transferred into a Hamilton 1 mL gastight syringe and the syringe was placed in an Avanti Polar Lipids Mini-Extruder with a second collection syringe on the opposite side. The lipid solution was then passed through a 0.20 μm Whatman polycarbonate filter (supported on both sides by a 10 mm Whatman drain disk) 21 times. The resulting large unilamellar vesicle (LUV) suspension was collected in the syringe that did not contain the original suspension of MLVs to prevent the carryover of MLVs into the LUV solution. All LUV suspensions were added to separate clean 12 x 75 mm test tubes.

Preparation of blank sample: Blank liposome samples were directly purified following extrusion. The LUVs were purified by gel exclusion chromatography with a Sephadex G50-150 column (1 cm column, 1.0 g unswelled resin, resin swelled with K buffer, eluted with K buffer). The purified LUVs were collected in 13 x 100 mm test tubes for phosphorous analysis and dilution.

Preparation of carotenoid-containing samples: Carotenoid solutions were prepared. Astaxanthin and β-carotene stock solutions were prepared in uninhibited THF, and stock solutions for octaene **2.41** and synechoxanthin **2.6** were prepared in DMSO + 5% Et_3N : THF solvent mixture. To a vortexing suspension of LUVs under a stream of dry nitrogen was dropwise added appropriate μL of the carotenoid stock solution.

Sample concentrations used are as follows:

- Astaxanthin in THF (8.3 mM) prepared, 60 μL addition led to 8.3% incorporation.
- β-carotene in THF (25 mM) prepared, 50 μL addition led to 6.4% incorporation.
- Octaene **2.41** in DMSO + 5% Et_3N : THF (1:1) (10 mM) prepared, 60 μL addition led to 3.2% incorporation.
- Synechoxanthin **2.6** [0.783 mg dissolved in DMSO + 5% Et_3N (100 uL) + THF (50 uL) + Et_3N (3 uL)], 60 μL addition led to 3.9% incorporation.
- Blank: 50 μL of DMSO + 5% Et_3N : THF (1:1) was added as an additional control.

All carotenoid-impregnated LUVs were purified by gel exclusion chromatography with a Sephadex G50-150 column (1 cm column, 1.0 g unswelled resin, resin swelled with K buffer, eluted with K buffer). Separate columns were used for astaxanthin, β-carotene, octaene, and synechoxanthin containing liposomes. The purified carotenoid containing LUVs were collected in 13 x 100 mm test tubes for phosphorous analysis and dilution.

Determination of phosphorus content and liposome dilution

The total phosphorous content for each liposome suspension was determined to allow dilution to 1 mM phosphorous. Determination of total phosphorus was adapted from the report of Chen and coworkers.[10]

Preparation of a standard curve: To 7 mL vials in triplicate were added the following amount of phosphorus standard solution (0.65 mM phosphorus as KH_2PO_4, Sigma Aldrich, catalog number P3869): 20 μL, 40 μL, 60 μL, 80 μL, 100 μL, and 120 μL. To these vials and to 3 separate vials containing no phosphorus to be used as blanks, was added 450 μL of 8.9 M aqueous H_2SO_4. The samples were incubated open to ambient atmosphere in a 225 °C aluminum heating block for 25 min and then removed to 23 °C for 5 min. To each sample was added 150 μL of 30% w/v aqueous hydrogen peroxide and the vials were returned to the 225 °C heating block for 30 min after which the samples were removed to 23 °C for 5 min. To each sample was added 4.0 mL DI H_2O. To each vial was then added 500 μL of 2.5% w/v ammonium molybdate tetrahydrate. The vials were capped and the resulting mixtures were vortexed briefly and vigorously. Subsequently,

500 μL of 10% w/v L-(+)-ascorbic acid was added to each vial. The vials were capped and the resulting mixtures were vortexed briefly and vigorously. The capped vials were then placed in a 100 °C aluminum heating block for 7 min. The samples were removed to 23 °C and cooled for approximately 20 minutes to 23 °C prior to analysis by UV/Vis spectroscopy. Total phosphorus was determined by observing the absorbance at 820 nm. A standard curve was prepared by plotting μmol of phosphorus vs the absorbance at 820 nm.

Analysis of phosphorous content in liposomes: To 7 mL vials in triplicate was added 10 μL of the purified LUV suspensions. Three separate vials containing no LUVs to be used as blanks were prepared. Total phosphorous content in each LUV suspension was analyzed as described above. Total phosphorus was determined by observing the absorbance at 820 nm and comparing these values to the standard curve. The liposome suspensions were each diluted to a phosphorous concentration of 1 mM.

Determination of carotenoid content

To HPLC vials were added 100 μL of the 1 mM liposome suspension and 200 μL of 4:1:1 acetone : MeOH : 0.2 M BHT in EtOH. The mixtures were shaken to give clear solutions. The samples were analyzed by analytical HPLC (Agilent Technologies, 1200 Series) and the carotenoid content was determined by comparing the peak area to standard curves prepared from carotenoid solutions of known concentrations.

HPLC method: Agilent Zorbax Eclipse XDB-C18 column, 75 μL sample injection, flow 2 mL/min.

Astaxanthin: 90 : 10, MeOH : H_2O; detect at 478 nm
β-carotene: 25 : 40 : 35, THF : MeCN : MeOH; detect at 464 nm
Octaene **2.41**: 70 : 30, MeOH : 25 mM NH_4OAc: detect at 478 nm
Synechoxanthin **2.6**: 70 : 30, MeOH : 25 mM NH_4OAc: detect at 478 nm

Copper-based lipid peroxidation assay (TBARS)

To 7 mL vials in triplicate was added 2 mL of the 1 mM liposome suspensions. To each sample was added 20 µL of 11 mM $CuCl_2$ in DI H_2O. The vials were capped and incubated in a 37 °C aluminum heating block. At 1.5 h intervals (including an initial time point directly following $CuCl_2$ addition), the vials were inverted to mix the suspensions and aliquots were removed from each sample and analyzed for TBARS. At each timepoint, a 100 µL aliquot was removed from each liposome assay sample to a 1.5 mL HPLC vial containing 500 µL of TBA solution (0.4% w/v thiobarbituric acid in 0.1 M NaOAc, pH 3.5). The vials were capped and incubated in a 100 °C aluminum heating block for 15 min. The samples were removed to 23 °C and cooled for approximately 10 min to 23 °C prior to analysis by HPLC.

HPLC method: Agilent Zorbax Eclipse XDB-C18 column, inject 75 µL sample, flow 2 mL/min. TBA/MDA adduct: 72 : 17 : 11, 50 mM KH_2PO_4 : MeOH : MeCN; detect at 535 nm.

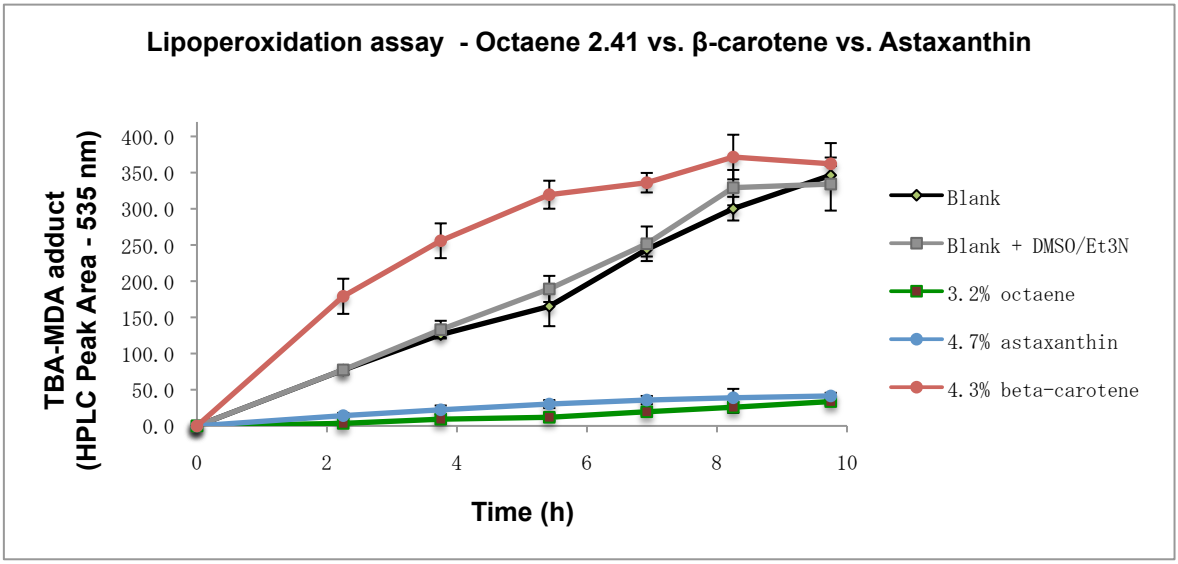

Figure 2-7. TBA-MDA adduct formation over time was evaluated with octaene **2.41**, β-carotene and astaxanthin-incorporated liposomes. Each sample was run in triplicate (plotted as average ±1 standard deviation). Peak area of 400 ≈ 6 x 10^{-3} mM TBA-MDA adduct. DMSO + 5% Et_3N control had no effect compared to the blank liposome.

Control experiments

Following the standard protocols for copper-based lipid peroxidation assay, formation of MDA-TBA adduct was measured over time while incubated at 100 °C (Figure 2-8A). Following the standard liposome preparation and carotenoid incorporation, changes in percent incorporation of astaxanthin was monitored after subsequent size-exclusion columns (Figure 2-8B). In addition, changes in percent incorporation of the carotenoid content was assessed at two different temperatures, 37 ^{o}C (incubation temperature) and 3 ^{o}C (fridge temperature) over the course of 65 h following the general carotenoid content determination protocol (Figure 2-8C).

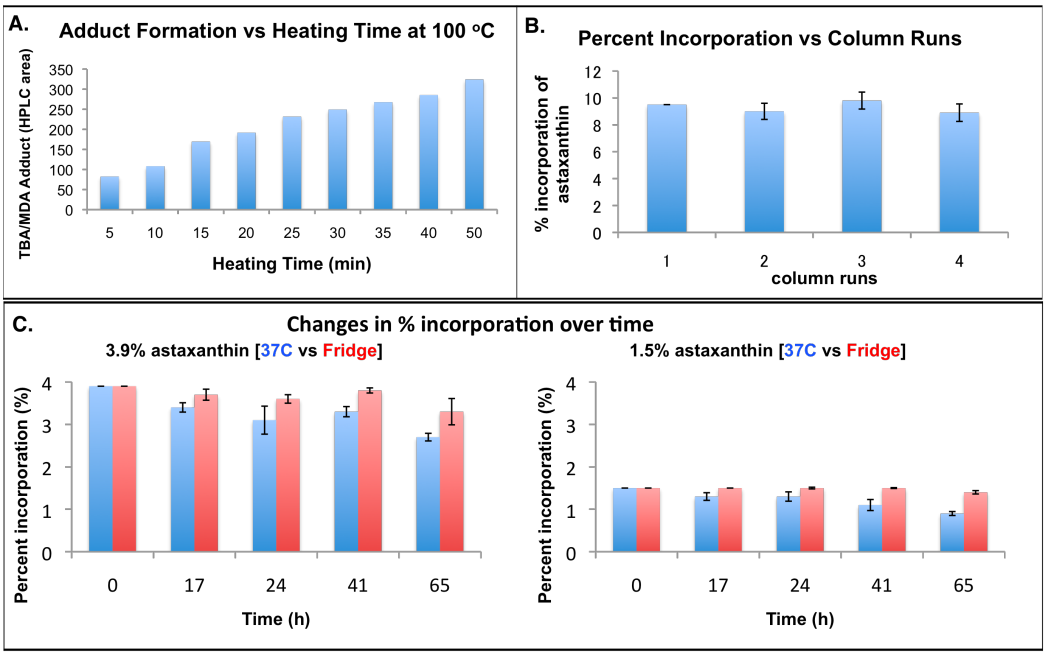

Figure 2-8. Control experiments for TBARS assay. **A.** Longer heating times increase production of MDA. **B.** The change in percent incorporation of astaxanthin in liposomes is not affected by the number of times the liposome is passed through a size exclusion column. **C.** Changes in percent incorporation of astaxanthin were measured at two different temperatures (37 ^{o}C and 3 ^{o}C) over the course of 3 days. Error bars = ±1 standard deviation, runs in duplicate.

IV. REFERENCES

[1] Pangborn, A. B.; Giardello, M. A.; Grubbs, R. H.; Rosen, R. K.; Timmers, F. J. *Organometallics* **1996**, *15*, 1518-1520.

[2] Kaiser, F.; Schwink, L.; Velder, J.; Schmalz, H-G. *Tetrahedron* **2003**, *59*, 3201-3217.

[3] Negishi, E.; Alimardanov, A.; Xu, C. *Org. Lett.* **2000**, *2*, 65-67.

[4] Stavber, S.; Kralj, P.; Zupan, M. *Synlett* **2002**, *4*, 598 - 600.

[5] Lee, S. J.; Anderson, T. M.; Burke, M. D. *Angew. Chem. Int. Ed.* **2010**, *49*, 8860-8863.

[6] Struble, J. R.; Lee, S. J.; Burke, M. D. *Tetrahedron* **2010**, *66*, 4710-4718.

[7] Woerly, E. M.; Cherney, A. H.; Davis, E. K.; Burke, M. D. *J. Am. Chem. Soc.* **2010**, *132*, 6941-6943.

[8] Still, W. C.; Kahn, M.; Mitra, A. *J. Org. Chem.* **1978**, *43*, 2923.

[9] Graham, J. E.; Lecomte, J. T.; Bryant, D. A. *J. Nat. Prod.* **2008**, *71*, 1647-1650.

[10] Chen, P. S.; Toribara, T. Y.; Warner, H. *Anal. Chem.* **1956**, *28*, 1756.

CHAPTER 3
SYNTHESIS OF SMALL MOLECULES VIA A COMMON AND AUTOMATED ICC PLATFORM

ABSTRACT

More than a century of advances have enabled the laboratory synthesis of many small molecules. However, because the strategies and reactions employed are usually customized to each target or class of targets, the synthesis process has remained a complex and time-intensive process practiced exclusively by specialists. As a collective result, synthesis is still the slow step in efforts to access the extraordinary functional potential that these compounds possess. Building on the work described in Chapter 2, this chapter describes a major step toward generalizing and automating the iterative cross-coupling (ICC) strategy to access a range of different small molecules. Specifically, this chapter describes the collaborative effort to develop a small molecule synthesizer. The key to establishing this automated platform for small molecule synthesis was the discovery that *N*-methyliminodiacetic acid (MIDA) boronates have general binary elution properties on silica gel, which permits any intermediate that contains this functional group motif to be automatically purified via a novel type of catch-and-release chromatography. This small molecule synthesizer employed cross-coupling reactions to iteratively assemble a variety of MIDA boronate building blocks into many different types of small molecules including materials, pharmaceuticals, complex natural products, and their derivatives. In concert with the development of the synthesizer, the ICC platform was expanded to include C-N and Csp^3-Csp^2 bond formations, dramatically increasing the chemical space of the small molecule targets that can be accessed using this synthesis strategy.

Dr. Steven G. Ballmer contributed to the construction and implementation of the current small molecule synthesizer and conducted the majority of the automated syntheses in collaboration with Gregory F. Morehouse and Michael J. Schmidt. For small molecule targets listed in Figures 3-8 and 3-11, Dr. Steven G. Ballmer (oligothiophene **3.9**, BTP2 **3.78**), Junqi Li (oligophenylene **3.14**, crocacin C **3.22**), and Gregory F. Morehouse (β-parinaric acid **3.26**) contributed to the synthesis of non-commercial building blocks and performed manual experiments used to determine and optimize reaction conditions used for automation. Gram-scale synthesis of building block **3.27** was accomplished in collaboration with Matthew J. Clark.

Manual optimization of ratanhine library synthesis was conducted in collaboration with Junqi Li. Junqi Li executed the post-automation manual deprotections for the ratanhine library. Manual experiments for cyclic target **3.83** were performed in collaboration with Andrea M. E. Palazzolo, and synthesis of building block **3.101** was performed in collaboration with Jonathan W. Lehmann. Manual experiments for citreofuran **3.79** and indene core **3.81** were conducted by Junqi Li. Dr. Eric P. Gillis contributed to the design and construction of the initial synthesizer and early configurations of the software.

3-1 AUTOMATING ITERATIVE CROSS-COUPLING TOWARD A GENERAL PLATFORM FOR SMALL MOLECULE SYNTHESIS

As described in Chapter 1, peptides, oligonucleotides, and oligosaccharides can now be synthesized using automated synthesis platforms.[1] These advances have increased the efficiency with which these compounds can be prepared and even extended this access to non-specialists. Developing a similarly generalized and automated platform capable of accessing many different types of small molecules is challenging because of the high level of structural diversity that this class of compounds represents. However, these and many others small molecules are inherently modular and many of them can be viewed as a collection of building blocks linked by C-C or C-heteroatom bonds. In fact, many materials, pharmaceuticals, and biological probes represent oligomers of aryl or heteroaryl fragments. Many natural products are inherently modular because they are biosynthesized via iterative assembly of common building blocks. Even many topologically complex macrocyclic and polycyclic natural products are biosynthetically derived from relatively simple and modular linear precursors that are then cyclized into the final framework.[2]

To harness this modularity, ICC strategy was developed by Dr. Eric Gillis in 2007 to enable the precise iterative assembly of haloboronic acid building blocks employing *N*-methyliminodiacetic acid (MIDA) as a protecting group that can reversibly attenuate the reactivity of a boronic acid, similar to the way a fluorenylmethoxycarbonyl (Fmoc) group protects an amine.[3] This permits recursive C–C bond formation between a free boronic acid and the halide terminus of a MIDA protected haloboronic acid building block using the Suzuki-Miyaura cross-coupling,[4] an increasingly general reaction for making certain types of C–C bonds. Since its initial report, this ICC strategy has been applied to the manual synthesis of many different types of small molecules including natural products,[5] natural product derivatives,[6] and pharmaceuticals.[7] More than 160 MIDA boronate building blocks are now commercially available from Sigma Aldrich, extending the use of this method to a wider range of scientists.

Even with a general strategy and commercially available building blocks in hand, the process of making small molecules still requires considerable amount of person time. This provides very little time for the researcher to explore other aspects of the small molecule discovery process while the synthesis is in progress. We recognized that if we wanted to accelerate the understanding of small molecule function, the synthesis process needed to be

simple and ideally, automated. Importantly, it was crucial to have a general platform capable of accessing a wide range of small molecules instead of a customized platform specific for each target. Inspired by the way peptides, oligonucleotides, and oligosaccharides can now be made in a fully automated fashion, we questioned whether automating the ICC strategy would provide a starting point to achieving a similarly general and automated platform for small molecule synthesis.

3-2 CHALLENGES FOR AUTOMATION

Transforming the ICC platform into a fully automated process foremost required the development of a general strategy for purifying synthetic intermediates. Peptides, oligonucleotides and oligosaccharides, all contain common functional group handles for attachment to a solid support (Figure 3-1A). This enables automated purification by solid-phase synthesis, in which excess reagents and byproducts are removed via simple filtration (Figure 3-1B).[1] In contrast, small molecules do not contain such a universal functional group handle, thus cannot be generally purified using solid-phase purification (Figure 3-2A).[8] We noted, however, that all of the intermediate coupling products in an ICC-based synthesis contain a MIDA boronate motif (Figure 3-2B).

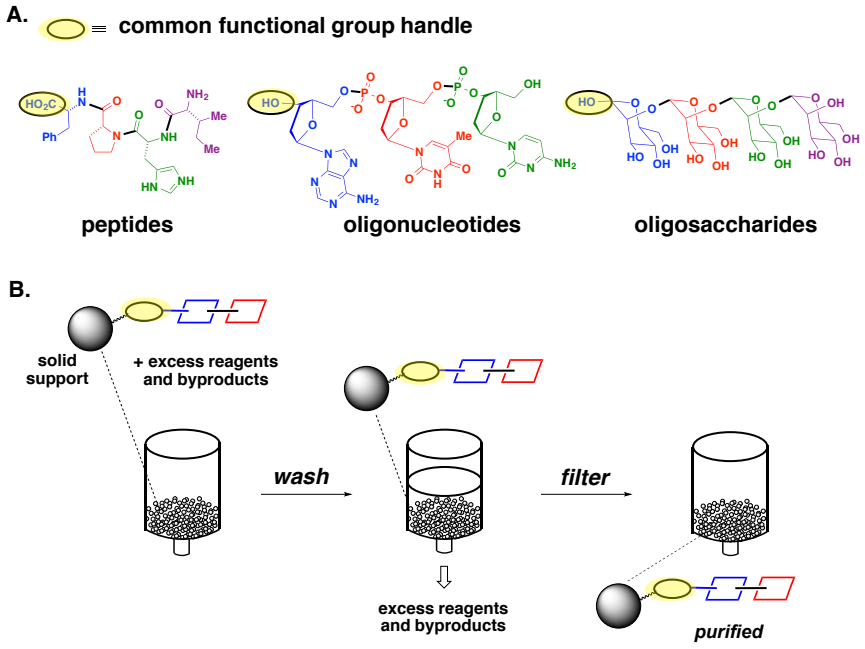

Figure 3-1. A. Peptides, oligonucleotides, and oligosaccharides all contain common functional group handles for attachment to a solid support. **B.** Schematic of an automated solid-phase purification.

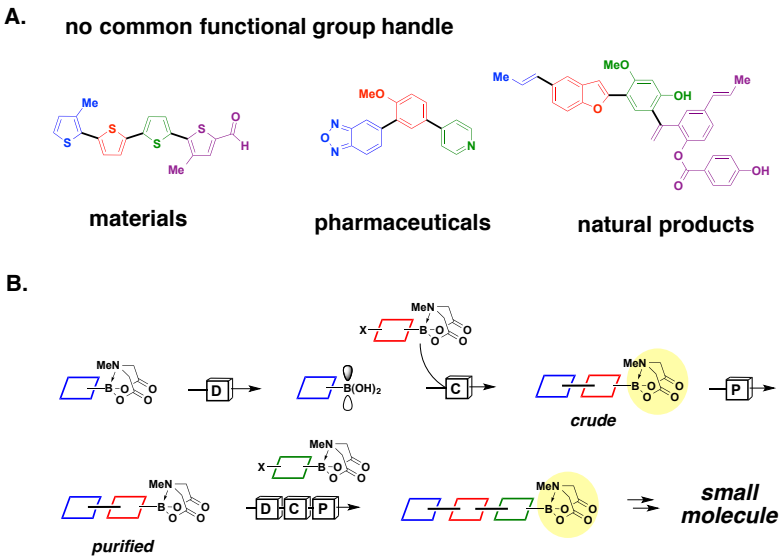

Figure 3-2. A. Small molecules do not contain a common functional group handle that is required for generalized purification via solid-phase synthesis. **B.** MIDA boronate serves as a common functional group handle in an ICC-based synthesis. [D] = deprotection, [C] = cross-coupling, [P] = purification.

This prompted us to develop a general strategy for purifying compounds that contain this functional group. In this vein, we had observed ad hoc that certain MIDA boronates demonstrate binary elution properties on silica gel with specific pairs of eluents. We thus questioned whether we could identify a single pair of eluents in which all MIDA boronates would demonstrate such behaviour and thereby enable generalized purification via a novel type of catch-and-release chromatography.

Silica gel chromatography is a standard method for purifying small molecules, but variable affinities of different compounds for this stationary phase typically necessitate optimization of a customized eluent for each purification. In stark contrast, after surveying many solvent combinations, we discovered that MIDA boronates of different sizes, polarities, and functional group content, **3.1a-3.1t**, all show zero mobility on a thin layer chromatography (TLC) plate eluted with a mixture of 1.5% MeOH in Et_2O, a polar eluent that causes rapid elution of most other compounds and reagents (Figure 3-3, left). In contrast, all of the same MIDA boronates are rapidly eluted with tetrahydrofuran (THF) (Figure 3-3, right).

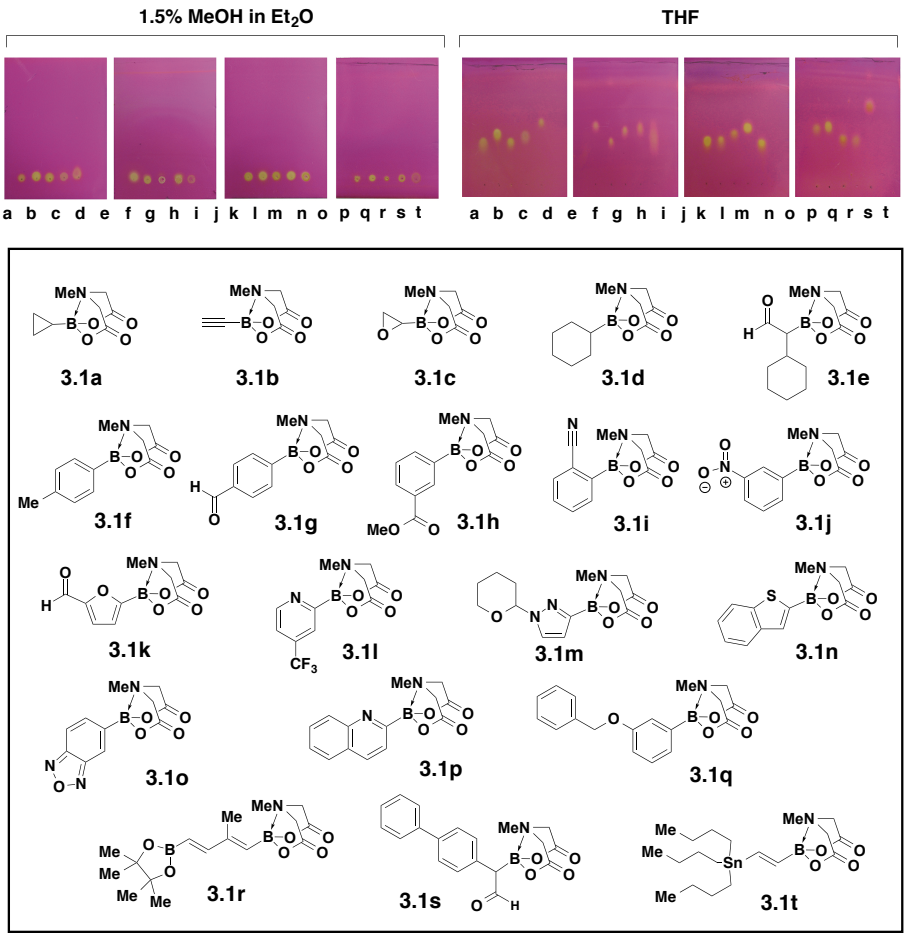

Figure 3-3. Universal binary elution of MIDA boronates on silica gel is illustrated in a photograph of TLC plates spotted with a wide range of commercially available MIDA boronates, eluted with 1.5% (v/v) MeOH in Et_2O or THF and stained with $KMnO_4$.

This universal binary elution profile enabled the development of a general and readily automatable catch-and-release purification system (Figure 3-4). In this approach, the MIDA boronate is temporarily caught on a plug of silica gel while excess reagents and byproducts are removed via washing with a copious volume of 1.5% (v/v) MeOH in Et_2O. Thereafter, the MIDA boronate is cleanly and rapidly released by switching the eluent to THF. This purification strategy has the added advantage of permitting all of the deprotection and coupling reactions to be executed in solution phase, thus avoiding the substantial challenges associated with running heterogeneous reactions in the solid phase format.

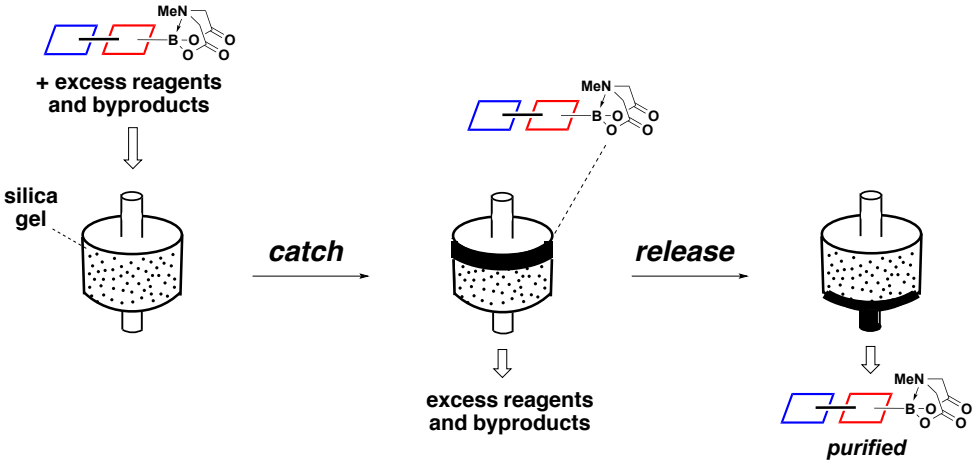

Figure 3-4. The binary elution profile of MIDA boronates on silica gel enabled the development of an automated catch-and-release purification strategy for MIDA boronates.

Further facilitating the automation of ICC, we found additional features of MIDA boronates that collectively enable general conditions for the deprotection and cross-coupling steps. In contrast to other boronic acid derivatives,[9] the rates of hydrolysis of MIDA boronates are exceptionally similar.[10] MIDA deprotections are also generally free of side reactions, and the water-soluble ligand can be easily separated from the resulting boronic acid. For the cross-coupling reactions, some generality was achieved using PdXPhos as catalyst,[11] anhydrous K_3PO_4 as base, and THF as solvent, but these conditions still failed to provide good yields in some cases. We identified boronic acid decomposition, both before and during the cross-coupling reaction, as a major cause.[10] Overcoming this limitation, we found that clean hydrolysis of bench-stable MIDA boronates immediately prior to a cross-coupling ensures that every reaction starts with a pure boronic acid. Moreover, slow addition of such freshly prepared boronic acids into reactions minimizes the in situ decomposition caused by heat, base, and/or catalyst in the reaction mixture.

3-3 DEVELOPMENT OF A SMALL MOLECULE SYNTHESIZER

Based on all these enabling features of MIDA boronates, a small molecule synthesizer was designed and constructed by Dr. Eric Gillis and Dr. Steven Ballmer (Figure 3-5).[8] The execution of each automated synthesis simply requires the placement of pre-loaded cartridges onto the synthesizer and pressing "Start". Thus, the person time required to execute the synthesizer is minimal.

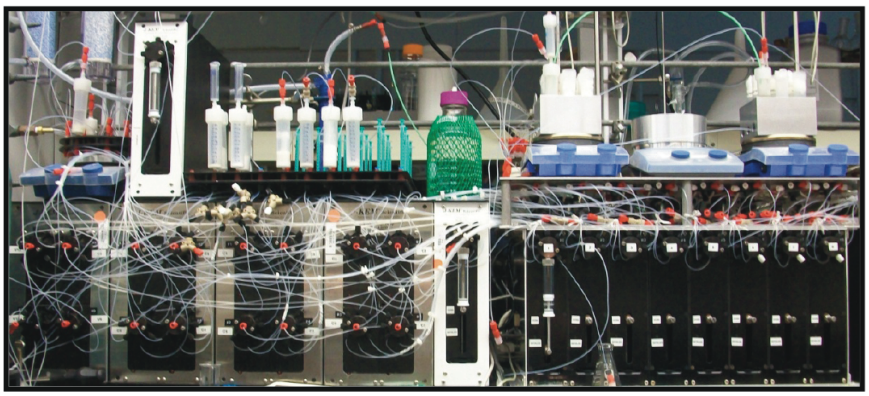

Figure 3-5. A photograph of the small molecule synthesizer, which is comprised of three modules that promote the deprotection, cross-coupling, and purification steps required for each ICC cycle. Each module is a computer-controlled liquid-handling system that uses syringe pumps to transfer substrates through a series of reagent-containing disposable cartridges.

A schematic representation of one automated ICC cycle is described in Figure 3-6. Specifically, the deprotection module (Figure 3-6, top) adds THF and water to a cartridge containing the starting MIDA boronate and solid NaOH. This system is agitated using pulses of argon gas at room temperature for 20 minutes. This is followed by a reaction quench with pH 6 potassium phosphate buffer and diethyl ether and the resulting ethereal solution of the freshly prepared boronic acid is separated from the water-soluble MIDA ligand. The organic layer is dried over anhydrous $MgSO_4$ and molecular sieves mixed with Celite. The organic solution is then concentrated and deoxygenated with argon sparging to remove diethyl ether and afford a dry, deoxygenated THF solution of freshly prepared boronic acid.

The cross-coupling module then heats and stirs a reaction cartridge containing a coupling partner, PdXPhos, K_3PO_4, THF, and a magnetic stir bar (Figure 3-6, middle). The solution of boronic acid in THF is then slowly added to the cross-coupling reaction. Finally, the purification module (Figure 3-6, bottom) executes catch-and-release chromatography on the crude reaction mixture using a series of eluents (4:1 hexanes:THF → 1.5% (v/v) MeOH in diethyl ether → diethyl ether → THF). The first three series of eluents remove non-MIDA boronate containing impurities including unreacted boronic acid, decomposition byproducts associated with protodeborylation, and catalyst components. THF is conveniently used to release the purified MIDA boronate, enabling transfer of the resulting concentrated solution of the purified MIDA boronate product directly into the deprotection module to start the next ICC cycle.

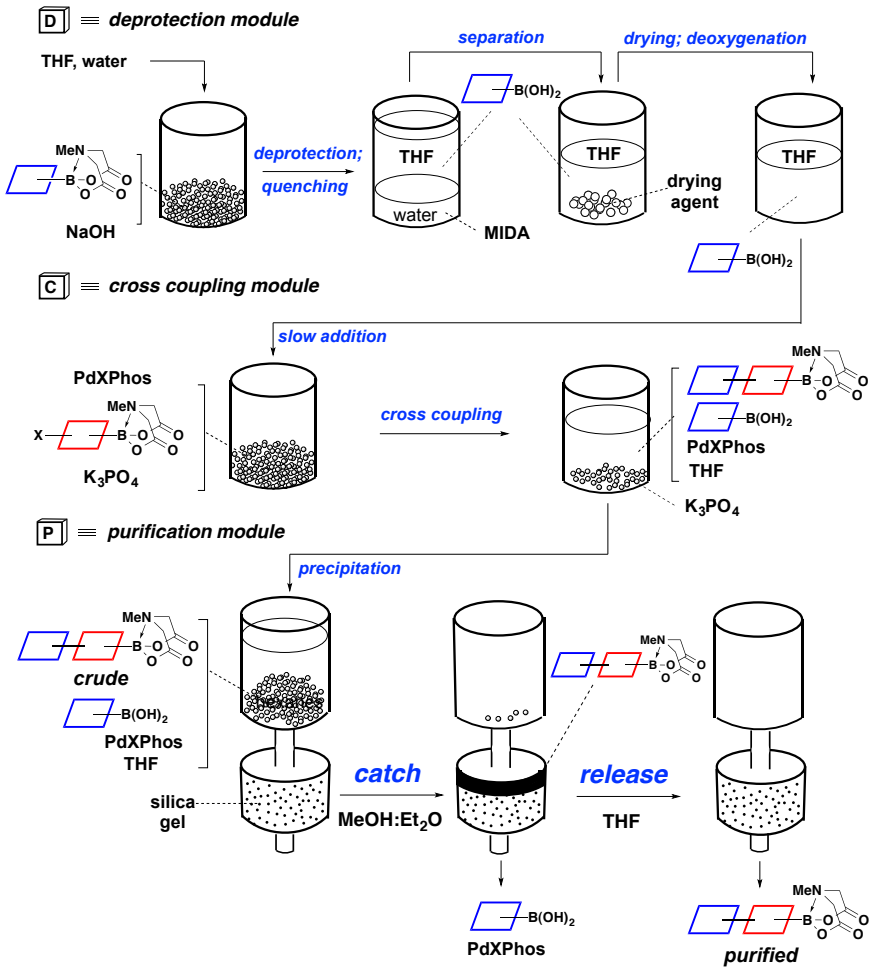

Figure 3-6. Schematic representations of fully automated modules for the deprotection [D], cross-coupling [C], and purification [P] steps of ICC.

Having constructed the modules for deprotection, cross-coupling, and purification, Dr. Steven Ballmer in collaboration with Gregory Morehouse first tested this platform to automatically execute one cycle of ICC with a series of commercially available aryl (**3.2a-c**), heteroaryl (**3.2d-f**), and vinyl MIDA boronates (**3.2g-i**) using the same conditions for each module to construct C-C bonds (Figure 3-7). The conversion at each step was quantified as well as yield and purity of the final MIDA boronate products. Without any modifications of any of the general conditions, excellent conversions of all MIDA boronates **3.2** to the corresponding boronic acids **3.3**, and excellent conversions of bifunctional building block **3.4** to provide good isolated yields of the desired cross-coupling products **3.5** were observed (Figure 3-7). Most importantly, all of the final MIDA boronate products **3.5a-i** were isolated in excellent purity as analyzed by ^{1}H NMR.

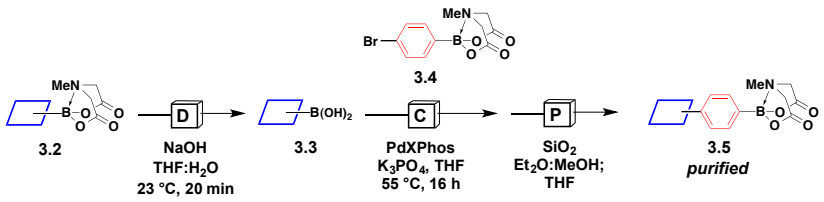

entry	MIDA boronate 3.2	% conversion (3.2 to 3.3)	boronic acid 3.3	% conversion (3.4 to 3.5)	MIDA boronate 3.5	% isolated yield of 3.5	% purity of 3.5
1	3.2a	99	3.3a	98	3.5a	61	>95
2	3.2b	99	3.3b	99	3.5b	65	>90
3	3.2c	97	3.3c	86	3.5c	61	>80
4	3.2d	98	3.3d	98	3.5d	75	>95
5	3.2e	97	3.3e	93	3.5e	72	>90
6	3.2f	99	3.3f	99	3.5f	83	>95
7	3.2g	98	3.3g	95	3.5g	67	>90
8	3.2h	98	3.3h	99	3.5h	67	>95
9	3.2i	99	3.3i	98	3.5i	71	>90

Figure 3-7. A range of structurally diverse MIDA boronate building blocks were subjected to one fully automated cycle of deprotection [D], cross-coupling [C], and purification [P] using the same set of general conditions in each module. General condition for deprotection: MIDA boronate **3.2** (1 mmol, 3 equiv.) NaOH (9 equiv.), THF (0.1 M), 23 ^{o}C, 20 min. General condition for cross-coupling: MIDA boronate **3.4** (1 equiv.), PdXPhos (5 mol%, XPhos = 2-dicyclohexylphosphino-2′,4′,6′-triisopropylbiphenyl), K_3PO_4 (9 equiv.), THF (0.028 M), 55 ^{o}C, 16 h. General condition for catch-and-release purification: SiO_2, MeOH:Et_2O (1.5:98.5, 36 mL), Et_2O (36 mL), THF (12 mL). % Conversions and % purity were determined via ^{1}H NMR.

3-4 TOTAL SYNTHESIS OF A RANGE OF DIFFERENT SMALL MOLECULES VIA AUTOMATED ICC

We next tested whether the synthesizer could prepare a wide range of structurally and functionally diverse small molecules that are composed mainly of C-C bonds in their backbones. We targeted milligram quantities of these small molecules, sufficient for discovery assays. Since small molecules are not as large as macromolecules, it was expected that most small molecules could be synthesized from three or four building blocks. The results summarized in Figure 3-8 demonstrate that a single automated run of two or three ICC cycles successfully delivered each of the targeted compounds in milligram quantities, fulfilling the requirements of most functional discovery assays. The percent yields reported represent the yield of the final step starting from 1 equiv. of the capping building block. Importantly, while at least 4 days of full time commitment is required to manually synthesize each of these targets from the same building blocks, loading the reaction cartridges and starting the synthesizer takes only 1 hour of person time. This difference represents 4 days that could be committed to many other aspects of the small molecule discovery process.

Specifically, we first targeted a pair of materials components that are comprised of repeating heteroaryl or phenylene units, important structures found in solar cells and light-emitting diodes, respectively.[12] Using the same set of previously described general conditions for the deprotection, cross-coupling, and purification, building blocks **3.6-3.8** were readily assembled to generate quaterthiophene **3.9** (Figure 3-8, entry 1). In a similar fashion, building blocks **3.10** – **3.12** were assembled to synthesize oligophenylene **3.14** (Figure 3-8, entry 2). We next questioned whether the synthesizer could also prepare important pharmaceutical compounds. Encouragingly, phosphodiesterase inhibitor **3.18**,[13] a small molecule for treating asthma, was readily prepared from building blocks **3.15** – **3.17** under the same exact conditions used to make the two materials targets (Figure 3-8, entry 3).

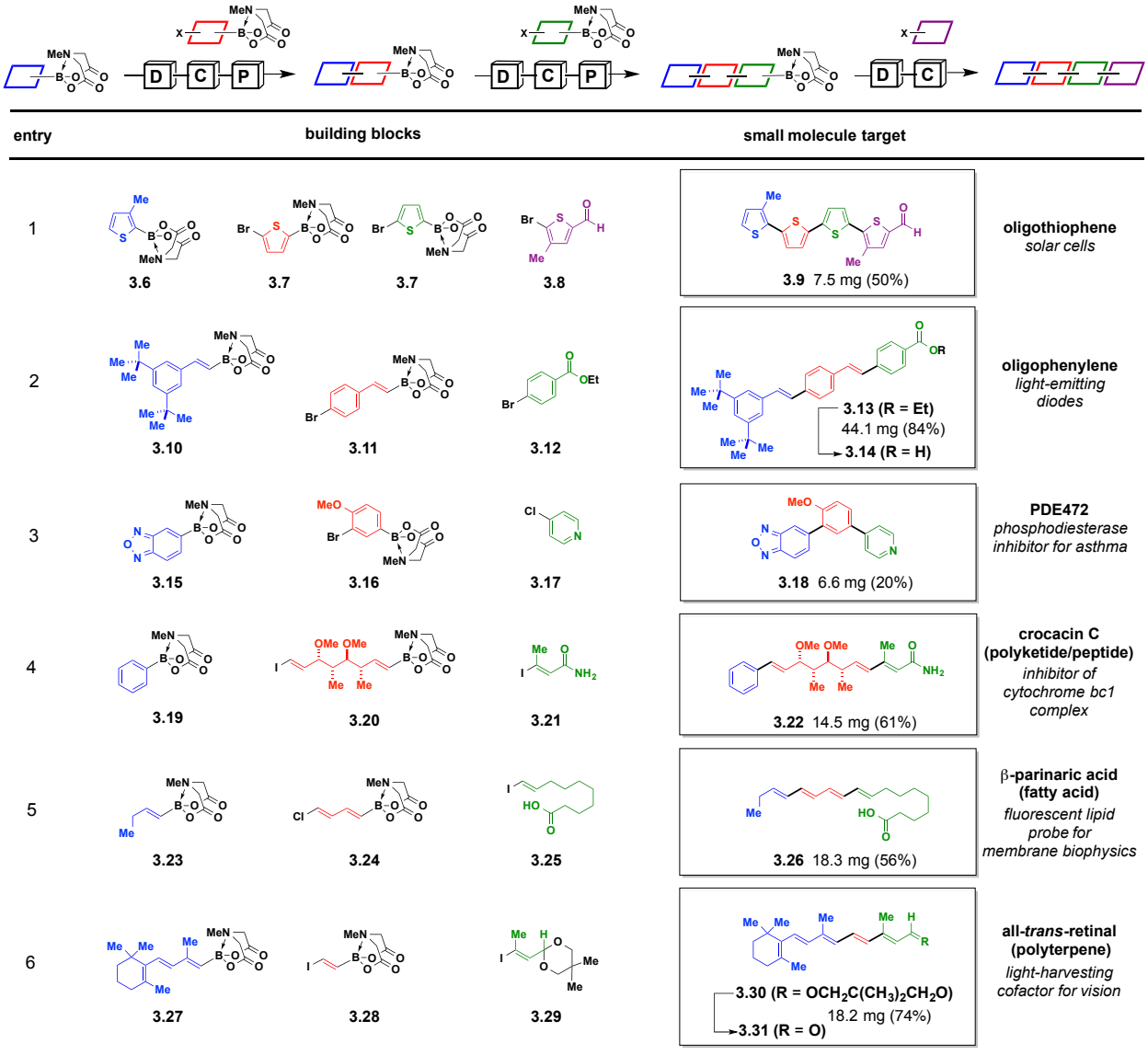

Figure 3-8. Automated synthesis of materials, pharmaceuticals, and natural products. Similar to automated peptide, oligonucleotide and oligosaccharide syntheses, all of the synthesizer-generated products were readily purified using standard chromatographic techniques, and any protecting groups (Et = ethyl) other than MIDA were easily removed in a separate step. Yield reflects the quantity of each small molecule target that was generated with a single run on the synthesizer. All % yields are based on one equivalent of the final halide building block.

Natural products represent the most structurally complex and diverse class of small molecules and are thus the most challenging targets for a general and automated synthesis platform. Similar to the changes in reaction conditions often employed for automated synthesis of more complex peptides, minor modifications to the phosphine ligand, base, and/or reaction temperature in some cases enabled us to successfully expand the scope to include natural product targets representing common small molecule biosynthetic pathways (Figure 3-8, entries 4-6).

Hybrid polyketide/peptide crocacin C (**3.22**),[14] an antifungal natural product with potential to inhibit the mitochondrial cytochrome bc1 segment of complex III in the respiratory transport chain,[15] was readily assembled from stereochemically complex building blocks **3.19-3.21** (Figure 3-8, entry 4). We then synthesized fatty acid *β*-parinaric acid (**3.26**)[16], a widely used fluorescent probe for structural and functional studies of lipid bilayer membranes.[17] Assembly of alkenyl building blocks **3.23-3.25** afforded **3.26** with complete retention of olefin stereochemistry (Figure 3-8, entry 6).[16]

Polyterpene all-*trans*-retinal (**3.31**) has the ability to transduce solar energy into mechanical energy and is a critical functional component of the light-driven proton pump found in bacteria and the photoreception machinery utilized by most animals.[18] A modular and flexible automated synthesis toward this natural product will enable systematic structure-function studies of this natural product. Synthesis of **3.31** required manual optimization and development before an automated synthesis can be achieved due to the inaccessibility of building block **3.27**, the instability of the polyenyl boronic acid intermediates, and the potential for isomerization before or after cross-coupling.

First, synthesis of building block **3.27** was investigated using known reaction conditions starting from commercially available β-ionone to afford boronic acid **3.32** in four steps[19] followed by complexation with MIDA anhydride[20] to afford the target building block (Scheme 3-1). Through this route, **3.27** was synthesized in only 16% overall yield over 5 steps via handling of unstable intermediates that could not be isolated. In particular, boronic acid **3.32** is an unstable boronic acid and decomposes upon concentration and isolation.[19] We therefore sought an alternate method to synthesize this building block that involved stable intermediates and fewer steps. Since all-*trans* retinal structurally represents half of β-carotene, we questioned whether building block **3.27** could be constructed in the same manner carotenoid intermediates were constructed (see Chapter 2 for details). This involved coupling sterically hindered and unactivated vinyl iodide **3.33**[21] and **3.1r**, a key bisborylated building block used in the synthesis of synechoxanthin[5b] and renierapurpurin that is now commercially-available (Scheme 3-1). Encouragingly, this approach afforded building block **3.27** in 70% yield on gram-scale. This synthetic route further highlighted the potential utility of building block **3.1r** as a general building block for polyene synthesis. Unlike boronic acid **3.32**, the corresponding MIDA boronate **3.27** was stable to isolation and silica gel chromatography.

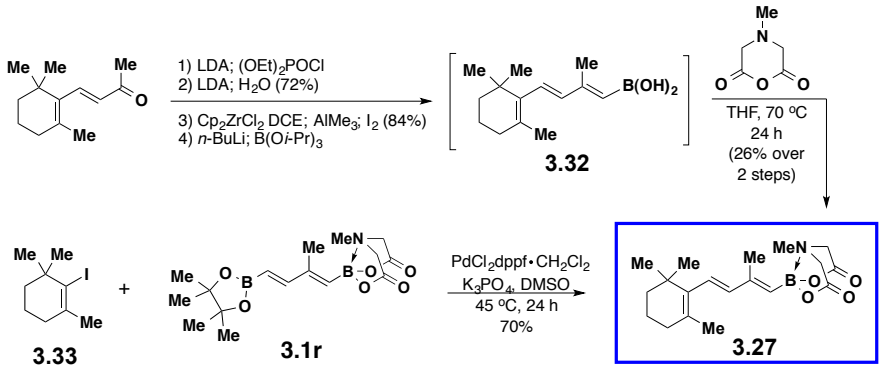

Scheme 3-1. Synthesis of building block **3.27**.

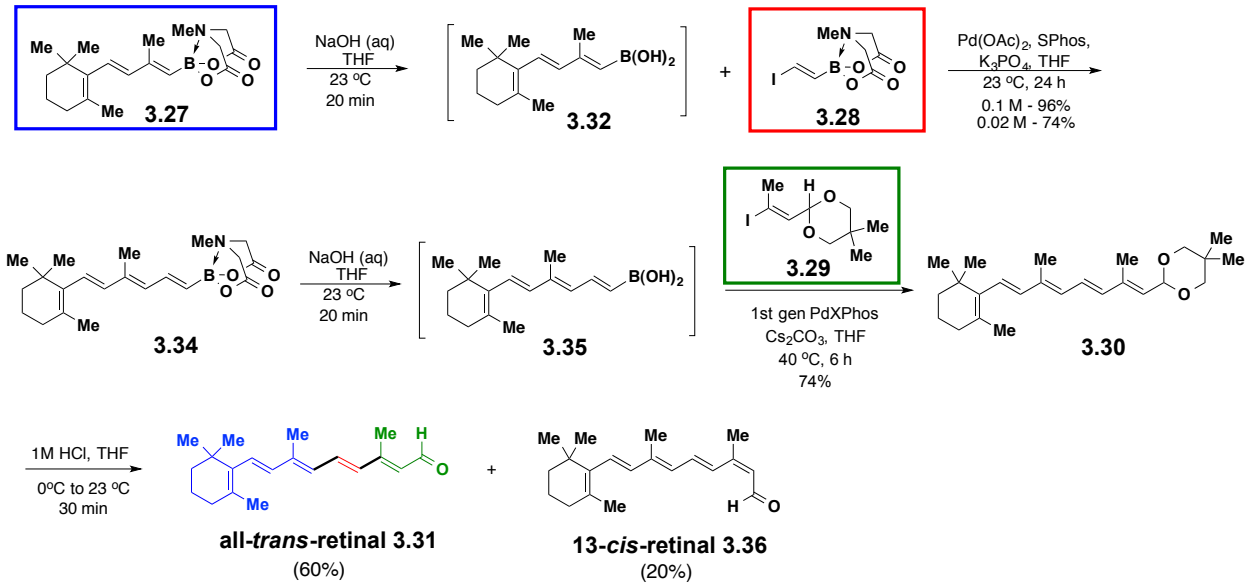

Scheme 3-2. Manual synthesis of all-*trans* retinal **3.31**.

With the key building block in hand, synthetic route toward **3.31** was first investigated manually. Conditions from the literature were translated to the first deprotection and coupling steps to afford tetraenyl MIDA boronate **3.34** (Scheme 3-2).[16] However, the second coupling proved problematic under similar conditions. We discovered that unprotected version of aldehyde building block **3.29** was prone to isomerization and gave at best 50% yield of the target. This prompted us to protect this capping building block as an acetal. Cross-coupling boronic acid **3.35** with acetal **3.29** encouragingly provided protected all-*trans* retinal **3.30** in 74% yield with >95% *trans* stereochemistry.[22]

3-5 AUTOMATED LIBRARY SYNTHESIS OF NATURAL PRODUCT DERIVATIVES

The development of new medicines, biological probes, and materials with optimized functional properties often requires access to many structural derivatives of a specific small molecule. In medicinal chemistry, natural products are rich sources for identification of a drug lead. However, as described in Chapter 2, isolation of small molecules from natural sources is difficult, thus biological studies are sometimes conducted with a mixture of natural product isolates which makes the specific source of the activity, such as in herbal drugs, challenging to probe. In order to facilitate understanding and optimization of the active compounds and/or their modes of action, a systematic understanding of structure-activity relationships is required for each member of the natural product family as well as their derivatives.

This is especially true for polyphenolpropanoid natural products[23] of the medicinal plant *Ratanhiae radix*, an anti-inflammatory herb, some of which have shown promise to contribute to the biological activity of this plant.[24] For this reason, we targeted an automated synthesis of natural products previously isolated from this medicinal plant with the larger goal of creating a library of natural product derivatives to drive understanding of their functions. Specifically, ratanhiaphenol III (**3.36**) has shown promising activity in the inhibition of protein tyrosine phosphate 1B (PTP1B) that is considered to be effective for combating insulin resistance and type II diabetes,[25] and ratanhine (**3.37**) [26] represents the largest and most complex natural product isolated from this medicinal plant and intriguingly, its biological activity has not yet been tested (Figure 3-9).

To accomplish this goal, we set out to realize a 20-membered library of natural product derivatives and questioned whether the small molecule synthesizer could execute this experiment without ad-hoc optimizing the deprotection, cross-coupling, and purification steps for each library member. Given the modularity of small molecules, we retrosynthesized natural product ratanhiaphenol III (**3.36**) and family member ratanhine (**3.37**) into three and four building blocks respectively (Figure 3-9). Guided by this retrosynthesis, we incorporated four sets of building blocks representing common sub-structural elements found throughout the neolignan family of medicinal natural products and other pharmaceutically relevant motifs to create a diverse set of building blocks (Figure 3-9). These building blocks include variations in oxidation states, methylation patterns, fluorine content, aromatic ring identity, and size. We planned to mix and

match these building blocks in all possible combinations for both the trimer (2 x 2 x 3 = 12 members) and tetramer (2 x 2 x 1 x 2 = 8 members) libraries.

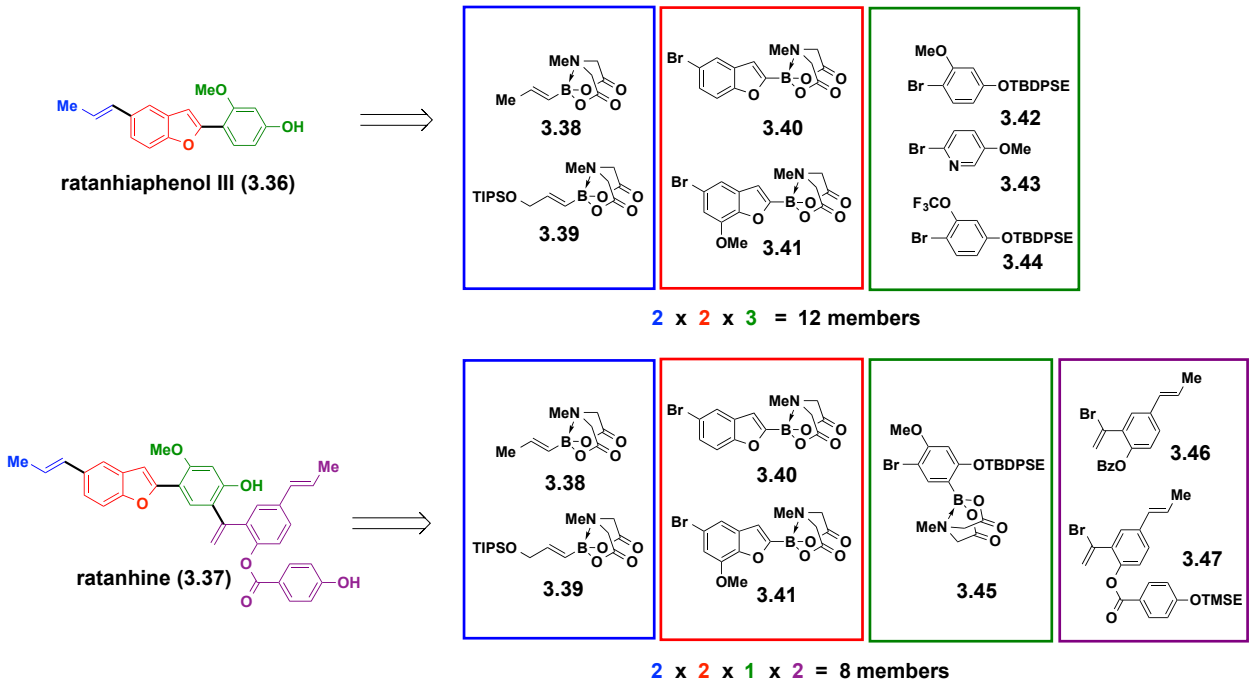

Figure 3-9. Strategy for a 20-membered natural product library synthesis.

Two main challenges had to be solved for this library synthesis to be efficient and practical. First, identification of orthogonal protecting groups were important for compatibility with cross-coupling and deprotection reactions in addition to achieving general conditions for a global deprotection. Second, a general set of cross-coupling conditions to couple a variety of different coupling partners was necessary to avoid ad hoc optimizations for each library target. Moreover, ratanhine (**3.37**) is a challenging target for cross-coupling due to its acid-sensitive functionality and relatively unstable boronic acid intermediates.[3a] To solve the initial challenge, various protecting groups were first explored in a manual fashion in collaboration with Junqi Li, including MOM and SEM, but these protecting groups were difficult to remove. After optimization, we discovered that silyl protecting groups (TIPS, TMSE, TBDPSE) were appropriate protecting groups that have the capacity to survive cross-coupling conditions as well as be readily deprotected under milder conditions.

To solve the second challenge, we started by manually optimizing the Suzuki-Miyaura cross-coupling conditions for the most challenging target of the trimer library **3.48** (Scheme 3-3).

After optimization, employing SPhos as the ligand and K_2CO_3 as the base, building blocks **3.39** and **3.41** were coupled under otherwise standard cross-coupling conditions used in Figure 3-2, affording MIDA boronate **3.49** in 81% yield. Deprotection of MIDA boronate **3.49** to its corresponding boronic acid and slow addition of this intermediate to the second cross-coupling reaction with capping halide **3.42** afforded the protected library member **3.50** in 89% yield. After some investigation, TBAF in DMPU and DMSO was identified as a potentially general deprotection condition for silyl protecting groups. This condition was employed by Junqi Li to deprotect both TIPS and TBDPSE protecting groups in one pot to afford the fully-deprotected trimer library member **3.48** (Scheme 3-3).

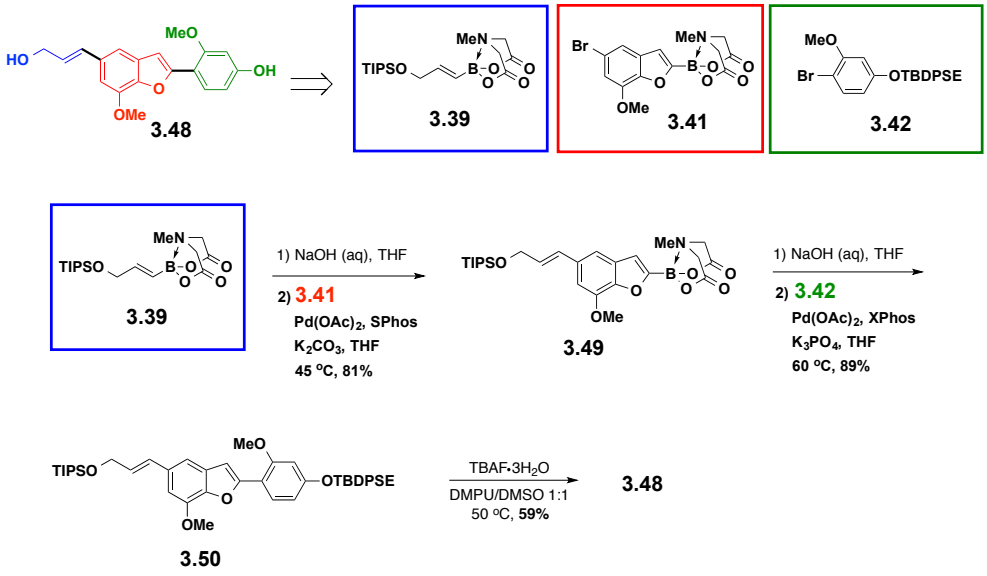

Scheme 3-3. Cross-coupling and deprotection conditions for trimer library members.

In a similar fashion, the synthesis of the most challenging target of the tetramer library **3.51** was first investigated manually in the laboratory (Scheme 3-4). Encouragingly, the same exact reaction conditions employed to make **3.50** translated well to the synthesis of MIDA boronate **3.52** in the second cross-coupling step. Increased equivalents of NaOH (4.5 equiv compared to 3 equiv) were necessary to complete full hydrolysis of MIDA boronate **3.52**. For the third cross-coupling reaction, switching the phosphine ligand from XPhos to Sphos with slightly higher catalyst loading (10 mol% vs. originally 5 mol%) and longer reaction time (24 h vs. originally 16 h) afforded the protected library member **3.53m** in modest, yet acceptable 51% yield for the TBDPSE-protected derivative. Protodeborylated compound from the boronic acid

intermediate was identified as the major byproduct in this reaction. Finally, a two-step deprotection sequence was developed by Junqi Li to remove all three silyl protecting groups. With TBDPSE as the protecting group for capping building block **3.47**, there was a ~1:4 ratio of benzoate-cleaved byproduct to **3.51**. To optimize this reaction even further, we switched this protecting group to TMSE, which cleanly afford the fully-deprotected tetramer library member **3.51** without formation of any benzoate-cleaved byproduct (Scheme 3-4). Moreover, it was later discovered that the conversion of triply protected derivative such as **3.53m** can be deprotected using just CsF in DMSO in a one-step procedure.

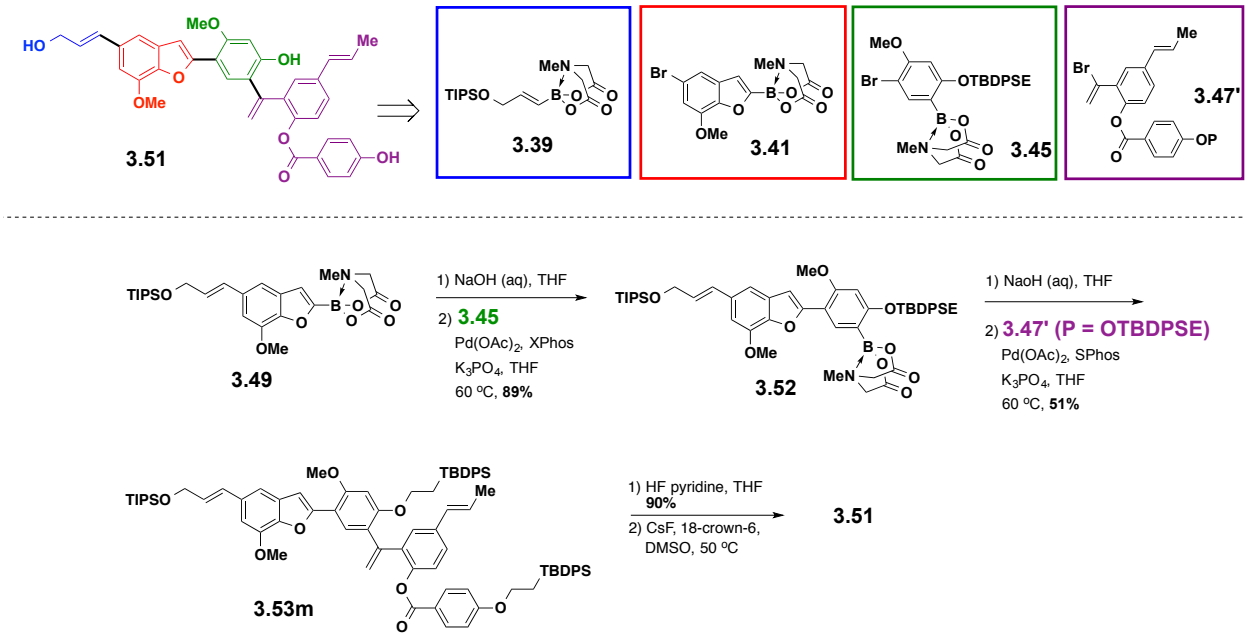

Scheme 3-4. Cross-coupling and deprotection conditions for tetramer library members.

With general cross-coupling conditions in hand, we turned towards translating these conditions on the synthesizer to prepare the 20-membered library without ad hoc optimizations of conditions. We reasoned that both the general deprotection and purification conditions (Figure 3-7) could be applied for this library synthesis. Encouragingly, the manual conditions translated smoothly to the automated platform to synthesize protected ratanhiaphenol III (**3.36**) from building blocks **3.38**, **3.40**, and **3.42** in 75% yield (Figure 3-10). Impressively, even the highly

complex target ratanhine (**3.37**) was readily prepared via fully automated ICC of building blocks **3.38**, **3.40**, **3.45**, and **3.47** (Figure 3-10).

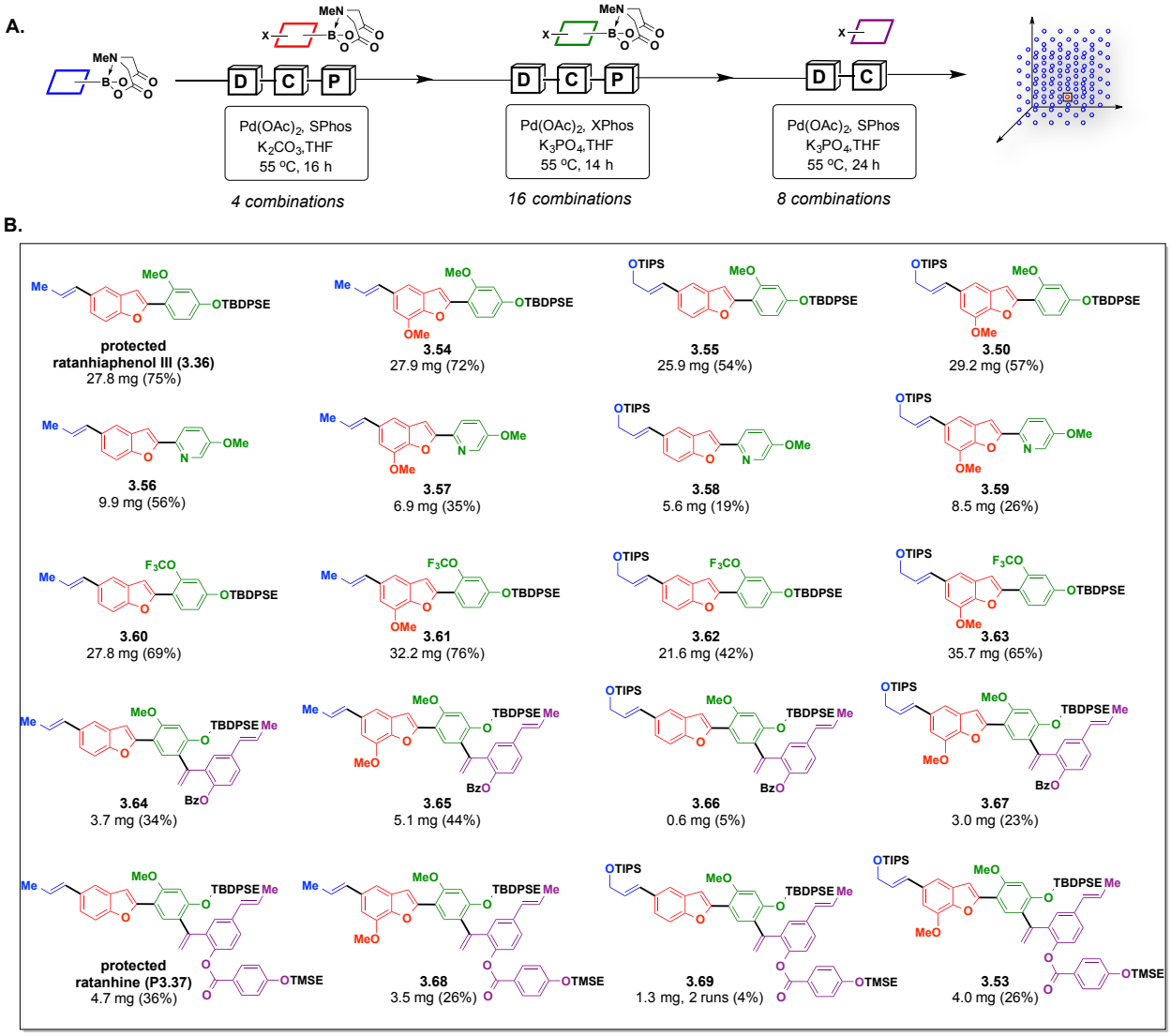

Figure 3-10. Automated synthesis of a 20-membered natural product library. A. General scheme of the automated ICC sequence, highlighting the general cross-coupling conditions for each step. **B**. All 20 targeted library members were successfully synthesized in a fully automated fashion using the same series of deprotection, cross-coupling, and purification conditions for each step. Unless otherwise noted, the quantity of material indicated below each product represents the yield from a single run on the synthesizer. All percent yields are based on one equivalent of the final halide building block. All protecting groups other than MIDA (TIPS (triisopropylsilyl), TBDPSE = *tert*-butylpdiphenylsilylethyl, TMSE = trimethylsilylethyl, or Bz (benzoyl)) were successfully removed in a separate manual step.

For the remaining library members, we did not permit any optimizations to any of the conditions used to construct **3.36** and **3.37**. In the event, the synthesizer successfully generated 20 out of 20 of the targeted derivatives, collectively representing all possible combinations of

this four-component matrix of building blocks (Figure 3-10). It is worth mentioning that in addition to **3.36** and **3.37**, library member **3.55** (CAS # 143001-80-3) is a known isolate from both roots of *Krameria grayi* and *Krameria interior*, a genus of plants used medicinally to fight eye infections and body weakness.[27] If preformed independently in a manual fashion, these 20 syntheses would have required about three months of full time commitment. In contrast, initiating all of the corresponding automated assembly of 3-4 building blocks required a total of only 20 hours of person time.

3-6 EXPANDING ICC TO INCLUDE FORMATION OF CARBON-HETEROATOM BONDS

Up to this point, all of our small molecule targets were made by using the Suzuki-Miyaura cross-coupling reaction to form Csp^2-Csp^2 bonds. This reaction alone has allowed access to functionally and structurally diverse small molecules. However, we questioned whether we could expand this strategy to access chemical space that has not yet been accessed to date using ICC, especially in the context of this automated platform. In this vein, not all small molecules can be assembled via only C-C bond-formations; in fact, many pharmaceuticals contain C-N bonds in their backbones.[28] Because many C-heteroatom bonds can also be formed using cross-coupling,[7a] we envisioned employing the same modular ICC platform to incorporate not only different building blocks, but also different types of bond formations. We further recognized that, as long as the intermediate contains a MIDA boronate in the ICC sequence, the same automated catch-and-release purification would be effective. Combined with the compatibility of MIDA boronates with many different types of reactions,[14] this opened the possibility of expanding the coupling chemistry to access a wider range of different linkages including C-N bonds.

In this vein, we targeted the automated synthesis of two pharmaceutical compounds with C-N linkages in their backbones. For the synthesis of anticancer B-Raf kinase inhibitor **3.74**,[29] the first step involved a Buchwald-Hartwig cross coupling between pyrimidine **3.71** and isoquinoline **3.72**. Remarkably, the same general conditions employed for the previously described materials and pharmaceutical targets (Figure 3-8) enabled efficient C-N bond formation between these building blocks. In the second step, Suzuki-Miyaura cross-coupling of an intermediate boronic acid with capping building block **3.73** completed the sequence to yield **3.74** (Figure 3-11, entry 1).

As a second example, we questioned whether BTP 2 (**3.78**), an inhibitor of Ca influx in T-cells,[30] can be prepared on this synthesizer simply by inputting different building blocks under appropriate reaction conditions. Synthesis of this pharmaceutical involved an amide bond formation and a C-N bond formation. Supporting our hypothesis, amide bond formation between carboxylic acid **3.75** and amine **3.76** was successful using DCC. In the second step, we took advantage of the fact that boronic acids are versatile functional groups that can undergo useful transformations other than Suzuki-Miyaura cross-coupling, such as Chan-Lam couplings[31]. The intermediate MIDA boronate formed from union of building blocks **3.75** and **3.76** was thus deprotected to its corresponding boronic acid under general deprotection conditions and reacted with heterocycle **3.77** to afford target **3.78** (Figure 3-11, entry 2).

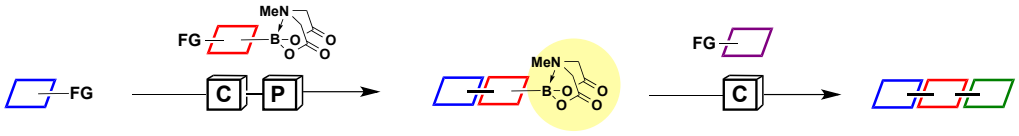

entry	building blocks			small molecule target	
1	 3.71	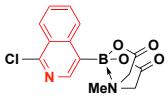 3.72	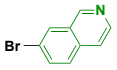 3.73	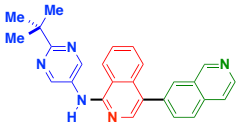 3.74 12.9 mg (28%)	pharmaceutical *B-Raf kinase inhibitor for cancer*
2	 3.75	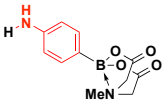 3.76	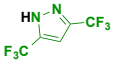 3.77	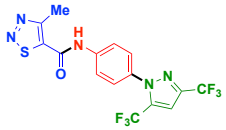 3.78 6.7 mg (9%)	BTP2 *inhibitor of Ca influx in T-cells*

Figure 3-11. Automated synthesis of pharmaceuticals via C-N and C-C bond formations. Similar to automated peptide, oligonucleotide and oligosaccharide syntheses, all of the synthesizer-generated products were readily purified using standard chromatographic techniques. Yield reflects the quantity of each small molecule target that was generated with a single run on the synthesizer. All % yields are based on one equivalent of the final building block. Entry 1 conditions: see Figure 3-8. Entry 2 conditions: 1st [C] = *N,N*'-dicyclohexylcarbodiimide (DCC), THF, RT, 4 h. 2nd [C] = pyridine, $Cu(OAc)_2$, molecular sieves, THF, RT, 48 h. [D] and [P] unchanged from general conditions.

3-7 EXPANDING ICC TO ACCESS CYCLIC SMALL MOLECULES

As a final test for this synthesis platform, we are currently pursuing whether the same automated iterative assembly of building blocks could enable access to complex macrocyclic and polycyclic natural products and natural product-like skeletons (Figure 3-12). At first glance, these targets may appear beyond reach with this approach. However, we were encouraged by the recognition that Nature makes many such small molecules via a common strategy in which a linear precursor is first prepared via an iterative building block assembly followed by cyclization(s) that ultimately yield the complex cyclic architecture found in the corresponding natural product (Scheme 3-5A).[2]

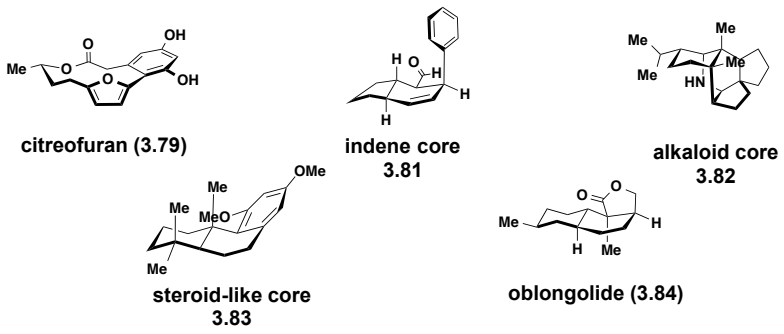

Figure 3-12. Selected structures of cyclic natural products and natural product-like skeletons.

For example, natural product citreofuran (**3.79**) can be retrosynthesized to linear precursor **3.85**, which, in the forward direction can undergo a macrocyclization to afford the cyclic small molecule.[32] We also recognized that both the steroid lanosterol (**3.86**)[33] and the highly complex daphniphyllum alkaloid (**3.88**)[34] could be prepared from similar linear precursors (**3.87** and **3.89**) derived from terpene-like building blocks (Scheme 3-5B). These linear precursors can then be retrosynthesized into building blocks that can be mapped back to the target molecules highlighting the fact that even in these complex cases, small molecules are inherently modular in their constitution.

Furthermore, in total synthesis efforts, the time and labor-intensive requirements of linear precursor syntheses often represent the slow step in completion of the target molecule. Addressing this unmet challenge by developing a general strategy to access these motifs in a method that has potential for rapid derivatization can have great impact. The time relieved from making linear precursors can now be shifted towards designing different linear precursors,

developing better methods to cyclize these linear precursors, and/or understanding the functions of these cyclic natural products.

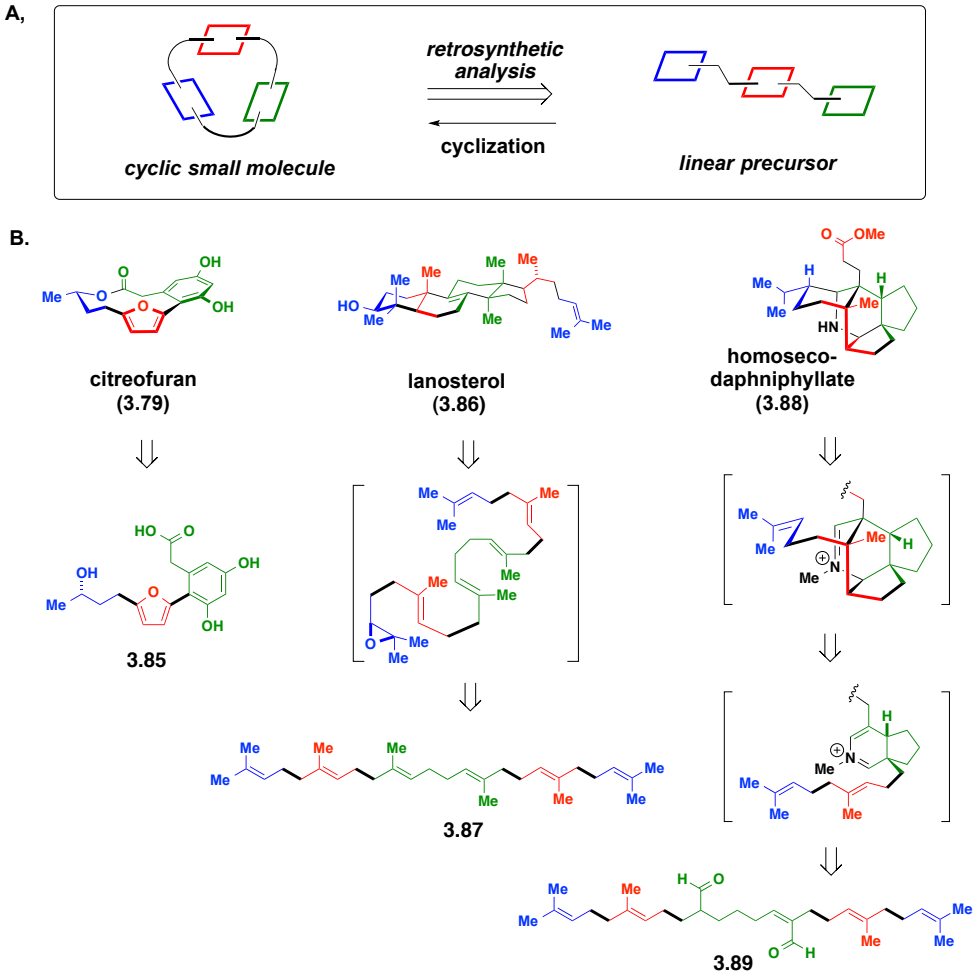

Scheme 3-5. A. Retrosynthesis of cyclic small molecules to linear precursors. In the forward direction, linear precursors can be cyclized to form cyclic targets. **B.** Biosynthesis-inspired retrosynthesis of cyclic natural products to their corresponding linear precursors.

Topologically complex small molecules are derived from linear precursors that contain an increased amount of saturation and flexibility capable of cyclization (Scheme 3-5B). Thus, in order to access these natural product frameworks through this automated synthesis platform, two main challenges had to be addressed: 1) synthesis of building blocks that contain increased abundance of saturated Csp^3 carbon atoms pre-installed and 2) development of efficient methods to cross-couple Csp^3 carbons. ICC can now be routinely used to synthesize targets with Csp^2-Csp^2 linkages in their backbones via assembly of aryl, heteroaryl, and vinyl MIDA boronate building blocks. However, as described in Chapter 1, there have been fewer reports on Csp^3-Csp^2

or Csp^3-Csp^3 variants for Suzuki-Miyaura cross-coupling and it is currently an area of intense interest in the synthetic community.

To explore this potential on the synthesizer, we sought to prepare complex cyclic small molecules through automated assembly of corresponding MIDA boronate building blocks via formation of Csp^3-Csp^2 bonds to synthesize biosynthesis-inspired linear precursors (Figure 3-13). After automated preparation of linear precursors, we planned to execute manual application of state-of-the-art chemical methods to promote the desired stereoselective macrocyclizations or polycyclizations (Figure 3-13).

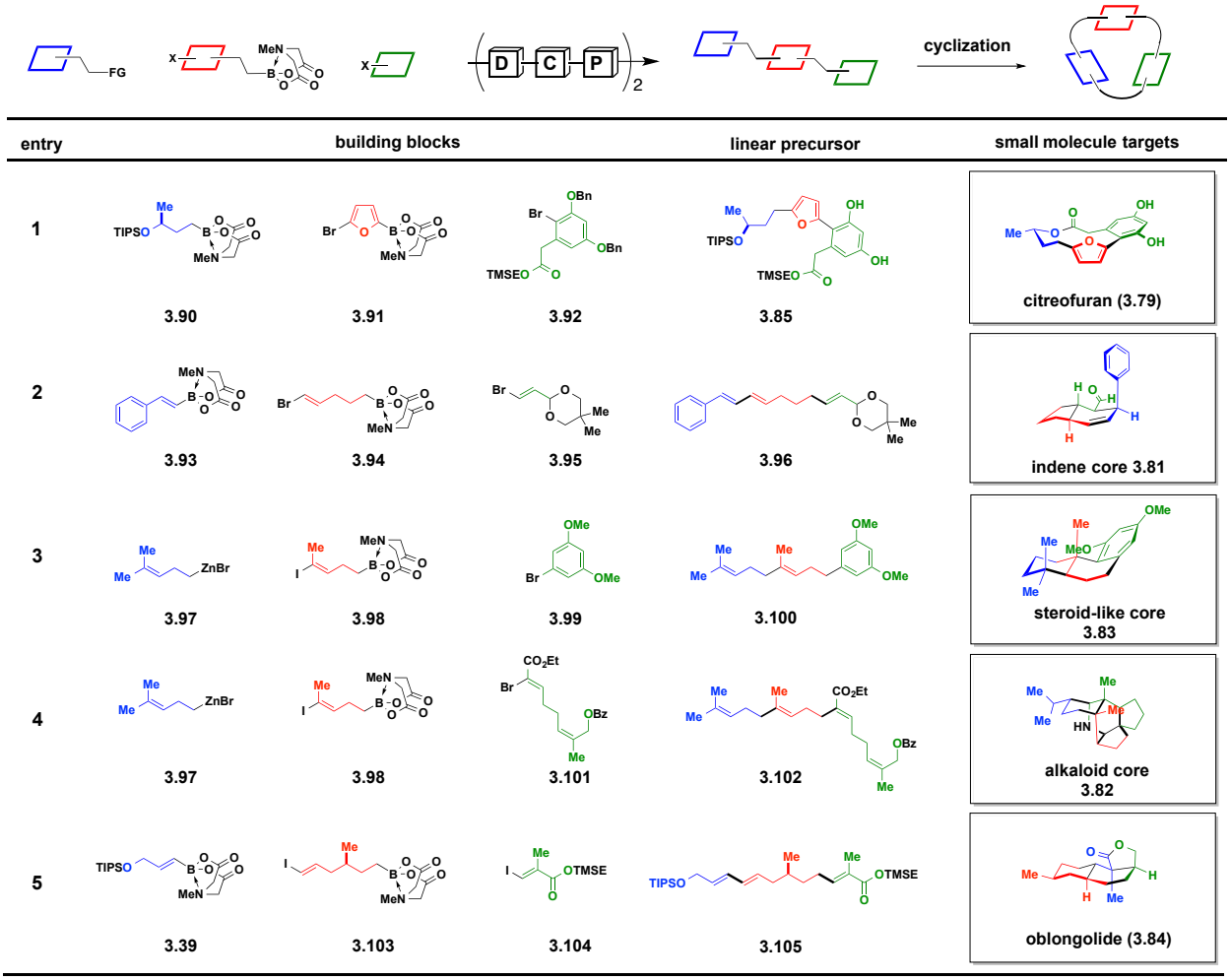

Figure 3-13. Outline of the synthetic plan toward automated synthesis of linear precursors for five cyclic small molecules.

3-8 BUILDING BLOCK SYNTHESIS AND MANUAL INVESTIGATIONS OF Csp^3-Csp^2 CROSS-COUPLING CONDITIONS

Synthesis of most building blocks that contain increased number of Csp^3 carbons were readily accessed in a few steps from commercial or known starting materials. For example, bifunctional building block **3.98** was synthesized in four steps starting from known homoallylic alcohol **3.106** (Scheme 3-6). After conversion of alcohol **3.106** to iodide **3.107**,[35] this unactivated iodide was subjected to Miyaura borylation with bispinacolatodiboron to afford pinacol boronic ester **3.108**.[36] Transesterification of **3.108** yielded the corresponding MIDA boronate **3.109**,[5a] followed by iododesilyation of the dimethyl(phenyl)silyl group with hexafluoroisopropanol (HFIP)[37] as the solvent completed the synthesis of bifunctional building block **3.98** (Scheme 3-6).

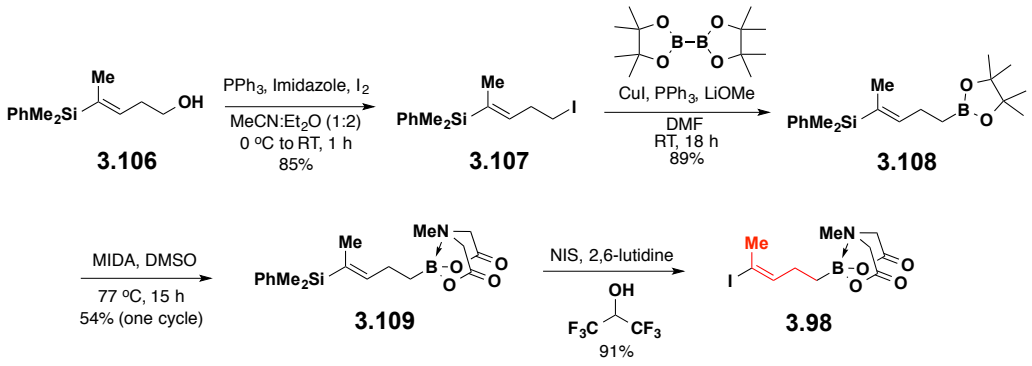

Scheme 3-6. Synthesis of bifunctional building block **3.98**.

Several larger building blocks that also contain increased saturation such as **3.101** and **3.103** were synthesized by joining two fragments together using Negishi cross-coupling. Specifically, synthesis of capping building block **3.101** for the alkaloid target was accomplished in seven linear steps from known phosphonoacetate **3.111**[38] and aldehyde **3.110**[39] (Scheme 3-7). Horner-Wadsworth-Emmons reaction of the two starting materials afforded α,β-unsaturated methyl ester **3.112**, and this ester was reduced to alcohol **3.113** using DIBAL-H. Alcohol **3.113** was protected as a benzoate to afford **3.70**, and the TBS group was cleanly deprotected to afford **3.114** in high yields. Next, the homoallylic alcohol was converted to the corresponding bromide **3.115**. Zn metal insertion to the C-Br bond afforded the Negishi reagent in situ, which then enabled a bromide-selective Csp^3-Csp^2 Negishi cross-coupling with vinyl bromide **3.116**[40] to afford building block **3.101** in 70% yield (Scheme 3-7).

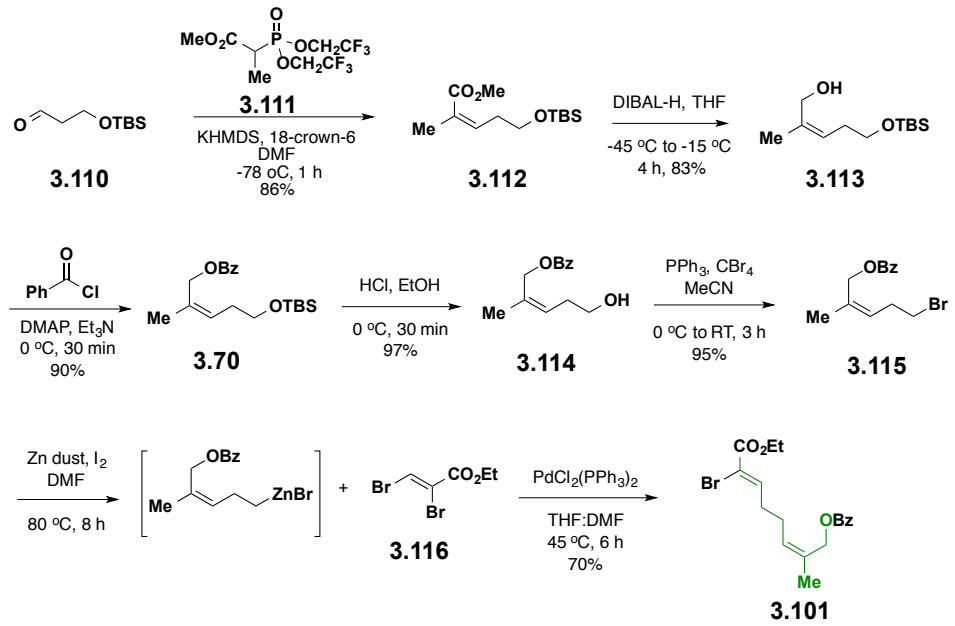

Scheme 3-7. Synthesis of vinyl bromide building block **3.101**.

With these building blocks in hand, our focus shifted toward assembling these building blocks. We recognized that all of the targets shown in Figure 3-12 require at least one Csp^3-Csp^2(vinyl) cross-coupling of a primary alkyl boronic acid to a vinyl halide, which is a challenging bond formation due to increased propensity for an alkyl boronic acid to undergo side reactions such as β-hydride elimination compared to its Csp^2 counterparts. In addition, there are only a limited number of reports on Suzuki-Miyaura cross-coupling of alkyl boron reagents with vinyl halides compared to aryl halides in the literature.[41] In constrast, Negishi cross-coupling with alkyl zinc reagents and vinyl halides are well precedented.[42] We thus sought to investigate both of these cross-coupling reactions manually to decide which reaction would be most applicable to the current synthesizer.

First, Suzuki-Miyaura cross-coupling between boronic acid **3.119** derived form MIDA boronate **3.118** and bifunctional building block **3.98** was investigated (Scheme 3-8). Silver (I) oxide has been shown to be effective in promoting Suzuki-Miyaura cross-coupling with primary alkyl boronic acids and activated boronic esters.[43] Building on this precedent, several Pd sources and phosphine ligands were investigated in combination with Ag_2O or Ag_2O/K_2CO_3. However, these conditions, in addition to conditions employing other bases, showed no successful cross-coupling, either resulting in no conversion or consumption of the starting materials toward

unproductive side reactions (Scheme 3-8, entries 1-4). As a model system, commercially available octyl boronic acid was subjected to cross-coupling with **3.98**. Product formation was observed employing the conditions described for entries 4-6 (Scheme 3-8), as analyzed by ^{1}H NMR and high-resolution mass spectrometry. Additional control experiments showed that boronic acid **3.119** smoothly coupled to 4-bromoacetophenone affording the desired product under conditions shown for entries 5-7 (Scheme 3-8). However, switching from the aryl halide to the vinyl halide **3.98** resulted in >5 different MIDA boronates, product formation being minor (Scheme 3-8). To further understand the reactivity landscape for this reaction, we also explored a general cross-coupling condition for vinyl halides[44] (Scheme 3-8, entry 8). However, in this condition, boronic acid **3.119** was recovered while vinyl halide **3.98** was fully consumed to form undesired byproducts. These results indicated that further development of optimal conditions are needed to efficiently couple these two unactivated substrates under conditions that are compatible with the MIDA boronate and amenable to automation.

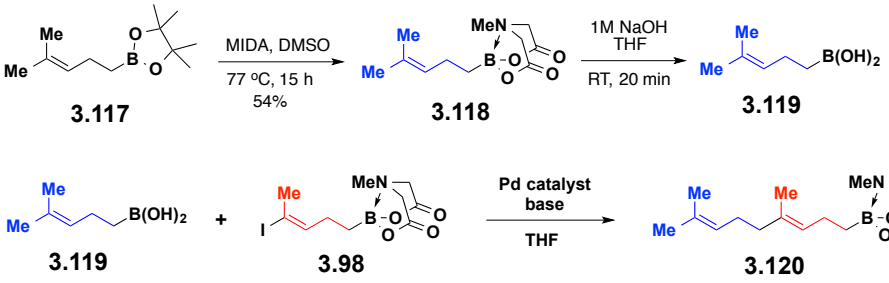

Entry	Catalyst	Ligand	Base	Temperature (°C)	Conversion
1	Pd_2dba_3	P(o-tol)$_3$	Ag_2O:K_2CO_3	60	iodide 3.98 recovered + decomposition
2	Pd_2dba_3	P(tBu)$_3$	KF	60	mainly iodide 3.98 recovered
3	Pd_2dba_3	P(Cy)$_3$	KF	60	mainly iodide 3.98 recovered
4	$PdCl_2$dppf.DCM	-	Ag_2O:K_2CO_3	60	mainly decomposition
5	$PdCl_2$dppf.DCM	-	Ag_2O	85	>5 MIDA boronates
6	Pd[P(o-tol)$_3$]$_2$		Ag_2O	85	>5 MIDA boronates
7	Pd(PPh$_3$)$_4$		Ag_2O	85	>5 MIDA boronates
8	PdXPhos		Cs_2CO_3	60	mainly decomposition

mass spec hit for product

Scheme 3-8. Suzuki-Miyaura cross-coupling of alkyl boronic acid **3.119** to vinyl iodide **3.98**.

In order to overcome this challenge, we turned our attention to Negishi cross-coupling which had substantial promise for forming Csp^3-Csp^2(vinyl) bonds. First, we looked for a simple solution employing THF as the reaction solvent (Scheme 3-9 top). However, greater than 12 equivalents of alkyl zinc bromide **3.97** was needed to reach >95% conversion from **3.98**, indicating that using a common activation method was not optimal to activate the C-Br bond and afford alkyl zinc bromide **3.97** in situ. Transferring this method to the synthesizer was

complicated by the necessity to quench the excess **3.97** and other byproducts. Alternatively starting from 5-iodo-2-methyl-2-pentene, an alkyl halide with a lower bond dissociation energy, was briefly explored, but a simpler activation method showed greater promise. Specifically, Zn insertion into the C-Br bond of 5-bromo-2-methyl-2-pentene using Zn dust and I_2 in DMF[45] formed alkyl zinc bromide **3.97** in situ, which was reacted with **3.98** (Scheme 3-9 bottom). With this approach, the intermediate MIDA boronate was successfully synthesized in 70% yield. The key to transferring this method onto the synthesizer required optimization of the solvent composition. With >5% DMF in THF as the reaction solvent, a biphasic mixture was observed in the purification module, thus disabling the catch-and-release purification to operate efficiently. However, with increasing the concentration of the alkyl zinc bromide to 2.5 M and decreasing the overall amount of DMF in the reaction to <5%, the intermediate was successfully purified using a simple aqueous work up and the general catch-and-release purification module.

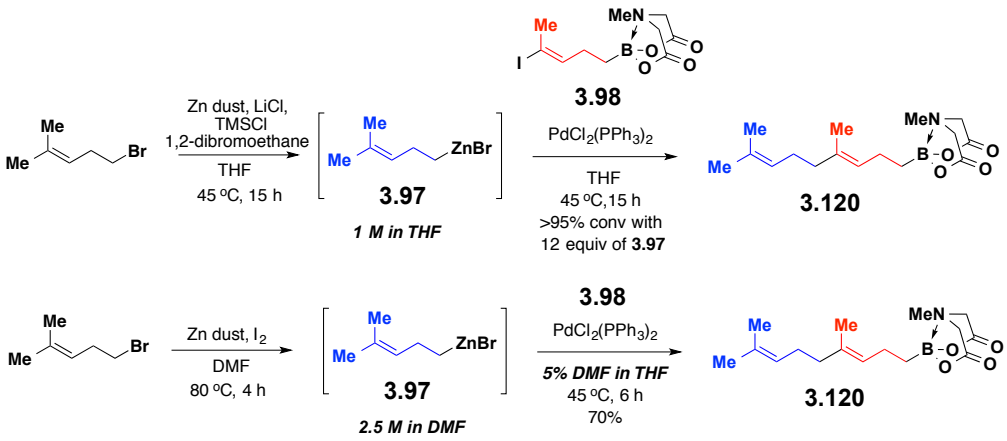

Scheme 3-9. Negishi cross-coupling of alkyl zinc bromide **3.97** to vinyl iodide **3.98**.

With the first step of the cross-coupling conditions established, manual optimization of the second step toward polyterpene linear precursor **3.100** was investigated. Deprotection of MIDA boronate **3.120** to boronic acid **3.121** and coupling **3.121** to aryl bromide **3.99** employing $Pd[P(o\text{-tol})_3]_2$, an air-stable and commercially available catalyst, and a base combination of Ag_2O/K_2CO_3[46] afforded linear precursor **3.100** in 60% yield (Scheme 3-10). The *ortho*-methyl groups of $Pd[P(o\text{-tol})_3]_2$ are proposed to block the open coordination site of Pd, thus minimizing the unproductive β-hydride elimination pathway.[47] This condition also afforded the Csp^3-Csp^2(heteroaryl) coupling between **3.90** and **3.91** toward citreofuran linear precursor **3.85**.

Employing only Ag_2O as the base at higher concentration (0.3 M) resulted in less than 50% conversion to product. In the final cyclization step, a catalyst-controlled enantioselective cation-π cyclization of linear precursor **3.100** was promoted by the 1:1 complex of *o,o'*-dichloro-BINOL and $SbCl_5$ to afford the tricyclic steroid-like skeleton **3.83** using conditions reported in the literature.[48]

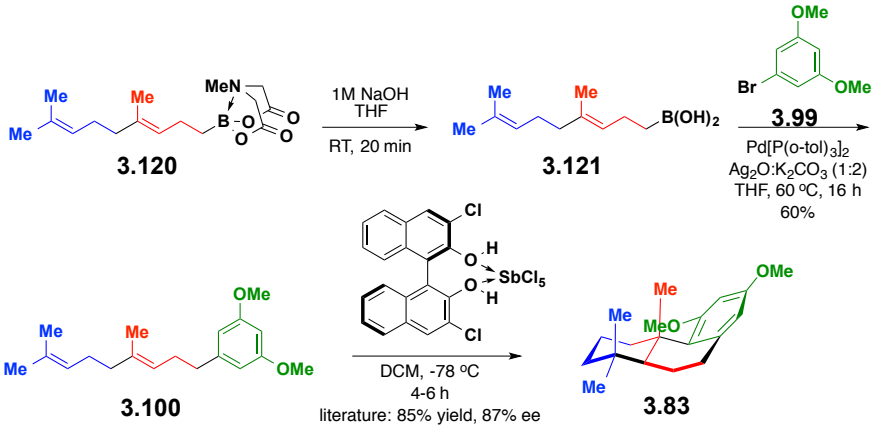

Scheme 3-10. Manual Csp^3-Csp^2 Suzuki-Miyaura cross-coupling of boronic acid **3.121** to aryl bromide **3.99** affords linear precursor **3.100**, which can be cyclized to form steroid-like tricyclic core **3.83**.

Taking advantage of the modularity that exists even between natural product classes, linear precursor **3.102** and alkaloid **3.82** share the same two out of three building blocks required for linear precursor synthesis. Thus, we next explored the final step toward the alkaloid target, which also involved a Csp^3-Csp^2 Suzuki-Miyaura cross-coupling with a potentially challenging trisubstitued vinyl halide with several sensitive functionalities. However, under the same exact cross-coupling conditions that yielded **3.100** in 60% yield, linear precursor **3.102** was synthesized in only 10% isolated yield. After a number of screens exploring the effects of solvent composition, temperature, base identity, Pd, and ligand sources, it was discovered that addition of an electron-rich phosphine ligand, P(*t*-Bu)$_2$Me,[49] improved the ratio of product to side products qualitatively analyzed by crude ^{1}H NMR (Scheme 3-11). Quantitative analysis either through analytical HPLC or ^{1}H NMR of the crude reaction mixture was difficult due to the presence of many side products with very similar chemical shifts to that of **3.102**. Preliminary results indicate that the conditions described in Scheme 3-11 provides **3.102** in higher yield (15-25%) than the cross-coupling condition without the addition of P(*t*-Bu)$_2$Me. To further improve on this yield, different carbonate bases were screened (Cs_2CO_3, Na_2CO_3, Ag_2CO_3) while keeping

the rest of the parameters constant, but all of these conditions showed no improvements on the ratios of product to side products. The use of K_2CO_3 alone led to decomposition of the starting materials and the use of Ag_2O alone led to incomplete conversion with the presence of side products. The use of CsF showed complete decomposition of both starting materials, and the use of other bases (KF and K_3PO_4) resulted in no conversion of **3.101**. Future work in this area involves exploring different Pd(0) and Pd(II) sources with P(*t*-Bu)$_2$Me.

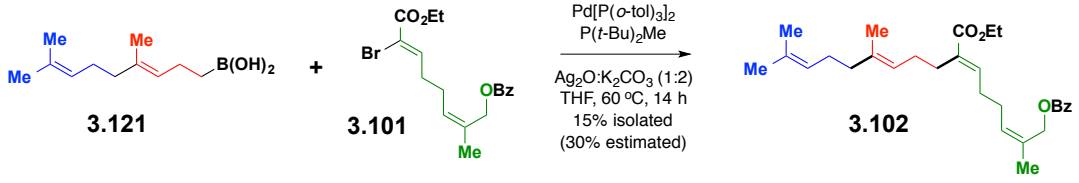

Scheme 3-11. Prelimiary study on the manual Csp^3-Csp^2 Suzuki-Miyaura cross-coupling of boronic acid **3.121** to vinyl bromide **3.101**.

After identification of a cross-coupling condition that can be translated to the synthesizer for automation, the following sequence could be applied for the cyclization of this linear precursor to its corresponding alkaloid target. Following two reductions and an oxidation to afford **3.124**, a Heathcock-like biosynthesis-inspired cascade of intramolecular ammonium condensation, trans-annular Diels-Alder, and Prins-type cyclizations are expected to afford alkaloid core **3.82** (Scheme 3-12).[50]

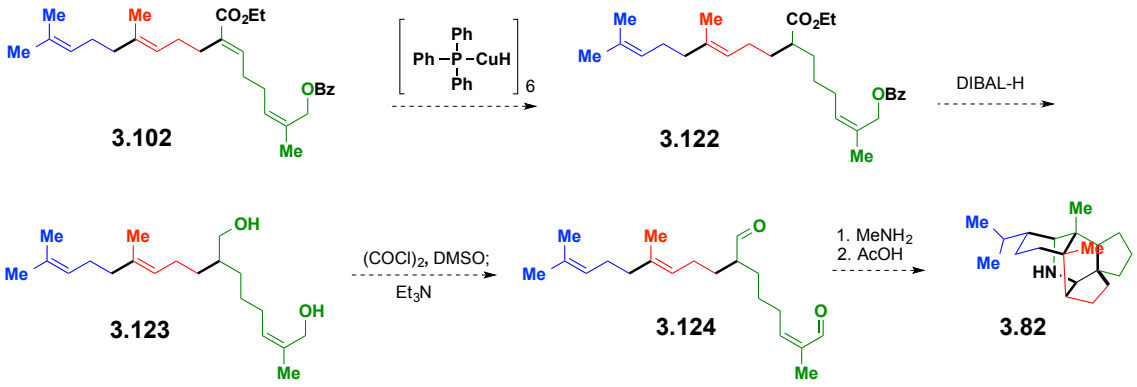

Scheme 3-12. Manual cyclization plan from linear precursor **3.102** to alkaloid core **3.82**.

3-9 SEMI-AUTOMATED SYNTHESIS OF CYCLIC SMALL MOLECULES

We very recently achieved the semi-automated synthesis of a natural product and several natural-product cores on the synthesizer applying the cross-coupling conditions mentioned above. Specifically, in an automated fashion, the complex macrocyclic natural product citreofuran **3.79** was prepared by my colleagues Junqi Li and Dr. Steve Ballmer by the iterative assembly of building blocks **3.90**-**3.92** via fully automated cross-coupling of challenging Csp^3 and 2-furanyl halide boronic acid intermediates to generate linear precursor **3.85** (Scheme 3-13). A subsequent substrate-controlled diasteroselective macrocyclization and benzyl ether deprotections provided rapid access to citreofuran as a single stereoisomer.[32] Importantly, the required stereochemical information for this synthesis is pre-encoded in the chiral nonracemic MIDA boronate building block **3.90**.

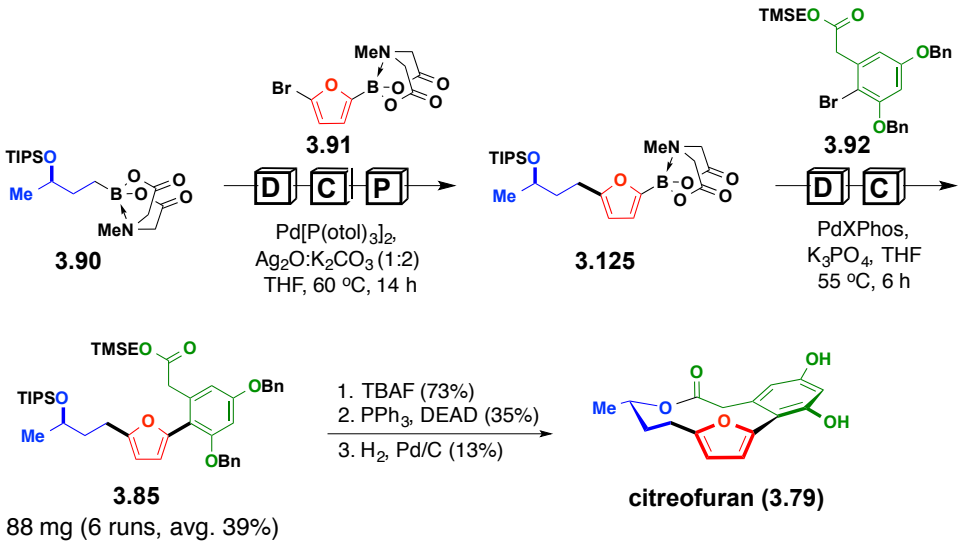

Scheme 3-13. Semi-automated synthesis of citreofuran natural product (**3.79**).

In a similar fashion, linear precursor **3.96** of an indene natural product derivative was readily prepared by Dr. Steve Ballmer in collaboration with Michael Schmidt via fully automated stereospecific assembly of stereo-defined building blocks **3.93**-**3.95** using the manually optimized conditions developed by Junqi Li (Scheme 3-14). Catalyst-controlled intramolecular Diels-Alder reaction is expected to generate the targeted tricycle in a highly stereoselective fashion.[51]

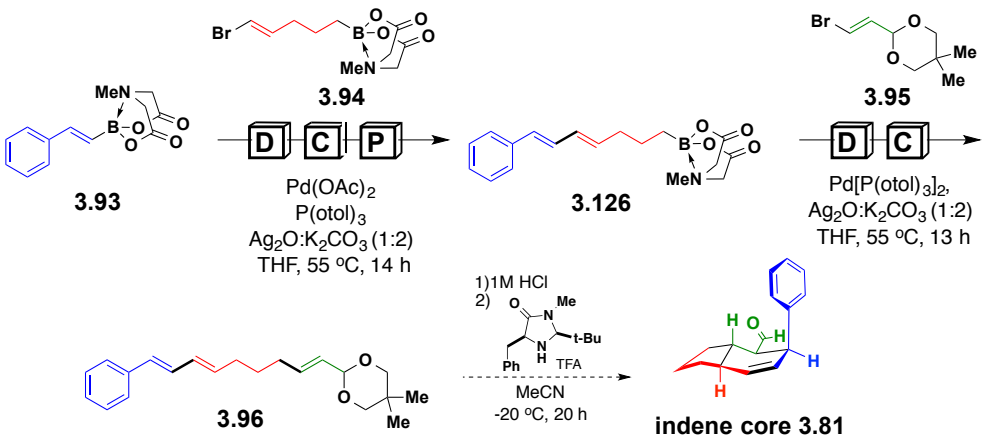

Scheme 3-14. Semi-automated synthesis of indene core **3.81**.

In a similar fashion, translating the manual experimental results, linear precursor **3.100** was prepared via fully automated stereospecific assembly of building blocks **3.97** and **3.98** via Negishi cross-coupling under the conditions described in Scheme 3-10 (Scheme 3-15). In the second step, building block **3.99** was successfully coupled to the boronic acid derived form MIDA boronate **3.120** to afford **3.100** (Scheme 3-15). Polycyclization of this linear precursor is expected to generate the targeted tricycle in a highly stereoselective fashion.[49]

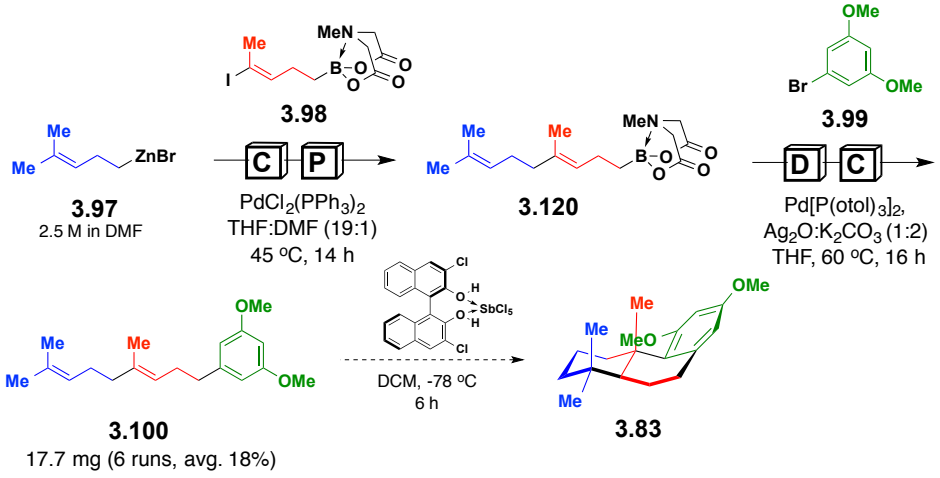

Scheme 3-15. Semi-automated synthesis of polyterpene core **3.83**.

3-10 SUMMARY AND CONCLUSIONS

With the ultimate goal of accelerating the functional discoveries of small molecules, a small molecule synthesizer has been developed. This synthesizer is capable of making a wide range of small molecules: materials, pharmaceuticals, natural products, and natural product derivatives via fully-automated iterative assembly of MIDA boronate building blocks. In concert with automation of ICC, we have expanded this platform to include C-N and Csp^3-Csp^2 bond formations, thus increasing the scope and flexibility of this building block approach. Moreover, this platform can provide simple, rapid, and flexible access to even topologically complex cyclic small molecule targets by automated synthesis of their respective linear precursors. All of these small molecules can be prepared in the manner of 1 h of person time regardless of the number of building blocks required, significantly decreasing the overall time commitment of a researcher by several days. In the future, with thousands of potentially applicable building blocks already commercially available, we envision that a wide range of small molecules can be delivered on-demand to all scientists through this automated platform, thus leading to the advancement and acceleration of the small molecule discovery process.

However, we recognize that this is only the starting point. Increases in the scope of this automated platform and access to a larger chemical space will continue to be driven by rapidly expanding new methods for making and cross-coupling suitable building blocks. Specifically, efficient and general methods to make new types of heterocycles will contribute to adding a new collection of reoccurring structures in materials, pharmaceuticals, as well as natural products. In addition, further advances in developing efficient and general methods to couple heteroatoms to form C-O and C-S bonds, in addition to C-N bonds, will substantially expand the chemical space this platform can access. As described in Chapter 2, MIDA boronates represent protecting groups for not only boronic acids, but also halides. In addition, since boronic acids are versatile functional groups, they can be oxidized to their corresponding phenols in one-step. Therefore, this platform shows promise to incorporate coupling reactions with functional groups other than boronic acids, as long as all the intermediates contain a MIDA boronate. Lastly, the development of increasingly general conditions to couple Csp^3-hybridized atoms will be crucial in accessing flexible, cyclic, and topologically complex small molecules. Harnessing these advances in concert with further improvements in the speed and generality of this synthesizer will ultimately

broaden the access of small molecules to non-specialists and accelerate the discovery of small molecule function.

3-11 REFERENCES

[1] (a) Merrifield, R. B. *Science* **1965**, *150*, 178-185. (b) Merrifield, R. B.; Stewart, J. M. *Nature* **1965**, 207, 522-523. (c) Caruthers, M. H. *Science* **1985**, *230*, 281-285. (d) Plante, O. J.; Palmacci, E. R.; Seeberger, P. H. *Science* **2001**, *291*, 1523-1527.

[2] Fischbach, M. A.; Walsh, C. T. *Chem. Rev.* **2006**, *106*, 3468-3496.

[3] (a) Gillis, E. P.; Burke, M. D. *J. Am. Chem. Soc.* **2007**, *129*, 6716-6717. (b) Gillis, E. P.; Burke, M. D. *Aldrichimica Acta* **2009**, *42*, 17-27.

[4] Miyaura, N.; Suzuki, A. *Chem. Rev.* **1995**, *95*, 2457-2483.

[5] (a) Woerly, E. M.; Cherney, A. H.; Davis, E. K.; Burke, M. D. *J. Am. Chem. Soc.* **2010**, *132*, 6941-6943. (b) Fujii, S.; Chang, S. Y.; Burke, M. D. *Angew. Chem. Int. Ed.* **2011**, *50*, 7862-7864. (c) Fujita, K.; Matsui, R.; Suzuki, T.; Kobayashi, S. *Angew. Chem. Int. Ed.* **2012**, *51*, 7271-7274.

[6] Gray, K. C.; Palacios, D. S.; Dailey, I.; Endo, M. M.; Uno, B. E.; Wilcock, B. C.; Burke, M. D. *Proc. Natl. Acad. Sci. U.S.A.* **2012**, *109*, 2234-2239.

[7] (a) Grob, J. E.; Dechantsreiter, M. A.; Tichkule, R. B.; Connolly, M. K.; Honda, A.; Tomlinson, R. C.; Hamann, L. G. *Org. Lett.* **2012**, *14*, 5578-5581. (b) Li, J.; Burke, M. D. *J. Am. Chem. Soc.* **2011**, *133*, 13774-13777.

[8] For preliminary studies on the development of a solid-phase purification module for MIDA boronates in the context of automation, see: (a) Gillis, E. P. Iterative Cross-Coupling with MIDA Boronates. PhD Dissertation, University of Illinois at Urbana-Champaign, 2011. (b) Ballmer, S. G. A Small Molecule Synthesizer. PhD Dissertation, University of Illinois at Urbana-Champaign, 2013.

[9] Lennox, A. J. J.; Lloyd-Jones, G. C. *J. Am. Chem. Soc.* **2012**, *134*, 7431-7441.

[10] Knapp, D. M.; Gillis, E. P.; Burke, M. D. *J. Am. Chem. Soc.* **2009**, *131*, 6961-6963.

[11] Kinzel, T.; Zhang, Y.; Buchwald, S. L. *J. Am. Chem. Soc.* **2010**, *132*, 14073-14075.

[12] Müller, T. J. J.; Bunz, U. H. F. eds. *Functional Organic Materials: Syntheses, Strategies and Applications*; Wiley-VCH, Weinheim, Germany, 2007.

[13] Manley, P. W.; Acemoglu, M.; Marterer W.; Pachinger, W. *Org. Proc. Res. Dev.* **2003**, 7, 436-445.

[14] Gillis, E. P.; Burke, M. D. *J. Am. Chem. Soc.* **2008**, *130*, 14084-14085.

[15] Kunze, B.; Jansen, R.; Hofle, G.; Reichenbach, H. *J. Antibiot.* **1994**, *47*, 881-886.

[16] Lee, S. J.; Gray, K. C.; Paek, J. S.; Burke, M. D. *J. Am. Chem. Soc.* **2008**, *130*, 466-468.

[17] (a) Sklar, L. A.; Hudson, B. S.; Simoni, R. D. *Proc. Natl. Acad. Sci. U.S.A.* **1975**, *72*, 1649-1653. (b) Kuerschner, L.; Ejsing, C. S.; Ekroos, K.; Schevchenko, A.; Anderson, K. I.; Thiele, C. *Nat. Methods* **2005**, *2*, 39-45.

[18] (a) Luecke, H.; Schobert, B.; Richter, H.-T.; Cartailler, J.-P.; Lanyi, J. K. *Science* **1999**, *286*, 255-260. (b) Kobayashi, T.; Saito, T.; Ohtani, H. *Nature* **2001**, *414*, 531-534. (c) Zhong, Q.; Ruhman, S.; Ottolenghi, M.; Sheves, M.; Friedman, N.; Atkinson, G. H.; Delaney, J. K. *J. Am. Chem. Soc.* **1996**, *118*, 12828-12829.

[19] Uenishi, J.; Matsui, K.; Wada, A. *Tetrahedron* **2003**, *44*, 3093-3096.

[20] Klubnick, J. A. Expansion of the Iterative Cross-Coupling Synthesis Strategy through Csp^3 Halide Cross-Coupling, Mida Boronate Synthesis, and Chan-Lam Couplings. Thesis, University of Illinois at Urbana-Champaign, 2011.

[21] Duclos, B. A.; Jung, M. E. *Teterahedron* **2006**, *62*, 9321-9334.

[22] $Pd(OAc)_2$ and SPhos combination also provided good conversion to product and minimal side products. Surveying different bases revealed that Cs_2CO_3 is a better base than K_2CO_3 or K_3PO_4 for this reaction. For the latter, only ~50% conversion to product was observed under otherwise identical conditions.

[23] Hahlbrock, K.; Scheel, D. *Annu. Rev. Plant Physiol. Plant Mol. Biol.* **1989**, *40*, 347-369.

[24] Baumgartner, L.; Sosa, S.; Atanasov, A. G.; Bodensieck, A.; Fakhrudin, N.; Bauer, J.; Del Favero, G.; Ponti, C.; Heiss, E. H.; Schwaiger, S.; Ladurner, A.; Widowitz, U.; Loggia, R. D.; Rollinger, J. M.; Werz, O.; Bauer, R.; Dirsch, V. M.; Tubaro, A.; Stuppner, H. *J. Nat. Prod.* **2011**, *74*, 1779–1786.

[25] Heiss, E. H.; Baumgartner, L.; Schwaiger, S.; Heredia, R. J.; Atanasov, A. G.; Rollinger, J. M.; Stuppner, H.; Dirsch, V. M. *Planta Med* **2012**, *78*, 678-681.

[26] Arnone, A.; Modugno, V. D.; Nasini, G.; de Pava, O. V. *Gazz. Chim. Ital.* **1990**, *120*, 397-401.

[27] (a) Dominguez, X. A.; Sanchez V., H.; Espinoza B., G. C.; Verde S., J.; Achenbach, H.; Utz, W. *Phytochemistry* **1990**, *29*, 2651-2653. (b) Achenbach, H.; Utz, W.; Sánchez V., H.; Touché, E. M. G.; Verde, J.; Domínguez, X. A. *Phytochemistry* **1995**, *39*, 413-415.

[28] Hili, R.; Yudin, A. K. *Nat. Chem. Biol.* **2006**, *2*, 284-287.

[29] Denni-Dischert, D.; Marterer, W.; Bänziger, M.; Yusuff, N.; Batt, D.; Ramsey, T.; Geng, P.; Michael, W.; Wang, R-M. B.; Taplin Jr., F.; Versace, R.; Cesarz, D.; Perez, P. B. *Org. Proc. Res. Dev.* **2006**, *10*, 70-77.

[30] Yonetoku, Y.; Kubota, H.; Miyazaki, Y.; Okamoto, Y.; Funatsu, M.; Yoshimura-Ishikawa, N.; Ishikawa, J.; Yoshino, T.; Takeuchi, M.; Ohta, M. *Bioorg. Med. Chem.* **2008**, *16*, 9457-9466. (b) Yonetoku, Y.; Kubota, H.; Okamoto, Y.; Ishikawa, J.; Takeuchi, M.; Ohta, M.; Tsukamoto, S. *Bioorg. Med. Chem.* **2006**, *14*, 5370-5383. (c) Djuric, S. W. et al. *J. Med. Chem.* **2000**, *43*, 2975-2981.

[31] Qiao, J. X.; Lam, P. Y. S. *Synthesis*, **2011**, 829-856.

[32] Bracher, F.; Schulte, B. *Natural Product Res.* **2003**, *17*, 293-299.

[33] Yoder, R. A.; Johnston, J. N. *Chem. Rev.* **2005**, *105*, 4730-4756.

[34] Heathcock, C. H. *Proc. Natl. Acad. Sci. U.S.A.* **1996**, *93*, 14323-14327.

[35] Aaroz, R.; Servent, D.; Molgó, J.; Iorga, B. I.; Fruchart-Gaillard, C.; Benoit, E.; Gu, Z.; Stivala, C.; Zakarian, A. *J. Am. Chem. Soc.* **2011**, *133*, 10499-10511.

[36] (a) Yang, C-T.; Zhang, Z-Q.; Tajuddin, H.; Wu, C-C.; Liang, J.; Liu, J-H.; Fu, Y.; Czyzewska, M.; Steel, P. G.; Marder, T. B.; Liu, L. *Angew. Chem. Int. Ed.* **2012**, *51*, 528-532. For an alternate condition for borylation of primary alkyl bormides, see: (b) Joshi-Pangu, A.; Ma, X.; Diane, M.; Iqbal, S.; Kribs, R. J.; Huang, R.; Wang, C-Y.; Biscoe, M. R. *J. Org. Chem.* **2012**, *77*, 6629-6633.

[37] Ilardi, E. A.; Stivala, C. E.; Zakarian, A. *Org. Lett.* **2008**, 10, 1721-1730.

[38] Synthesized using a literature procedure: Lifchits, O.; Reisinger, C. M.; List, B. *J. Am. Chem. Soc.* **2010**, *132*, 10227-10229.

[39] Synthesized using a literature procedure: Ghadigaonkar, S.; Koli, M. R.; Gamre, S. S.; Choudhary, M. K.; Chattopadhyay, S.; Sharma, A. *Tetrahedron: Asymmetry* **2012**, *23*, 1093-1099.

[40] Synthesized using a literature procedure: Myers, A. G.; Dragovich, P. S. *Org. Synth.* **1995**, *72*, 104.

[41] (a) Jana, R.; Pathak, T. P.; Sigman, M. S. *Chem. Rev.* **2011**, *111*, 1417-1492. (b) Doucet, H. *Eur. J. Org. Chem.* **2008**, 2013-2030. (b) Fall, Y.; Coucet, H.; Santelli, M. *Appl. Organometal. Chem.* **2008**, *22*, 503-509.

[42] Placzek, A. T.; Gibbs, R. A. *Org. Lett.* **2011**, *13*, 3576-3579.

[43] (a) Falck, J. R.; Kumar, P. S.; Reddy, Y. K.; Zou, G.; Capdevila, J. H. *Tetrahedron Lett.* **2001**, *42*, 7211-7212. (b) Glasspoole, B. W.; Ghozati, K.; Moir, J. W.; Crudden, C. M. *Chem. Commun.* **2012**, *48*, 1230-1232.

[44] (a) Woerly, E. M.; Roy, J. R.; Burke, M. D. *Nature Chem.* **2014**, *submitted*. (b) Woerly, E. W. Total Synthesis and Study of the Antilipoperoxidant Peridinin, Synthesis of Versatile MIDA Boronate Building Blocks, and a General Strategy for the Synthesis of Polyenes. PhD. Dissertation, University of Illinois at Urbana-Champaign, 2013.

[45] Huo, S. *Org. Lett.* **2003**, *5*, 423-425.

[46] Zou, G.; Reddy, K.; Falck, J. R. *Tetrahedron Lett.* **2001**, *42*, 7213-7215.

[47] (a) Paul, F.; Joe Patt, J.; Hartwig, J. F. *Organometallics* **1995**, *14*, 3030-3039. (b) Hartwig, J. F.; Richards, S.; Barañano, D.; Paul, F. *J. Am. Chem. Soc.* **1996,** *118,* 3626-3633.

[48] Surendra, K.; Corey, E. J. *J. Am. Chem. Soc.* **2012**, *134*, 11992-11994.

[49] Hills, I. D.; Netherton, M. R.; Fu, G. C. *Angew. Chem. Int. Ed.* **2003**, *42*, 5749-5752.

[50] Heathcock, C. H.; Piettre, S.; Ruggeri, R. B.; Ragan, J. A.; Kath, J. C. *J. Org. Chem.* **1992**, *57*, 2554-2566.

[51] Wilson, R. M.; Jen, W. S.; MacMillan, D. W. C. *J. Am. Chem. Soc.* **2005**, *127*, 1616-1617.

CHAPTER 3
EXPERIMENTAL SECTION

Materials. Commercial reagents were purchased from Sigma-Aldrich, EMD Millipore, Fisher Scientific, Alfa Aesar, Frontier Scientific, Oakwood Products, or Strem and were used without further purification unless otherwise noted. Most of the building blocks used in these studies are available from Sigma-Aldrich® [**3.1a** (697311), **3.1b** (700231), **3.1c** (721573), **3.1d** (710032), **3.1e** (MIDA071), **3.1f** (698229), **3.1g** (697494), **3.1h** (698164), **3.1i** (698016), **3.1j** (698148), **3.1k** (704547), **3.1l** (MIDA032), **3.1m** (736600), **3.1n** (748714), **3.1o** (723711), **3.1p** (738514), **3.1q** (699861), **3.1r** (MIDA020), **3.1s** (MIDA076), **3.1t** (704873), **3.2a** (730335), **3.2b** (699853), **3.2c** (699160), **3.2d** (708828), **3.2e** (701017), **3.2f** (733539), **3.2g** (710024), **3.2h** (703710), **3.2i** (707252), **3.4** (698083), **3.6** (MIDA080), **3.7** (701092), **3.10** (MIDA083), **3.11** (MIDA084), **3.12** (363774), **3.15** (723711), **3.16** (MIDA081), **3.17** (C70223), **3.72** (MIDA085), **3.19** (698032), **3.23** (MIDA034), **3.28** (MIDA013), **3.38** (701831), **3.40** (MIDA014), **3.45** (MIDA017), **3.39** (MIDA039), **3.41** (MIDA015), **3.76**, **3.77**, **3.75**, **3.93** (699292)], Frontier Scientific, Inc. [**3.8** (B1644), **3.73** (B10713), **3.43** (B1851)], or Aurora Fine Chemicals LLC [**3.71** (A00.242.706)].

General Experimental Procedures. Unless otherwise noted, manual building block syntheses were carried out in oven- or flame-dried glassware under a dry inert atmosphere. Unless otherwise noted: Celite™ refers to Celite™ 545 filter aid (not acid washed); Darco® refers to activated carbon, Darco® G-60, -100 mesh, powder; and K_3PO_4 and K_2CO_3 were both anhydrous and were freshly and finely ground in a 120 °C mortar and pestle. XPhos 2nd generation palladacycle refers to chloro(2-dicyclohexylphosphino-2′,4′,6′-triisopropyl-1,1′-biphenyl)[2-(2′-amino-1,1′-biphenyl)]palladium(II) (741825, Sigma-Aldrich) (21). Solvents were purified via passage through packed columns as described by Pangborn and coworkers[1] (THF, Et_2O, CH_3CN, CH_2Cl_2: dry neutral alumina; hexanes, benzene, toluene: dry neutral alumina and Q5 reactant; DMSO, DMF: activated molecular sieves. Water was deionized. Thin layer chromatography (TLC) was performed using the indicated eluent on E. Merck silica gel 60 F254 plates (0.25 mm). Compounds were visualized by exposure to a UV lamp (λ = 254 and/or 366 nm) and/or a basic solution of $KMnO_4$ followed by brief heating with a Varitemp® heat gun. Flash chromatography was performed as described by Still and coworkers[2] using EM Merck silica gel 60 (230-400

mesh). RP-HPLC purification was performed on Agilent 1100 series HPLC system equipped with an Agilent Prep-C18, 10 μm, 30 x 150 mm (product number: 413910-302) column or Sunfire Prep-C18, 5 μm, 30 x 150 mm (product number: 186002797) with indicated eluent, flow rate, and wavelength.

Structural Analysis. ^{1}H NMR spectra were recorded at room temperature on one of the following instruments: Varian Unity 500, Varian VXR 500, or Varian Unity Inova 500NB. Chemical shifts (δ) are reported in parts per million (ppm) downfield from tetramethylsilane and referenced to residual protium in the NMR solvent ($CDCl_3$, δ = 7.26; $(CD_3)_2CO$, δ = 2.05, center line; CD_2Cl_2, δ = 5.32, center line; $(CD_3)_2SO$, δ = 2.50, center line). Data are reported as follows: chemical shift, multiplicity (s = singlet, d = doublet, t = triplet, q = quartet, sept = septet, m = multiplet, br = broad, app = apparent, dd = doublet of doublets, dt = doublet of triplets, dq = doublet of quartets), coupling constant (*J*) in Hertz (Hz), and integration. ^{13}C NMR spectra were recorded at room temperature on one of the following instruments: Varian Unity 500 or Varian VXR 500. Chemical shifts (δ) are reported in ppm downfield from tetramethylsilane and referenced to carbon resonances in the NMR solvent ($CDCl_3$, δ = 77.16, center line; $(CD_3)_2CO$, δ = 29.84, center line; CD_2Cl_2, δ = 53.84; $(CD_3)_2SO$, δ = 39.52, center line). Carbons bearing boron substituents were not observed due to quadrupolar relaxation. High-resolution mass spectra (HRMS) were performed by Furong Sun and Elizabeth Eves at the University of Illinois School of Chemical Sciences Mass Spectrometry Laboratory.

EXPERIMENTAL PROCEDURES

I. DESIGN OF THE SMALL MOLECULE SYNTHESIZER[3]

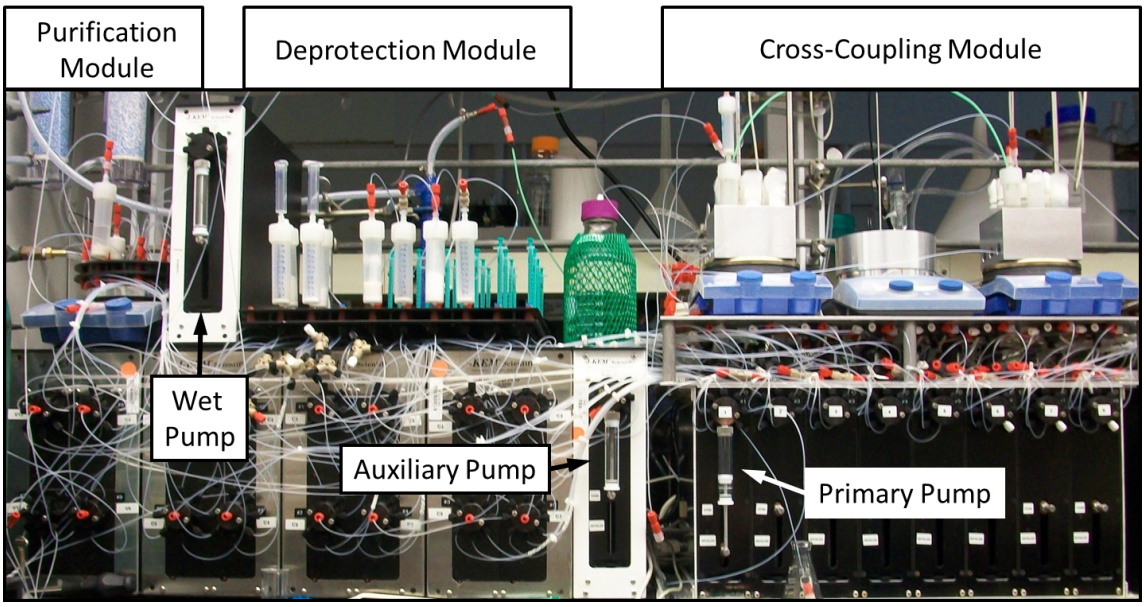

Design of the Deprotection Module

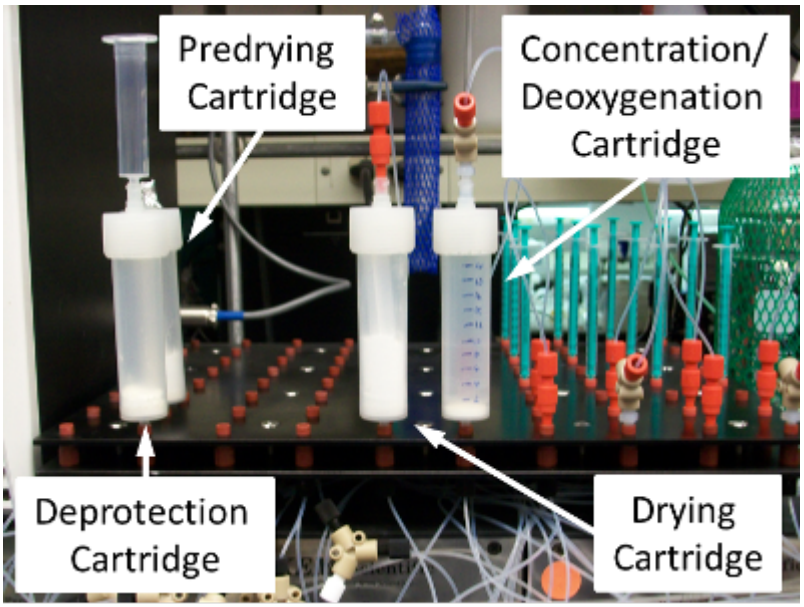

The deprotection module consists of two J-KEM® Scientific V6 programmable syringe pumps (part # SYR-1400PC). Both are fitted with a 10-mL glass/PTFE syringe (part # SPGS-10000) and an 8-port distribution valve (part # SPDV-8). One pump (the Primary Pump) is utilized as the organic liquid handling pump and the other (the Wet Pump) is used exclusively as the aqueous liquid handling pump. The module utilizes an additional five 8-port distribution valves (part # SPDV-CS8) housed in four separate quad stack KEM select distribution modules (part # SYR-CS4) for liquid handling. A source of dry nitrogen and dry argon are used for liquid handling and deoxygenation/concentration processes. Connections between valves are made with FEP tubing (1/16'' OD, 0.030'' ID).

To the Deprotection Cartridge, the Primary Pump adds THF and the Wet Pump adds water. The reaction is then agitated with pulses of argon gas. The Wet Pump then adds aqueous potassium phosphate buffer (pH = 6) and the Primary Pump adds Et_2O. The resulting biphasic system is agitated with pulses of nitrogen gas and the aqueous layer is drawn off and disposed of by the Wet Pump. The Wet Pump adds 50% saturated aqueous NaCl. The resulting biphasic system is agitated with pulses of nitrogen and the aqueous layer is drawn off and disposed of by the Wet Pump. The Primary Pump transfers the wet organic solution to a Predrying, and subsequently Drying Cartridge, containing drying agents and agitates the mixture by repeatedly withdrawing/injecting the solution. The Primary Pump transfers the dried organic solution to a Concentration/Deoxygenation Cartridge and concentrates/deoxygenates the solution with pulses of argon gas.

Design of the Cross-Coupling Module

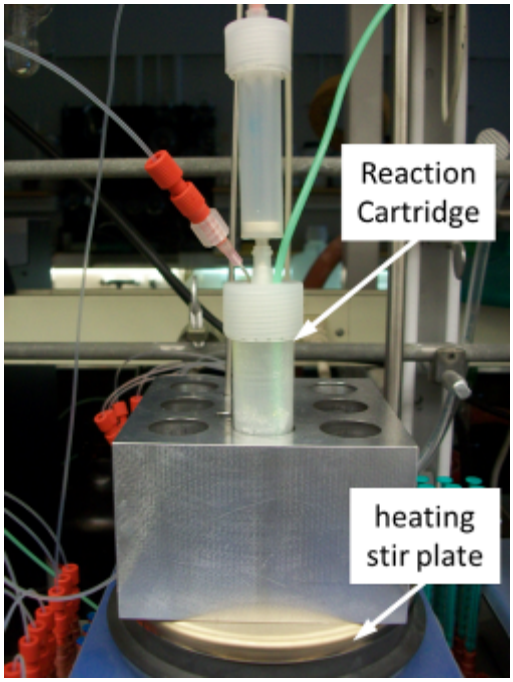

The cross-coupling module consists of one J-KEM® Scientific V6 programmable syringe pump (part # SYR-1400PC), the Primary Pump described above. The module utilizes one additional 8-port distribution valve (part # SPDV-CS8) housed in one separate quad stack KEM select distribution module (part # SYR-CS4) for liquid handling (shared with the deprotection module). A source of dry nitrogen and dry argon are used for liquid handling and deoxygenation processes (shared with the deprotection module). Two IKA® RET control visc IKAMAG® safety control heating stir plates (part # 3364001) and one IKA® RCT basic IKAMAG® safety control heating stir plate (part # 3810001) are used for reaction stirring and temperature control. Connections between valves are made with FEP tubing (1/16'' OD, 0.030'' ID).

The Reaction Cartridge, agitated with a magnetic stir bar, is deoxygenated with pulses of argon gas. The Primary Pump adds THF to the reaction cartridge and then slowly adds the dried/deoxygenated THF solution of boronic acid. After the addition, the reaction is allowed to agitate.

Design of the Purification Module

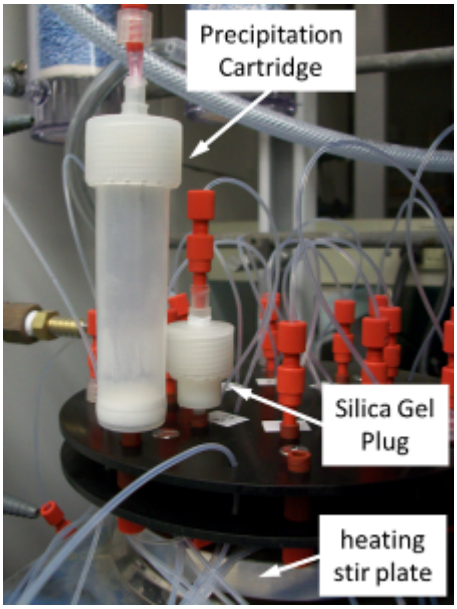

The purification module consists of two J-KEM® Scientific V6 programmable syringe pumps (part # SYR-1400PC). One is the Primary Pump described above. The other pump (the Auxillary Pump) is used exclusively as the column eluent and waste handling pump. The module utilizes an additional six 8-port distribution valves (part # SPDV-CS8) housed in three separate quad stack KEM select distribution modules (part # SYR-CS4) for liquid handling. Five of these distribution valves are shared with the deprotection and cross-coupling modules. Two IKA® RET control visc IKAMAG® safety control heating stir plates (part # 3364001), shared with the cross-coupling module, and one IKA® RCT basic IKAMAG® safety control heating stir plate (part # 3810001) are used. Connections between valves are made with FEP tubing (1/16'' OD, 0.030'' ID).

The Auxillary Pump adds hexanes to the Precipitation Cartridge, agitated with a magnetic stir bar. The Primary Pump adds portions of the crude reaction solution to the Precipitation Cartridge. The Auxillary Pump then withdraws the solvent through the Silica Gel Plug. This process is repeated until the Reaction Cartridge is empty. The Primary Pump then adds 1.5% MeOH in Et_2O to the Precipitation Cartridge and then the Auxillary Pump withdraws the solvent through the Silica Gel Plug. The Primary Pump then adds Et_2O to the Precipitation Cartridge and then the

Auxillary Pump withdraws the solvent through the Silica Gel Plug. The Auxillary Pump then adds THF to the Precipitation Cartridge and the Primary Pump removes the resulting solution and transfers it to the next Deprotection Cartridge.

Description of the Software

The synthesizer is controlled remotely on a Windows-based computer by a custom software program written in VB.NET (based on code written for the J-KEM® Scientific V6 programmable syringe pumps). The software program is designed to interpret instructions to the synthesizer written in simple custom scripting language. Pre-set series of instructions enable all of the steps required for a synthesis to be executed in a fully automated fashion after the operator simply presses "Start."

II. GENERAL METHOD FOR ONE AUTOMATED ICC CYCLE

The following cartridges (unless otherwise noted, cartridge refers to a 12-g Luknova column capped with a 12-g Luknova column screw cap) were prepared:

First Deprotection Cartridges contain solid NaOH and the starting MIDA boronate.

Second and Third Deprotection Cartridges contain solid NaOH.

Predrying Cartridges contain Celite™ (800 mg) and anhydrous $MgSO_4$ (2.1 g). These solids are mixed thoroughly and a plastic 5-mL syringe plunger is placed on top of the mixed solids. This is topped with an aluminum foil cover.

Drying Cartridges contain Celite™ (300 mg) with 4 Å molecular sieves (activated, powder, -325 mesh) (3.6 g) layered on top. A plastic 5-mL syringe plunger is placed on top of the layered solids.

Concentration/Deoxygenation Cartridges are empty.

First Reaction Cartridges contain a PTFE-coated magnetic stir bar, coupling partner, catalyst and ligand, and base. For this cartridge, the factory-supplied fiber frit has been removed and a medium porosity glass frit installed. The cap is pierced with a 1.5-inch 18 G needle and topped with an empty 4-g Luknova column (capped with a 4-g Luknova column screw cap). This cap is tethered to another cap PTFE tubing (1/16-inch I.D., 1/8-inch O.D.). This additional cap, pierced

with a 1.5-inch 18 G needle, is attached to the Reaction Filtration Cartridge. The PTFE tubing is adjusted to place the end of the tubing approximately 5 mm above the frit of the First Reaction Cartridge and approximately 20 mm below the screw cap of the Reaction Filtration Cartridge. The luer ports of both screw caps are packed with a small ball of rolled Kimberly-Clark® Kimwipes™.

Reaction Filtration Cartridges contain a PTFE-coated magnetic stir bar and a mixture of Celite™ (2.5 g) and Florisil® (1.25 g). This is tethered to the First Reaction Cartridge as described above.

Second and Third Reaction Cartridges contain a PTFE-coated magnetic stir bar, coupling partner, catalyst and ligand, and base.

Precipitation Cartridges contain a PTFE-coated magnetic stir bar, Celite™ (150 mg), and 3-aminopropyl functionalized silica gel (250 mg). Hexanes (10 mL) is added and the cartridge is swirled vigorously to suspend and homogenize the mixture of solids. The stir bar and solids are allowed to settle over 30 seconds and the supernatant hexanes is pushed out of the cartridge with an overhead pressure of air. The stir bar is now embedded in the mixture of solids wet with hexanes.

Silcia Gel Plugs contain silica gel, tightly packed, topped with a 4-g Luknova column frit. This is capped with a 4-g Luknova column screw cap, using four layers of PTFE tape on the sealing insert to ensure a leak-free seal.

General Automated Procedure for One ICC Cycle

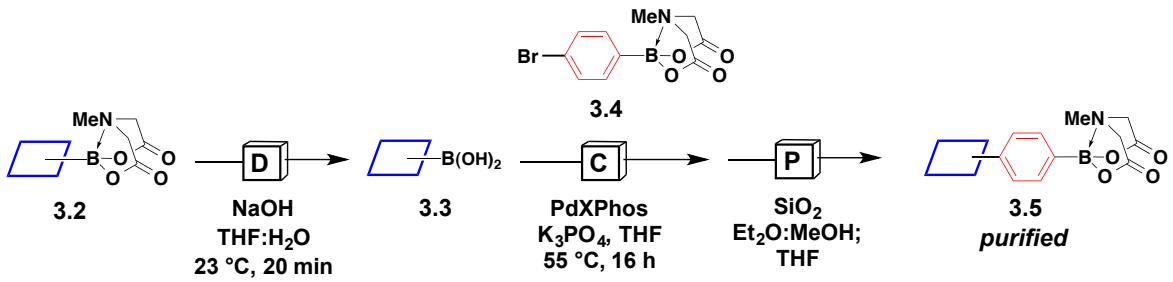

The following set of cartridges [Predrying, Drying, Concentration/Deoxygenation, Reaction Filtration, Precipitation, Silica Gel Plug] were prepared. In addition, the Deprotection Cartridge was charged with the starting MIDA boronate **3.2** (1.0 mmol) and NaOH (3.0 mmol), and the

Reaction Cartridge was equipped with a magnetic stir bar, coupling partner (0.33 mmol), XPhos 2nd generation palladacycle (0.017 mmol), and K_3PO_4 (3.0 mmol). The cap was pierced with a 1.5-inch 18 G needle and topped with an empty 4-g Luknova column with a screw cap. All cartridges were placed on the synthesizer and the reaction was initiated by pressing "Start" on a computer. The reaction was stirred at 55 °C for a total of 16 h. No human intervention was required throughout the completion of the synthesis and purification of the targeted product.

Detailed Automated Procedure for One ICC Cycle

The small molecule synthesizer executes the following steps once the operator presses "Start".
In the deprotection module, to a Deprotection Cartridge containing a starting MIDA boronate **3.2** (1.0 mmol) and NaOH (3.0 mmol, 120 mg) is added 12 mL THF followed by 3 mL water. After 20 minutes agitation at 23 °C, 3 mL aqueous potassium phosphate buffer (pH = 6) and 5 mL Et_2O are added and the layers are separated. Then 3 mL 50% saturated aqueous NaCl are added and the layers are separated. The THF/Et_2O solution of boronic acid is dried using a Predrying and Drying Cartridge. The resulting dry THF/Et_2O solution is transferred to a Concentration/Deoxygenation Cartridge. The drying agents are washed with 6 mL THF, which is added to the Concentration/Deoxygenation Cartridge. The organic solution is concentrated to 10 mL (evaporating most of the Et_2O) and the drying agents are washed with an additional 6 mL THF, which is added to the Concentration/Deoxygenation Cartridge. The organic solution (now only THF) is concentrated to 9 mL.

In the cross-coupling module, to a deoxygenated First Reaction Cartridge agitated and heated at 55 °C and containing bifunctional MIDA boronate **3.4** (0.33 mmol, 104 mg), XPhos 2nd generation palladacycle (0.017 mmol, 13.1 mg, 5 mol%), and K_3PO_4 (3.0 mmol, 637 mg), is added 3 mL THF. The THF solution of boronic acid is added over 4 h (0.0375 mL/min). At the end of the addition the reaction is stirred for an additional 12 h.

In the purification module, to a Reaction Filtration Cartridge is added the crude cross-coupling solution and to a Precipitation Cartridge/Silica Gel Plug is added 12 mL hexanes. Then 3 mL of the crude cross-coupling solution (filtered through the Reaction Filtration Cartridge) is added and

the solvent is removed. This process is performed ten times, using 3 mL THF to wash the Reaction Cartridge and Reaction Filtration Cartridge for each cycle. Then 12 mL 1.5% MeOH in Et_2O are added and the solvent is removed a total of three times (36 mL total). Then 12 mL Et_2O are added and the solvent is removed a total of three times (36 mL total). Finally, 12 mL THF are added and the resulting purified solution of **3.5** is added to the Second Deprotection Cartridge. In the event, all cartridges are connected to the synthesizer and the synthesis is initiated by pressing "Start". From this point forward, no human intervention is required throughout the completion of the synthesis and purification of targeted product **3.5**.

Analysis of Conversion and Yield (Figure 3-7)

In order to characterize the progress of the automated reaction sequences, the following analysis was performed. At the end of the deprotection quench, a 500-µL aliquot of the organic layer is removed manually from the First Deprotection Cartridge. The sample is concentrated, a ^1H NMR sample is prepared and a spectrum is acquired immediately. The percent conversion for the deprotection step is determined via integration of the resonances corresponding to the boronic acid product and any remaining MIDA boronate starting material. At the end of the synthesis, the final THF solution of purified **3.5** is concentrated and a ^1H NMR spectrum is acquired. The percent conversion for the cross-coupling is determined via integration of the resonances corresponding to the cross-coupling product **3.5** and any remaining MIDA boronate starting material **3.4**. The purity of cross-coupling product **3.5** is determined via integration of the resonances corresponding to **3.5** and any impurities observed in the spectrum.

Representative ^{1}H NMR analysis:

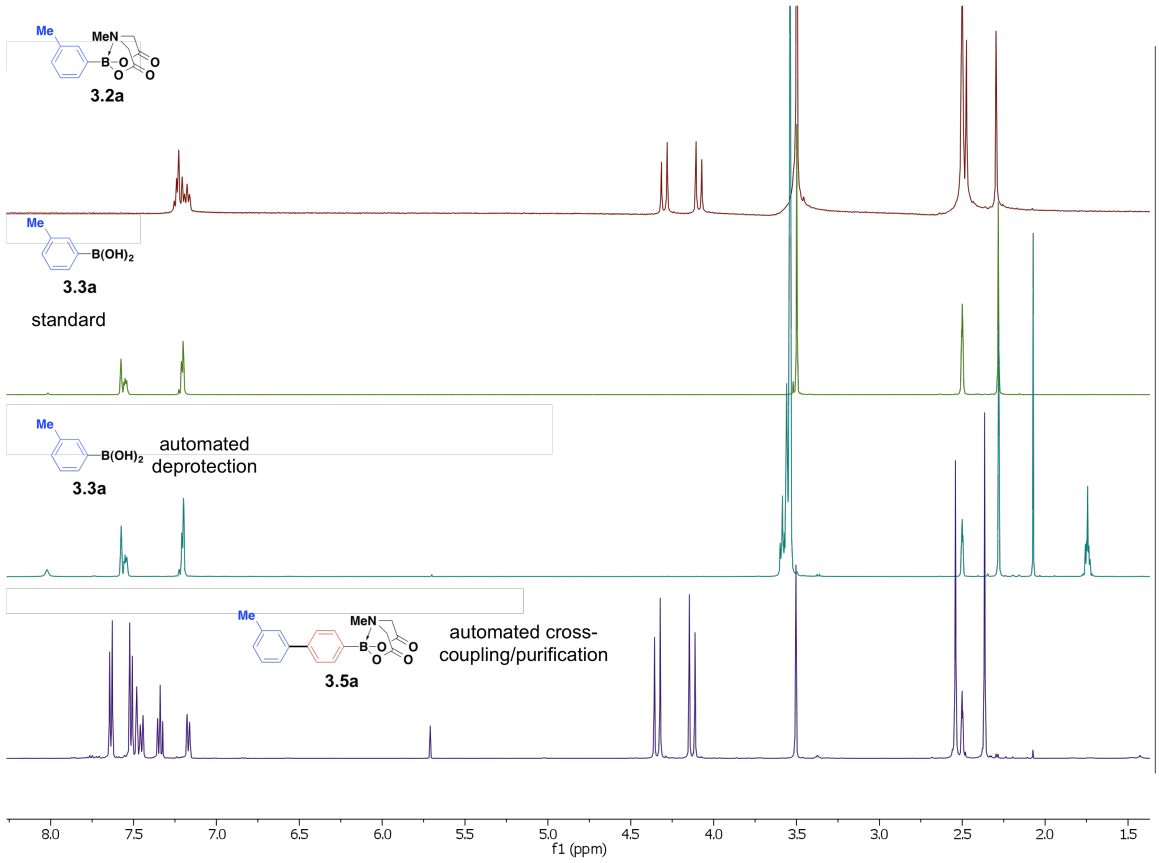

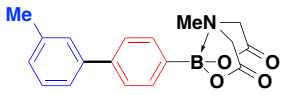

3.5a

(3'-methyl-[1,1'-biphenyl]-4-yl)boronic acid MIDA ester (3.5a). The general procedure was followed using 251.7 mg (1.02 mmol) aryl MIDA boronate **3.2a** and 104.0 mg (0.333 mmol) bifunctional MIDA boronate **3.4**. The conversion for the deprotection step was 99% and the conversion for the cross-coupling step was 98%. The desired aryl MIDA boronate **3.5a** was obtained as a colorless solid of >95% purity (65.3 mg, 0.202 mmol, 61% yield).

TLC (20% MeCN in Et_2O)

$R_f = 0.37$, visualized by UV and $KMnO_4$ stain

^{1}H-NMR (500 MHz, DMSO-d_6:D_2O, 95:5)

δ 7.64 (d, J = 8.5 Hz, 2H), 7.51 (d, J = 8.5 Hz, 2H), 7.48 (s, 1H), 7.45 (dd, J = 7.5, 0.5 Hz, 1H), 7.34 (t, J = 7.5 Hz, 1H), 7.17 (dd, J = 7.5, 0.5 Hz, 1H), 4.34 (d, J = 17.5 Hz, 2H), 4.13 (d, J = 17 Hz, 2H), 2.54 (s, 3H), 2.37 (s, 3H).

^{13}C-NMR (125 MHz, DMSO-d_6:D_2O, 95:5)

δ 169.1, 140.7, 140.1, 138.0, 132.9, 128.7, 128.0, 127.2, 125.9, 123.7, 61.8, 47.6, 21.0.

HRMS (EI+)

Calculated for $C_{18}H_{18}BNO_4$:	323.13289
Found:	323.13253

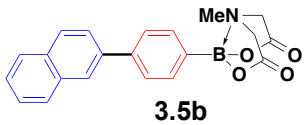

3.5b

(4-(naphthalen-2-yl)phenyl)boronic acid MIDA ester (3.5b). The general procedure was followed using 284.5 mg (1.00 mmol) aryl MIDA boronate **3.2b** and 104.3 mg (0.334 mmol) bifunctional MIDA boronate **3.4**. The conversion for the deprotection step was 99% and the conversion for the cross-coupling step was 99%. The desired aryl MIDA boronate **3.5b** was obtained as an off-white solid of >90% purity (77.7 mg, 0.216 mmol, 65% yield).

TLC (20% MeCN in Et_2O)

R_f = 0.28, visualized by UV and $KMnO_4$ stain

^{1}H-NMR (500 MHz, DMSO-d_6:D_2O, 95:5)

δ 8.23 (d, J = 1 Hz, 1H), 7.99 (d, J = 8 Hz, 2H), 7.92 (dd, J = 7.5, 1.5 Hz, 1H), 7.85 (dd, J = 9.0, 2 Hz, 1H), 7.82 (d, J = 8 Hz, 2H), 7.59 (d, J = 8 Hz, 2H), 7.56-7.49 (m, 2H), 4.38 (d, J = 17 Hz, 2H), 4.16 (d, J = 17 Hz, 2H), 2.57 (s, 3H).

^{13}C-NMR (125 MHz, DMSO-d_6:D_2O, 95:5)

δ 169.6, 140.5, 137.6, 133.5, 133.3, 132.4, 128.7, 128.4, 127.6, 126.6, 126.4, 126.3, 125.3, 125.2, 62.0, 47.8.

HRMS (EI+)

Calculated for $C_{21}H_{18}BNO_4$: 359.13289

Found: 359.13333

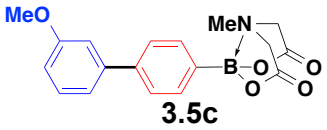

3.5c

(3'-methoxy-[1,1'-biphenyl]-4-yl)boronic acid MIDA ester (3.5c). The general procedure was followed using 263.5 mg (1.00 mmol) aryl MIDA boronate **3.2c** and 104.4 mg (0.335 mmol) bifunctional MIDA boronate **3.4**. The conversion for the deprotection step was 97% and the conversion for the cross-coupling step was 86%. The desired aryl MIDA boronate **3.5c** was obtained as a colorless solid of >80% purity (69.2 mg, 0.204 mmol, 61% yield).

TLC (20% MeCN in Et_2O)

R_f = 0.31, visualized by UV and $KMnO_4$ stain

^{1}H-NMR (500 MHz, DMSO-d_6:D_2O, 95:5)

δ 7.66 (d, J = 8 Hz, 2H), 7.52 (d, J = 7.5 Hz, 2H), 7.37 (t, J = 7.5 Hz, 1H), 7.23 (d, J = 7.5 Hz, 1H), 7.18 (s, 1H), 6.93 (dd, J = 8, 2.5 Hz, 1H), 4.35 (d, J = 17.5 Hz, 2H), 4.13 (d, J = 17 Hz, 2H), 3.80 (s, 3H), 2.54 (s, 3H).

^{13}C-NMR (125 MHz, DMSO-d_6:D_2O, 95:5)

δ 169.7, 160.0, 141.8, 140.7, 133.3, 130.3, 126.3, 119.2, 113.3, 112.3, 62.0, 55.3, 47.8.

HRMS (EI+)

Calculated for $C_{18}H_{18}BNO_5$: 339.12780

Found: 339.12732

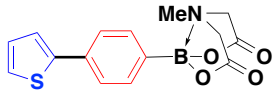

3.5d

(4-(thiophen-2-yl)phenyl)boronic acid MIDA ester (3.5d). The general procedure was followed using 242.1 mg (1.01 mmol) aryl MIDA boronate **3.2d** and 104.1 mg (0.3334 mmol) bifunctional MIDA boronate **3.4**. The conversion for the deprotection step was 98% and the conversion for the cross-coupling step was 98%. The desired aryl MIDA boronate **3.5d** was obtained as an off-white solid of >95% purity (78.7 mg, 0.250 mmol, 75% yield).

TLC (20% MeCN in Et_2O)

R_f = 0.38, visualized by UV and $KMnO_4$ stain

^{1}H-NMR (500 MHz, DMSO-d_6:D_2O, 95:5)

δ 7.64 (d, J = 8.5 Hz, 2H), 7.52 (m, 2H), 7.47 (d, J = 8 Hz, 2H), 7.13 (dd, J = 4.5, 4 Hz, 1H), 4.34 (d, J = 17 Hz, 2H), 4.12 (d, J = 17 Hz, 2H), 2.53 (s, 3H).

^{13}C-NMR (125 MHz, DMSO-d_6:D_2O, 95:5)

δ 169.7, 143.6, 134.4, 133.4, 128.8, 125.9, 124.9, 124.0, 62.0, 47.8.

HRMS (EI+)

Calculated for $C_{15}H_{14}BNO_4S$:	315.07366
Found:	315.07412

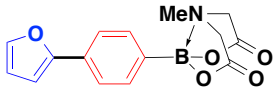

3.5e

(4-(furan-2-yl)phenyl)boronic acid MIDA ester (3.5e). The general procedure was followed using 225.5 mg (1.01 mmol) aryl MIDA boronate **3.5e** and 104.4 mg (0.335 mmol) bifunctional MIDA boronate **3.4**. The conversion for the deprotection step was 97% and the conversion for the cross-coupling step was 93%. The desired aryl MIDA boronate **3.5e** was obtained as an off-white solid of >90% purity (72.4 mg, 0.242 mmol, 72% yield).

TLC (20% MeCN in Et_2O):

R_f = 0.33, visualized by UV and $KMnO_4$ stain

^{1}H-NMR (500 MHz, DMSO-d_6:D_2O, 95:5)

δ 7.73 (d, *J* = 2 Hz, 1H), 7.68 (d, *J* = 8.5 Hz, 2H), 7.48 (d, *J* = 8 Hz, 2H), 6.95 (d, *J* = 3 Hz, 1H), 6.58 (dd, *J* = 3.5, 2 Hz, 1H), 4.34 (d, *J* = 17 Hz, 2H), 4.12 (d, *J* = 17.5 Hz, 2H), 2.51 (s, 3H).

^{13}C-NMR (125 MHz, DMSO-d_6:D_2O, 95:5)

δ 169.7, 153.3, 143.2, 133.2, 131.0, 123.0, 112.4, 106.3, 62.0, 47.8.

HRMS (EI+)

Calculated for $C_{15}H_{14}BNO_5$:	299.09650
Found:	299.09715

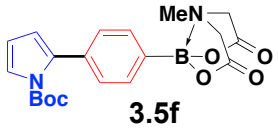

3.5f

(4-(1-(tert-butoxycarbonyl)-1H-pyrrol-2-yl)phenyl)boronic acid MIDA ester (3.5f). The general procedure was followed using 325.4 mg (1.01 mmol) aryl MIDA boronate **3.2f** and 104.4 mg (0.335 mmol) bifunctional MIDA boronate **3.4**. The conversion for the deprotection step was 99% and the conversion for the cross-coupling step was 99%. The desired aryl MIDA boronate **3.5f** was obtained as an off-white solid of >95% purity (110.9 mg, 0.278 mmol, 83% yield).

TLC (20% MeCN in Et_2O)

R_f = 0.46, visualized by UV and $KMnO_4$ stain

^{1}H-NMR (500 MHz, DMSO-d_6:D_2O, 95:5)

δ 7.43 (d, *J* = 8 Hz, 2H), 7.33 (dd, *J* = 3, 1.5 Hz, 1H), 7.30 (d, *J* = 8.5 Hz, 2H), 6.26 (t, *J* = 3.5 Hz, 1H), 6.23 (dd, *J* = 3, 1.5 Hz, 1H), 4.34 (d, *J* = 17 Hz, 2H), 4.13 (d, *J* = 17 Hz, 2H), 2.54 (s, 3H), 1.28 (s, 9H).

^{13}C-NMR (125 MHz, DMSO-d_6:D_2O, 95:5)

δ 169.7, 149.1, 134.7, 134.4, 132.0, 128.2, 123.0, 114.7, 111.2, 83.9, 62.1, 47.9, 27.3.

HRMS (ESI+)

Calculated for $C_{20}H_{24}BN_2O_6$: 399.1727

Found: 399.1723

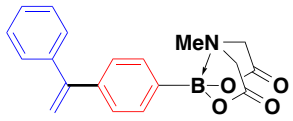

3.5g

(4-(1-phenylvinyl)phenyl)boronic acid MIDA ester (3.5g). The general procedure was followed using 261.1 mg (1.01 mmol) aryl MIDA boronate **3.2g** and 105.1 mg (0.337 mmol) bifunctional MIDA boronate **3.4**. The conversion for the deprotection step was 98% and the conversion for the cross-coupling step was 95%. The desired aryl MIDA boronate **3.5g** was obtained as a colorless solid of >90% purity (75.7 mg, 0.226 mmol, 67% yield).

TLC (20% MeCN in Et_2O)

R_f = 0.36, visualized by UV and $KMnO_4$ stain

^{1}H-NMR (500 MHz, DMSO-d_6:D_2O, 95:5)

δ 7.44 (d, J = 8.5 Hz, 2H), 7.38-7.32 (m, 3H), 7.28 (app dd, J = 8 Hz, 4H), 5.50 (s, 1H), 5.47 (s, 1H), 4.34 (d, J = 17 Hz, 2H), 4.12 (d, J = 17 Hz, 2H), 2.54 (s, 3H).

^{13}C-NMR (125 MHz, DMSO-d_6:D_2O, 95:5)

δ 169.7, 149.4, 141.4, 140.9, 132.7, 128.6, 128.2, 128.1, 127.4, 115.0, 62.0, 47.8.

HRMS (EI+)

Calculated for $C_{19}H_{18}BNO_4$: 335.13289

Found: 335.13356

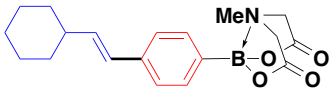

3.5h

(E)-(4-(2-cyclohexylvinyl)phenyl)boronic acid MIDA ester (3.5h). The general procedure was followed using 265.9 mg (1.00 mmol) aryl MIDA boronate **3.2h** and 105.6 mg (0.339 mmol) bifunctional MIDA boronate **3.4**. The conversion for the deprotection step was 98% and the conversion for the cross-coupling step was 99%. The desired aryl MIDA boronate **3.5h** was obtained as an off-white solid of >95% purity (77.7 mg, 0.228 mmol, 67% yield).

TLC (20% MeCN in Et_2O)

R_f = 0.44, visualized by UV and $KMnO_4$ stain

^{1}H-NMR (500 MHz, DMSO-d_6:D_2O, 95:5)

δ 7.35 (s, 4H), 6.34 (d, J = 16.5 Hz, 1H), 6.25 (dd, J = 16.5, 7 Hz, 1H), 4.31 (d, J = 17 Hz, 2H), 4.08 (d, J = 17 Hz, 2H), 2.47 (s, 3H), 2.13-2.06 (m, 1H), 1.74-1.68 (m, 4H), 1.63-1.60 (m, 1H), 1.31-1.23 (m, 2H), 1.18-1.11 (m, 3H).

^{13}C-NMR (125 MHz, DMSO-d_6:D_2O, 95:5)

δ 169.6, 138.1, 136.8, 132.7, 127.3, 125.4, 61.9, 47.7, 40.6, 32.6, 25.8, 25.6.

HRMS (EI+)

Calculated for $C_{19}H_{24}BNO_4$:	341.17984
Found:	341.18030

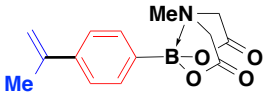

3.5i

(4-(prop-1-en-2-yl)phenyl)boronic acid MIDA ester (3.5i). The general procedure was followed using 199.4 mg (1.01 mmol) aryl MIDA boronate **3.2i** and 104.2 mg (0.334 mmol) bifunctional MIDA boronate **3.4**. The conversion for the deprotection step was 99% and the

conversion for the cross-coupling step was 98%. The desired aryl MIDA boronate **3.5i** was obtained as a colorless solid of >90% purity (64.9 mg, 0.238 mmol, 71% yield).

TLC (20% MeCN in Et_2O)

R_f = 0.36, visualized by UV and $KMnO_4$ stain

^{1}H-NMR (500 MHz, DMSO-d_6:D_2O, 95:5)

δ 7.49 (d, *J* = 8.5 Hz, 2H), 7.42 (d, *J* = 8 Hz, 2H), 5.45 (s, 1H), 5.10 (t, *J* = 1.5 Hz, 1H), 4.33 (d, *J* = 17 Hz, 2H), 4.10 (d, *J* = 17 Hz, 2H), 2.50 (s, 3H), 2.10 (s, 3H).

^{13}C-NMR (125 MHz, DMSO-d_6:D_2O, 95:5)

δ 169.7, 142.7, 141.0, 132.7, 124.8, 112.9, 61.9, 47.8, 21.6.

HRMS (EI+)

Calculated for $C_{14}H_{16}BNO_4$:	273.11724
Found:	273.11679

III. AUTOMATED SYNTHESIS OF SMALL MOLECULES VIA MULTIPLE ICC CYCLES

General Automated Procedure for Multiple ICC Cycles

The general procedure for one ICC cycle is followed with the following additions:

If three building blocks are being assembled, the Second Deprotection Cartridge contains NaOH (1.0 mmol, 40 mg) and the Second Reaction Cartridge contains the second bifunctional MIDA boronate or the capping building block (0.11 mmol), XPhos 2nd generation palladacycle (0.0056 mmol, 4.4 mg, 5 mol%), and K_3PO_4 (1.0 mmol, 212 mg). This cartridge is identical to a First Reaction Cartridge, but is not tethered to a Reaction Filtration Cartridge.

If four building blocks are being assembled, the Third Deprotection Cartridge contains NaOH (0.33 mmol, 13.3 mg) and no Drying Cartridge is used for the third reaction. The Third Reaction Cartridge is a 7-mL glass vial containing a PTFE-coated magnetic stir, the capping building block (0.037 mmol), XPhos 2nd generation palladacycle (0.00185 mmol, 1.5 mg, 5 mol%), and

K_3PO_4 (0.33 mmol, 71 mg). The vial is sealed under argon with a septum-top screw cap. At the end of the synthesis, the crude reaction is purified by silica gel chromatography or preparative HPLC as noted.

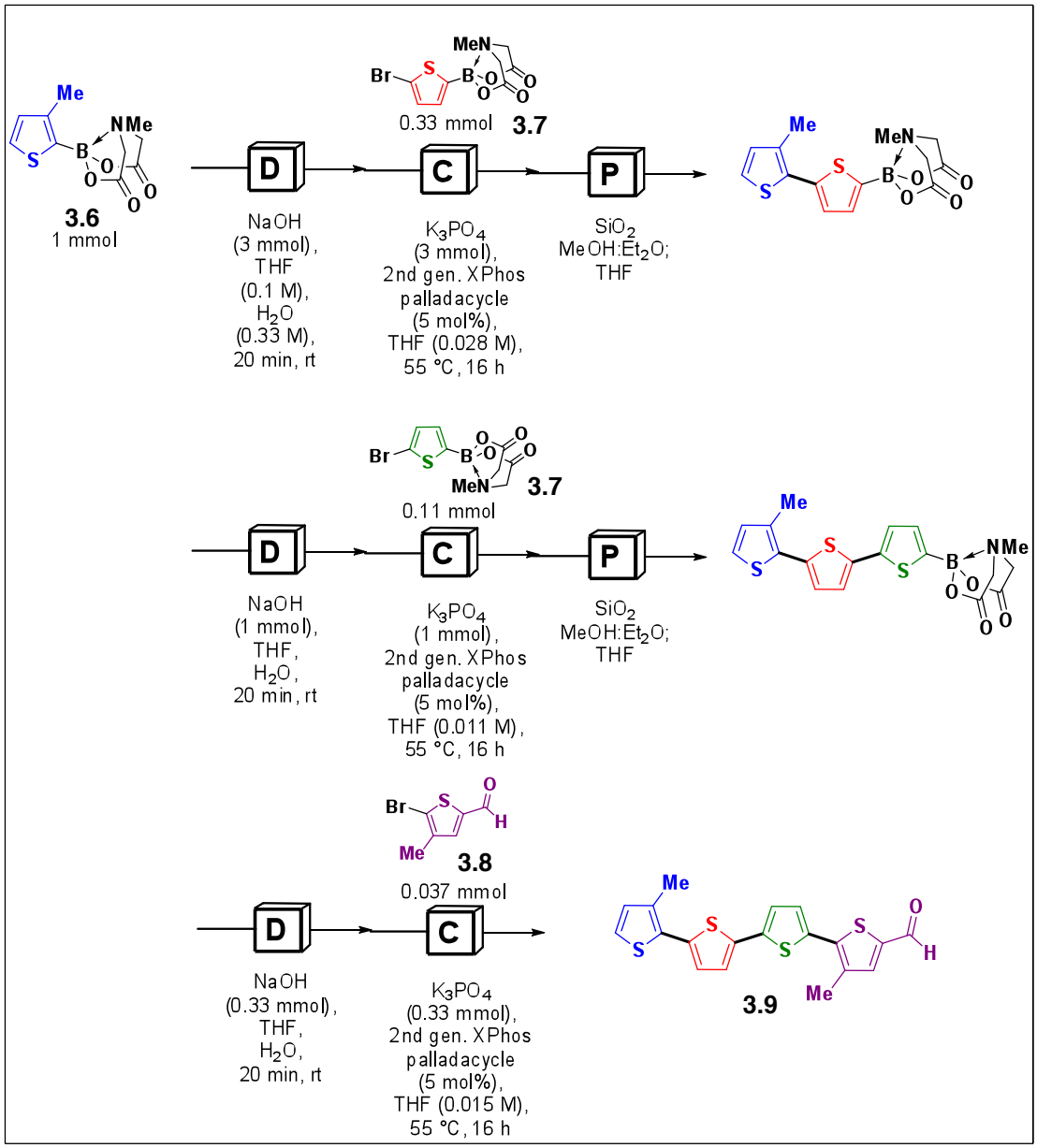

Oligothiophene (3.9). The general procedure was followed. Crude **3.9** as purified via silica gel chromatography (100% hexanes → 20% EtOAc in hexanes) to afford **3.9** as a red/orange solid (7.5 mg, 0.0194 mmol, 50% yield).

TLC (20% EtOAc in hexanes)

R_f = 0.29, visualized by longwave UV

^{1}H-NMR (500 MHz, $CDCl_3$)

δ 9.81 (s, 1H), 7.54 (s, 1H), 7.24 (d, *J* = 3.5 Hz, 1H), 7.17 (m, 3H), 7.06 (d, *J* = 3.5 Hz, 1H), 6.90 (d, *J* = 5.0 Hz, 1H), 2.48 (s, 3H), 2.43 (s, 3H).

^{13}C-NMR (125 MHz, $CDCl_3$)

δ 182.6, 141.6, 140.6, 139.7, 139.2, 136.7, 135.8, 134.8, 134.5, 134.2, 131.7, 130.7, 128.2, 126.2, 124.8, 124.2, 123.8, 16.1, 15.7.

HRMS (EI+)

Calculated for $C_{19}H_{14}OS_4$: 385.99277

Found: 385.99217

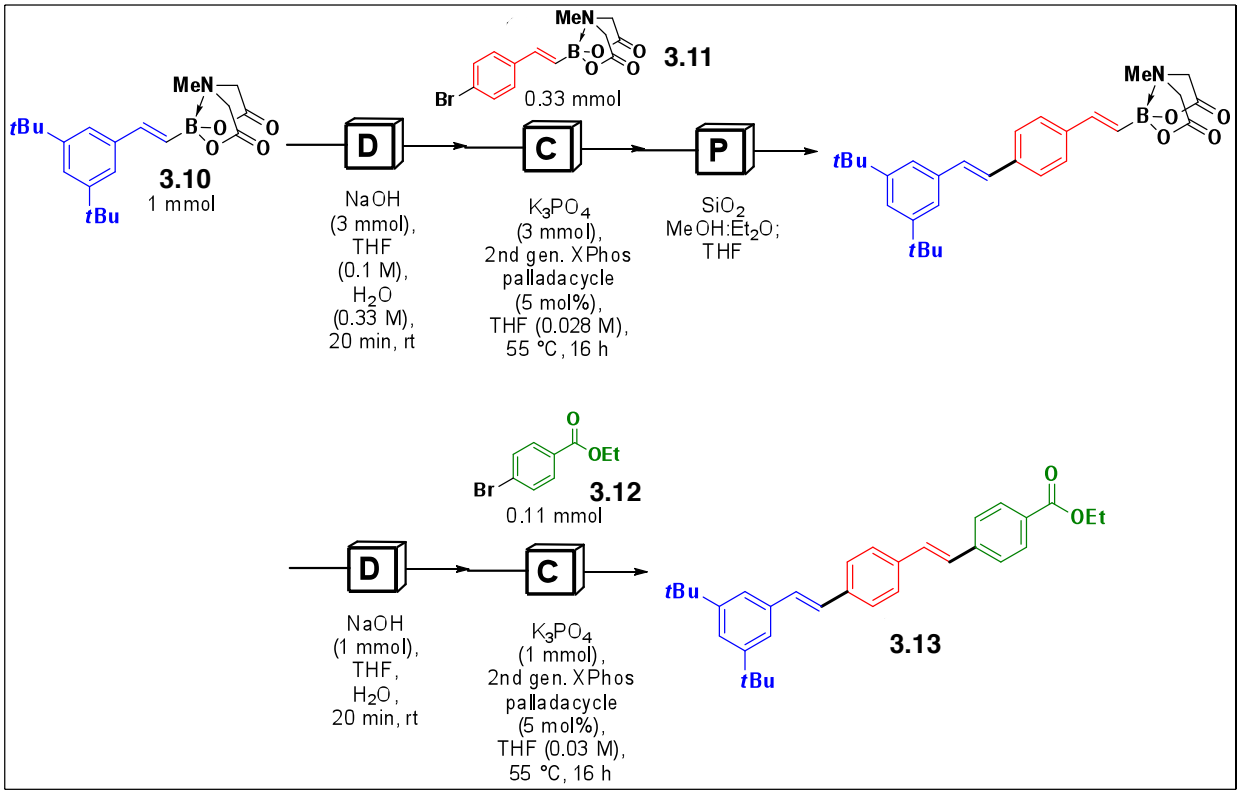

Protected oligophenylene (3.13). The general procedure was followed with the following modifications: In the second cross-coupling reaction, the concentration was 0.03 M with respect to **3.12**, the addition of the boronic acid was performed over 1 minute, and the coupling was run in a 7-mL glass vial. **3.13** was afforded as a yellow solid (44.1 mg, 0.0945 mmol, 84% yield).

TLC (40% DCM in hexanes)

R_f = 0.31, visualized by UV

^{1}H-NMR (500 MHz, CDCl3)

δ 8.06 (d, *J* = 8 Hz, 2H), 7.59-7.54 (m, 6H), 7.41-7.39 (m, 3H), 7.23 (d, *J* = 16.5 Hz, 1H), 7.22 (d, *J* = 16 Hz, 1H), 7.15 (d, *J* = 15.5 Hz, 1H), 7.12 (d, *J* = 16 Hz, 1H), 4.40 (q, *J* = 7 Hz, 2H), 1.42 (t, *J* = 7.5 Hz, 3H), 1.40 (s, 18H).

^{13}C-NMR (125 MHz, CDCl3)

δ 166.5, 151.2, 141.9, 137.8, 136.5, 136.0, 130.9, 130.2, 130.1, 129.3, 127.5, 127.4, 127.3, 127.0, 126.4, 122.4, 121.0, 61.0, 35.0, 31.6, 14.5.

HRMS (ESI+)

Calculated for $C_{33}H_{39}O_2$:	467.2950
Found:	467.2943

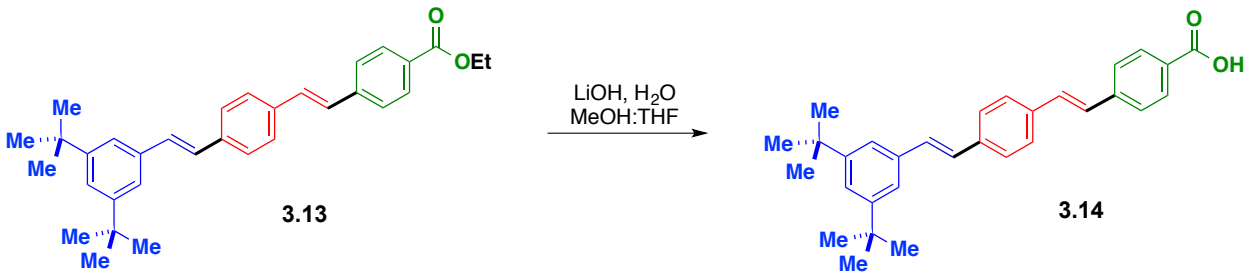

Oligophenylene (3.14). To a solution of ethyl ester **3.13** (44.1 mg, 0.0945 mmol) in MeOH/THF 1:1 (2 mL) was added LiOH solution (18 mg, 0.752 mmol in 0.4 mL H_2O) in one portion. The mixture was stirred vigorously at 45 °C for 3.5 h. The reaction was cooled briefly in an ice-water bath and 0.2 mL of 2 N HCl was added. The mixture was diluted with 5 mL H_2O and extracted

with EtOAc (10 mL, then 2 × 5 mL). The combined organic layers were washed with brine, dried over anhydrous Na_2SO_4, filtered, and concentrated. The crude product was purified by recrystallization from hot toluene. A second crop was obtained by precipitation from toluene/hexanes and combined with the first crop to afford **3.14** as a bright yellow solid (20.5 mg, 0.047 mmol, 50% yield).

^{1}H-NMR (500 MHz, DMSO-d_6)

δ 12.88 (s, 1H), 7.92 (d, J = 8 Hz, 2H), 7.70 (d, J = 8.5 Hz, 2H), 7.64 (s, 3H), 7.43 (d, J = 1.5 Hz, 2H), 7.40 (d, J = 16.5 Hz, 1H), 7.34 (d, J = 16.5 Hz, 1H), 7.32 (d, J = 17 Hz, 1H), 7.30 (s, 2H), 7.26 (d, J = 16.5 Hz, 1H), 1.31 (s, 18 H).

^{13}C-NMR (125 MHz, DMSO-d_6)

δ 167.0, 150.5, 141.5, 137.2, 136.2, 135.7, 130.6, 129.7 (2C), 129.4, 127.2, 127.1, 126.8, 126.4, 121.6, 120.8, 34.5, 31.2.

HRMS (EI+)

Calculated for $C_{31}H_{34}O_2$:	438.25588
Found:	438.25538

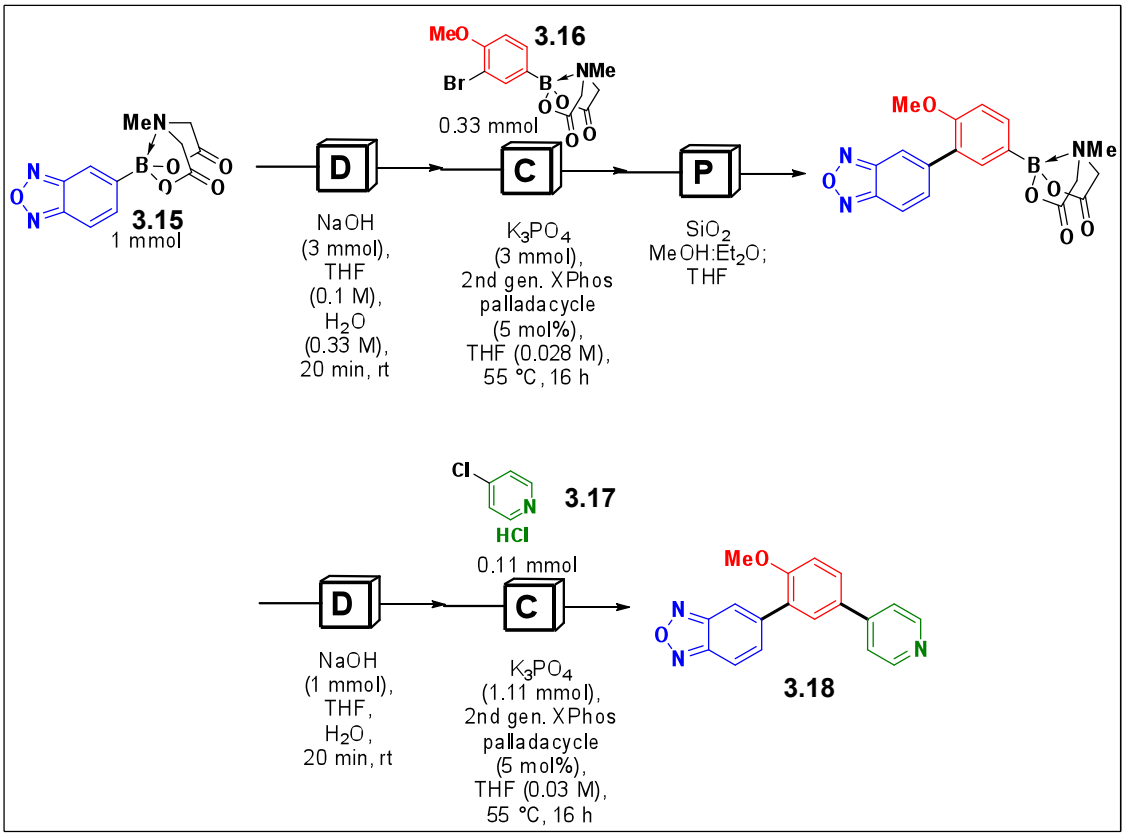

PDE472 (3.18). The general procedure was followed with the following modifications: In the second cross-coupling reaction, the concentration was 0.03 M with respect to **3.17**, 1.11 mmol of K_3PO_4 were used, the addition of the boronic acid was performed over 1 minute, and the coupling was run in a 7-mL glass vial. **3.18** was afforded as a colorless solid (6.6 mg, 0.0218 mmol, 20% yield).

TLC (EtOAc)

R_f = 0.30, visualized by UV

HPLC

tR = 17.5 min; flow rate = 25 mL/min, gradient: 5% → 95% MeCN in H_2O over 20 min.

^{1}H-NMR (500 MHz, acetone-d_6)

δ 8.63 (br s, 2H), 8.12 (t, J = 1 Hz, 1H), 7.97 (dd, J = 9.5, 1 Hz, 1H), 7.96 (d, J = 2.5 Hz, 1H), 7.93 (dd, J = 9, 2.5 Hz, 1H), 7.87 (dd, J = 9.5, 1.5 Hz, 1H), 7.74 (app d, J = 6 Hz, 2H), 7.35 (d, J = 9 Hz, 1H), 3.98 (s, 3H).

^{13}C-NMR (125 MHz, DMSO-d_6)

δ 157.3, 150.1, 149.3, 148.1, 146.1, 142.2, 135.8, 129.8, 129.1, 129.0, 128.2, 120.9, 114.9 (2C), 112.7, 56.1.

HRMS (ESI+)

Calculated for $C_{18}H_{14}N_3O_2$: 304.1086

Found: 304.1081

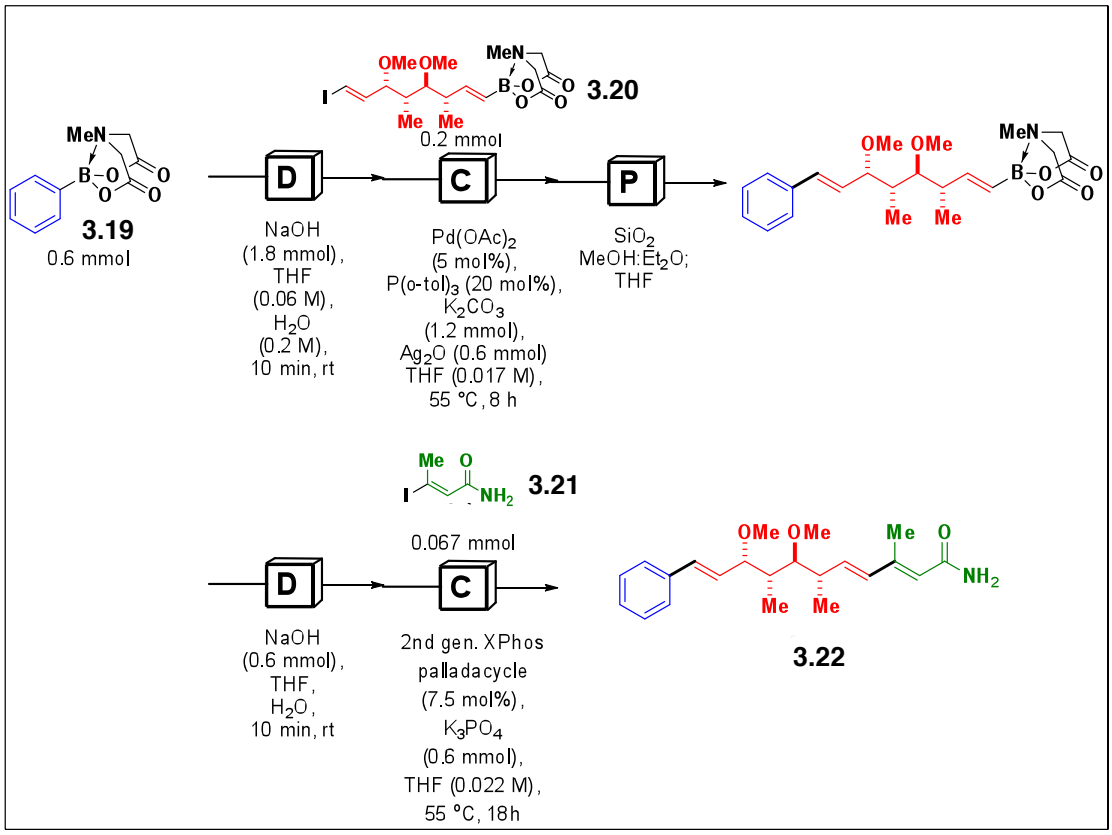

(+)-Crocacin C (3.22). The general procedure was followed with the following modifications: In the first cross-coupling reaction, P(*o*-tol)$_3$ was used as the ligand and K_2CO_3 and Ag_2O were

used as the base and the reaction was run for 8 hours. Both deprotection reactions were run for 10 minutes. The second cross-coupling reaction was run for 18 hours in a 7-mL glass vial. Crude **3.22** was purified via silica gel chromatography (40% EtOAc in hexanes to 50% EtOAc in hexanes) to afford **3.22** as an off-white solid (14.5 mg, 0.0406 mmol, 61% yield).

TLC (20% EtOAc in hexanes)

R_f = 0.08, visualized by UV

^{1}H-NMR (500 MHz, $CDCl_3$)

δ 7.39 (d, *J* = 7.5 Hz, 2H), 7.32 (t, *J* = 7 Hz, 2H), 7.23 (t, *J* = 7 Hz, 1H), 6.56 (d, *J* = 16.5 Hz, 1H), 6.17-6.01 (m, 3H), 5.63 (s, 1H), 5.38 (br s, 2H), 4.08 (dd, *J* = 7.5, 1 Hz, 1H), 3.54 (s, 3H), 3.32 (s, 3H), 3.19 (dd, *J* = 10, 2 Hz, 1H), 2.56-2.53 (m, 1H), 2.25 (d, *J* = 1 Hz, 3H), 1.56-1.52 (m, 1H), 1.19 (d, *J* = 7 Hz, 3H), 0.84 (d, *J* = 7 Hz, 3H).

^{13}C-NMR (125 MHz, $CDCl_3$)

δ 169.4, 149.7, 137.2, 136.8, 134.1, 132.1, 129.3, 128.7, 127.7, 126.5, 119.7, 86.5, 81.1, 61.6, 56.6, 42.7, 40.2, 18.9, 13.9, 9.8.

HRMS (ESI+)

Calculated for $C_{22}H_{32}NO_3$: 358.2382

Found: 358.2392

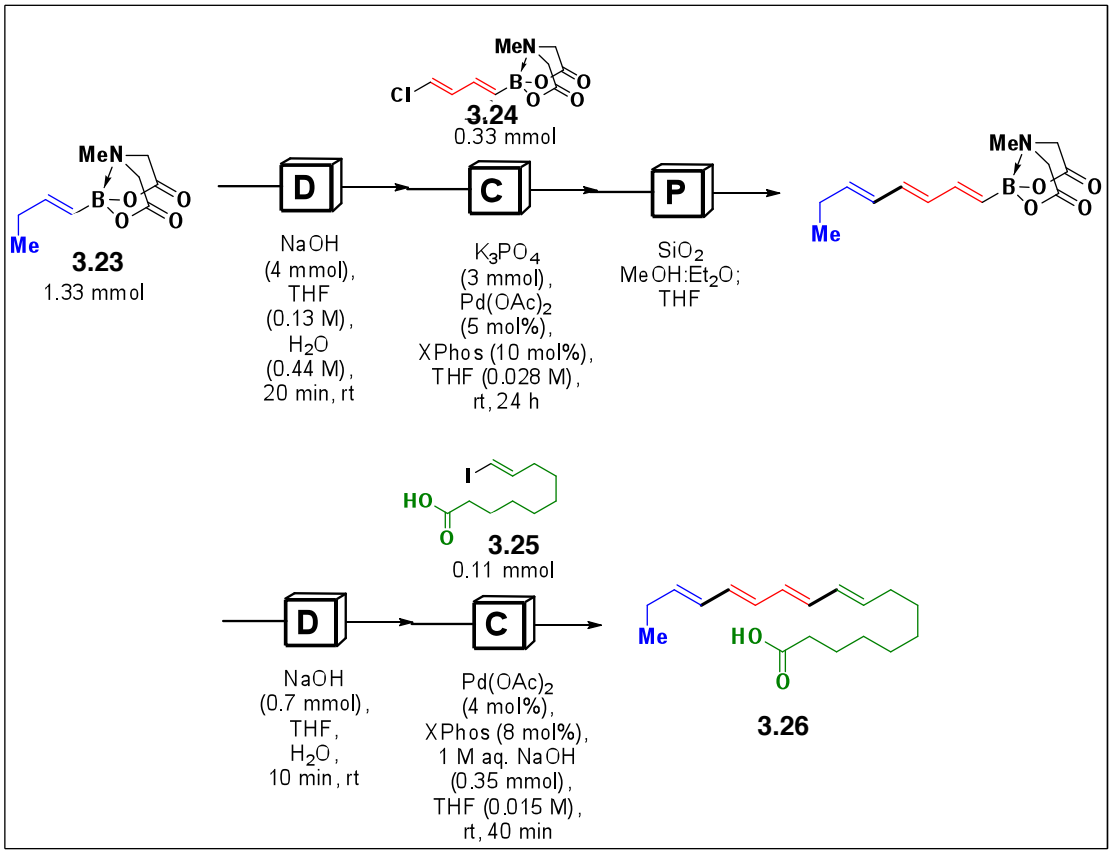

β-parinaric acid (3.26). The general procedure was followed with the following modifications: The first cross-coupling reaction was run at room temperature for 24 h. The second deprotection reaction was run for 10 minutes, and the second cross-coupling reaction was run in a 20-mL glass vial at room temperature using aqueous NaOH as the base for 40 minutes. The procedure was also conducted under subdued light conditions to protect against isomerization of the polyene framework. **3.26** was afforded as a fluorescent solid (18.3 mg, 0.0662 mmol, 56% yield). ^{1}H NMR indicated a 10:1 mixture of the desired β-parinaric acid (**3.26**):9-(*Z*)-parinaric acid (arising from 10:1 *E*:*Z* mixture of starting material vinyl iodide **3.25**).

TLC (50% Et_2O in hexanes)

R_f = 0.13, visualized by UV

HPLC

tR = 23.7 min; flow rate = 25 mL/min, gradient of 5% → 95% MeCN in H_2O over 15 min followed by 100% MeCN for 30 min. Detected at λ= 254 nm.

^{1}H-NMR (500 MHz, $CDCl_3$)

δ 6.21-6.05 (m, 6H), 5.76-5.63 (m, 2H), 2.34 (t, J = 7 Hz, 2H), 2.15-2.07 (m, 4H), 1.66-1.60 (m, 2H), 1.43-1.26 (m, 8H), 1.01 (t, J = 7.5 Hz, 3H).

^{13}C-NMR (125 MHz, $CDCl_3$)

δ 179.2, 136.7, 135.1, 132.6, 132.6, 131.0, 131.0, 130.8, 129.8, 34.0, 33.0, 29.4, 29.2, 29.1, 29.1, 26.0, 24.8, 13.7.

HRMS (ESI+)

Calculated for $C_{18}H_{29}O_2$: 277.2168

Found: 277.2175

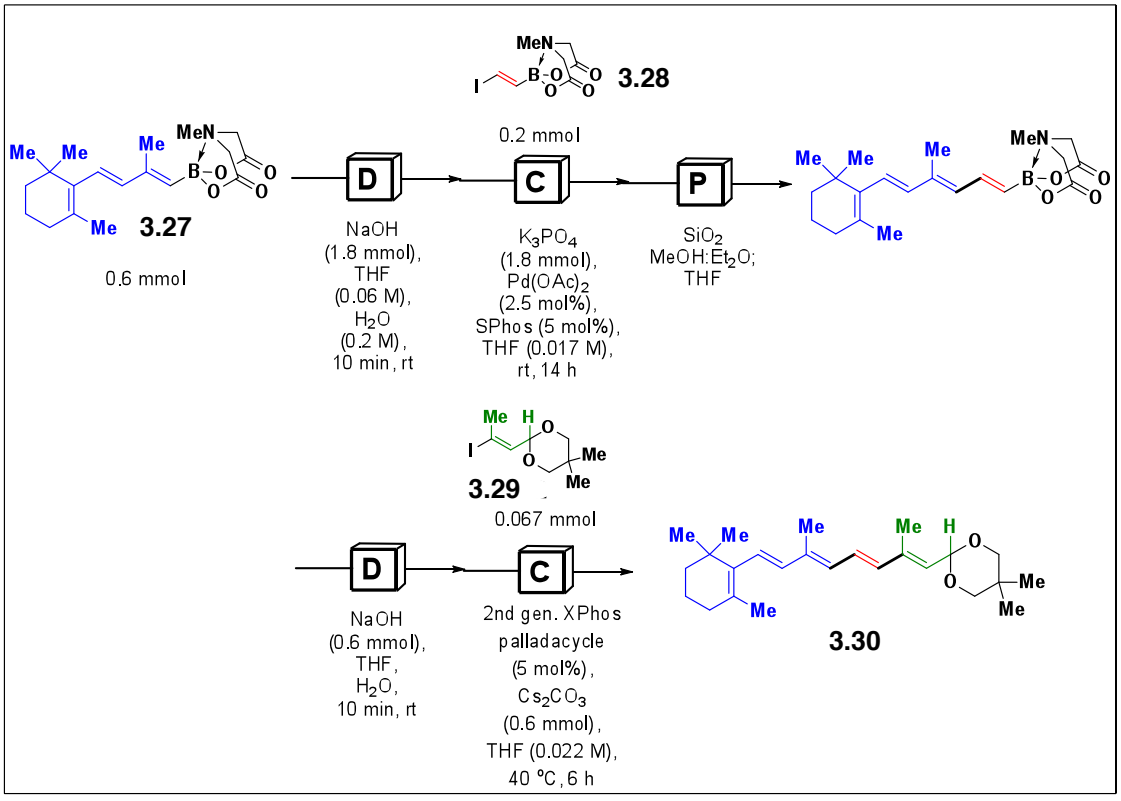

Protected all-*trans*-retinal (3.30). The general procedure was followed with the following modifications: In the first cross-coupling reaction, SPhos was used as the ligand and the reaction was run for 14 hours at room temperature. Both deprotection reactions were run for 10 minutes.

The second cross-coupling reaction was run in a 7-mL glass vial at 40 °C for 6 h using Cs_2CO_3 as the base. The procedure was also conducted under subdued light conditions to protect against isomerization of the polyene framework. Crude **3.30** was purified via silica gel chromatography (100% hexanes to 30% EtOAc in hexanes) to afford **3.30** as a single stereoisomer and a yellow oil (18.2 mg, 0.0491 mmol, 74% yield).

TLC (petroleum ether:ether 4:1)

R_f = 0.86, stained by $KMnO_4$

^{1}H-NMR (500 MHz, $CDCl_3$)

δ 6.66 (dd, *J* = 14.8, 11.2 Hz, 1H), 6.27 (d, *J* = 15.2 Hz, 1H), 6.19-6.08 (m, 3H), 5.54 (d, *J* = 6 Hz, 1H), 5.21 (d, *J* = 6.4 Hz, 1H), 3.66 (d, *J* = 11.2 Hz, 2H), 3.53 (d, *J* = 10.8 Hz, 2H), 2.01 (t, *J* = 6.4 Hz, 2H), 1.95 (s, 3H), 1.91 (s, 3H), 1.70 (s, 3H), 1.62-1.59 (m, 2H), 1.47-1.44 (m, 2H), 1.23 (s, 3H), 1.01 (s, 6H), 0.75 (s, 3H).

^{13}C-NMR (125 MHz, $CDCl_3$)

δ 139.3, 137.8, 137.6, 136.6, 135.8, 130.0, 129.3, 127.2, 127.0, 126.2, 109.8, 98.8, 39.6, 34.2, 33.0, 30.0, 28.9, 23.0, 22.0, 21.7, 19.2, 13.4, 12.7.

HRMS (ESI+)

Calculated for $C_{25}H_{39}O_2$:	371.2950
Found:	371.2950

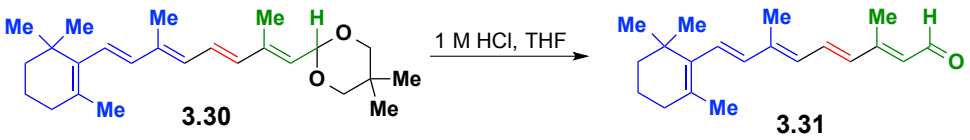

All-*trans*-retinal (3.31). A 7-mL vial charged with **3.30** (18.2 mg, 0.049 mmol, 1.0 equiv.) was sealed with a PTFE-lined cap and purged with N_2 and THF (1.0 mL, 0.05M) was added to afford a clear yellow solution. The vial was cooled to 0 °C in an ice bath for 5 minutes. Aqueous HCl (1M, 0.5 mL) was added dropwise to the reaction vial and the reaction mixture was allowed to warm to 23 °C with stirring over 30 minutes. After 30 minutes, the reaction mixture was

transferred to a separatory funnel containing aqueous saturated $NaHCO_3$ (5 mL), rinsing with diethyl ether (10 mL) and the phases were separated. The aqueous layer was back-extracted with diethyl ether (5 mL) and the combined organic layers were dried over anhydrous $MgSO_4$, filtered, and concentrated *in vacuo* to afford a yellow-orange oil. The resulting crude material (4:1 ratio of all-*trans* retinal (**3.31**):13-*cis*-retinal) was adsorbed onto Celite™ from an acetone solution and purified by silica gel chromatography (32:1 hexanes:EtOAc) to afford **3.31** as an orange solid (8.9 mg, 0.0313 mmol, 64% yield).

^{1}H-NMR (500 MHz, $CDCl_3$)

δ 10.11 (d, J = 8 Hz, 1H), 7.14 (dd, J = 15, 11.5 Hz, 1H), 6.37 (d, J =15 Hz, 1H), 6.34 (d, J = 15 Hz, 1H), 6.19 (d, J = 9.5 Hz, 1H), 6.16 (d, J = 16 Hz, 1H), 5.97 (d, J = 8.5 Hz, 1H), 2.33 (d, J = 1 Hz, 3H), 2.04-2.02 (m, 2H), 2.03 (s, 3H), 1.72 (s, 3H), 1.63-1.60 (m, 2H), 1.49-1.46 (m, 2H), 1.03 (s, 6H).

IV. AUTOMATED SYNTHESIS OF RATANHINE LIBRARY MEMBERS

General Scheme for Automated Synthesis of Trimer Library Members

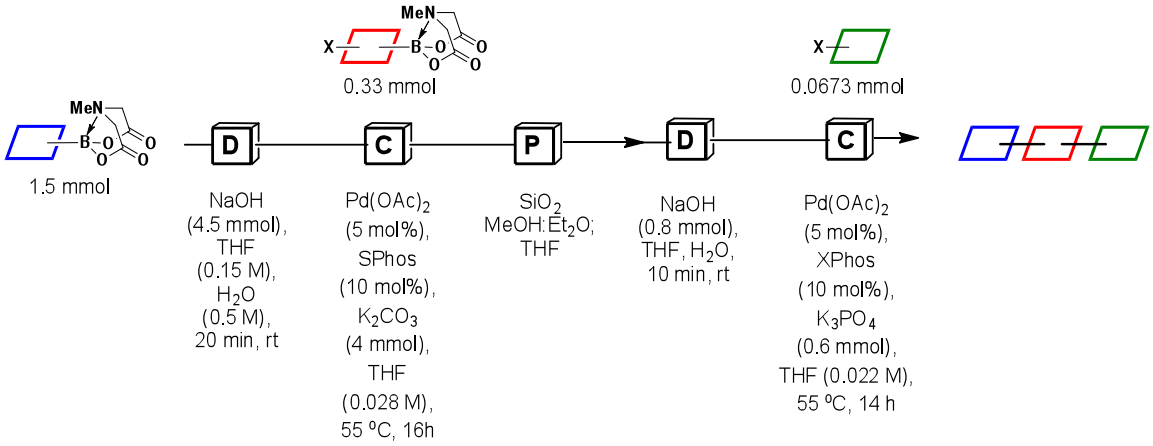

The general procedure was executed with the conditions stated above for all of the trimer library members.

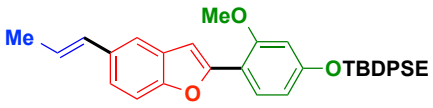

protected ratanhiaphenol III (3.36)
27.8 mg (75%)

Protected ratanhiaphenol III (3.36). TLC (50% DCM in hexanes): R_f = 0.51, stained by $KMnO_4$; ^{1}H-NMR (500 MHz, acetone-d_6): δ 7.82 (d, J = 8.5 Hz, 1H), 7.74-7.71 (m, 4H), 7.53 (d, J = 1.5 Hz, 1H), 7.47-7.42 (m, 6H), 7.39 (d, J = 8.5 Hz, 1H), 7.29 (dd, J = 8.5, 1.5 Hz, 1H), 7.17 (d, J = 1 Hz, 1H), 6.52-6.46 (m, 3H), 6.24 (dq, J = 15.5, 6.5 Hz, 1H), 4.14-4.11 (m, 2H), 3.93 (s, 3H), 1.88-1.84 (m, 5H), 1.09 (s, 9H); ^{13}C-NMR (125 MHz, acetone-d_6): δ 161.3, 158.8, 153.8 (2C), 136.7, 134.8, 134.0, 132.2, 131.2, 130.3, 128.7, 128.3, 124.5, 122.8, 118.7, 112.8, 111.2, 106.6, 105.0, 100.0, 66.2, 55.9, 28.1, 18.6, 18.5, 12.6; HRMS (ESI+) calculated for $C_{36}H_{39}O_3Si$ $[M+H]^+$ *m/z* 547.2668, found 547.2673.

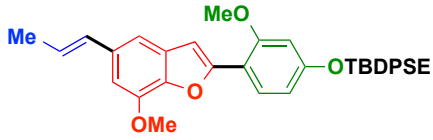

3.54
27.9 mg (72%)

Library member (3.54). TLC (50% DCM in hexanes): R_f = 0.23, visualized by UV; ^{1}H-NMR (500 MHz, acetone-d_6): δ 7.84 (dd, J = 8, 0.5 Hz, 1H), 7.74-7.72 (m, 4H), 7.47-7.43 (m, 6H), 7.14 (s, 1H), 7.10 (d, J = 1.5 Hz, 1H), 6.93 (d, J = 1.5 Hz, 1H), 6.50-6.45 (m, 3H), 6.24 (dq, J = 15.5, 6.5 Hz, 1H), 4.14-4.10 (m, 2H), 4.01 (s, 3H), 3.93 (s, 3H), 1.87-1.84 (m, 5H), 1.09 (s, 9H); ^{13}C-NMR (125 MHz, acetone-d_6): δ 161.3, 158.7, 153.7, 145.9, 143.0, 136.7, 135.0, 134.8, 132.6, 132.5, 130.3, 128.7, 128.3, 124.6, 112.8, 111.6, 106.6, 105.2 (2C), 100.0, 66.2, 56.3, 56.0, 28.1, 18.5 (2C) 12.6; HRMS (ESI+) calculated for $C_{37}H_{41}O_4Si$ $[M+H]^+$ *m/z* 577.2774, found 577.2767.

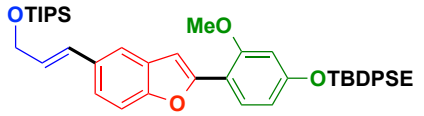

3.55
25.9 mg (54%)

Library member (3.55). TLC (50% DCM in hexanes): R_f = 0.49, stained by $KMnO_4$; ^{1}H-NMR (500 MHz, acetone-d_6): δ 7.83 (d, J = 8.5 Hz, 1H), 7.74-7.72 (m, 4H), 7.61 (d, J = 1.5 Hz, 1H),

7.47-7.42 (m, 7H), 7.35 (dd, J = 8.5, 2 Hz, 1H), 7.19 (d, J = 0.5 Hz, 1H), 6.77 (dt, J = 16, 1.5 Hz, 1H), 6.51-6.47 (m, 2H), 6.35 (dt, J = 15.5, 5 Hz, 1H), 4.47 (dd, J = 4.5, 1.5 Hz, 2H), 4.14-4.11 (m, 2H), 3.94 (s, 3H), 1.88-1.84 (m, 2H), 1.22-1.08 (m, 30H); ^{13}C-NMR (125 MHz, acetone-d_6):δ 161.4, 158.8, 154.1, 154.0, 136.7, 134.8, 133.2, 131.3, 130.3, 130.2, 128.8, 128.7, 128.3, 123.3, 119.3, 112.8, 111.3, 106.7, 105.0, 100.0, 66.2, 64.8, 56.0, 28.1, 18.6, 18.4, 12.8, 12.6; HRMS (ESI+) calculated for $C_{45}H_{59}O_4Si_2$ $[M+H]^+$ m/z 719.3952, found 719.3925.

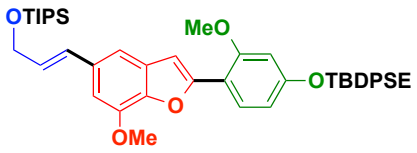

3.50
29.2 mg (57%)

Library member (3.50). TLC (50% DCM in hexanes): R_f = 0.40, visualized by UV; ^{1}H-NMR (500 MHz, acetone-d_6):δ 7.84 (app d, J = 9 Hz, 1H), 7.74-7.71 (m, 4H), 7.48-7.43 (m, 6H), 7.17 (d, J = 1 Hz, 1H), 7.16 (s, 1H), 7.00 (d, J = 1.5 Hz, 1H), 6.73 (dt, J = 15.5, 1.5 Hz, 1H), 6.50 (s, 1H), 6.50--6.48 (m, 1H), 6.36 (dt, J = 16, 4.5 Hz, 1H), 4.47 (dd, J = 5, 1.5 Hz, 2H), 4.14-4.11 (m, 2H), 4.02 (s, 3H), 3.93 (s, 3H), 1.88-1.84 (m, 2H), 1.20-1.09 (m, 30H); ^{13}C-NMR (125 MHz, acetone-d_6): δ 161.3, 158.7, 153.8, 146.0, 143.2, 136.7, 143.7, 134.2, 132.7, 130.5, 130.3, 128.8, 128.7, 128.3, 112.8, 112.3, 106.6, 105.5, 105.2, 100.0, 66.2, 64.8, 56.3, 55.9, 28.1, 18.6, 18.4, 12.8, 12.6; HRMS (ESI+) calculated for $C_{46}H_{61}O_5Si_2$: $[M+H]^+$ m/z 749.4058, found 749.4056.

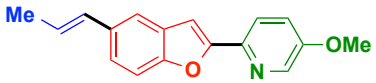

3.56
9.9 mg (56%)

Library member (3.56). TLC (20% EtOAc in hexanes): R_f = 0.28, stained by $KMnO_4$; ^{1}H-NMR (500 MHz, acetone-d_6): δ 8.37 (dd, J = 3, 0.5 Hz, 1H), 7.89 (dd, J = 8.5, 0.5 Hz, 1H), 7.63 (dd, J = 2 Hz, 1H), 7.50 – 7.48 (m, 2H), 7.39 (dd, J = 8.5, 2 Hz, 1H), 7.31 (d, J = 1 Hz, 1H), 6.53 (dd, J = 16, 1.5 Hz, 1H), 6.29 (dq, 15.5, 6.5 Hz, 1H), 3.95 (s, 3H), 1.87 (dd, J = 6.5, 1.5 Hz, 3H); ^{13}C-NMR (125 MHz, acetone-d_6):δ 157.0, 156.6, 155.2, 142.5, 139.2, 134.5, 132.0, 130.4, 125.1, 123.7, 121.2, 120.9, 119.3, 111.9, 103.6, 56.2, 18.6; HRMS (ESI+) calculated for $C_{17}H_{16}NO_2$ $[M+H]^+$ m/z 266.1181, found 266.1180.

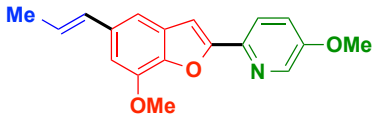

3.57
6.9 mg (35%)

Library member (3.57). TLC (20% EtOAc in hexanes): R_f = 0.23, stained by $KMnO_4$; ^{1}H-NMR (500 MHz, acetone-d_6): δ 8.36 (dd, *J* = 3, 0.5 Hz, 1H), 7.89 (dd, *J* = 8.5, 0.5 Hz, 1H), 7.49 (dd, *J* = 8.5, 3.0 Hz, 1H), 7.28 (s, 1H), 7.19 (d, *J* = 1.5 Hz, 1H), 7.01 (d, *J* = 1.5 Hz, 1H), 6.50 (d, *J* = 15.5, 1.5 Hz, 1H), 6.29 (dq, *J* = 16, 6.5 Hz, 1H), 4.05 (s, 3H), 3.95 (s, 3H), 1.87 (dd, *J* = 6.5, 1.5 Hz, 3H); ^{13}C-NMR (125 MHz, acetone-d_6): δ 156.9, 156.6, 146.3, 144.5, 142.5, 139.2, 135.5, 132.3, 131.8, 125.1, 121.2, 120.8, 112.0, 105.8, 103.9, 56.3, 56.2, 18.5; HRMS (ESI+) calculated for $C_{18}H_{18}NO_3$ $[M+H]^+$ *m/z* 296.1287, found 296.1282.

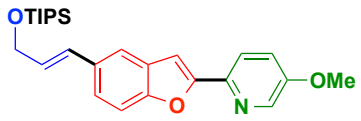

3.58
5.6 mg (19%)

Library member (3.58). Library member **3.58** was isolated as an off-white solid containing **3.58** (5.6 mg, 19% yield) and a small amount of a byproduct and was carried on to the manual deprotection without further purification. TLC (20% EtOAc in hexanes): R_f = 0.33, visualized by UV; ^{1}H-NMR (500 MHz, acetone-d_6): δ 8.37 (dd, *J* = 3, 1 Hz, 1H), 7.89 (dd, *J* = 9, 1 Hz, 1H), 7.71 (d, *J* = 1.5 Hz, 1H), 7.52 (d, *J* = 8.5, 1H), 7.49 (dd, *J* = 8.5, 3 Hz, 1H), 7.46 (dd, *J* = 8.5, 1H), 7.34 (d, *J* = 1 Hz, 1H), 6.80 (dt, *J* = 15.5, 2 Hz, 1H), 6.40 (dt, *J* = 15.5, 5 Hz, 1H), 4.50 (dd, *J* = 4.5, 2 Hz, 2H), 3.96 (s, 3H), 1.22-1.10 (m, 21H); HRMS (ESI+) calculated for $C_{26}H_{36}NO_3Si$ $[M+H]^+$ *m/z* 438.2464, found 438.2468.

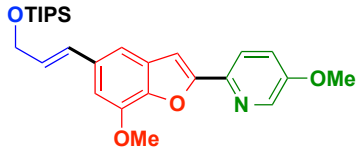

3.59
8.5 mg (26%)

Library member (3.59). TLC (20% EtOAc in hexanes): R_f = 0.26, visualized by UV; ^{1}H-NMR (500 MHz, acetone-d_6): δ 8.36 (dd, *J*= 3, 0.5 Hz, 1H), 7.90 (dd, *J* = 9, 0.5 Hz, 1H), 7.49 (dd, *J* =

8.5, 3 Hz, 1H), 7.30 (s, 1H), 7.26 (d, J = 1.5 Hz, 1H), 7.08 (d, J = 1.5 Hz, 1H), 6.76 (dt, J = 15.5, 2 Hz, 1H), 6.41 (dt, J = 16, 4.5 Hz, 1H), 4.49 (dd, J = 5, 2 Hz, 2H), 4.06 (s, 3H), 3.95 (s, 3H), 1.21-1.11 (m, 21H); ^{13}C-NMR (125 MHz, acetone-d_6):δ 157.0, 156.6, 146.4, 144.7, 142.5, 139.2, 134.8, 131.9, 130.2, 129.3, 121.2, 120.8, 112.8, 106.0, 103.9, 64.7, 56.4, 56.2, 18.4, 12.8; HRMS (ESI+) calculated for $C_{27}H_{38}NO_4Si$ $[M+H]^+$ *m/z* 468.2570, found 468.2572.

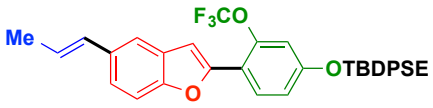

3.60
27.8 mg (69%)

Library member (3.60). TLC (20% DCM in hexanes): R_f = 0.27, visualized by UV; ^{1}H-NMR (500 MHz, acetone-d_6): δ 7.94 (d, J = 9 Hz, 1H), 7.74-7.72 (m, 4H), 7.62 (d, J = 1.5 Hz, 1H), 7.48-7.42 (m, 7H), 7.37 (dd, J = 8.5, 1.5 Hz, 1H), 7.10 (d, J = 0.5 Hz, 1H), 6.91 (dd, J = 9, 2.5 Hz, 1H), 6.82 (quint, J = 1.5 Hz, 1H), 6.51 (dd, J = 16, 2 Hz, 1H), 6.27 (dq, J = 16, 7 Hz, 1H), 4.17-4.14 (m, 2H), 1.90-1.87 (m, 2H), 1.86 (dd, J = 6.5, 1.5 Hz, 3H), 1.10 (s, 9H); ^{13}C-NMR (125 MHz, acetone-d_6): δ 160.7, 154.2, 151.7, 147.0, 136.7, 134.6, 134.5, 132.0, 130.4, 130.3, 129.8, 128.7, 125.1, 123.8, 121.5 (J_{C-F} = 257 Hz), 119.2, 116.8, 114.2, 111.6, 109.0, 105.7, 67.0, 28.1, 18.6 (2C), 12.4; HRMS (ESI+) calculated for $C_{36}H_{36}F_3O_3Si$ $[M+H]^+$ *m/z* 601.2386, found 601.2386.

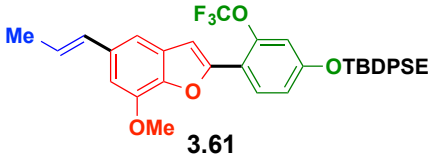

3.61
32.2 mg (76%)

Library member (3.61). TLC (20% DCM in hexanes): R_f = 0.09, visualized by UV; ^{1}H-NMR (500 MHz, acetone-d_6): δ 7.94 (d, J = 9 Hz, 1H), 7.74-7.72 (m, 4H), 7.48-7.42 (m, 6H), 7.18 (d, J = 1.5 Hz, 1H), 7.07 (s, 1H), 7.00 (d, J = 1.5 Hz, 1H), 6.92 (dd, J = 9, 2.5 Hz, 1H), 6.81 (quint, J = 2 Hz, 1H), 6.48 (dd, J = 16, 2 Hz, 1H), 6.27 (dq, J = 16, 6.5 Hz, 1H), 4.17-4.14 (m, 2H), 4.03 (s, 3H), 1.90-1.86 (m, 2H), 1.86 (dd, J = 6.5, 1.5 Hz, 3H), 1.09 (s, 9H); ^{13}C-NMR (125 MHz, acetone-d_6): δ 160.7, 151.5, 146.9, 146.1, 143.6, 136.7, 135.5, 134.6, 132.3, 131.9, 130.3, 129.7, 128.7, 125.1, 121.5 (J_{C-F} = 257 Hz), 116.8, 114.2, 111.8, 109.0, 105.9 (2C), 67.0, 56.4, 28.1, 18.6, 18.5, 12.4; HRMS (ESI+) calculated for $C_{37}H_{38}O_4F_3Si$ $[M+H]^+$ *m/z* 631.2491, found 631.2488.

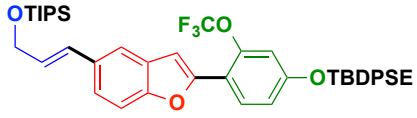

3.62
21.6 mg (42%)

Library member (3.62). Library member **3.62** was isolated as a colorless oil containing **3.62** (21.6 mg, 42% yield) and a small amount of a byproduct and was carried on to the manual deprotection without further purification. TLC (10% DCM in hexanes): R_f = 0.11, visualized by UV; ^{1}H-NMR (500 MHz, acetone-d_6): δ 7.95 (d, J = 9 Hz, 1H), 7.74-7.70 (m, 5H), 7.50-7.41 (m, 8H), 7.13 (d, J = 0.5 Hz, 1H), 6.92 (dd, J = 9, 2.5 Hz, 1H), 6.82 (quint, J = 1.5 Hz, 1H), 6.79 (dt, J = 16, 1.5 Hz, 1H), 6.39 (dt, J = 16, 4.5 Hz, 1H), 4.48 (dd, J = 5, 2 Hz, 2H), 4.18-4.14 (m, 2H), 1.90-1.87 (m, 2H), 1.21-1.08 (m, 30H); HRMS (ESI+) calculated for $C_{45}H_{54}F_3O_4Si_2$ $[M+H]^+$ *m/z* 771.3513, found 771.3550.

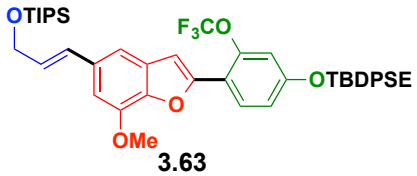

3.63
35.7 mg (65%)

Library member (3.63). TLC (20% DCM in hexanes): R_f = 0.11, visualized by UV; ^{1}H-NMR (500 MHz, acetone-d_6): δ 7.95 (d, J = 8.5 Hz, 1H), 7.74-7.72 (m, 4H), 7.46-7.42 (m, 6H), 7.26 (d, J = 1.5 Hz, 1H), 7.09 (s, 1H), 7.06 (d, J = 1 Hz, 1H), 6.93 (dd, J = 8.5, 2.5 Hz, 1H), 6.81 (quint, J = 1.5 Hz, 1H), 6.79 (dt, J = 15.5, 2 Hz, 1H), 6.39 (dq, J = 16, 4.5 Hz, 1H), 4.47 (dd, J = 4.5, 1.5 Hz, 2H), 4.17-4.14 (m, 2H), 4.04 (s, 3H), 1.90-1.86 (m, 2H), 1.20-1.09 (m, 30H); ^{13}C-NMR (125 MHz, acetone-d_6): δ 160.7, 151.6, 146.9, 146.2, 143.8, 136.7, 134.8, 134.6, 132.0, 130.3, 130.2, 129.8, 129.3, 128.7, 121.5 ($J_{C\text{-}F}$ = 257 Hz), 116.8, 114.2, 112.6, 109.0, 106.2, 106.0, 67.0, 64.7, 56.4, 28.1, 18.5, 18.4, 12.8, 12.4; HRMS (ESI+) calculated for $C_{46}H_{57}F_3O_5Si_2Na$ $[M+H]^+$ *m/z* 825.3594, found 825.3600.

General Scheme for Automated Synthesis of Tetramer Library Members

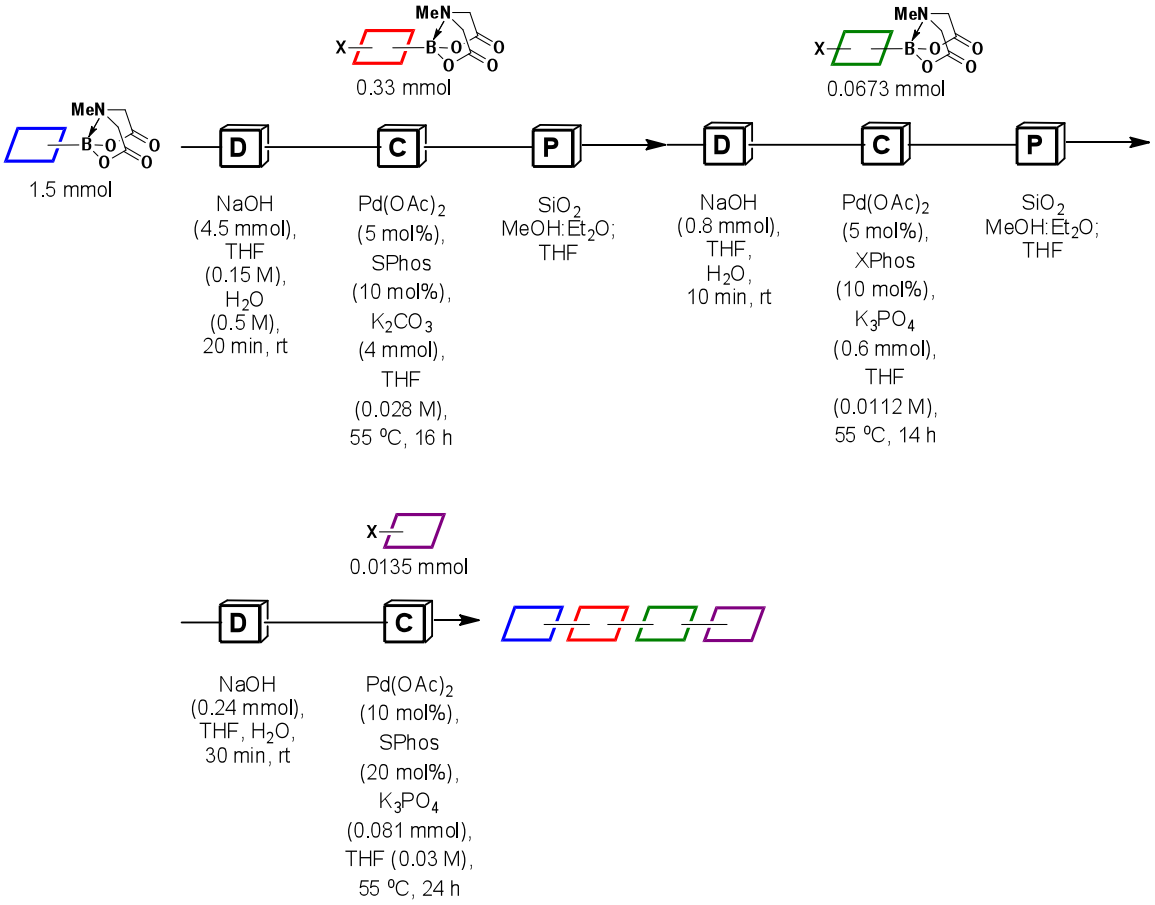

The general procedure was executed with the conditions stated above for all of the tetramer library members.

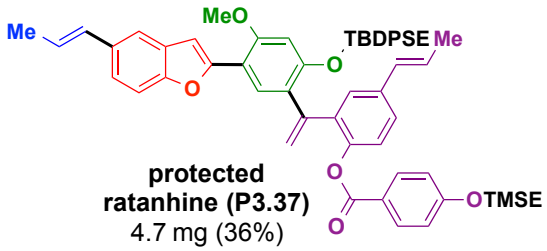

protected ratanhine (P3.37)
4.7 mg (36%)

Protected ratanhine (P3.37). HPLC [tR = 13.4, flow rate = 25 mL/min, gradient: 20% → 100% THF:MeCN (1:4) in H_2O over 50 min]. ^{1}H-NMR (500 MHz, acetone-d_6): δ 7.67 (s, 1H), 7.64-7.62 (m, 4H), 7.54 (d, J = 9 Hz, 2H), 7.50 (s, 1H), 7.45-7.43 (m, 8H), 7.25 (d, J = 2 Hz, 1H), 7.21 (d, J = 8.5 Hz, 1H), 7.10 (d, J = 8.5 Hz, 1H), 6.95 (d, J = 1 Hz, 1H), 6.56 (dd, J = 16, 2 Hz, 1H), 6.51-6.46 (m, 3H), 6.38 (dq, J = 15.5, 6.5 Hz, 1H), 6.35 (s, 1H), 6.26 (dq, J = 15.5, 6.5 Hz,

1H), 5.46 (s, 2H), 3.86-3.83 (m, 2H), 3.81 (s, 3H), 3.57-3.54 (m, 2H), 1.91 (dd, J = 6.5, 1.5 Hz, 3H), 1.88 (dd, J = 5, 1.5 Hz, 3H), 1.20-1.17 (m, 2H), 0.99 (s, 9H), 0.89-0.86 (m, 2H), 0.02 (s, 9H); HRMS (ESI+) calculated for $C_{59}H_{65}O_6Si_2$ $[M+H]^+$ *m/z* 925.4320, found 925.4316.

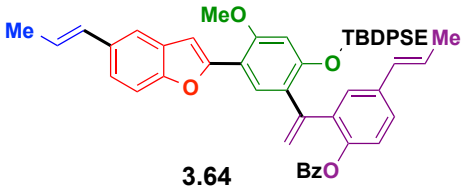

3.64
3.7 mg (34%)

Library member (3.64). HPLC [25 mL/min, gradient: A = water, B = 10% THF in MeCN, 0 min: 80% A, 20% B; 5 min: 0% A, 100% B; 50 min: 0% A, 100% B): 17.1 min; ^{1}H-NMR (500 MHz, acetone-d_6): δ 7.71 (s, 1H), 7.68-7.61 (m, 6H), 7.60 (d, J = 2.5 Hz, 1H), 7.50 (d, J = 1.5 Hz, 1H), 7.47-7.41 (m, 7H), 7.36 (d, J = 8.5 Hz, 1H), 7.29 (dd, J = 8.5, 1.5 Hz, 1H), 7.17-7.13 (m, 2H), 7.10-7.06 (m, 2H), 6.95 (d, J = 1 Hz, 1H), 6.56 (dd, J = 16, 2 Hz, 1H), 6.51 (dd, J = 16, 1.5 Hz, 1H), 6.38 (dq, J = 16, 6.5 Hz, 1H), 6.34 (s, 1H), 6.25 (dq, J = 15.5, 7 Hz, 1H), 5.50 (d, J = 1.5 Hz, 1H), 5.49 (d, J = 2 Hz, 1H), 3.88-3.86 (m, 2H), 3.79 (s, 3H), 1.90 (dd, J = 6.5, 1.5 Hz, 3H), 1.87 (dd, J = 6.5, 1.5 Hz, 3H), 1.27-1.23 (m, 2H), 0.99 (s, 9H); HRMS (ESI+) calculated for $C_{54}H_{53}O_5Si$ $[M+H]^+$ *m/z* 809.3662, found 809.3658.

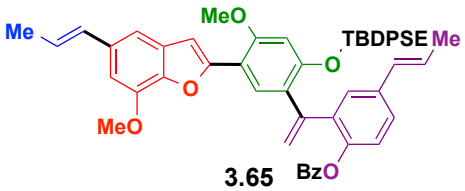

3.65
5.1 mg (44%)

Library member (3.65). HPLC (25 mL/min, gradient: A = water, B = 10% THF in MeCN, 0 min: 80% A, 20% B; 5 min: 0% A, 100% B; 50 min: 0% A, 100% B): 14.3 min; TLC (70% DCM in hexanes): R_f = 0.5, visualized by UV; ^{1}H-NMR (500 MHz, acetone-d_6): δ 7.75 (s, 1H), 7.68-7.63 (m, 6H), 7.59 (d, J = 2.5 Hz, 1H), 7.47-7.41 (m, 8H), 7.17-7.14 (m, 2H), 7.10-7.07 (m, 3H), 6.93 (s, 1H), 6.55 (dd, J = 16, 1.5 Hz, 1H), 6.48 (dd, J = 16, 1.5 Hz, 1H), 6.38 (dq, J = 16, 6.5 Hz, 1H), 6.34 (s, 1H), 6.26 (dq, J = 15.5, 6.5 Hz, 1H), 5.51 (d, J = 2 Hz, 1H), 5.50 (d, J = 2 Hz, 1H), 4.00 (s, 3H), 3.88-3.85 (m, 2H), 3.78 (s, 3H), 1.90 (dd, J = 6.5, 1.5 Hz, 3H), 1.87 (dd, J

= 6.5, 1.5 Hz, 3H), 1.27-1.23 (m, 2H), 0.99 (s, 9H); HRMS (ESI+) calculated for $C_{55}H_{55}O_6Si$ $[M+H]^+$ *m/z* 839.3768, found 839.3772.

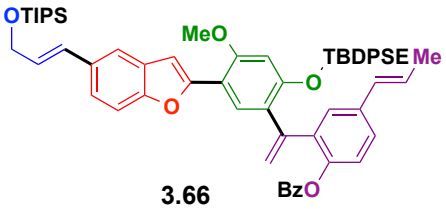

3.66
0.6 mg (5%)

Library member (3.66). HPLC (25 mL/min, gradient: A = water, B = 10% THF in MeCN, 0 min: 80% A, 20% B; 5 min: 0% A, 100% B; 50 min: 0% A, 100% B): 48.3 min; ^{1}H-NMR (500 MHz, acetone-d_6): δ 7.71 (s, 1H), 7.67-7.58 (m, 7H), 7.47-7.37 (m, 10H), 7.16-7.14 (m, 2H), 7.10-7.07 (m, 2H), 6.97 (s, 1H), 6.78 (app d, *J* = 16 Hz, 1H), 6.56 (dd, *J* = 15.5, 1.5 Hz, 1H), 6.41-6.36 (m, 2H), 6.35 (s, 1H), 5.51 (d, *J* = 1.5 Hz, 1H), 5.50 (d, *J* = 1.5 Hz, 1H), 4.50 (dd, *J* = 5, 2 Hz, 2H), 3.88-3.85 (m, 2H), 3.79 (s, 3H), 1.91 (dd, *J* = 6.5, 1.5 Hz, 3H), 1.29-1.07 (m, 23H), 0.94 (s, 9H); HRMS (ESI+) calculated for $C_{63}H_{73}O_6Si_2$ $[M+H]^+$ *m/z* 981.4946, found 981.4949.

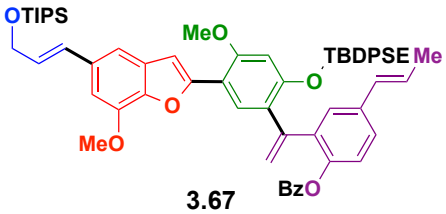

3.67
3.0 mg (23%)

Library member (3.67). HPLC (25 mL/min, gradient: A = water, B = 10% THF in MeCN, 0 min: 80% A, 20% B; 5 min: 0% A, 100% B; 50 min: 0% A, 100% B): 33.4 min; TLC (50% DCM in hexanes): R_f = 0.18, visualized by UV; ^{1}H-NMR (500 MHz, acetone-d_6):δ 7.75 (s, 1H), 7.69-7.62 (m, 6H), 7.60 (d, *J* = 2.5 Hz, 1H), 7.47-7.40 (m, 7H), 7.17-7.13 (m, 3H), 7.10-7.06 (m, 2H), 7.00 (d, *J* = 1.5 Hz, 1H), 6.95 (s, 1H), 6.76 (dt, *J* = 15.5, 1.5 Hz, 1H), 6.56 (dd, *J* = 15.5, 1.5 Hz, 1H), 6.40-6.35 (m, 2H), 6.34 (s, 1H), 5.52 (d, *J* = 1.5 Hz, 1H), 5.50 (d, *J* = 1.5 Hz, 1H), 4.49 (dd, *J* = 5, 2 Hz, 2H), 4.02 (s, 3H), 3.88-3.85 (m, 2H), 3.78 (s, 3H), 1.90 (dd, *J* = 6.5, 2.5 Hz, 3H), 1.29-1.23 (m, 2H), 1.23-1.08 (m, 21H), 0.99 (s, 9H); HRMS (ESI+) calculated for $C_{64}H_{74}O_7Si_2Na$ $[M+Na]^+$ *m/z* 1033.4871, found 1033.4895.

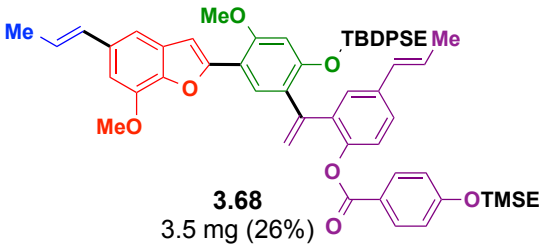

3.68
3.5 mg (26%)

Library member (3.68). HPLC (25 mL/min, gradient: A = water, B = 20% THF in MeCN, 0 min: 80% A, 20% B; 5 min: 0% A, 100% B; 50 min: 0% A, 100% B): 12.2 min; ^{1}H-NMR (500 MHz, acetone-d_6): δ 7.71 (s, 1H), 7.64-7.62 (m, 4H), 7.56-7.53 (m, 2H), 7.46-7.41 (m, 8H), 7.10 (d, J = 8 Hz, 1H), 7.08 (d, J = 1 Hz, 1H), 6.94 (d, J = 1.5 Hz, 1H), 6.93 (s, 1H), 6.56 (dd, J = 15.5, 1.5 Hz, 1H), 6.51-6.47 (m, 3H), 6.38 (dq, J = 15.5, 6.5 Hz, 1H), 6.34 (s, 1H), 6.27 (dq, J = 15.5, 6.5 Hz, 1H), 5.46 (s, 2H), 4.02 (s, 3H), 3.87-3.84 (m, 2H), 3.80 (s, 3H), 3.56 (app t, J = 8 Hz, 2H), 1.90 (dd, J = 6.5, 1.5 Hz, 3H), 1.88 (dd, J = 6.5, 1.5 Hz, 3H), 1.23-1.20 (m, 2H), 0.98 (s, 9H), 0.91-0.88 (m, 2H), 0.03 (s, 9H); HRMS (ESI+) calculated for $C_{60}H_{67}O_7Si_2$ $[M+H]^+$ *m/z* 955.4425, found 955.4437.

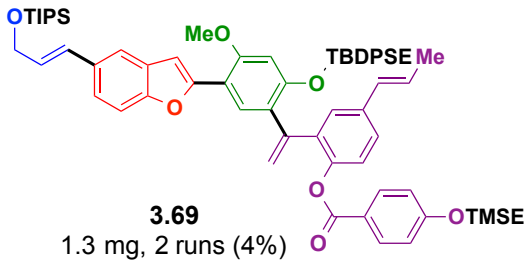

3.69
1.3 mg, 2 runs (4%)

Library member (3.69). HPLC (25 mL/min, gradient: A = water, B = 20% THF in MeCN, 0 min: 80% A, 20% B; 5 min: 0% A, 100% B; 50 min: 0% A, 100% B): 26.8 min; ^{1}H-NMR (500 MHz, acetone-d_6): δ 7.69 (s, 1H), 7.64-7.61 (m, 5H), 7.57 (s, 1H), 7.55 (d, J = 9 Hz, 2H), 7.46-7.34 (m, 9H), 7.10 (d, J = 8.5 Hz, 1H), 6.97 (s, 1H), 6.80 (dt, J = 16, 1.5 Hz, 1H), 6.56 (dd, J = 15.5, 1.5 Hz, 1H), 6.49 (d, J = 7 Hz, 2H), 6.41-6.34 (m, 3H), 5.46 (s, 2H), 4.51 (dd, J = 5, 2 Hz, 2H), 3.90-3.85 (m, 2H), 3.81 (s, 3H), 3.58 (app t, J = 8 Hz, 2H), 1.91 (dd, J = 6.5, 1 Hz, 3H), 1.24-1.17 (m, 5H), 1.15-1.12 (m, 18H), 0.99 (s, 9H), 0.88 (m, 2H), 0.03 (s, 9H); HRMS (ESI+) calculated for $C_{68}H_{85}O_7Si_3$ $[M+H]^+$ *m/z* 1097.5603, found 1097.5591.

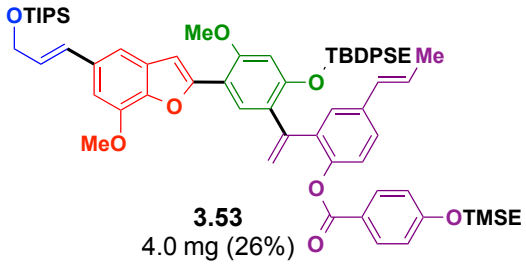

3.53
4.0 mg (26%)

Library member (3.53). HPLC (25 mL/min, gradient: A = water, B = 20% THF in MeCN, 0 min: 80% A, 20% B; 5 min: 0% A, 100% B; 50 min: 0% A, 100% B): 22.3 min; ^{1}H-NMR (500 MHz, acetone-d_6): δ 7.72 (s, 1H), 7.64-7.62 (m, 5H), 7.55 (d, J = 8.5 Hz, 2H), 7.46-7.41 (m, 7H), 7.14 (d, J = 1 Hz, 1H), 7.10 (d, J = 8 Hz, 1H), 7.00 (d, J = 1.5 Hz, 1H), 6.95 (s, 1H), 6.76 (dt, J = 15.5, 1.5 Hz, 1H), 6.56 (dd, J = 16, 2 Hz, 1H), 6.49 (d, J = 8.5 Hz, 2H), 6.42-6.34 (m, 3H), 5.44 (d, J = 2 Hz, 1H), 5.43 (d, J = 2 Hz, 1H), 4.50 (dd, J = 5, 2 Hz, 2H), 4.03 (s, 3H), 3.88-3.82 (m, 2H), 3.80 (s, 3H), 3.59 (app t, J = 8 Hz, 2H), 1.91 (dd, J = 6.5, 1.5 Hz, 3H), 1.24-1.17 (m, 5H), 1.15-1.13 (m, 18H), 0.99 (s, 9H), 0.91-0.88 (m, 2H), 0.03 (s, 9H); HRMS (ESI+) calculated for $C_{69}H_{86}O_8Si_3Na$ $[M+Na]^+$ *m/z* 1149.5528, found 1149.5552.

V. MANUAL DEPROTECTION OF LIBRARY MEMBERS

Deprotection Condition 1

To a 7-mL vial containing the protected library member and a PTFE-coated magnetic stir bar was added TBAF•3H_2O (2.2–15 equiv) followed by 1:1 DMSO/DMPU under ambient atmosphere. The vial was sealed with a Teflon-lined cap and stirred at 50 °C for 30 minutes–6 hours. The reaction was then cooled to room temperature and diluted with a solution of 1:1 saturated NH_4Cl/H_2O (1.5–2 mL). The layers were mixed and the aqueous layer was removed. The organic layer was washed with H_2O (2 × 1.5 mL). The combined aqueous phase was extracted with EtOAc (3 mL). The organic phase was dried over anhydrous $MgSO_4$, filtered, and concentrated *in vacuo*. The crude product was purified by silica gel chromatography to give the pure product as a white or off-white solid.

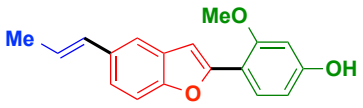

ratanhiaphenol III (3.36)
(7.1 mg, 50% yield)

Ratanhiaphenol III (3.36). Deprotection condition 1 was followed to give **3.36** (7.1 mg, 50% yield). TLC (20% EtOAc/hexanes): $R_f = 0.14$, visualized by shortwave UV; ^{1}H-NMR (500 MHz, acetone-d_6): δ 8.77 (br s, 1H), 7.83 (d, $J = 8.5$ Hz, 1H), 7.54 (d, $J = 2.0$ Hz, 1H), 7.41 (d, $J = 8.5$ Hz, 1H), 7.29 (dd, $J = 8.5$, 2.0 Hz, 1H), 7.16 (d, $J = 1.0$ Hz, 1H), 6.64 (d, $J = 2.0$ Hz, 1H), 6.60 (dd, $J = 8.0$, 2.0 Hz, 1H), 6.51 (d, $J = 16$, 1.5 Hz, 1H), 6.25 (dq, $J = 15.5$, 7 Hz, 1H), 3.99 (s, 3H), 1.86 (dd, $J = 7.0$, 2.0 Hz, 3H); ^{13}C-NMR (125 MHz, acetone-d_6): δ 160.2, 159.2, 154.2, 153.8, 134.0, 132.3, 131.3, 128.5, 124.5, 122.7, 118.7, 111.9, 111.2, 108.5, 104.6, 100.2, 55.9, 18.6; HRMS (ESI+) calculated for $C_{18}H_{17}O_3$ $[M+H]^+$ *m/z* 281.1178, found 281.1181.

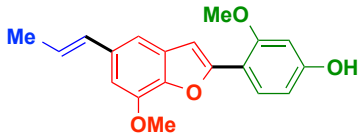

deprotected 3.54
(11.7 mg, 78% yield)

Deprotected 3.54. Deprotection condition 1 was followed to give **deprotected 3.54** (11.7 mg, 78% yield). TLC (30% EtOAc/hexanes): $R_f = 0.3$, visualized by shortwave UV; ^{1}H-NMR (500 MHz, acetone-d_6): δ 8.73 (br s, 1H), 7.84 (d, $J = 8.5$ Hz, 1H), 7.13 (s, 1H), 7.11 (d, $J = 1.0$ Hz, 1H), 6.93 (d, $J = 1.0$ Hz, 1H), 6.64 (d, $J = 2.0$ Hz, 1H), 6.60 (dd, $J = 8.5$, 2.0 Hz, 1H), 6.48 (dd, $J = 16$, 1.5 Hz, 1H), 6.25 (dq, $J = 16$, 6.5 Hz, 1H), 4.03 (s, 3H), 3.98 (s, 3H), 1.86 (dd, $J = 6.5$, 1.5 Hz, 3H); ^{13}C-NMR (125 MHz, acetone-d_6): δ 160.2, 159.1, 154.0, 145.9, 142.9, 135.0, 132.7, 132.6, 128.5, 124.6, 111.9, 111.6, 108.5, 105.1, 104.8, 100.2, 56.4, 55.9, 18.6; HRMS (ESI+) calculated for $C_{19}H_{19}O_4$ $[M+H]^+$ *m/z* 311.1283, found 311.1277.

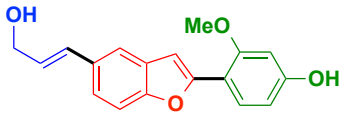

deprotected 3.55
(6.0 mg, 56% yield)

Deprotected 3.55. Deprotection condition 1 was followed to give **deprotected 3.55** (6.0 mg, 56% yield). TLC (50% EtOAc/hexanes): $R_f = 0.27$, visualized by shortwave UV; ^{1}H-NMR (500

MHz, acetone-d_6): δ 8.78 (br s, 1H), 7.83 (d, J = 8.5 Hz, 1H), 7.61 (d, J = 1.5 Hz, 1H), 7.43 (d, J = 8.5 Hz, 1H), 7.36 (dd, J = 9.0, 2.0 Hz, 1H), 7.18 (d, J = 0.5 Hz, 1H), 6.70 (d, J = 16.0 Hz, 1H), 6.64 (d, J = 2.5 Hz, 1H), 6.60 (dd, J = 8.5, 2.5 Hz, 1H), 6.38 (dt, J = 16, 5.5 Hz, 1H), 4.25 (t, J = 5.5 Hz, 2H), 3.99 (s, 3H), 3.84 (t, J = 5.5 Hz, 1H); ^{13}C-NMR (125 MHz, acetone-d_6): δ 160.2, 159.1, 154.2, 153.9, 133.3, 131.3, 130.5, 129.6, 128.5, 123.0, 119.2, 111.8, 111.2, 108.4, 104.5, 100.2, 63.4, 55.8; HRMS (ESI+) calculated for $C_{18}H_{17}O_4$ $[M+H]^+$ *m/z* 297.1127, found 297.1128.

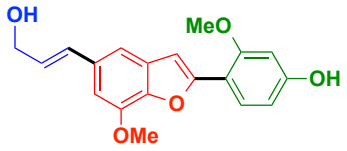

3.48
(7.4 mg, 35% yield)

3.48. Deprotection condition 1 was followed to give **3.48** (7.4 mg, 35% yield). TLC (60% EtOAc/hexanes): R_f = 0.22, visualized by shortwave UV; ^{1}H-NMR (500 MHz, acetone-d_6): δ 8.75 (br s, 1H), 7.85 (d, J = 8.0 Hz, 1H), 7.18 (d, J = 1.5 Hz, 1H), 7.15 (s, 1H), 6.99 (d, J = 1.0 Hz, 1H), 6.66 (dt, J = 17, 1.5 Hz, 1H), 6.64 (d, J = 2.0 Hz, 1H), 6.60 (dd, J = 8.5, 2.5 Hz, 1H), 6.38 (dt, J = 16, 5.5 Hz, 1H), 4.25 – 4.24 (m, 2H), 4.04 (s, 3H), 3.99 (s, 3H), 3.84 (br s, 1H); ^{13}C-NMR (125 MHz, acetone-d_6): δ 160.2, 159.1, 154.2, 146.0, 143.2, 134.4, 132.8, 130.9, 129.7, 128.5, 112.3, 111.9, 108.5, 105.4, 104.8, 100.2, 63.4, 56.4, 55.9; HRMS (ESI+) calculated for $C_{19}H_{19}O_5$ $[M+H]^+$ *m/z* 327.1232, found 327.1223.

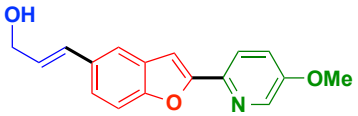

deprotected 3.58
(3.1 mg, 63% yield)

Deprotected 3.58. Deprotection condition 1 was followed to give **deprotected 3.58** (3.1 mg, 63% yield). TLC (60% EtOAc/hexanes): R_f = 0.36, visualized by shortwave UV; ^{1}H-NMR (500 MHz, acetone-d_6): δ 8.37 (dd, J = 2.5, 0.5 Hz, 1H), 7.90 (d, J = 8.5 Hz, 1H), 7.70 (d, J = 1.5 Hz, 1H), 7.52 (d, J = 8.5 Hz, 1H), 7.50 (dd, J = 9.0, 3.0 Hz, 1H), 7.45 (dd, J = 8.5, 1.5 Hz, 1H), 7.33 (d, J = 1 Hz, 1H), 6.72 (dt, J = 15.5, 1.5 Hz, 1H), 6.41 (dt, J = 16.0, 5.5 Hz, 1H), 4.26 (t, J = 8.0 Hz, 2H), 3.96 (s, 3H), 3.87 (br t, J = 5.0 Hz, 1H); ^{13}C-NMR (125 MHz, acetone-d_6): δ 157.1,

156.6, 155.4, 142.4, 139.2, 133.8, 130.4, 130.2, 130.1, 124.1, 121.2, 120.9, 119.8, 111.9, 103.5, 63.3, 56.2; HRMS (ESI+) calculated for $C_{17}H_{16}NO_3$ $[M+H]^+$ *m/z* 282.1130, found 282.1132.

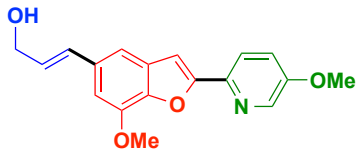

deprotected 3.59
(3.9 mg, 67% yield)

Deprotected 3.59. Deprotection condition 1 was followed to give **deprotected 3.59** (3.9 mg, 67% yield). TLC (60% EtOAc/hexanes): R_f = 0.27, visualized by shortwave UV; ^{1}H-NMR (500 MHz, acetone-d_6): δ 8.36 (dd, *J* = 2.5, 0.5 Hz, 1H), 7.90 (d, *J* = 8.5 Hz, 1H), 7.49 (dd, *J* = 9.0, 3.0 Hz, 1H), 7.30 (s, 1H), 7.25 (d, *J* = 1.0 Hz, 1H), 7.08 (d, *J* = 1.5 Hz, 1H), 6.68 (app d, *J* = 15.5 Hz, 1H), 6.41 (dt, *J* = 16, 5.5 Hz, 1H), 4.25 (t, *J* = 5.5 Hz, 2H), 4.06 (s, 3H), 3.95 (s, 3H), 3.86 (br t, *J* = 5.5 Hz, 1H); ^{13}C-NMR (125 MHz, acetone-d_6): δ 159.9, 156.5, 146.3, 144.6, 142.4, 139.2, 134.8, 131.8, 130.4, 130.2, 121.2, 120.8, 112.6, 105.9, 103.8, 63.3, 56.3, 56.2; HRMS (ESI+) calculated for $C_{18}H_{18}NO_4$ $[M+H]^+$ *m/z* 312.1236, found 312.1239.

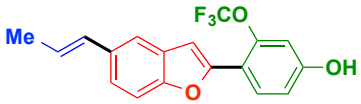

deprotected 3.60
(12.6 mg, 81% yield)

Deprotected 3.60. Deprotection condition 1 was followed to give **deprotected 3.60** (12.6 mg, 81% yield). TLC (20% EtOAc/hexanes): R_f = 0.36, visualized by shortwave UV; ^{1}H-NMR (500 MHz, acetone-d_6): δ 9.30 (br s, 1H), 7.96 (d, *J* = 8.5 Hz, 1H), 7.63 (d, *J* = 1.0 Hz, 1H), 7.47 (d, *J* = 8.5 Hz, 1H), 7.38 (dd, *J* = 8.5, 1.5 Hz, 1H), 7.10 (s, 1H), 7.03 (dd, *J* = 8.5, 2.0 Hz, 1H), 6.98 (m, 1H), 6.52 (dd, *J* = 15.5, 1.5 Hz, 1H), 6.28 (dq, *J* = 15.5, 6.5 Hz, 1H), 1.87 (dd, *J* = 6.5, 1.5 Hz, 3H); ^{13}C-NMR (125 MHz, acetone-d_6): δ 159.7, 154.2, 152.0, 147.2, 134.4, 131.9, 130.5, 130.0, 125.0, 123.7, 121.5 ($J_{C\text{-}F}$ = 257 Hz), 119.1, 115.9, 115.7, 111.5, 109.3, 105.3, 18.5; HRMS (ESI+) calculated for $C_{18}H_{14}O_3F_3$ $[M+H]^+$ *m/z* 335.0895, found 335.0889.

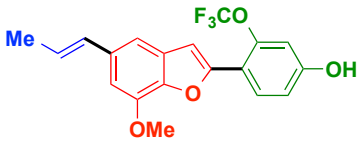

deprotected 3.61
(14.3 mg, 77% yield)

Deprotected 3.61. Deprotection condition 1 was followed to give **deprotected 3.61** (14.3 mg, 77% yield). TLC (20% EtOAc/hexanes): R_f = 0.27, visualized by shortwave UV; ^{1}H-NMR (500 MHz, acetone-d_6): δ 9.33 (br s, 1H), 7.96 (d, J = 9.0 Hz, 1H), 7.19 (d, J = 0.5 Hz, 1H), 7.07 (s, 1H), 7.03 (dd, J = 8.5, 2.0 Hz, 1H), 7.00 (d, J = 1.5 Hz, 1H), 6.97 (m, 1H), 6.49 (dd, J = 15.5, 1.5 Hz, 1H), 6.28 (dq, J = 16.0, 6.5 Hz, 1H), 4.04 (s, 3H), 1.86 (dd, J = 6.5, 3.0 Hz, 3H); ^{13}C-NMR (125 MHz, acetone-d_6): δ 159.7, 151.7, 147.1, 146.0, 143.5, 135.4, 132.2, 131.9, 129.9, 125.0, 121.5 ($J_{C\text{-}F}$ = 256 Hz), 115.9, 115.7, 111.8, 109.2, 105.8, 105.6, 56.3, 18.5; HRMS (ESI+) calculated for $C_{19}H_{16}O_4F_3$ $[M+H]^+$ *m/z* 365.1001, found 365.0997.

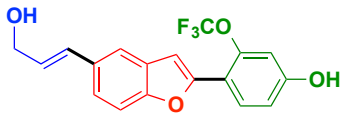

deprotected 3.62
(7.1 mg, 73% yield)

Deprotected 3.62. Deprotection condition 1 was followed to give **deprotected 3.62** (7.1 mg, 73% yield). TLC (40% EtOAc/hexanes): R_f = 0.21, visualized by shortwave UV; ^{1}H-NMR (500 MHz, acetone-d_6): δ 9.30 (br s, 1H), 7.97 (d, J = 8.5 Hz, 1H), 7.10 (d, J = 1.5 Hz, 1H), 7.50 (d, J = 8.5 Hz, 1H), 7.44 (dd, J = 8.5, 2.0 Hz, 1H), 7.12 (d, J = 0.5 Hz, 1H), 7.04 (dd, J = 8.5, 2.5 Hz, 1H), 6.98 (quint, J = 2 Hz, 1H), 6.72 (d, J = 16 Hz, 1H), 6.41 (dt, J = 16.0, 5.0 Hz, 1H), 4.26 (d, J = 5.0 Hz, 2H), 3.84 (br s, 1H); ^{13}C-NMR (125 MHz, acetone-d_6): δ 159.8, 154.4, 152.1, 147.2, 133.8, 130.6, 130.1, 130.0 (2C), 124.0, 121.5 ($J_{C\text{-}F}$ = 256 Hz), 119.7, 115.9, 115.7, 111.6, 109.3, 105.3, 63.3; HRMS (ESI+) calculated for $C_{18}H_{14}O_4F_3$ $[M+H]^+$ *m/z* 351.0844, found 351.0849.

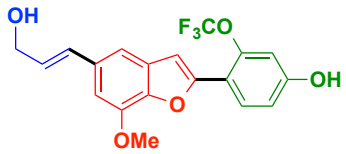

deprotected 3.63
(11.4 mg, 67% yield)

Deprotected 3.63. Deprotection condition 1 was followed to give **deprotected 3.63** (11.4 mg, 67% yield). TLC (40% EtOAc/hexanes): R_f = 0.13, visualized by shortwave UV; ^{1}H-NMR (500 MHz, acetone-d_6): δ 9.30 (br s, 1H), 7.97 (d, J = 8.5 Hz, 1H), 7.26 (d, J = 0.5 Hz, 1H), 7.09 (s, 1H), 7.06 (d, J = 1.0 Hz, 1H), 7.04 (dd, J = 8.5, 2.5 Hz, 1H), 6.97 (m, 1H), 6.68 (d, J = 15.5 Hz, 1H), 6.41 (dt, J = 16.0, 5.0 Hz, 1H), 4.26 (d, J = 5.0 Hz, 2H), 4.06 (s, 3H), 3.85 (br s, 1H); ^{13}C-NMR (125 MHz, acetone-d_6): δ 159.7, 151.8, 147.1, 146.1, 143.7, 134.8, 131.9, 130.4, 130.1, 129.9, 121.5 ($J_{C\text{-}F}$ = 256 Hz), 115.9, 115.7, 112.4, 109.2, 106.0, 105.6, 63.3, 56.4; HRMS (ESI+) calculated for $C_{19}H_{16}O_5F_3$ $[M+H]^+$ *m/z* 381.0950, found 381.0946.

Deprotection Condition 2

To a 1-mL Reacti-vial™ containing the protected tetramer library member and a PTFE-coated magnetic stir bar was added TBAF•3H_2O (15-20 equiv) followed by DMSO under ambient atmosphere. The vial was sealed with a cap and stirred at 50 °C for 5 hours. The reaction was then cooled to room temperature, diluted with 8 mL Et_2O and washed with a solution of 1:1 saturated NH_4Cl/H_2O (4 mL). The aqueous layer was extracted with 4 mL Et_2O. The combined organic layers were washed with H_2O (2 × 4 mL), then with brine (4 mL). The organic phase was dried over anhydrous $MgSO_4$, filtered, and concentrated *in vacuo*. The crude product was purified by silica gel chromatography.

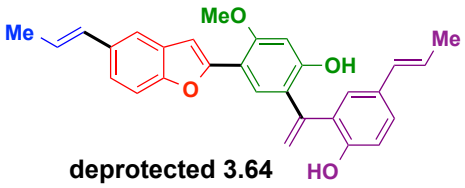

deprotected 3.64
(1.0 mg, 48% yield)

Deprotected 3.64. Deprotection condition 2 was followed to give **deprotected 3.64** (1.0 mg, 48% yield). TLC (40% EtOAc/pentane): R_f = 0.49, visualized by shortwave UV; ^{1}H-NMR (500 MHz, acetone-d_6): δ 7.77 (s, 1H), 7.53 (d, J = 1.5 Hz, 1H), 7.37 (d, J = 8.0 Hz, 1H), 7.27 (dd, J =

8.5, 2.0 Hz, 1H), 7.18-7.17 (m, 3H), 6.82 (dd, *J* = 6.5, 3.0 Hz, 1H), 6.68 (s, 1H), 6.50 (dd, *J* = 16.0, 1.5 Hz, 1H), 6.31 (dd, *J* = 15.5, 1.5 Hz, 1H), 6.24 (dq, *J* = 16.0, 6.5 Hz, 1H), 6.05 (dq, *J* = 15.5, 7.0 Hz, 1H), 5.69 (d, *J* = 2.5 Hz, 1H), 5.66 (d, *J* = 2.5 Hz, 1H), 3.99 (s, 3H), 1.85 (dd, *J* = 6.5, 1.5 Hz, 1H), 1.78 (dd, *J* = 6.5, 1.5 Hz, 1H); HRMS (ESI+) calculated for $C_{29}H_{27}O_4$ $[M+H]^+$ *m/z* 439.1909, found 439.1904.

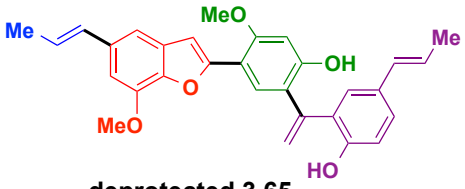

deprotected 3.65
(1.1 mg, 38% yield)

Deprotected 3.65. Deprotection condition 2 was followed to give **deprotected 3.65** (1.1 mg, 38% yield). TLC (40% EtOAc/pentane): R_f = 0.46, visualized by shortwave UV; ^{1}H-NMR (500 MHz, acetone-d_6): δ 7.81 (s, 1H), 7.18-7.14 (m, 3H), 7.10 (d, *J* = 1.0 Hz, 1H), 6.90 (d, *J* = 1.0 Hz, 1H), 6.82 (dd, *J* = 7.5, 1.5 Hz, 1H), 6.67 (s, 1H), 6.46 (dd, *J* = 16, 1.5 Hz, 1H), 6.30 (dd, *J* = 15.5, 1.0 Hz, 1H), 6.24 (dq, *J* = 15.5, 6.5 Hz, 1H), 6.04 (dq, *J* = 15.5, 6.5 Hz, 1H), 5.70 (d, *J* = 1.5 Hz, 1H), 5.67 (d, *J* = 2.0 Hz, 1H), 3.98 (s, 3H), 3.96 (s, 3H), 1.85 (dd, *J* = 7.0. 2.0 Hz, 3H), 1.78 (dd, *J* = 6.5, 1.5 Hz, 3H); HRMS (ESI+) calculated for $C_{30}H_{29}O_5[M+H]^+$ *m/z* 469.2015, found 469.2014.

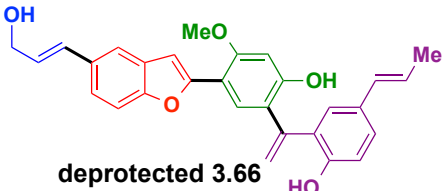

deprotected 3.66
(0.038 mg, 14% yield)

Deprotected 3.66. Deprotection condition 2 was followed to give **deprotected 3.66** (0.039 mg, 14% yield). The yield of the deprotection of **3.66** was determined by ^{1}H-NMR using an internal standard. ^{1}H-NMR (500 MHz, acetone-d_6): δ 7.78 (s, 1H), 7.60 (d, *J* = 1 Hz, 1H), 7.40 (d, *J* = 8 Hz, 1H), 7.33 (dd, *J* = 8.5, 1.5 Hz, 1H), 7.19-7.17 (m, 3H), 6.82 (d, *J* = 9 Hz, 1H), 6.70-6.68 (m, 2H), 6.37 (dt, *J* = 16, 5.5 Hz, 1H), 6.31 (dd, *J* = 15.5, 1 Hz, 1H), 6.05 (dq, *J* = 15.5, 6.5 Hz, 1H), 5.69 (d, *J* = 2 Hz, 1H), 5.66 (d, *J* = 2 Hz, 1H), 4.24 (dd, *J* = 5, 2 Hz, 2H), 3.99 (s, 3H), 1.78 (dd, *J*

= 6.5, 1.5 Hz, 3H); HRMS (ESI+) calculated for $C_{29}H_{27}O_5$ $[M+H]^+$ *m/z* 455.1858, found 455.1866.

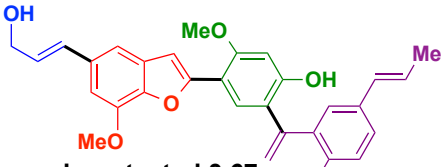

deprotected 3.67
(0.3 mg, 21% yield)

Deprotected 3.67. Deprotection condition 2 was followed to give **deprotected 3.67** (0.3 mg, 21% yield). TLC (40% EtOAc/pentane): R_f = 0.48, visualized by shortwave UV; ^{1}H-NMR (500 MHz, acetone-d_6): δ 7.81 (s, 1H), 7.18 – 7.14 (m, 4H), 6.97 (d, *J* = 1.0 Hz, 1H), 6.82 (dd, *J* = 7.0, 1.5 Hz, 1H), 6.67 – 6.63 (m, 2H), 6.37 (dt, *J* = 16, 5.5 Hz, 1H), 6.30 (dd, *J* = 15.5, 1.5 Hz, 1H), 6.04 (dq, *J* = 16.0, 7.0 Hz, 1H), 5.69 (d, *J* = 2.0 Hz, 1H), 5.66 (d, *J* = 2.0 Hz, 1H), 4.23 (d, *J* = 4.5 Hz, 2H), 3.98 (s, 3H), 3.98 (s, 3H), 1.78 (dd, *J* = 6.5, 2.0 Hz, 3H); HRMS (ESI+) calculated for $C_{30}H_{29}O_6$ $[M+H]^+$ *m/z* 485.1964, found 485.1952.

Deprotection Condition 3

To a 1-mL Reacti-vial™ containing the protected library member and a PTFE-coated magnetic stir bar was added CsF (25-30 equiv) and 18-crown-6 (2 equiv) followed by DMSO in a glovebox. The vial was sealed with a cap and stirred at 50 °C for 14 hours. The reaction was then cooled to room temperature, diluted with 8 mL EtOAc and washed with a solution of 1:1 saturated NH_4Cl/H_2O (8 mL). The aqueous layer was extracted with 4 mL EtOAc. The combined organic layers were washed with H_2O (2 × 4 mL), then with brine (8 mL). The organic phase was dried over anhydrous $MgSO_4$, filtered, and concentrated *in vacuo*. The crude product was purified by silica gel chromatography.

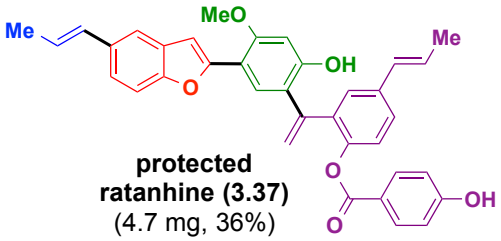

Ratanhine (3.37). TLC (40% EtOAc/pentane): R_f = 0.44, visualized by shortwave UV; ^{1}H-NMR (500 MHz, acetone-d_6): δ 7.83 (dt, J = 9.0, 2.0 H, 2H), 7.77 (s, 1H), 7.53 (s, 1H), 7.43 (dd, J = 8.5, 2.0 Hz, 1H), 7.37 (d, J = 8.5 Hz, 1H), 7.34 (d, J = 2.5 Hz, 1H), 7.28 (d, J = 8.0, 1.0 Hz, 1H), 7.17 (d, J = 8.5 Hz, 1H), 7.14 (s, 1H), 6.83 (dt, J = 8.5, 2.0 Hz, 2H), 6.55 (s, 1H), 6.50 (dd, J = 15.5, 1.5 Hz, 1H), 6.44 (dd, J = 16.0, 1.5 Hz, 1H), 6.31-6.21 (m, 2H), 5.61 (d, J = 1.5 Hz, 1H), 5.57 (d, J = 2.0 Hz, 1H), 3.96 (s, 3H), 1.87 (dd, J = 6.5, 1.5 Hz, 3H), 1.84 (dd, J = 6.5, 1.5 Hz, 3H). HRMS (ESI+) Calculated for $C_{36}H_{31}O_6$: 559.2121, found : 559.2128.

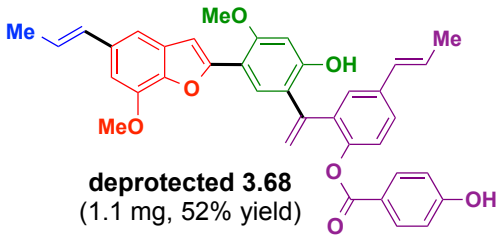

Deprotected 3.68. Deprotection condition 3 was followed to give **deprotected 3.68** (1.1 mg, 52% yield). TLC (40% EtOAc/pentane): R_f = 0.39, visualized by shortwave UV; ^{1}H-NMR (500 MHz, acetone-d_6): δ 7.85 (app d, J = 9.0 Hz, 2H), 7.81 (s, 1H), 7.43 (dd, J = 8.5, 2.5 Hz, 1H), 7.33 (d, J = 2.5 Hz, 1H), 7.18 (d, J = 8.5 Hz, 1H), 7.12 – 7.10 (m, 2H), 6.92 (d, J = 1.5 Hz, 1H), 6.84 (app d, J = 9.0 Hz, 2H), 6.55 (s, 1H), 6.49 – 6.42 (m, 2H), 6.30 – 6.21 (m, 2H), 5.62 (d, J = 2.0 Hz, 1H), 5.58 (d, J = 1.5 Hz, 1H), 3.97 (s, 3H), 3.96 (s, 3H), 1.86 (dd, J = 6.5, 1.5 Hz, 3H), 1.83 (dd, J = 7.0, 2.0 Hz, 3H); HRMS (ESI+) calculated for $C_{37}H_{33}O_7$ $[M+H]^+$ m/z 589.2226, found 589.2224.

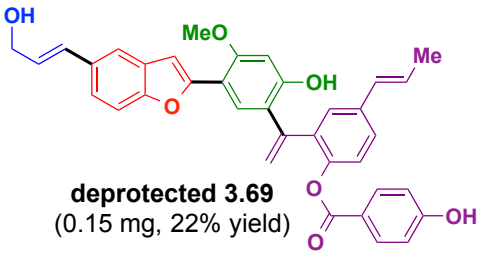

deprotected 3.69
(0.15 mg, 22% yield)

Deprotected 3.69. Deprotection condition 3 was followed to give **deprotected 3.69** (0.15 mg, 22% yield). TLC (60% EtOAc/pentane): R_f = 0.24, visualized by shortwave UV; ^{1}H-NMR (500 MHz, acetone-d_6): δ 7.82 (app d, J = 8.5 Hz, 2H), 7.77 (s, 1H), 7.60 (d, J = 1.5 Hz, 1H), 7.43 (dd, J = 8.0, 2.0 Hz, 1H), 7.40 (d, J = 8.0 Hz, 1H), 7.35-7.33 (m, 2H), 7.17 (d, J = 8.5 Hz, 1H), 7.15 (d, J = 1.0 Hz, 1H), 6.83 (app d, J = 9.0 Hz, 2H), 6.69 (app d, J = 16.0 Hz, 1H), 6.56 (s, 1H), 6.44 (d, J = 16 Hz, 1H), 6.38 (dt, J = 16.0, 5.5 Hz, 1H), 6.27 (dq, J = 16, 6.5 Hz, 1H), 5.61 (d, J = 1.5 Hz, 1H), 5.58 (d, J = 2.0 Hz, 1H), 4.25-4.24 (m, 2H), 3.97 (s, 3H), 1.84 (dd, J = 6.5, 1.5 Hz, 3H); HRMS (ESI+) calculated for $C_{36}H_{31}O_7$ $[M+H]^+$ *m/z* 575.2070, found 575.2070.

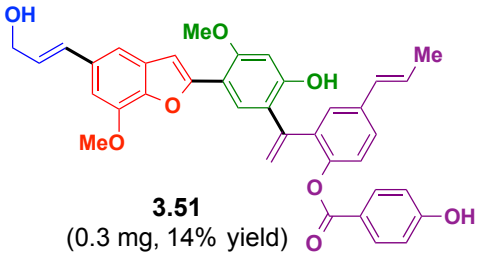

3.51
(0.3 mg, 14% yield)

3.51. Deprotection condition 3 was followed to give **3.51** (0.3 mg, 14% yield). TLC (60% EtOAc/pentane): R_f = 0.23, visualized by shortwave UV; ^{1}H-NMR (500 MHz, acetone-d_6): δ 7.85 (dt, J = 8.5, 2.0 Hz, 2H), 7.81 (s, 1H), 7.43 (dd, J = 8.0, 2.0 Hz, 1H), 7.33 (d, J = 2.0 Hz, 1H), 7.18-7.17 (m, 2H), 7.13 (s, 1H), 6.98 (s, 1H), 6.84 (dt, J = 9.0, 2.0 Hz, 2H), 6.66 (app d, J = 16.0 Hz, 1H), 6.55 (s, 1H), 6.44 (dd, J = 16.5, 1.5 Hz, 1H), 6.37 (dt, J = 16.0, 5.5 Hz, 1H), 6.27 (dq, J = 16.0, 6.5 Hz, 1H), 5.62 (d, J = 1.5 Hz, 1H), 5.58 (d, J = 1.5 Hz, 1H), 4.25-4.24 (m, 2H), 3.99 (s, 3H), 3.96 (s, 3H), 1.83 (dd, J = 6.5, 1.5 Hz, 3H); HRMS (ESI+) calculated for $C_{37}H_{33}O_8$ $[M+H]^+$ *m/z* 605.2175, found 605.2167.

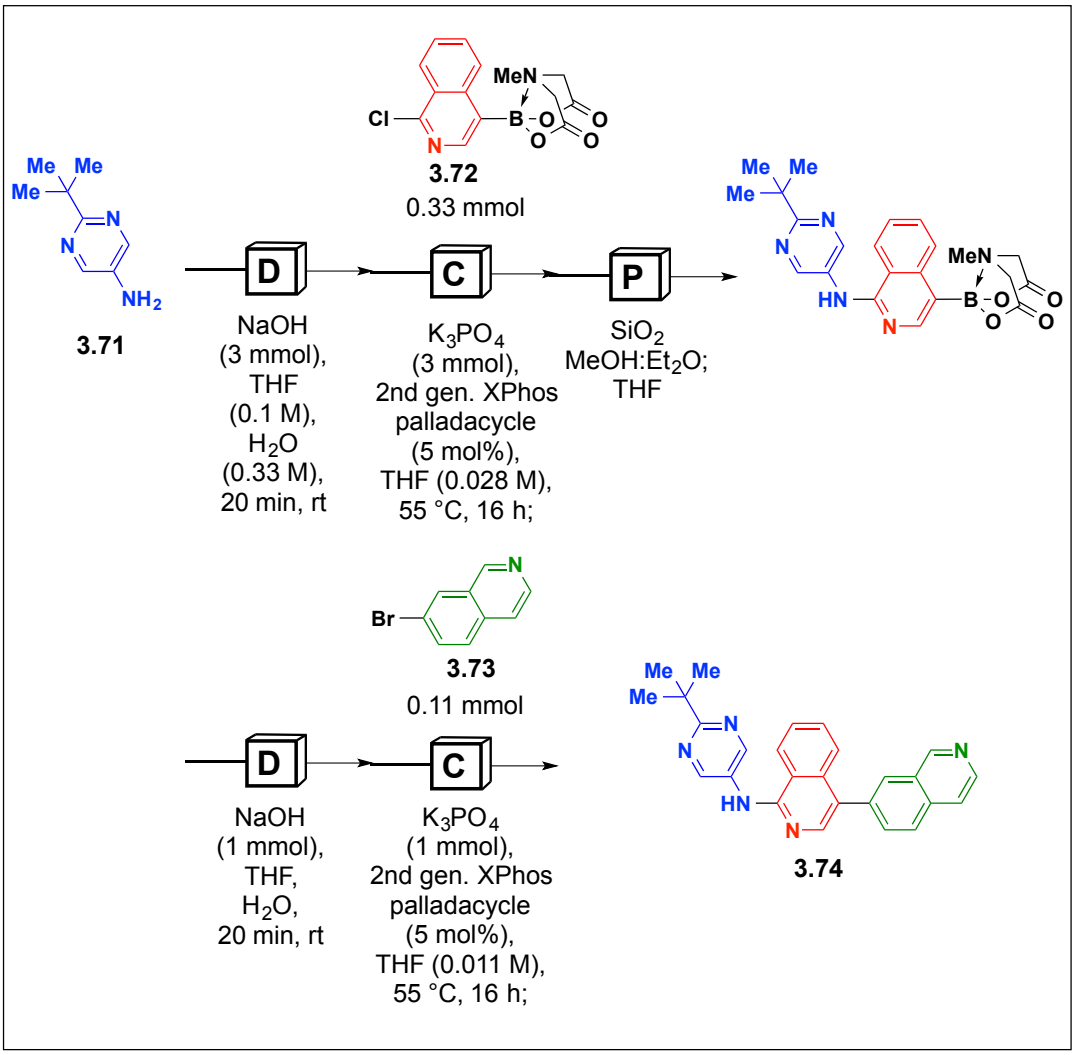

Pharmaceutical (3.74). The general procedure was followed (see EXPERIMENTAL SECTION III). Crude **3.74** was purified via silica gel chromatography (50% hexanes in EtOAc to 100% EtOAc) to afford **3.74** as a tan-orange solid (12.9 mg, 0.0318 mmol, 28% yield).

TLC (EtOAc)

R_f = 0.25, visualized by UV

^{1}H-NMR (500 MHz, $CDCl_3$)

δ 9.31 (br s, 1H), 9.19 (s, 2H), 8.58 (d, *J* = 5 Hz, 1H), 8.16 (d, *J* = 8 Hz, 1H), 8.10 (s, 1H), 8.05 (s, 1H), 7.95 (d, *J* = 8.5 Hz, 1H), 7.87-7.81 (m, 2H), 7.74 (d, *J* = 5.5 Hz, 1H), 7.68-7.60 (m, 2H), 7.56 (br s, 1H), 1.44 (s, 9H).

^{13}C-NMR (125 MHz, $CDCl_3$)

δ 171.2, 152.5, 151.6, 148.5, 143.2, 140.9, 136.9, 135.9, 135.2, 133.2, 132.7, 130.8, 128.9, 128.6, 127.2, 126.8, 126.3, 125.6, 121.9, 120.6, 118.2, 39.0, 29.9.

HRMS (ESI+)

Calculated for $C_{26}H_{24}N_5$: 406.2032

Found: 406.2031

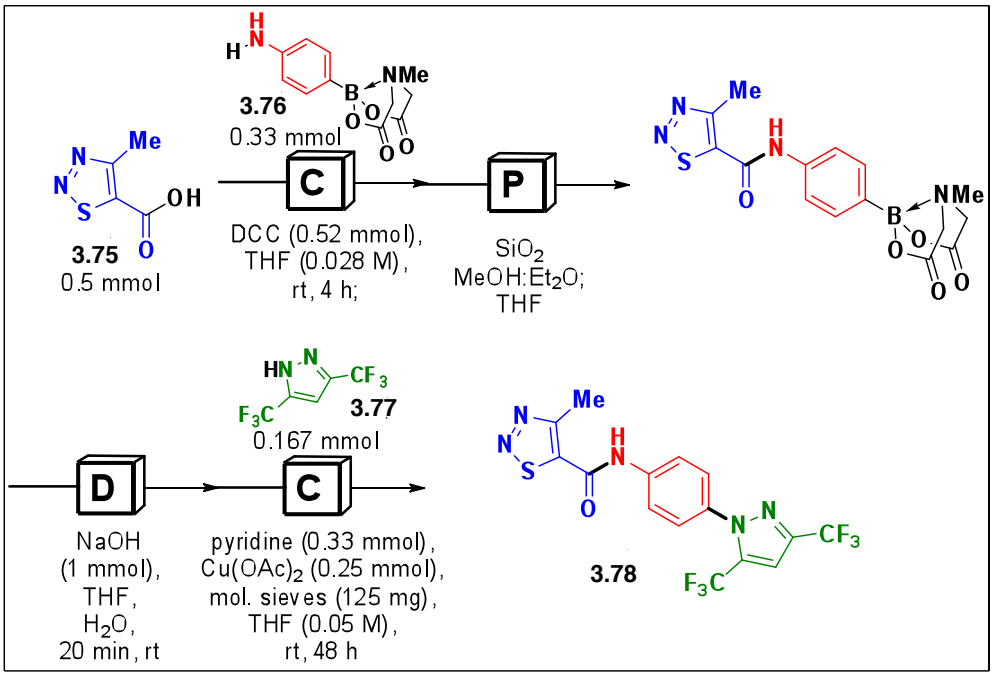

BTP2 (3.78). The general procedure was followed (see EXPERIMENTAL SECTION III) with the following modifications: In the first cross-coupling reaction, *N*,*N*'-dicyclohexylcarbodiimide (DCC) was used as a coupling agent. The DCC, carboxylic acid **3.75**, and amine MIDA boronate **3.76** all began in the First Reaction Cartridge and the coupling was run at room temperature for 4 h. In the second cross-coupling reaction, the concentration was 0.05 M with respect to **3.77**, 0.33

mmol of pyridine, 0.25 mmol of $Cu(OAc)_2$, and 125 mg of activated 4 Å powdered molecular sieves were used, the addition of the boronic acid was performed over 1 minute, and the coupling was run at room temperature for 48 hours in a 7-mL glass vial. **3.78** was afforded a colorless solid (6.7 mg, 0.0159 mmol, 9% yield).

TLC (20% EtOAc in hexanes)

R_f = 0.22, visualized by UV

HPLC

tR = 11.6 min; flow rate = 25 mL/min, gradient: 5% MeCN in H_2O over 10 min followed by 5% → 95% MeCN in H_2O over 15 min.

^{1}H-NMR (500 MHz, acetone-d_6):

δ 10.15 (br s, 1H), 8.01 (d, J = 9.0 Hz, 2H), 7.66 (d, J = 8.5 Hz, 2H), 7.52 (s, 1H), 2.92 (s, 3H).

^{13}C-NMR (125 MHz, acetone-d_6)

δ 160.8, 159.0, 144.5, 143.1 ($J_{C\text{-}F}$ = 39.2 Hz), 141.1, 135.2, 135.1 ($J_{C\text{-}F}$ = 40.1 Hz), 127.7, 121.7, ($J_{C\text{-}F}$ = 268.6 Hz), 121.5, 120.1 ($J_{C\text{-}F}$ = 269.6 Hz), 108.3, 13.6.

HRMS (ESI+)

Calculated for $C_{15}H_{10}N_5OSF_6$:	422.0510
Found:	422.0504

Building block **3.30** for crocacin C was synthesized according to Scheme 3-16:

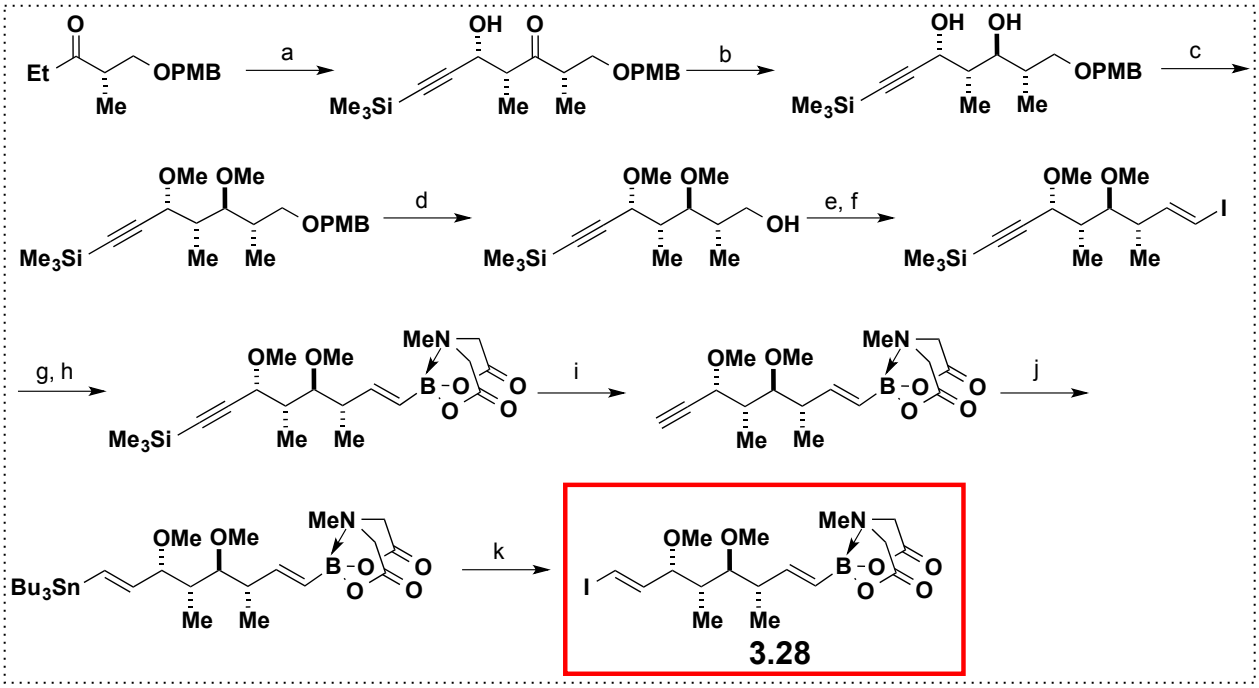

Scheme 3-16.[4] Conditions: (a) 3-(trimethylsilyl)propiolaldehyde, $Sn(OTf)_2$, NEt_3, CH_2Cl_2, -78 ^oC, 2 h; (b) $Me_4NBH(OAc)_3$, MeCN:AcOH 2:1, -25 ^oC, 16 h; (c) Me_3OBF_4, proton sponge, CH_2Cl_2, 23 ^oC, 2.5 h; (d) $(NH_4)_2Ce(NO_3)_6$, MeCN:H_2O, 10:1, 23 ^oC, 1 h; (e) Dess-Martin periodinane, CH_2Cl_2, 0 ^oC to 23 ^oC, 1.5 h; (f) CHI_3, $CrCl_2$, THF, 0 ^oC to 23 ^oC, 3 h; (g) *n*-BuLi, THF, $B(OMe)_3$, -78 ^oC; 1N HCl; (h) *N*-methyliminodiacetic acid, benzene:DMSO 10:1, 80 ^oC, 2 h; (i) $AgNO_3$, 2,6-lutidine, acetone:H_2O 1:1, 0 ^oC, 2.5 h; (j) $HSnBu_3$, Pd_2dba_3, RuPhos, CH_2Cl_2, 23 ^oC; (k) I_2, CH_2Cl_2, 23 ^oC.

Synthesis of Building Blocks for All-*Trans* Retinal

Synthesis of Building block 3.27

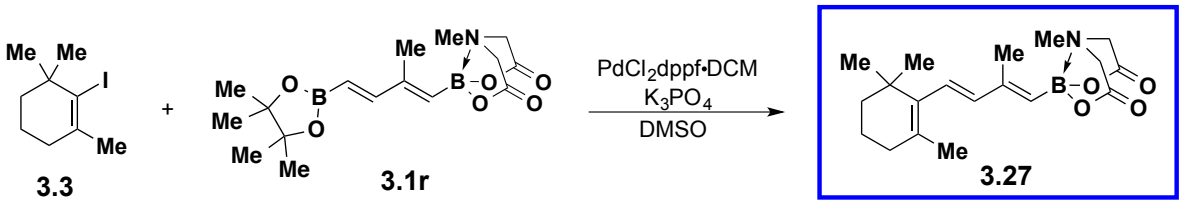

MIDA boronate building block 3.27. The following reaction was run in duplicate. In a glovebox, to a 40-mL vial charged with vinyl iodide **3.33**[5] (914 mg, 3.66 mmol, 1.2 equiv.) and bisborylated diene **3.1r**[6] (1064 mg, 3.05 mmol, 1.0 equiv.) was added $PdCl_2(dppf)•CH_2Cl_2$ (125 mg, 0.153 mmol, 5 mol%), K_3PO_4 (3884 mg, 18.3 mmol, 6.0 equiv.), and DMSO (20 mL, 0.15 M). The vial was sealed with a PTFE-lined cap and removed from the glovebox. The vial was placed in a 45 °C aluminum heat block and maintained at that temperature with stirring for 24 hours. The reaction was cooled to 23 °C and transferred to a separatory funnel, diluting with EtOAc (50 mL). The organic layer was washed with brine:H_2O (1:1, 2 x 50 mL) to remove DMSO, dried over anhydrous $MgSO_4$, filtered, and concentrated *in vacuo*. The crude material was adsorbed onto Celite™ from an acetone solution and purified by silica gel chromatography (hexanes:EtOAc 1:1 → EtOAc) to afford **3.27** as a pale yellow solid (1.0 g, 48%).

TLC (EtOAc)

R_f = 0.45, stained by $KMnO_4$

^{1}H-NMR (500 MHz, acetone-d_6)

δ 6.17 (d, *J* = 16.5 Hz, 1H), 6.11 (d, *J* = 16.5 Hz, 1H), 5.34 (s, 1H), 4.21 (d, *J* = 16.5 Hz, 2H), 4.04 (d, *J* = 17.0 Hz, 2H), 3.03 (s, 3H), 1.98 (s, 3H), 1.98-2.01 (m, 2H), 1.67 (s, 3H), 1.58-1.62 (m, 2H), 1.45-1.47 (m, 2H), 1.00 (s, 6H).

^{11}B-NMR (128 MHz, acetone-d_6)

δ 15.8.

^{13}C-NMR (125 MHz, acetone-d_6)

δ 169.0, 148.7, 141.2, 138.3, 129.3, 127.1, 62.3, 47.3, 40.2, 34.7, 33.4, 29.2, 21.8, 19.8, 15.4.

HRMS (ESI+)

Calculated for $C_{19}H_{29}O_4NB$:	346.2190
Found:	346.2192

Building block 3.29

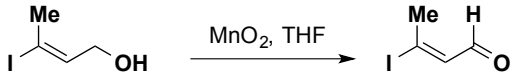

S1 **S2**

Aldehyde S2. Crotyl alcohol **S1**[7] (1.08 g, 5.54 mmol, 1.0 equiv.) and activated MnO_2 (14 g, 30 equiv.) was charged in a 100-mL round-bottom flask equipped with a PTFE-coated magnetic stir bar and topped with a rubber septum and purged with N_2. Dichloromethane (50 mL, 0.11 M) was added to the round-bottom flask and the resulting reaction mixture was stirred at 23 °C for 45 minutes. After 45 minutes, the reaction mixture was filtered through a plug of silica gel and Celite™ and concentrated *in vacuo* to afford **S2** as a yellow oil (500 mg, 46% yield).

TLC (petroleum ether:diethyl ether 4:1)

R_f = 0.51, stained by $KMnO_4$

^{1}H-NMR (500 MHz, $CDCl_3$)

δ 9.79 (d, J = 6.5 Hz, 1H), 6.84-6.86 (m, 1H), 3.00 (s, 3H).

^{13}C-NMR (125 MHz, $CDCl_3$)

δ 185.9, 141.8, 126.1, 29.9.

HRMS (ESI+)

Calculated for C_4H_6OI:	196.9463
Found:	196.9468

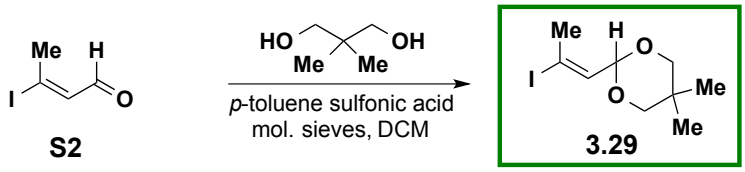

Building block 3.29. Aldehyde **S2** (150 mg, 0.77 mmol, 1.0 equiv.), neopentyl glycol (797 mg, 7.7 mmol, 10.0 equiv.), and *p*-toluene sulfonic acid (15 mg, 0.08 mmol, 0.1 equiv.) was charged in a 40-mL vial equipped with a PTFE-coated magnetic stir bar. The vial was sealed with a PTFE-lined cap and purged with N_2. Dichloromethane (15 mL, 0.05 M) was added to the vial and the resulting mixture was stirred for 1 minute until homogeneous. Activated 4 Å powdered molecular sieves (300 mg, 2:1 weight ratio to aldehyde) were added to the vial to afford a cloudy white solution. The resulting reaction mixture was stirred at 40 °C for 24 hours. After 24 hours, the reaction mixture was filtered through a filter funnel and concentrated *in vacuo*. The resulting white solid was adsorbed onto Celite™ from an acetone solution and purified by silica gel chromatography (4:1 petroleum ether:ether) to afford **3.29** as a pale yellow oil (150 mg, 69%).

TLC (petroleum ether:diethyl ether 4:1)

R_f = 0.71, stained by $KMnO_4$

^{1}H-NMR (500 MHz, $CDCl_3$)

δ 6.27 (d, *J* = 6.0 Hz, 1H), 5.02 (d, *J* = 6.0 Hz, 1H), 3.64 (d, *J* = 11.5 Hz, 2H), 3.88 (d, *J* = 11.0 Hz, 2H), 2.51 (s, 3H), 1.20 (s, 3H), 0.74 (s, 3H).

^{13}C-NMR (125 MHz, $CDCl_3$)

δ 138.0, 102.0, 97.9, 30.0, 29.1, 22.9, 21.9.

HRMS (ESI+)

Calculated for $C_9H_{16}O_2I$:	283.0195
Found:	283.0200

Synthesis of Library Building Block **3.45**

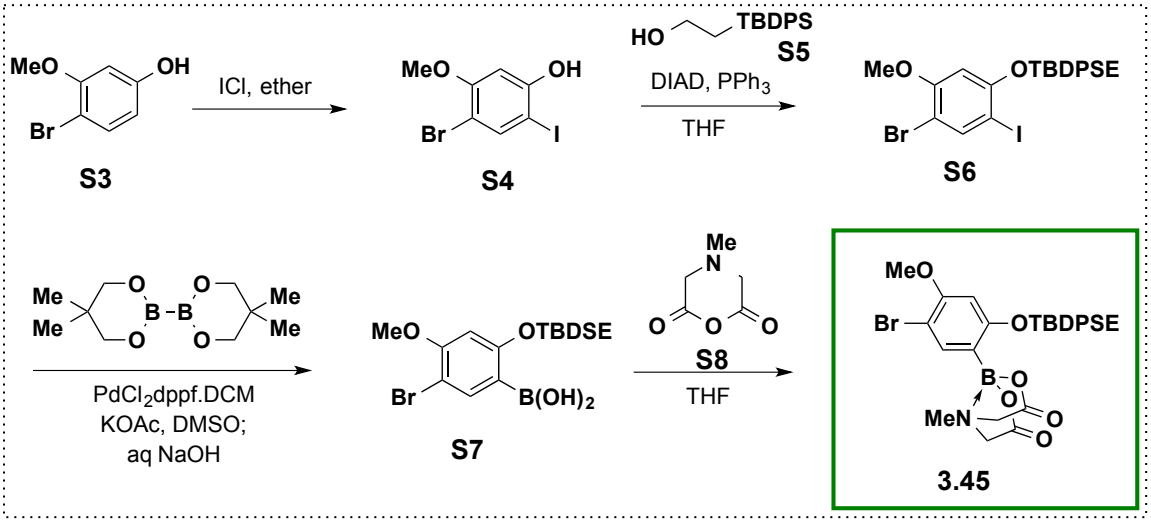

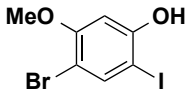

S4

4-bromo-2-iodo-5-methoxyphenol (S4). A 100-mL round-bottom flask charged with 4-bromo-3-methoxyphenol (**S3**) (5000 mg, 24.63 mmol, 1.0 equiv.) was sealed with a septum and purged with N_2 and diethyl ether (25 mL, 1.0 M) was added to afford a clear solution. The flask was cooled to 0 °C in an ice bath for 10 minutes. Iodine monochloride (1.3 mL, 1.05 equiv.) was added dropwise to the reaction flask and the reaction mixture was allowed to warm to 23 °C with stirring over 1.5 hours. After 1.5 hours, the reaction mixture was transferred to a separatory funnel containing aqueous saturated $Na_2S_2O_3$ (50 mL), rinsing with diethyl ether (50 mL) and the phases were separated. The aqueous layer was back-extracted with diethyl ether (50 mL × 3) and the combined organic layers were dried over anhydrous $MgSO_4$, filtered, and concentrated *in vacuo* to afford crude **S4** as a yellow-brown oil (7.86 g, 97% crude yield). This oil was used for the next step without further purification.

TLC (hexanes:diethyl ether 2:3)

R_f = 0.32, stained by $KMnO_4$

^{1}H-NMR (500 MHz, $CDCl_3$)

δ 7.73 (s, 1H), 6.62 (s, 1H), 5.23 (s, 1H), 3.86 (s, 3H).

HRMS (EI+)

Calculated for $C_7H_6O_2IBr$: 327.85961

Found: 327.85939

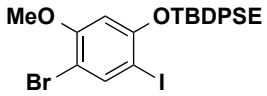

S6

Aryl iodide S6. Triphenylphosphine (PPh_3, 5054 mg, 19.3 mmol, 1.8 equiv.) was charged in a 100-mL Schlenk flask equipped with a PTFE-coated magnetic stir bar and back-filled with N_2. THF (57 mL) was added and the reaction mixture was cooled to 0 °C for 10 minutes. Diisopropyl azodicarboxylate (DIAD, 3.8 mL, 1.8 equiv.) was added dropwise to the reaction flask affording a white precipitate. This heterogeneous mixture was stirred at 0 °C for 10 minutes. Alcohol **S5** (5482 mg, 19.3 mmol, 1.8 equiv.) was added to the reaction flask and THF (4 mL) was added to dissolve all reagents and the resulting mixture was stirred at 0 °C for 10 minutes. Separately, **S4** (3511 mg, 10.7 mmol, 1.0 equiv.) was charged in a 20-mL vial, back-filled with N_2, and THF (6 mL) was added. This solution was added to the reaction flask at 0 °C and stirred at that temperature for 10 minutes. After 10 minutes, the reaction mixture was warmed to 23 °C with stirring for 16 hours. After 16 hours, the reaction mixture was transferred to a 200-mL round-bottom flask, rinsing with diethyl ether (20 mL), and concentrated *in vacuo* to afford an orange oil. The crude material was adsorbed onto Celite™ from an acetone solution and purified by SiO_2 chromatography (20% DCM:hexanes → 30% DCM:hexanes) to afford **S6** as a white solid (5.23 g, 82%).

TLC (hexanes:diethyl ether 2:3)

R_f = 0.68, stained by $KMnO_4$

^{1}H-NMR (500 MHz, $CDCl_3$)

δ 7.81 (s, 1H), 7.65 (d, *J* = 7.0 Hz, 4H), 7.43 – 1.38 (m, 6H), 6.09 (s, 1H), 4.02 – 3.98 (m, 2H), 3.68 (s, 3H), 1.86 – 1.83 (m, 2H), 1.07 (s, 9H).

^{13}C-NMR (125 MHz, $CDCl_3$)

δ 157.8, 156.8, 141.2, 135.8, 133.5, 129.5, 127.9, 103.0, 98.0, 75.6, 67.6, 56.2, 27.6, 18.0, 11.7.

HRMS (ESI+)

Calculated for $C_{25}H_{28}O_2SiBrINa$:	616.9984
Found:	616.9979

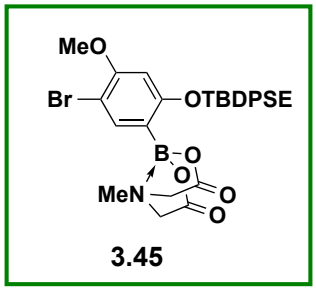

3.45

Building block 3.45. In a glove box, to a 100-mL round-bottom flask equipped with a PTFE-coated magnetic stir bar and containing **S6** (3572 mg, 6.0 mmol, 1.0 equiv.) was added potassium acetate (1767 mg, 18.0 mmol, 3.0 equiv.), bis(neopentylglycolato)diboron (1355 mg, 6.0 mmol, 1.0 equiv.) and $PdCl_2$dppf•CH_2Cl_2 (147 mg, 0.18 mmol, 3 mol%). The flask was sealed with a septum cap and removed from the glove box. Outside the glovebox, DMSO (50 mL, 0.12 M) was added to the reaction flask under N_2 atmosphere and the reaction mixture was placed in an 80 °C oil bath and stirred at that temperature for 18 hours. After 18 hours, the reaction mixture was cooled to 23 °C and 1 M aqueous NaOH (18.0 mL, 3.0 equiv) was added dropwise and the resulting heterogeneous mixture was stirred vigorously for 30 minutes at 23 °C. The reaction mixture was transferred to a separatory funnel with EtOAc (100 mL) and water (100 mL). The layers were separated and the aqueous phase was extracted with water (3 x 100 mL). Combined organic layers were dried over anhydrous $MgSO_4$, and concentrated *in vacuo* to afford a crude sample of **S7** as a brown oil. This crude boronic acid was concentrated in a 40-mL I-Chem vial and charged with *N*-methyliminodiacetic acid (MIDA) anhydride **S8**[8] (3873 mg, 30

mmol, 5.0 equiv.) and equipped with a PTFE-coated magnetic stir bar. The vial was flushed with N_2 and THF (20 mL, 0.3 M) was added and the reaction mixture was placed in a 70 °C aluminum heat block and stirred at that temperature for 24 hours. After 24 hours, the reaction mixture was cooled to 23 °C and transferred to a separatory funnel with EtOAc (100 mL) followed by deionized water (100 mL). The phases were separated and the aqueous layer was extracted with EtOAc (50 mL x 3). The combined organic layers were washed with brine (100 mL), dried over anhydrous $MgSO_4$, and concentrated *in vacuo* to afford an off-white solid. The crude material was adsorbed onto Celite™ from an acetone solution and purified by SiO_2 chromatography (hexanes:EtOAc 1:1 → EtOAc) and recrystallized from DCM/hexanes to afford **3.45** as a white solid (1.707 g, 46% over three steps).

TLC (EtOAc)

R_f = 0.66, stained by $KMnO_4$

^{1}H-NMR (500 MHz, acetone-d_6)

δ 7.70 (d, *J* = 8.0 Hz, 2H), 7.63 (s, 1H), 7.42-7.45 (m, 6H), 6.45 (s, 1H), 4.35 (d, *J* = 17.0 Hz, 2H), 4.20 (d, *J* = 17.0 Hz, 2H), 4.11-4.14 (m, 2H), 3.72 (s, 3H), 2.84 (s, 3H), 1.91 – 1.88 (m, 2H), 1.05 (s, 9H).

^{13}C-NMR (125 MHz, acetone-d_6)

δ 169.3, 163.1, 158.5, 138.9, 136.5, 134.5, 130.3, 128.7, 98.5, 70.1, 67.2, 64.5, 56.3, 48.2, 27.9, 21.7, 18.5, 11.8.

HRMS (ESI+)

Calculated for $C_{30}H_{36}O_6BNSiBr$:	624.1588
Found:	624.1602

Synthesis of Building Block **3.42**

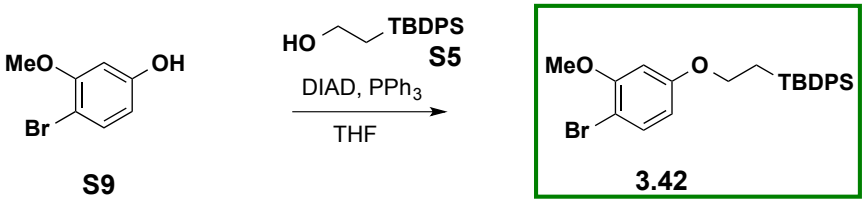

Building block 3.42. To a stirred solution of triphenylphosphine (1.10 g, 4.2 mmol, 1.2 equiv) in THF (10 mL) at 0 °C was added dropwise diisopropylazodicarboxylate (DIAD; 830 µL, 4.2 mmol, 1.2 equiv) to generate a yellow suspension. In one portion, 4-bromo-3-methoxyphenol (**S9**) (711 mg, 3.5 mmol, 1 equiv) and **S5** (1.19 g, 4.2 mmol, 1.2 equiv) were added. The mixture was stirred for 15 minutes, after which the ice bath was then removed and the reaction warmed to ambient temperature. After stirring for 1 hour, the reaction was diluted with diethyl ether and adsorbed onto Celite™ *in vacuo*. The Celite™ pad was loaded onto a silica gel column and eluted with hexanes/DCM gradient (4:1 to 3:7). Fractions containing a minor impurity were re-adsorbed on Celite™ and eluted from a silica gel column using a hexanes/DCM gradient (4:1 to 3:1). Purified fractions were combined to afford **3.42** as a colorless amorphous solid (1.19g, 72%).

^{1}H-NMR (500 MHz, acetone-d_6)

δ 7.74 – 7.72 (m, 4H), 7.50 – 7.44 (m, 6H), 7.34 (d, J = 8.5 Hz, 1H), 6.43 (d, J = 2.5 Hz, 1H), 6.27 (dd, J = 9.0, 3.0 Hz, 1H), 4.08 – 4.05 (m, 2H), 3.81 (s, 3H) 1.86 – 1.83 (m, 2H), 1.11 (s, 9H).

^{13}C-NMR (125 MHz, acetone-d_6)

δ 160.5, 157.5, 136.6, 134.7, 133.8, 130.3, 128.7, 107.7, 102.4, 101.3, 66.3, 56.4, 28.1, 18.5, 12.5.

HRMS (EI+)

Calculated for $C_{25}H_{29}O_2SiBr$:	468.11202
Found:	468.11118

Synthesis of Building Block **3.44**

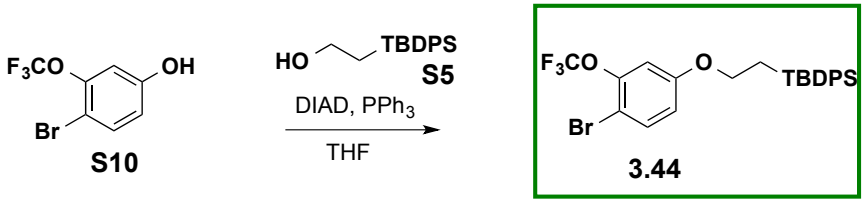

Building block 3.44. To a stirred solution of triphenylphosphine (765 mg, 3.0 mmol, 1.5 equiv) in THF (7.5 mL) at 0 °C was added dropwise diisopropylazodicarboxylate (DIAD; 570 µL, 3.0 mmol, 1.5 equiv) to generate a yellow suspension. In one portion, 4-bromo-3-(trifluoromethoxy)phenol (**S10**) (500 mg, 2.0 mmol, 1 equiv) and **S5** (830 mg, 3.0 mmol, 1.5 equiv) were added. The mixture was stirred for 15 minutes, after which the ice bath was then removed and the reaction warmed to ambient temperature. After stirring for 16 hours, the reaction was diluted with diethyl ether and adsorbed onto Celite™ *in vacuo*. The Celite™ pad was loaded onto a silica gel column and eluted with 4:1 hexanes/DCM. The colorless oil from this column was re-adsorbed onto Celite™, loaded onto silica gel, and eluted with a hexanes/DCM gradient (hexanes to 9:1 hexanes/DCM) to afford **3.44** as a colorless oil (785 mg, 77%).

^{1}H-NMR (500 MHz, acetone-d_6)

δ 7.71 – 7.69 (m, 4H), 7.55 (d, J = 8.5 Hz, 1H), 7.47 – 7.41 (m, 6H), 6.82 – 6.81 (m, 1H), 6.75 (dd, J = 8.5, 2.5 Hz, 1H), 4.11 – 4.07 (m, 2H), 1.86 – 1.83 (m, 2H), 1.08 (s, 9H).

^{13}C-NMR (125 MHz, acetone-d_6)

δ 160.5, 157.5, 136.6, 134.7, 133.8, 130.3, 128.7, 107.7, 102.4, 101.3, 66.3, 56.4, 28.1, 18.5, 12.5.

Synthesis of Building Block **3.47**

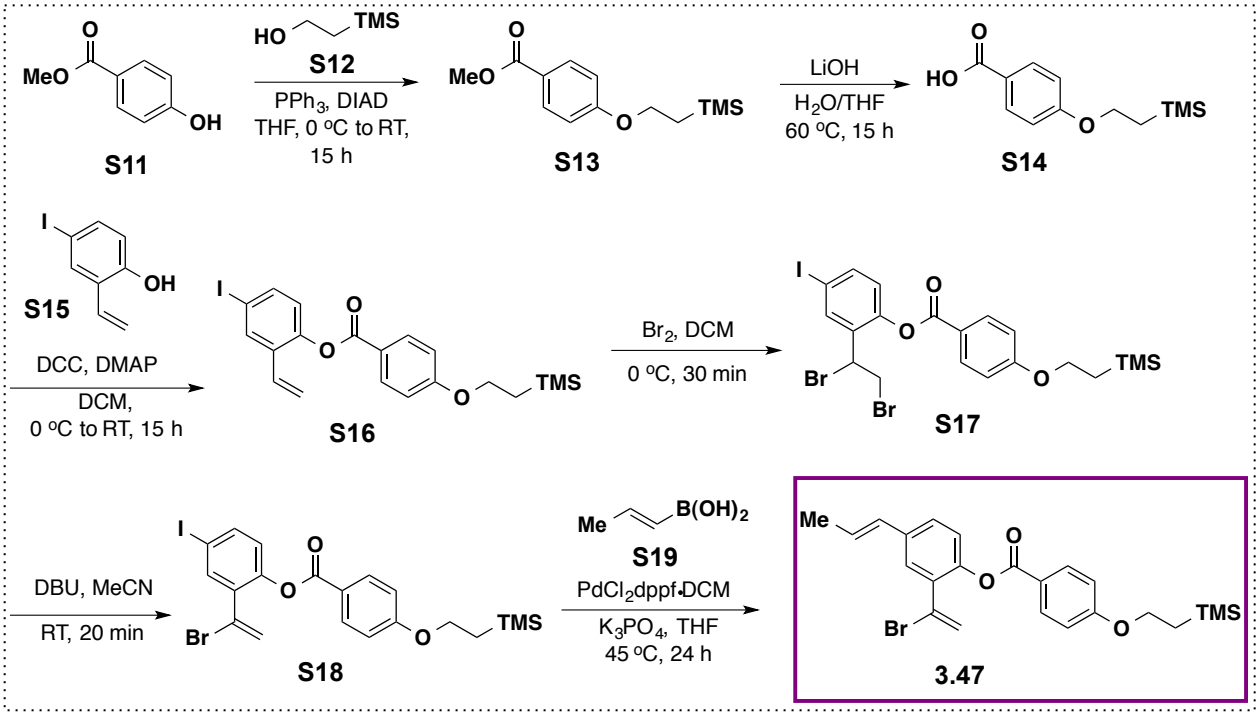

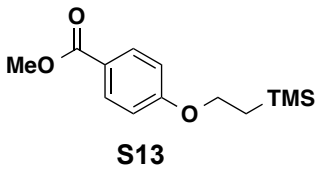

Methyl benzoate S13. Triphenylphosphine (PPh_3, 7450 mg, 28.4 mmol, 1.8 equiv.) was charged in a 250-mL round-bottom flask equipped with a PTFE-coated magnetic stir bar and back-filled with N_2. THF (70 mL) was added and the reaction mixture was cooled to 0 °C for 10 minutes. Diisopropyl azodicarboxylate (DIAD, 5.6 mL, 28.4 mmol, 1.8 equiv.) was added dropwise to the reaction flask affording a white precipitate. This heterogeneous mixture was stirred at 0 °C for 10 minutes. TMS ethanol **S12** (4.1 mL, 28.4 mmol, 1.8 equiv.) was added to the reaction flask and the resulting mixture was stirred at 0 °C for 10 minutes. Phenol **S11** (2400 mg, 15.8 mmol, 1.0 equiv.) was added to the flask in one portion followed by THF (10 mL) and the resulting reaction mixture was and stirred at 0 °C for 10 minutes. After 10 min, the reaction mixture was warmed to 23 °C with stirring for 16 hours. After 16 hours, the reaction mixture was concentrated *in vacuo* to afford a clear oil. This crude oil was dissolved in minimum amount of diethyl ether (5

mL). Hexanes (100 mL) were added and the solution was stirred at 23 °C for 5 minutes until white solid precipitated. The solid was filtered through a fritted filter funnel rinsing with hexanes. The filtrate was concentrated *in vacuo* to afford a clear oil, which was adsorbed onto Celite™ from an acetone solution and purified by SiO_2 chromatography (20% DCM:hexanes → 50% DCM:hexanes) to afford **S13** as a clear oil (434 mg, 11%).

TLC (dichloromethane:hexanes 1:1)

R_f = 0.28, shortwave UV

^{1}H-NMR (500 MHz, $CDCl_3$)

δ 7.97 (d, *J* = 9.5 Hz, 2H), 6.88 (d, *J* = 9.0 Hz, 2H), 4.13 (t, *J* = 7.5 Hz, 2H), 3.88 (s, 3H), 1.15 (t, *J* = 8.0 Hz, 2H), 0.09 (s, 9H).

^{13}C-NMR (125 MHz, $CDCl_3$)

δ 216.4, 172.1, 163.5, 132.3, 121.4, 114.2, 65.8, 17.6, -1.35.

HRMS (ESI+)

Calculated for $C_{13}H_{20}O_3SiNa$:	275.1079
Found:	275.1084

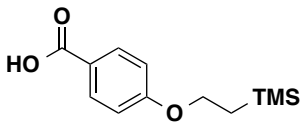

S14

Benzoic acid S14. A 40-mL vial equipped with a PTFE-coated magnetic stir bar was charged with $LiOH.H_2O$ (722 mg, 17.2 mmol, 10 equiv.) and deionized H_2O (4 mL). The vial was placed in a 60 °C aluminum heating block and stirred at that temperature for 5 minutes until a clear solution was afforded. The vial was removed from the heating block and a solution of **S13** (434 mg, 1.72 mmol, 1.0 equiv.) in THF (9 mL, 0.2 M) was added to the reaction vial. The vial was sealed with a PTFE-lined cap and placed in a 60 °C aluminum heating block and stirred at that temperature for 14 hours. The reaction mixture was cooled to 23 °C, then to 0 °C for 10 minutes. 6 N HCl was added dropwise to the crude reaction mixture with stirring until pH ≤ 1. The reaction mixture was transferred to a separatory funnel with H_2O (20 mL) and EtOAc (40 mL).

The phases were separated and the aqueous layer was extracted with EtOAc (40 mL x 2). The combined organic layers were washed with brine (50 mL), dried over anhydrous $MgSO_4$, and concentrated *in vacuo* to afford a white solid. The crude solid was adsorbed onto Celite™ from an acetone solution and purified by SiO_2 chromatography (1:4 EtOAc:hexanes → 2:1:7 EtOAc:EtOH:hexanes) to afford **S14** as a white solid (361 mg, 88%).

TLC (EtOAc:hexanes 1:4)

R_f = 0.22, shortwave UV

^{1}H-NMR (500 MHz, $CDCl_3$)

δ 8.03 (d, *J* = 9.0 Hz, 2H), 6.91 (d, *J* = 8.5 Hz, 2H), 4.15 (t, *J* = 7.5 Hz, 2H), 1.16 (t, *J* = 8.0 Hz, 2H), 0.09 (s, 9H).

^{13}C-NMR (125 MHz, $CDCl_3$)

δ 172.2, 163.5, 132.3, 121.4, 114.2, 65.8, 17.6, -1.35.

HRMS (ESI+)

Calculated for $C_{12}H_{18}O_3SiNa$:	261.0923
Found:	261.0934

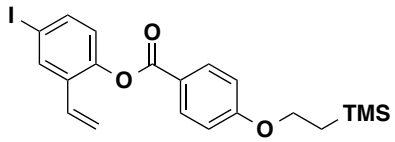

S16

Aryl iodide S16. A 100-mL flask equipped with a PTFE-coated magnetic stir bar was charged with **S14** (361 mg, 1.51 mmol, 1.0 equiv.) and back-filled with N_2. **S15** (447 mg, 1.82 mmol, 1.2 equiv.), DMAP (222 mg, 1.82 mmol, 1.2 equiv.), and dichloromethane (20 mL, 0.08 M) were added to the reaction flask. The clear, colorless solution was cooled to 0 °C and stirred at that temperature for 10 minutes. DCC (375 mg, 1.82 mmol, 1.2 equiv.) was added in one portion at 0 °C under N_2 and stirred at that temperature for 10 minutes. The ice bath was removed after 10 minutes and the reaction flask was allowed to warm to 23 °C with stirring over 15 hours. After

15 hours, the reaction mixture was concentrated *in vacuo* to afford a yellow sludge. The crude material was adsorbed onto Celite™ from an acetone solution and purified by SiO_2 chromatography (30% DCM:hexanes → 40% DCM:hexanes) to afford **S16** as a clear oil (575 mg, 81%).

TLC (30% DCM:hexanes)

R_f = 0.21, shortwave UV

^{1}H-NMR (500 MHz, $CDCl_3$)

δ 8.14 (d, *J* = 8.5 Hz, 2H), 7.92 (s, 1H), 7.61 (d, *J* = 8.5 Hz, 1H), 6.96 (d, *J* = 9.0 Hz, 2H), 6.92 (d, *J* = 8.5 Hz, 1H), 6.70 (dd, *J* = 11.0 Hz, *J* = 14.5 Hz, 1H), 5.78 (s, 1H), 5.74 (s, 1H), 5.32 (d, *J* = 11.0 Hz, 1H), 4.17 (t, *J* = 8.0 Hz, 2H), 1.18 (t, *J* = 7.5 Hz, 2H), 0.10 (s, 9H).

^{13}C-NMR (125 MHz, $CDCl_3$)

δ 164.4, 163.6, 148.2, 137.5, 135.3, 132.8, 132.4, 129.2, 124.9, 120.8, 117.5, 114.4, 90.4, 65.9,17.5, -1.33.

HRMS (ESI+)

Calculated for $C_{20}H_{24}O_3SiI$: 467.0540

Found: 467.0534

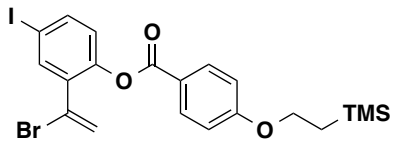

S18

Vinyl bromide S18. A 50-mL flask equipped with a PTFE-coated magnetic stir bar was charged with **S16** (575 mg, 1.23 mmol, 1.0 equiv.), sealed with a septum, and back-filled with N_2. Dichloromethane (12 mL, 0.1 M) was added to afford a clear, colorless solution. This solution was cooled to 0 °C and stirred at that temperature for 10 minutes. Bromine (0.14 mL, 2.71 mmol, 2.2 equiv.) was added dropwise to the reaction mixture at 0 °C over the course of 20 minutes

until a bright red color persisted. The crude reaction mixture was concentrated *in vacuo* and azeotroped with DCM (3 x 15 mL) to afford dibromide **S17** as a yellow foamy solid (721 mg, 93% crude yield). **S17** (721 mg, 1.15 mmol, 1.0 equiv.) was concentrated in a 50-mL round-bottom flask. The flask was equipped with a PTFE-coated magnetic stir bar, sealed with a septum, and back-filled with N_2. Acetonitrile (11.5 mL, 0.1 M) was added and the reaction mixture was stirred at 23 °C for 5 minutes. DBU (0.2 mL, 1.34 mmol, 1.2 equiv.) was added dropwise and the resulting mixture was stirred for 10 minutes. After 10 minutes, incomplete conversion was observed by TLC analysis, so another 0.3 mL of DBU was added dropwise. After 20 minutes of stirring at 23 °C, the reaction mixture was cooled to 0 °C and 1 N HCl (10 mL) was added. The reaction mixture was transferred to a separatory funnel with EtOAc (15 mL) and H_2O (15 mL) and the layers were separated. The phases were separated and the aqueous layer was extracted with EtOAc (10 mL x 2). The combined organic layers were dried over anhydrous $MgSO_4$ and concentrated *in vacuo* to afford a clear oil. The crude material was adsorbed onto Celite™ from an acetone solution and purified by SiO_2 chromatography (40% DCM:hexanes) to afford **S18** as a pale yellow oil (503 mg, 75% over two steps).

TLC (1:3 DCM:hexanes)

R_f = 0.25, shortwave UV

^{1}H-NMR (500 MHz, $CDCl_3$)

δ 8.13 (d, *J* = 9.0 Hz, 2H), 7.78 (s, 1H), 7.70 (d, *J* = 8.5 Hz, 1H), 6.98 (d, *J* = 8.5 Hz, 1H), 6.96 (d, *J* = 9.0 Hz, 2H), 5.91 (d, *J* = 1.5 Hz, 1H), 5.84 (d, *J* = 2.0 Hz, 1H), 4.17 (t, *J* = 8.0 Hz, 2H), 1.17 (t, *J* = 8.0 Hz, 2H), 0.10 (s, 9H)

^{13}C-NMR (125 MHz, $CDCl_3$)

δ 164.1, 163.6, 147.8, 138.9, 138.9, 135.4, 132.5, 125.3, 123.0, 122.7, 120.7, 114.4, 89.4, 65.9,17.5, -1.34.

HRMS (ESI+)

Calculated for $C_{20}H_{24}O_3SiI$: 467.0540

Found: 467.0534

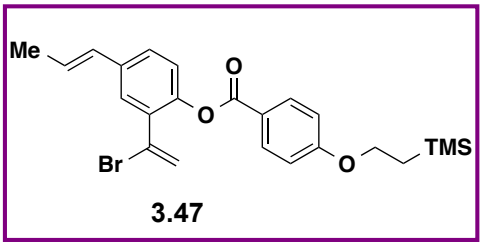

3.47

Building block 3.47. In a glove box, to a 7-mL vial equipped with a PTFE-coated magnetic stir bar and containing **S18** (20 mg, 0.037 mmol, 1.0 equiv.) and *trans*-propenyl boronic acid (**S19**) (4.73 mg, 0.055 mmol, 1.5 equiv.) was added ground potassium phosphate (23 mg, 0.11 mmol, 3.0 equiv.) and $PdCl_2dppf•CH_2Cl_2$ (1.5 mg, 0.002 mmol, 5 mol%) followed by THF (0.7 mL, 0.05 M). The vial was sealed with a cap and removed from the glove box. The vial was placed in a 45 °C aluminum heating block and stirred at that temperature for 24 hours. After 24 hours, the reaction mixture was cooled to 23 °C, filtered through a pad of Celite™, and concentrated *in vacuo*. The crude material was adsorbed onto Celite™ from an acetone solution and purified by SiO_2 chromatography (30% DCM;hexanes) to afford **3.47** as a pale yellow oil (13.5 mg, 80% yield).

TLC (1:1 DCM:hexanes)

R_f = 0.31, shortwave UV

^{1}H-NMR (500 MHz, $CDCl_3$)

δ 8.15 (d, *J* = 8.5 Hz, 2H), 7.40 (s, 1H), 7.35 (d, *J* = 8.5 Hz, 1H), 7.13 (d, *J* = 8.5 Hz, 1H), 6.96 (d, *J* = 9.0 Hz, 2H), 6.39 (d, *J* = 16.0 Hz, 1H), (dq, *J* = 15.5 Hz, *J* = 6.5 Hz, 1H), 5.89 (d, *J* = 1.5 Hz, 1H), 5.82 (d, *J* = 1.5 Hz, 1H), 4.17 (t, *J* = 8.0 Hz, 2H), 1.90 (d, *J* = 7.0 Hz, 3H), 1.17 (t, *J* = 8.0 Hz, 2H), 0.10 (s, 9H).

^{13}C-NMR (125 MHz, $CDCl_3$)

δ 164.6, 163.4, 146.4, 135.8, 133.2, 132.4, 129.6, 127.6, 127.2, 126.8, 124.6, 123.2, 122.1, 121.2, 114.3, 65.9, 18.5, 17.5, -1.33.

HRMS (ESI+)

Calculated for $C_{23}H_{28}O_3SiBr$:	459.0991
Found:	459.0987

Synthesis of Building Block **3.46**

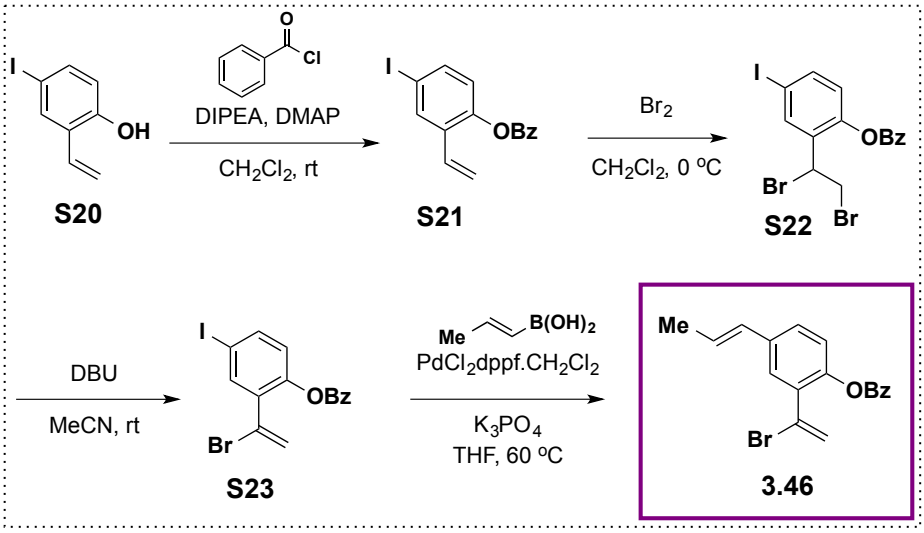

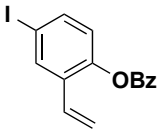

S21

4-iodo-2-vinylphenyl benzoate (S21). A dry 25-mL Schlenk flask equipped with a PTFE-coated magnetic stir bar was charged with **S20** (738 mg, 3 mmol) and DMAP (73.3 mg, 0.6 mmol) under N_2. The flask was sealed with a rubber septum and CH_2Cl_2 (15 mL) was added via syringe. To this solution was added DIPEA (2.1 mL, 12.1 mmol) in one portion. Benzoyl chloride (0.7 mL, 6.03 mmol) was then added neat dropwise over 5 minutes. The reaction was stirred for another 19 hours at room temperature, then transferred into a separatory funnel containing 1 N HCl (10 mL). After mixing and phase separation, the organic layer was washed with another portion of 1 N HCl (10 mL) and then with H_2O (20 mL). The combined aqueous layer was extracted with CH_2Cl_2 (20 mL). The organic phase was washed with brine (20 mL), dried over anhydrous $MgSO_4$, filtered and concentrated. The crude product was purified by silica gel

chromatography (30 - 35% CH_2Cl_2/hexanes) to afford **S21** as a colorless viscous oil (643 mg, 61%).

TLC (50% DCM/hexanes)

R_f = 0.44, visualized by shortwave UV.

^{1}H-NMR (500 MHz, $CDCl_3$)

δ 8.21 (d, *J* = 7 Hz, 2H), 7.94 (d, *J* = 2 Hz, 1H), 7.66 (tt, *J* = 7.5, 1.5 Hz, 1H), 7.63 (dd, *J* = 8, 1.5 Hz, 1H), 7.56 (t, *J* = 7.5 Hz, 2H), 6.94 (d, *J* = 8.5 Hz, 1H), 6.71 (dd, *J* = 17.5, 11 Hz, 1H), 5.77 (dd, *J* = 18, 1 Hz, 1H), 5.34 (d, *J* = 11 Hz, 1H).

^{13}C-NMR (125 MHz, $CDCl_3$)

δ 164.6, 148.0, 137.5, 135.4, 133.9, 132.7, 130.2, 129.0, 128.9, 128.7, 124.7, 117.7, 90.6.

HRMS (ESI+)

Calculated for $C_{15}H_{12}O_2I$:	350.9882
Found:	350.9890

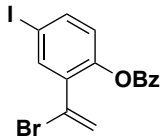

S23

2-(1-bromovinyl)-4-iodophenyl benzoate (S23). A solution of **S21** (3.37 g, 9.62 mmol) in CH_2Cl_2 (120 mL) in a 200-mL round-bottom flask was cooled to 0 °C under N_2. Bromine (0.49 mL, 9.62 mmol) was added neat dropwise over 15 minutes. After the addition was complete, the reaction was stirred for a further 5 minutes. The reaction was concentrated *in vacuo* to give an orange solid (**S22**). Residual bromine was removed by azeotroping the residue with CH_2Cl_2 (15 mL × 2). The round bottom flask containing the crude product and equipped with a PTFE-coated magnetic stir bar was sealed with a rubber septum and back-filled with N_2 twice. MeCN (120 mL) was added to dissolve most of the solid. DBU (1.4 mL, 9.5 mmol) was then added neat dropwise via syringe over 15 minutes. The reaction was stirred for 15 minutes before being

charged with another portion of DBU (0.2 mL, 1.34 mmol) added neat dropwise into the reaction. After another 15 minutes, another portion of DBU (0.2 mL, 1.34 mmol) was added. The reaction was poured slowly into 2 N HCl solution (100 mL) cooled to 0 °C with vigorous stirring. EtOAc (50 mL) was added and the mixture stirred. After phase separation, the aqueous layer was extracted with EtOAc (50 mL). The combined organic phase was washed with brine (100 mL), then dried over anhydrous $MgSO_4$, filtered and concentrated *in vacuo*. The crude product was purified by silica gel chromatography (30-35% CH_2Cl_2/hexanes) to afford **S23** as an off-white solid (2.67g, 66% over 2 steps).

TLC (40% CH_2Cl_2/hexanes)

R_f = 0.47, visualized by shortwave UV.

^{1}H-NMR (500 MHz, $CDCl_3$)

δ 8.20 (d, *J* = 7.5 Hz, 2H), 7.79 (d, *J* = 2 Hz, 1H), 7.72 (dd, *J* = 8.5, 2 Hz, 1H), 7.66 (tt, *J* = 7.5, 1H), 7.52 (tt, *J* = 8, 1.5 Hz, 2H), 6.99 (d, *J* = 8.5 Hz, 1H), 5.92 (d, *J* = 2 Hz, 1H), 5.85 (d, *J* = 1.5 Hz, 1H).

^{13}C-NMR (125 MHz, $CDCl_3$)

δ 164.4, 147.6, 138.9 (2C), 135.4, 133.9, 130.3, 128.8, 128.6, 125.1, 123.1, 122.5, 89.7.

HRMS (ESI+)

Calculated for $C_{15}H_{10}O_2BrINa$:	450.8807
Found:	450.8809

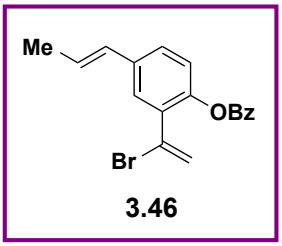

3.46

Building block 3.46. A dry 40-mL vial equipped with a PTFE-coated magnetic stir bar was charged with **S23** (858 mg, 2.0 mmol) and propenyl boronic acid (223 mg, 2.6 mmol). The vial was brought into a glovebox and charged with K_3PO_4 (1.27 g, 3 equiv.), $PdCl_2dppf.CH_2Cl_2$ (849 mg, 4 mmol) and THF (20 mL, 0.1 M). The vial was sealed with a Teflon-lined cap and stirred at 60 °C for 18 hours. The reaction was cooled to 23 °C and filtered through a pad of Celite™ and concentrated *in vacuo*. The crude product was purified by silica gel chromatography (30-40% CH_2Cl_2/hexanes) to give **3.46** as an off-white solid (268 mg, 39%).

TLC (40% CH_2Cl_2/hexanes)

R_f = 0.43, visualized by shortwave UV

^{1}H-NMR (500 MHz, $CDCl_3$)

δ 8.22 (dd, *J* = 8.0, 1.0 Hz, 2H), 7.65 (t, *J* = 7.5 Hz, 1H), 7.52 (app t, *J* = 8.0 Hz, 2H), 7.41 (d, *J* = 2.0 Hz, 1H), 7.36 (dd, *J* = 8.5, 2.0 Hz, 1H), 7.15 (d, *J* = 8.5 Hz, 1H), 6.40 (dd, *J* = 16.0, 1.5 Hz, 1H), 6.26 (dq, *J* = 15.5, 6.5 Hz, 1H), 5.90 (d, *J* = 1.5 Hz, 1H), 5.83 (d, *J* = 2.0 Hz, 1H), 1.90 (dd, *J* = 7.0, 1.5 Hz, 3H).

^{13}C-NMR (125 MHz, $CDCl_3$)

δ 164.8, 146.2, 136.0, 133.6, 133.3, 130.3, 129.5, 129.3, 128.6, 127.6, 127.2, 127.0, 124.5, 123.1, 122.2, 18.5.

HRMS (ESI+)

Calculated for $C_{18}H_{16}O_2Br$:	343.0334
Found:	343.0336

VIII. BUILDING BLOCK SYNTHESIS AND MANUAL EXPERIMENTS FOR POLYTERPENE **3.83** AND ALKALOID **3.82** TARGETS

Synthesis of Bifunctional Building Block **3.98**

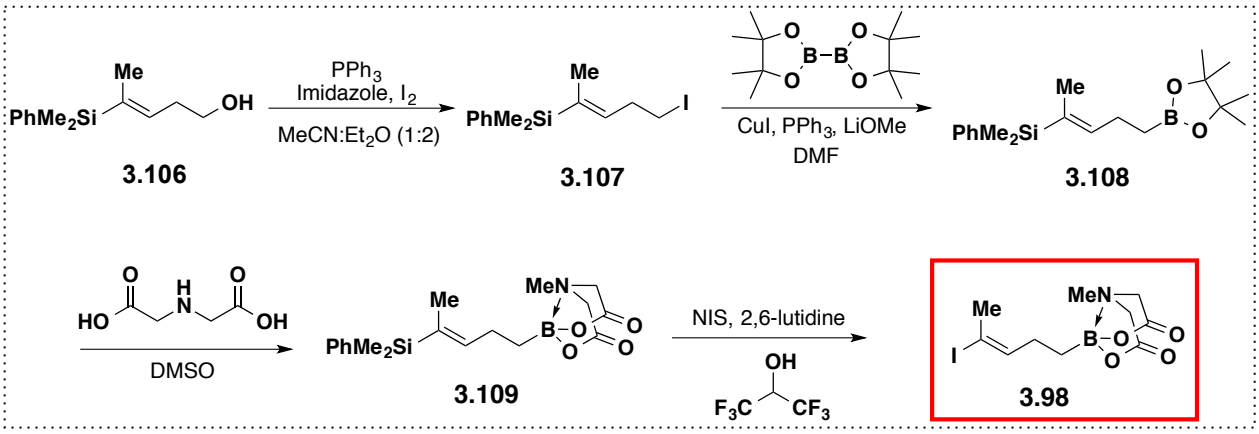

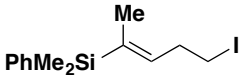

3.107

Alkyl iodide 3.107. To a flame-dried 250 mL round bottom flask was added triphenylphosphine (4.81 g, 18.35 mmol, 1.1 equiv.) and imidazole (1.71 g, 25 mmol, 1.5 equiv.). The reaction flask was fitted with a septum, purged with N_2, and charged with MeCN (16.8 mL, 1 M) and Et_2O (28.0 mL, 0.6 M). After stirring at room temperature for 5 min as a clear solution, the reaction was cooled to 0 ºC and iodine was added portionwise (4.24 g, 16.7 mmol, 1.0 equiv.). The reaction mixture was allowed to stir at 0 ºC for 15 minutes as a bright yellow, clear solution. Meanwhile, a flame-dried 20 mL vial was charged with alcohol **3.106** (3.70 g, 16.8 mmol; 1.0 equiv.). The vial was sealed with a PTFE-lined cap, purged with N_2 and charged with Et_2O (7 mL, 2.5 M). The solution of alcohol in diethyl ether was added to the reaction flask dropwise via syringe. The reaction mixture was allowed to stir at 0 ºC for 15 minutes as a pale yellow solution at which point the reaction was warmed to room temperature and stirred for 1 h. The reaction was diluted with hexanes (100 mL), filtered through a short silica plug eluting with hexanes, and concentrated *in vacuo* to afford a yellow oil. The crude material was purified by SiO_2 column chromatography on silica gel (hexanes) to afford **3.107** as a yellow oil (4.61 g, 85%). Characterization matched what is reported in the literature.[9]

TLC (hexanes)

R_f = 0.19, visualized with UV, stained with $KMnO_4$

^{1}H-NMR (500 MHz, $CDCl_3$)

δ 7.59 – 7.57 (m, 2H), 7.42 – 7.41 (m, 3H), 5.80 (tq, *J* = 6.8 Hz, *J* = 2.0 Hz, 1H), 3.22 (t, *J* = 7.4 Hz, 2H), 2.79 (q, *J* = 7.4 Hz, 2H), 1.74-1.73 (m, 3H), 0.43 (s, 6H).

^{13}C-NMR (125 MHz, $CDCl_3$)

δ 139.1, 138.1, 137.5, 134.1, 129.0, 127.8, 32.6, 15.2, 5.1, -3.4.

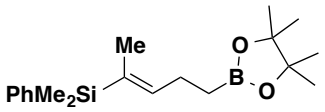

3.107

Alkyl pinacol ester 3.107. In a glovebox, to a 100 mL recovery equipped with magnetic stir bar and charged with alkyl ioidide **3.106** (4.61 g, 13.97 mmol, 1.0 equiv.) and triphenylphosphine (478 mg, 1.82 mmol, 0.13 equiv.) was added bis(pinacolato)diboron (5.32 g, 20.96 mmol, 1.5 equiv.), lithium methoxide (1.06 g, 27.99 mmol, 2.0 equiv.), and copper(I) iodide (287 mg, 1.51 mmol, 0.1 equiv.) The reaction flask was fitted with a septum, removed from the glovebox, and was charged with DMF (28 mL, 0.50 M). The resulting reaction mixture was allowed to stir at room temperature for 18 h, and the reaction mixture was diluted with EtOAc (50 mL), filtered through a short silica plug eluting with EtOAc, and concentrated *in vacuo* to afford a slurry in residual DMF. Crude mixture was transferred to a separatory funnel and washed with H_2O (slow, dropwise, 200 mL). The aqueous layer was back-extracted with EtOAc (2 x 50 mL). Combined organic layers were dried over Na_2SO_4, filtered, and concentrated *in vacuo* to afford a pale yellow oil. The crude material was adsorbed onto Celite from an acetone solution and purified by SiO_2 chromatography (hexanes:EtOAc 4:1 to afford **3.107** as a yellow oil (4.13 g, 89%).

TLC (4:1 hexanes:EtOAc)

R_f = 0.69, visualized by UV, stained with $KMnO_4$

^{1}H-NMR (500 MHz, $CDCl_3$)

δ 7.51-7.49 (m, 2H), 7.36-7.32 (m, 3H), 5.83 (tq, *J* = 6.5 Hz, 2.0 Hz, 1H), 2.25 (q, *J* = 7.5 Hz, 2H), 1.67 (s, 3H), 1.23 (s, 12H), 0.89 (t, *J* = 7.5 Hz, 2H), 0.32 (s, 6H)

^{13}C-NMR (125 MHz, $CDCl_3$)

δ 143.7, 139.0, 134.1, 133.0, 128.8, 127.7, 83.1, 29.8, 24.9, 23.0, 14.8, -3.3.

HRMS (EI+)

Calculated for $C_{19}H_{31}O_2BSi$: 330.2186

Found: 330.2186

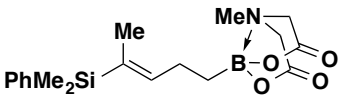

3.108

MIDA boronate 3.108. To a 1 L recovery flask was added pinacol ester **3.107** (7.26 g, 22.0 mmol, 1.0 equiv.) and *N*-methyliminodiacetic acid (30.0 g, 204 mmol, 9.3 equiv.). The reaction flask was fitted with a septum, purged with N_2, and charged with DMSO (220 mL, 0.1 M). The vial was placed in a 77 ^{o}C oil bath and maintained at that temperature with stirring for 15 h. The reaction mixture was diluted with EtOAc (100 mL) and transferred to a separatory funnel rinsing with EtOAc (50 mL). The layers were separated and the aqueous layer was extracted with EtOAc (3 x 75 mL). The combined organic layers were washed with H_2O (slowly dropwise, 600 mL), dried over Na_2SO_4, filtered, and concentrated *in vacuo* to afford a yellow oil/off-white solid precipitate. The crude material was adsorbed onto Celite from an acetone solution and purified by SiO_2 chromatography (hexanes:EtOAc 1:1 → EtOAc) to recover **3.107** as a yellow oil (2.62 g, 36% recovery) and afford **3.108** as a white solid (4.29 g, 54%).

TLC (EtOAc)

R_f = 0.26, visualized by UV, stained with $KMnO_4$

^{1}H-NMR (500 MHz, acetone-d_6)

δ 7.53 – 7.51 (m, 2H), 7.37 – 7.31 (m, 3H), 5.94 (tq, *J* = 7.0, 1.5 Hz, 1H), 4.19 (d, *J* = 16.5 Hz, 2H), 4.03 (d, *J* = 16.5 Hz, 2H), 3.10 (s, 3H), 2.23 – 2.17 (m, 2H), 1.17 (s, 3H), 0.75 – 0.69 (m, 2H), 0.31 (s, 6H).

^{13}C-NMR (125 MHz, acetone-d_6)

δ 168.8, 145.6, 139.4, 134.7, 132.6, 129.6, 128.5, 62.6, 46.2, 25.2, 23.9, 14.8, -3.2.

HRMS (ESI+)

Calculated for $C_{18}H_{27}BNO_4Si$:	360.1802
Found:	360.1802

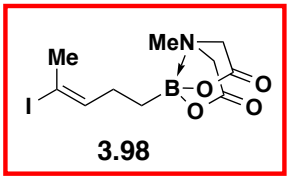

3.98

Building block 3.98. To a 100 mL recovery flask equipped with magnetic stir bar was added MIDA boronate **3.108** (1.141 g; 3.18 mmol, 1.0 equiv.), 2,6-lutidine (0.26 mL, 2.22 mmol, 0.7 equiv.) and hexafluoroisopropanol (12.8 mL, 0.25 M). After stirring at room temperature for 5 min as an off-white/pale yellow solution, the reaction was cooled to 0 ºC and NIS (637 mg, 4.76 mmol, 1.5 equiv.) was added in one portion. The reaction mixture was allowed to stir at 0 ºC for 15 minutes as a deep red, clear solution at which point the reaction was warmed to room temperature and stirred for 15 minutes. The reaction was quenched with saturated aqueous $Na_2S_2O_3$ (13 mL) and transferred to a separatory funnel as a pale yellow solution rinsing with EtOAc (20 mL) and the layers were separated. The aqueous layer was extracted with EtOAc (2 x 15 mL). The combined organic layers were dried over Na_2SO_4, filtered, and concentrated *in vacuo* to afford an off-white solid. The crude material was adsorbed onto Celite from an acetone solution and purified by SiO_2 chromatography (hexanes:acetone 4:1 → hexanes:acetone 3:1 → hexanes:acetone 2:1 → hexanes:acetone 1:1) to afford **3.98** as a off-white solid. Solid was dissolved in a minimal amount of DCM and layered with hexanes causing a white precipitated to form. Precipitate isolated by vacuum filtration (1.01 g, 91%).

TLC (EtOAc)

R_f = 0.30, visualized by UV, stained with $KMnO_4$

^{1}H-NMR (500 MHz, acetone-d_6)

δ 6.24 (tq, *J* = 7.5, 1.5 Hz, 1H), 4.19 (d, *J* = 17.0 Hz, 2H), 4.02 (d, *J* = 17.0 Hz, 2H), 3.10 (s, 3H), 2.36 (s, 3H), 2.13 – 2.07 (m, 2H), 0.74 – 0.71 (m, 2H).

^{13}C-NMR (125 MHz, acetone-d_6)

δ 168.7, 145.0, 92.7, 62.6, 46.3, 27.6, 26.1.

HRMS (ESI+)

Calculated for $C_{10}H_{16}BNO_4I$: 352.0217

Found: 352.0218

Manual Synthesis of Polyterpene Linear Precursor **3.100**

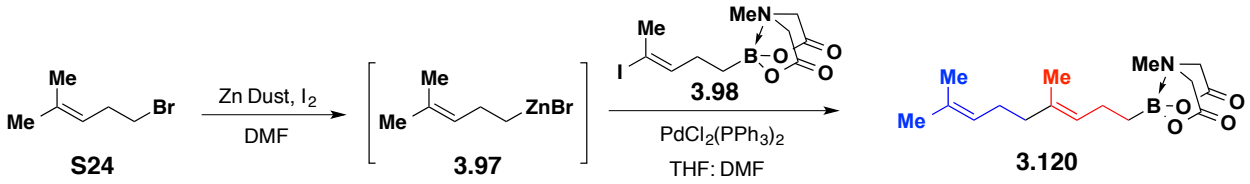

MIDA boronate 3.120.

To a flame-dried 20 mL vial equipped was added zinc dust (981 mg, 15 mmol, 1.5 equiv.) and iodine (127 mg, 0.5 mmol, 0.5 equiv.). The vial was sealed with a PTFE-lined cap, purged twice with argon, and charged with DMF (4.0 mL, 2.5 M). After stirring at room temperature for 1 min, homoallylic bromide **3.97** (1.63 g, 1.43 mmol, 1.0 equiv.) was added to the reaction vial via syringe under a positive pressure of argon. The gas inlet needle was removed, and the vial was placed in an 80 °C aluminum heat block and maintained at that temperature with stirring for 4 h.

In a glovebox, to a flame-dried 40 mL vial charged with vinyl iodide **3.98** (351 mg, 1.0 mmol, 1.0 equiv.) was added $PdCl_2(PPh_3)_2$ (21 mg, 0.31 mmol, 0.03 equiv.), THF (18 mL, 0.05 M),

followed by alkyl zinc **3.97** solution in DMF (1.0 mL, 2.5 M, 2.5 equiv.). The vial was sealed with a PTFE-lined cap and removed from the glovebox. The vial was placed in a 45 ^{o}C aluminum heat block and maintained at that temperature with stirring for 14 h. After 14 h, the reaction mixture was cooled to RT and quenched with saturated aqueous NH_4Cl (20 mL) affording a white precipitate. This crude mixture was transferred into a separatory funnel rinsing with EtOAc (30 mL) and brine (30 mL) was added. The layers were separated and the aqueous layer was extracted with EtOAc (2 x 30 mL). The combined organic layers were washed with brine:H_2O (1:1, 50 mL), dried over $MgSO_4$, filtered, and concentrated *in vacuo* to afford an orange brown oil. The crude material was adsorbed onto Celite from an acetone solution and purified by SiO_2 chromatography (hexanes:EtOAc 1:1 → EtOAc) to afford **3.98** as a pale yellow solid (190 mg, 60%).

TLC (EtOAc)

R_f = 0.22, visualized by UV, stained with $KMnO_4$

^{1}H-NMR (500 MHz, $CDCl_3$)

δ 5.16 (t, *J* = 6.5 Hz, 1H), 5.08 (t, *J* = 7.0 Hz, 1H), 4.04 (d, *J* = 16.5 Hz, 2H), 3.71 (d, *J* = 16.5 Hz, 2H), 2.91 (s, 3H), 2.09 – 1.98 (m, 4H), 1.96 -1.93 (m, 2H), 1.66 (s, 3H), 1.59 (s, 3H), 1.58 (s, 3H), 0.66 – 0.63 (m, 2H).

^{13}C-NMR (125 MHz, $CDCl_3$)

δ 168.3, 134.3, 131.4, 126.9, 124.4, 62.0, 46.0, 39.8, 26.9, 25.8, 22.4, 17.8, 16.1.

HRMS (ESI+)

Calculated for $C_{16}H_{27}BNO_4Na$:	308.2033
Found:	308.2035

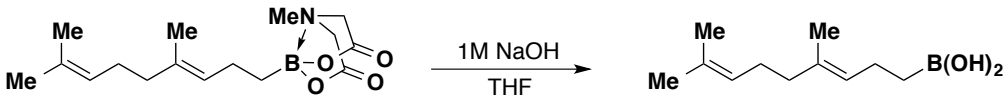

3.120 3.121

Boronic acid 3.121. To a 40 mL vial was added MIDA boronate **3.120** (163 mg, 0.53 mmol, 1.0 equiv.). The vial was sealed with a PTFE-lined cap, purged with N_2, charged with THF (5.3 mL, 0.1 M), and allowed to stir at room temperature. After 2 minutes, 1M NaOH (1.6 mL, 1.59 mmol, 3.0 equiv.) was added to the reaction vial. The reaction mixture was stirred vigorously at ambient temperature for 20 minutes. The reaction was quenched with pH 6 phosphate buffer (7 mL) and transferred to a separatory funnel rinsing with Et_2O (10 mL) and the layers were separated. The aqueous layer was extracted with Et_2O (15 mL). The combined organic layers were dried over Na_2SO_4, filtered, and concentrated *in vacuo* into a 20 mL vial to afford a pale yellow oil (112 mg, >100% crude yield). This material was used directly in the following reaction.

TLC (EtOAc)

Rf = 0.59, stained with $KMnO_4$

^{1}H-NMR (acetone-d_6)

δ 6.50 (s, 2H), 5.17 (t, *J* = 6.5 Hz, 1H), 5.10 (t, *J* = 6.5 Hz, 1H), 2.11 - 2.04 (m, 4H), 1.96 - 1.93 (m, 2H), 1.64 (s, 3H), 1.58 (s, 3H), 1.58 (s, 3H), 0.75 (t, *J* = 7.5 Hz, 2H).

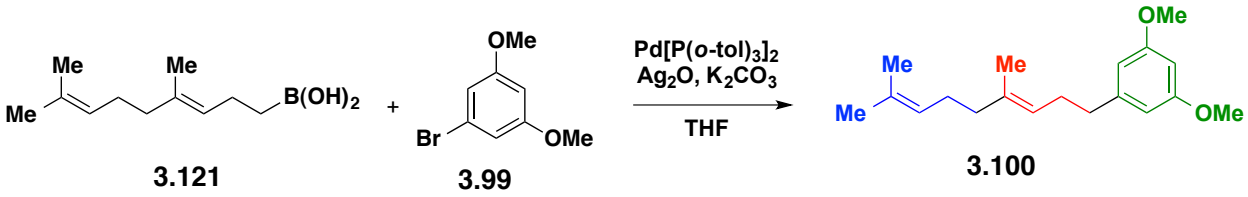

3.121 3.99 3.100

Linear precursor 3.100. In a glovebox, to a flame dried 20 mL vial charged with aryl bromide **3.99** (36 mg, 0.17 mmol, 1.0 equiv.) and Ag_2O (113 mg, 0.49 mmol, 3.0 equiv.) was added K_2CO_3 (134 mg, 0.97 mmol, 6.0 equiv.) and Pd[P(*o*-tol)$_3$]$_2$ (29 mg, 0.04 mmol, 0.25 equiv.). To the 20 mL vial containing boronic acid **3.121** was added THF (1.0 mL) and the boronic acid solution was transferred to the reaction vial rinsing with THF (2.4 mL). The vial was sealed with a PTFE-lined cap and removed from the glove box. The vial was placed in a 60 °C aluminum heat block and maintained at that temperature with stirring for 16 h. After 16 h, the reaction

mixture was cooled to 23 °C and diluted with Et_2O (10 mL), filtered through a short silica gel plug eluting with Et_2O, and concentrated *in vacuo* to afford a yellow oil. Crude material was purified by preparatory HPLC (50% MeCN → 95% MeCN) to afford **3.100** as a pale yellow oil (28.5 mg, 60%).

TLC (hexanes)

R_f = 0.31, visualized by UV, stained with $KMnO_4$

HPLC

tR = 19.89 min; flow rate = 25 mL/min, gradient of 50% → 95% MeCN in H_2O over 15 min followed by 95% MeCN in H_2O for 10 min. Detected at λ= 254 nm.

^{1}H-NMR (500 MHz, $CDCl_3$)

δ 6.38 (d, *J* = 2.3 Hz, 2H), 6.32 (t, *J* = 2.3 Hz, 1H), 5.20 (tq, *J* = 7.0, 1.3 Hz, 1H), 5.15 – 5.08 (m, 1H), 3.80 (s, 6H), 2.60 (dd, *J* = 9.0, 6.7 Hz, 2H), 2.35 – 2.28 (m, 2H), 2.11 – 2.04 (m, 2H), 2.00 (dd, *J* = 9.1, 5.9 Hz, 2H), 1.70 (d, *J* = 1.5 Hz, 3H), 1.63 – 1.59 (m, 6H).

^{13}C-NMR (125 MHz, $CDCl_3$)

δ 160.8, 145.0, 135.9, 131.5, 124.4, 123.7, 106.6, 97.8, 55.4, 39.9, 36.6, 29.9, 26.9, 25.8, 17.8, 16.2.

HRMS (ESI+)

Calculated for $C_{19}H_{29}O_2$:	289.2168
Found:	289.2175

Synthesis of Alkaloid Building Block **3.101**

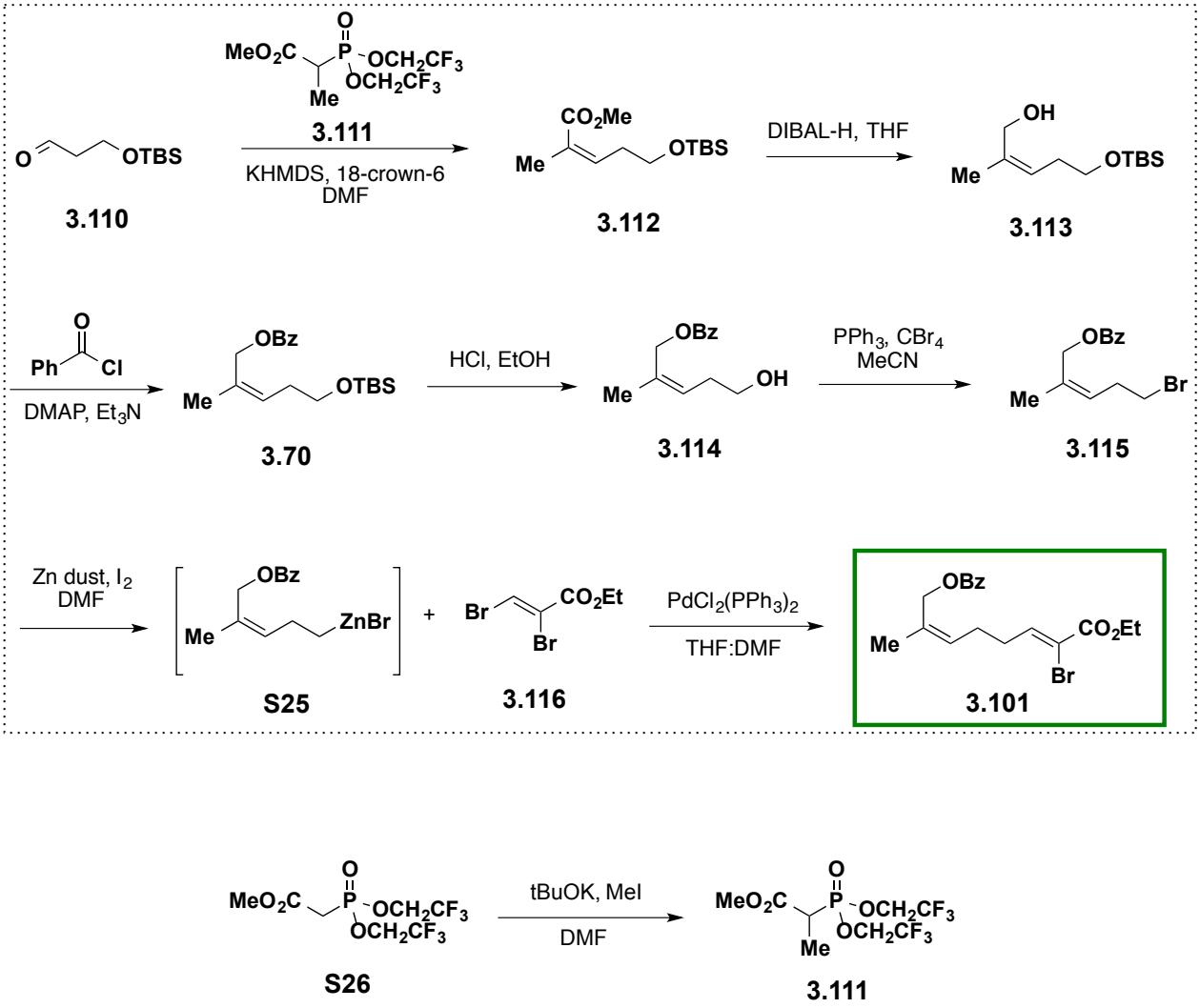

Phosphonoacetate 3.111. To a 500 mL flask was charged with potassium *tert*-butoxide (6.3420 g, 56.5 mmol, 1.2 equiv.), fitted with a septum, and back-filled with nitrogen was added DMF (x mL). The flask was cooled to 0 °C and phosphonoacetate **S26** (15.0 g, 47.2 mmol, 1.0 equiv.) was added dropwise over 10 min. After 40 min of stirring, methyl iodide (4.4 mL, 70.7 mmol, 1.5 equiv.) was added dropwise over 10 minutes at 0 °C. The reaction was slowly warmed to RT with stirring, then heated to 45 °C and the reaction was allowed to stir at that temperature for 24 h. After 24 h, the reaction mixture was cooled to RT, quenched with saturated NH_4Cl (100 mL), and transferred to a separatory funnel with water (50 mL) and diethyl ether (150 mL). The layers were shaken and separated. The aqueous layer was extracted with diethyl ether (3 x 150 mL). Combined organic layers were washed with brine (200 mL), dried over $MgSO_4$, filtered, and concentrated to yield a yellow oil that contained a mixture of starting material, product, and

bismethylated byproduct in a ratio of 0.08 : 1 : 0.28. The crude material was dissolved in 4:1 hexanes:ethyl acetate and purified by SiO_2 chromatography to afford **3.111** as a colorless oil (4.16 g, 27% yield). ^{1}H-NMR identical to literature.[10]

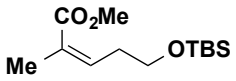

3.112

α-β-unsaturated ester 3.112. A 300 mL round bottom flask was charged with 18-crown-6 (6.13 g, 23 mmol, 5.0 equiv.) and the flask was sealed with rubber septa and back-filled with N_2. THF (80 mL) was added to afford a clear, colorless solution. To a 20 mL vial containing phosphonoacetate # (1.54 g, 4.64 mmol, 1.0 equiv.) was added THF (10 mL). This solution was transferred to the reaction flask via syringe. Additional THF (10 mL) was used for quantitative transfer. The reaction mixture was cooled to -78 ^{o}C in an IPA/dry ice bath for 5 min, KHMDS (0.5M in toluene, 9.3 mL, 10 equiv.) was added dropwise to the reaction flask over 5 min, and the resulting off-white cloudy solution was stirred at -78 ^{o}C for 30 min. To a 20 mL vial charged with aldehyde **3.110** (874 mg, 4.64 mmol, 1.0 equiv.) was added THF (5 mL). After 30 min of stirring, this solution was added to the reaction mixture at -78 ^{o}C, and additional THF (10 mL) was used for quantitative transfer. The resulting reaction mixture was stirred at -78 ^{o}C for 50 min. After 50 min, the IPA/dry ice bath was removed, and the reaction mixture was quenched with saturated aqueous NH_4Cl (100 mL) in which formation of a white precipitate was observed. The resulting biphasic mixture was transferred to a 500 mL separatory funnel, rinsing with diethyl ether (100 mL) for quantitative transfer. The layers were separated and the aqueous layer was extracted with diethyl ether (50 mL). The combined organic layers were washed with brine (100 mL), dried over $MgSO_4$, and concentrated *in vacuo* to afford a crude mixture. The crude material was dissolved in 10% diethyl ether in hexanes and purified by SiO_2 chromatography (10% diethyl ether in hexanes) to afford **3.112** as a clear, colorless oil (1.03 g, 86%).

TLC (10% diethyl ether in hexanes)

R_f = 0.57, stained by $KMnO_4$

^{1}H-NMR (500 MHz, $CDCl_3$)

δ 6.02 (t, *J* = 7.0 Hz, 1H), 3.72 (s, 3H), 3.67 (t, *J* = 6.5 Hz, 2H), 2.69 (q, *J* = 7.0 Hz, 2H), 1.90 (d, *J* = 1.5 Hz, 3H), 0.88 (s, 9H), 0.04 (s, 6H).

^{13}C-NMR (125 MHz, $CDCl_3$)

δ 168.5, 140.0, 128.3, 62.6, 51.4, 33.3, 26.1, 20.8, 18.5, -5.16.

HRMS (ESI+)

Calculated for $C_{13}H_{27}O_3Si$: 259.1729

Found: 259.1731

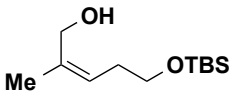

3.113

Allylic alcohol 3.113. A 100 mL Schlenk flask was sealed with a rubber septum and back-filled with N_2 and THF (20 mL) was added. To a 50 mL recovery flask charged with ester **3.112** (1.03 g, 4 mmol, 1.0 equiv.) was dissolved in THF (10 mL) and this solution was added to the reaction flask followed by quantitative transfer using THF (10 mL). The flask was placed in a -40 ^{o}C ethylene glycol/dry ice bath and stirred until the temperature stabilized to -45 ^{o}C. DIBAL-H (1.0 M in hexanes, 12.0 mL, 3.0 equiv.) was added dropwise to the reaction flask over 10 min, and the resulting reaction mixture was allowed to slowly warm to -15 ^{o}C with stirring over 4 h. After 4 h, saturated Rochelle's salt (15 mL) was added and the reaction mixture was vigorously stirred for 5 min followed by addition of glycerol (2.4 mL) to afford a biphasic mixture. The crude mixture was transferred to a 250 mL separatory funnel. The layers were separated and to the aqueous layer was added ethyl acetate (20 mL) and glycerol (1.0 mL) and layers were separated. The combined organic layers were washed with brine (30 mL), dried over sodium sulfate, filtered, and concentrated *in vacuo* to afford **3.113** as a cloudy oil (758.2 mg, 83%). This crude mixture was used in the next step without further purification.

TLC (33% diethyl ether in hexanes)

R_f = 0.34, stained by $KMnO_4$

^{1}H-NMR (500 MHz, $CDCl_3$)

δ 5.28 (td, *J* = 8.0 Hz, *J* = 1.5 Hz, 1H), 4.04 (s, 2H), 3.61 (t, *J* = 6.0 Hz, 2H), 2.45 (br s, 1H), 2.29 (q, *J* = 7.0 Hz, 2H), 1.80 (d, *J* = 1.0 Hz, 3H), 0.88 (s, 9H), 0.05 (s, 6H).

^{13}C-NMR (125 MHz, $CDCl_3$)

δ 138.1, 124.8, 62.7, 61.6, 31.2, 26.1, 22.4, 18.6, -5.29.

HRMS (ESI+)

Calculated for $C_{12}H_{27}O_2Si$: 231.1780

Found: 231.1781

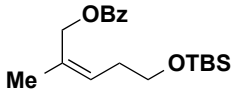

3.70

Benzoate 3.70. A 50 mL Schlenk flask was charged with DMAP (45 mg, 0.37 mmol, 11 mol%), sealed with a rubber septum, and back-filled with N_2. DCM (6 mL) was added to afford a clear, colorless solution. Benzoyl chloride (0.6 mL, 4.95 mmol, 1.5 equiv.) was added dropwise over 1 min and stirred for 5 min at RT. The reaction was then cooled to 0 ^{o}C in an ice bath. To a 50 mL pear flask charged with alcohol **3.113** (758 mg, 3.3 mmol, 1.0 equiv.) and sealed with a rubber septum was added DCM (3 mL) and the flask was cooled to 0 ^{o}C under positive pressure of N_2. Triethyl amine (0.7 mL, 4.95 mmol, 1.5 equiv.) was added dropwise to the alcohol solution turning the reaction pale yellow. After stirring for 5 min at 0 ^{o}C, this solution was cannulated to the reaction flask under positive N_2 pressure over 5 min. The resulting reaction mixture was allowed to stir at 0 ^{o}C for 30 min, turning bright yellow over time. After 30 min, H_2O (20 mL) was added to the reaction mixture at 0 ^{o}C. The crude mixture was transferred to a 125 mL separatory funnel using DCM (20 mL). The layers were separated and to the aqueous layer was extracted with DCM (20 mL). The combined organic layers were washed with brine (30 mL), dried over sodium sulfate, filtered, and concentrated *in vacuo*. The crude oil was dissolved in 5% diethyl ether in hexanes and purified by SiO_2 chromatography (5% diethyl ether in hexanes) to afford **3.70** as a clear, colorless oil (999 mg, 90%).

TLC (10% diethyl ether in hexanes)

R_f = 0.53, stained by $KMnO_4$

^{1}H-NMR (500 MHz, acetone-d_6)

δ 8.05-8.02 (m, 2H), 7.64 (tt, *J* = 7.5 Hz, *J* = 1.0 Hz, 1H), 7.52 (t, *J* = 7.5 Hz, 2H), 5.53 (td, *J* = 7.5 Hz, *J* = 1.0 Hz, 1H), 4.88 (s, 2H), 3.68 (t, *J* = 6.5 Hz, 2H), 2.40 (q, *J* = 6.5 Hz, 2H), 1.86 (d, *J* = 1.5 Hz, 3H), 0.89 (s, 9H), 0.06 (s, 6H).

^{13}C-NMR (125 MHz, acetone-d_6)

δ 166.6, 133.9, 132.7, 131.3, 130.2, 129.4, 128.0, 64.1, 63.4, 32.2, 26.3, 21.8, 18.8, -5.15.

HRMS (ESI+)

Calculated for $C_{19}H_{31}O_3Si$: 335.2042

Found: 335.2043

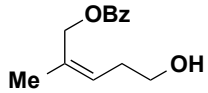

3.114

Alcohol 3.114. A 50 mL round bottom flask charged with TBS-protected alcohol **3.70** (999 mg, 2.99 mmol, 1.0 equiv.) was sealed with a rubber septum and back-filled with N_2. 1% HCl in EtOH solution (30 mL, 0.1 M) was added at RT to afford a clear, colorless solution and stirred for 25 min. After 30 min, reaction flask was cooled to 0 ^oC and slowly quenched with saturated $NaHCO_3$ (10 mL); white precipitate was observed. The crude mixture was transferred to a 125 mL separatory funnel with diethyl ether (30 mL) and H_2O (5 mL). The layers were separated with the addition of brine (10 mL). The organic layer was dried over $MgSO_4$, filtered, and concentrated *in vacuo* to afford a pale yellow oil. The crude oil was dissolved in 20% EtOAc in hexanes and purified by SiO_2 chromatography (20% EtOAc in hexanes → 50% EtOAc in hexanes) to afford **3.114** as a clear, colorless oil (638 mg, 97%).

TLC (20% EtOAc in hexanes)

R_f = 0.14, stained by $KMnO_4$

^{1}H-NMR (500 MHz, acetone-d_6)

δ 8.04 - 8.02 (m, 2H), 7.63 (tt, *J* = 7.5 Hz, *J* = 1.5 Hz, 1H), 7.51 (tt, *J* = 7.5 Hz, *J* = 1.5 Hz, 2H), 5.54 (t, *J* = 7.5 Hz, 1H), 4.88 (s, 2H), 3.62 (br t, *J* = 5.5 Hz, 1H), 3.60 - 3.56 (m, 2H), 2.39 (q, *J* = 7.0 Hz, 2H), 1.84 (q, *J* = 1.0 Hz, 3H).

^{13}C-NMR (125 MHz, acetone-d_6)

δ 166.7, 133.9, 132.6, 131.3, 130.2, 129.4, 128.2, 64.1, 62.3, 32.4, 21.7.

HRMS (ESI+)

Calculated for $C_{13}H_{16}O_3Na$: 243.0997

Found: 243.0998

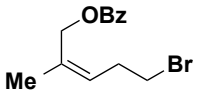

3.115

Bromide 3.115. A 100 mL Schlenk flask was charged with PPh_3 (1805 mg, 6.86 mmol, 1.2 equiv.), sealed with a rubber septum, and back-filled with N_2. MeCN (10 mL) was added to afford a heterogeneous solution which was cooled to 0 ^oC in an ice bath. A 40 mL vial charged with alcohol **3.114** (1.26 g, 5.72 mmol, 1.0 equiv.) was back-filled with N_2, and MeCN (10 mL) was added. This alcohol solution was transferred to the reaction flask with an additional MeCN (10 mL) rinse for quantitative transfer. To another 40 mL vial charged with CBr_4 (2277 mg, 6.86 mmol, 1.2 equiv.) and back-filled with N_2 was added MeCN (7 mL). This CBr_4 solution was transferred to the reaction flask with an additional MeCN (10 mL) rinse for quantitative transfer. The reaction mixture was stirred at 0 ^oC for 5 min and then was allowed to slowly warm to RT and stirred for 3 h. After 3 h, the crude mixture was transferred to a 200 mL round bottom flask with acetone (50 mL) and concentrated *in vacuo* to afford a heterogeneous mixture of yellow oil and white solid. The crude material was adsorbed onto Celite from an acetone solution and

purified by SiO_2 chromatography (hexanes → 10% EtOAc in hexanes) to afford **3.115** as a clear pale yellow oil (1.534 g, 95%).

TLC (30% EtOAc in hexanes)

R_f = 0.69, stained by $KMnO_4$

^{1}H-NMR (500 MHz, acetone-d_6)

δ 8.05 - 8.03 (m, 2H), 7.65-7.62 (m, 1H), 7.54-7.50 (m, 2H), 5.51 (t, *J* = 7.5 Hz, 1H), 4.88 (s, 2H), 3.51 (t, *J* = 7.0 Hz, 2H), 2.77 (q, *J* = 7.0 Hz, 2H), 1.87 (s, 3H).

^{13}C-NMR (125 MHz, acetone-d_6)

δ 166.6, 134.0, 133.9, 131.2, 130.2, 129.4, 127.9, 63.9, 33.6, 31.9, 21.7.

HRMS (ESI+)

Calculated for $C_{13}H_{15}O_2BrNa$: 305.0153

Found: 305.0157

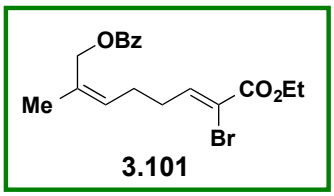

3.101

Building block 3.101. To a 20 mL vial was added zinc dust (531.4 mg, 8.13 mmol, 1.5 equiv.) and iodine (138 mg, 0.54 mmol, 0.1 equiv.). The vial was sealed with a PTFE-lined cap, purged twice with argon, and charged with DMF (1.4 mL). After stirring at RT for 1 min all of the dark purple color disappeared. In a separate 20 mL vial containing homoallylic bromide **3.115** (1.53 g, 5.42 mmol, 1.0 equiv.) was added DMF (2.0 ml). This solution was transferred to the reaction via syringe. Additional DMF (2.0 mL) was used for quantitative transfer. The argon inlet was removed, and the vial was placed in an 80 °C aluminum heat block and allowed to stir at that temperature for 8 h. After 8 h, the reaction mixture containing alkyl zinc bromide **S25**, now orange in color, was cooled to RT and stored in the glove box overnight allowing the zinc dust to settle.

In a glovebox, to a 40 mL vial equipped with a magnetic stir bar charged with vinyl iodide **3.116** (466 mg, 1.81 mmol, 1.0 equiv.) was added $PdCl_2(PPh_3)_2$ (38 mg, 0.054 mmol, 0.03 equiv.), THF (16.4 mL, 0.083 M), and alkyl zinc **S25** solution in DMF (5.4 mL, 0.1 M, 3.0 equiv.). The vial was sealed with a PTFE-lined cap and removed from the glovebox. The vial was placed in a 45 ^oC aluminum heat block and maintained at that temperature with stirring for 6 h. After 6 h, the reaction mixture was cooled to ambient temperature, quenched with saturated aqueous NH_4Cl (20 mL) causing a white precipitate to form, and transferred into a separatory funnel containing brine rinsing with diethyl ether (30 mL). The layers were separated and the aqueous layer was extracted with diethyl ether (2 x 30 mL). The combined organic layers were dried over $MgSO_4$, filtered, and concentrated *in vacuo* to afford a dark brown oil. The crude material was dissolved in MeCN and filtered through a short pad of silica gel and Celite and purified by prepatory HPLC purification to afford building block **3.101** as a clear yellow oil (250 mg, 45%) in addition to ~85% pure material (157 mg, additional 28%).

TLC (5% EtOAc in hexanes)

R_f = 0.25, stained by $KMnO_4$

HPLC

tR = 14.3 min; flow rate = 25 mL/min, gradient of 60% → 95% MeCN:H_2O over 10 min followed by 95% MeCN:H_2O over 7 min.

^{1}H-NMR (500 MHz, $CDCl_3$)

δ 8.04 (d, *J* = 8.0 Hz, 2H), 7.56 (t, *J* = 7.5 Hz, 1H), 7.44 (t, *J* = 8.0 Hz, 2H), 7.29 (d, *J* = 7.0 Hz, 1H), 5.45 (t, *J* = 7.0 Hz, 1H), 4.84 (s, 2H), 4.24 (q, *J* = 7.0 Hz, 2H), 2.45-2.41 (m, 2H), 2.39-2.34 (m, 2H), 1.85 (s, 3H), 1.31 (t, *J* = 7.0 Hz, 3H).

^{13}C-NMR (125 MHz, $CDCl_3$)

δ 166.7, 162.5, 145.0, 133.1, 131.8, 130.3, 129.7, 128.9, 128.5, 117.2, 63.5, 62.6, 32.4, 26.0, 21.7, 14.3.

HRMS (ESI+)

Calculated for $C_{18}H_{21}O_4BrNa$: 403.0521

Found: 403.0519

Manual Synthesis of Alkaloid Linear Precursor **3.102**

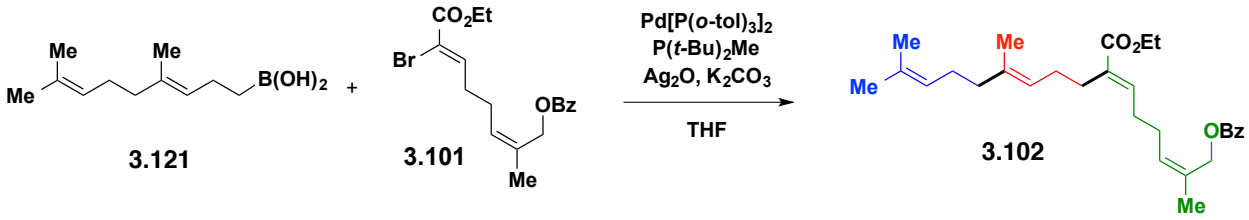

Linear precursor 3.102. Boronic acid **3.121** was prepared and concentrated in a 7 mL vial. In a glovebox, to a flame dried 7 mL vial charged with vinyl bromide **3.101** (38.1 mg, 0.1 mmol, 1.0 equiv.) was added $Pd[P(o\text{-tol})_3]_2$ (17.9 mg, 0.025 mmol, 0.25 equiv.), Ag_2O (57.9 mg, 0.25 mmol, 2.5 equiv.), K_2CO_3 (69.1 mg, 0.5 mmol, 5.0 equiv.) and THF (1.0 mL). To this vial was added $P(t\text{-Bu})_2Me$ solution in THF (14 mg/mL, 0.2 mL, 0.25 equiv.) and boronic acid **3.121** solution in THF (98 mg/mL, 0.5 mL, 2.5 equiv.) followed by THF (0.3 mL) rinse. The vial was sealed with a PTFE-lined cap and removed from the glovebox. The vial was placed in a 60 °C aluminum heat block and maintained at that temperature with stirring for 14 h. After 14 h, the reaction mixture was cooled to 23 °C and diluted with acetone, filtered through a short silica gel plug eluting with acetone, and concentrated *in vacuo* to afford a yellow oil. Crude material was first purified by SiO_2 chromatography (hexanes → 5% EtOAc in hexanes) to afford a clear pale yellow oil (33 mg, 69% semi-purified yield containing $P(o\text{-tol})_3$ and other minor byproducts). This material was further purified by preparatory HPLC (60% MeCN → 95% MeCN) to afford **3.102** as a pale yellow oil (6.6 mg, 15%).

TLC (5% EtOAc in hexanes)

R_f = 0.23, visualized by UV, stained with $KMnO_4$

HPLC

tR = 20.2 min; flow rate = 25 mL/min, gradient of 60% → 95% MeCN in H_2O over 10 min followed by 95% MeCN in H_2O for 15 min. Detected at λ= 254 nm.

^{1}H-NMR (500 MHz, $CDCl_3$)

δ 8.05 (dd, *J* = 8.0 Hz, *J* = 1.0 Hz, 2H), 7.56 (tt, *J* = 7.5 Hz, *J* = 1.0 Hz, 1H), 7.44 (t, *J* = 7.5 Hz, 2H), 6.74 (t, *J* = 7.5 Hz, 1H), 5.45 (t, *J* = 7.5, 1H), 5.14 (t, *J* = 7.0 Hz, 1H), 5.09 (tt, *J* = 7.0 Hz, *J* = 1.0 Hz, 1H), 4.84 (s, 2H), 4.17 (q, *J* = 7.0 Hz, 2H), 2.33 – 2.25 (m, 6H), 2.11 – 2.03 (m, 4H), 1.97 – 1.94 (m, 2H), 1.85 (s, 3H), 1.68 (s, 3H), 1.59 (s, 3H), 1.58 (s, 3H), 1.28 (t, *J* = 7.0 Hz, 3H).

^{13}C-NMR (125 MHz, $CDCl_3$)

δ 168.0, 166.7, 141.5, 136.0, 133.1, 132.9, 131.5, 131.2, 130.4, 129.7, 129.6, 128.6, 124.5, 123.6, 63.6, 60.5, 39.9, 29.0, 27.8, 27.23, 27.17, 26.9, 25.8, 21.7, 17.8, 16.1, 14.4.

HRMS (ESI+)

Calculated for $C_{29}H_{41}O_4$:	453.3005
Found:	453.2999

IX. AUTOMATED SYNTHESIS OF LINEAR PRECURSORS

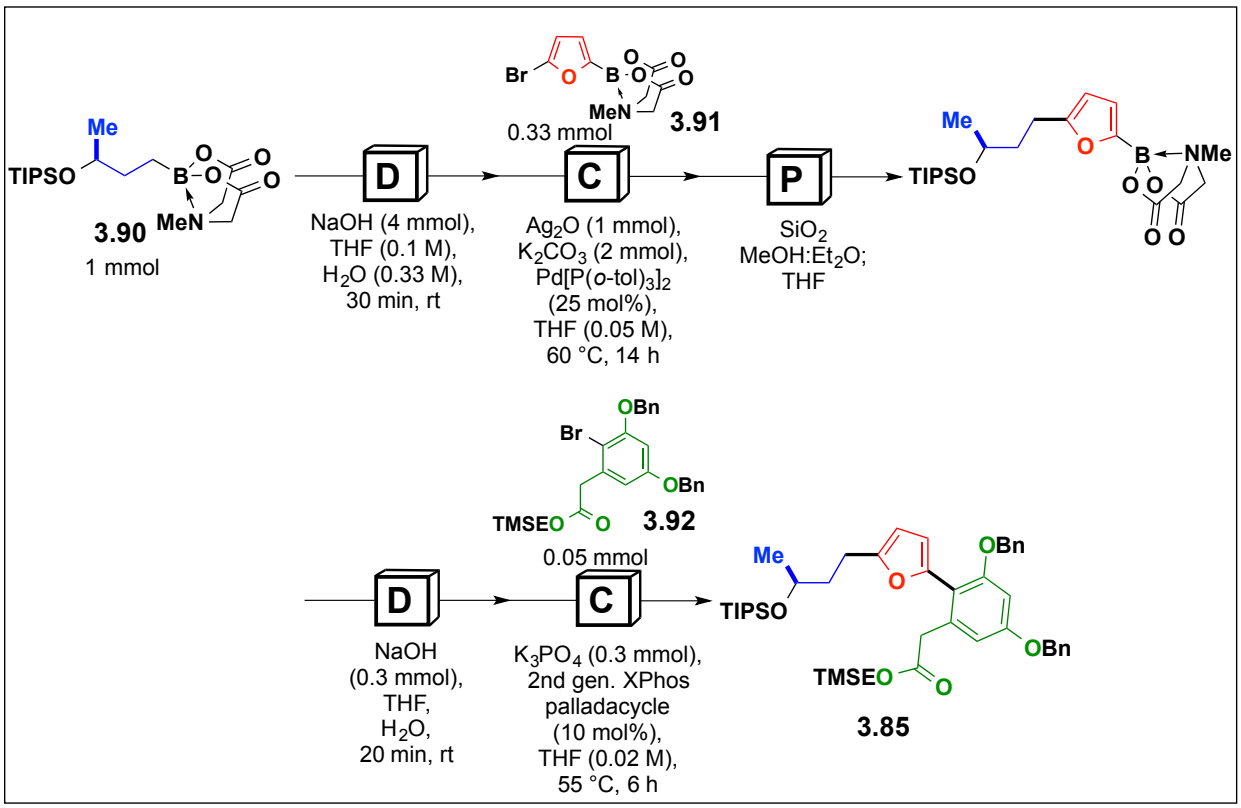

Citreofuran linear precursor (3.85). The general procedure was followed with the following modifications: In the first deprotection reaction, 4 mmol of NaOH were used and the reaction was run for 30 minutes. In the first cross-coupling reaction, the concentration was 0.05 M with respect to **3.91**, 1 mmol of Ag_2O, 2 mmol of K_2CO_3, and 25 mol% of $Pd[P(o\text{-tol})_3]_2$ were used, the addition of the boronic acid was performed over 1 minute, and the reaction was run at 60 °C for 14 h. In the second deprotection reaction, 0.3 mmol of NaOH were used. In the second cross-coupling reaction, the concentration was 0.02 M with respect to **3.92**, 0.3 mmol of K_3PO_4 and 10 mol% of 2nd generation XPhos palladacycle were used, and the reaction was run for 6 hours in a 7-mL glass vial. This automated cycle was performed 6 times to accumulate **3.85** as a slightly yellow residue (88.4 mg total; average of 14.7 mg, 0.020 mmol, 39% yield).

HPLC

tR = 18.5 min, flow rate = 25 mL/min, gradient: 100% MeCN over 10 min followed by 90% MeCN in EtOAc over 15 min.

^{1}H-NMR (500 MHz, acetone-d_6)

δ 7.50-7.48 (m, 2H), 7.43-7.39 (m, 4H), 7.37-7.32 (m, 3H), 7.31-7.28 (m, 1H), 6.77 (d, J = 2.5 Hz, 1H), 6.68 (d, J = 2.5 Hz, 1H), 6.37 (d, J = 3.0 Hz, 1H), 6.10 (d, J = 3.0 Hz, 1H), 5.14 (s, 2H), 5.13 (s, 2H), 4.14-4.08 (m, 3H), 3.64 (d, J = 1.5 Hz, 2H), 2.75 (t, J = 8.0 Hz, 2H), 1.92-1.80 (m, 2H), 1.24 (d, J = 6.5 Hz, 3H), 1.09-1.08 (m, 21H), 0.98-0.95 (m, 2H), 0.03 (s, 9H).

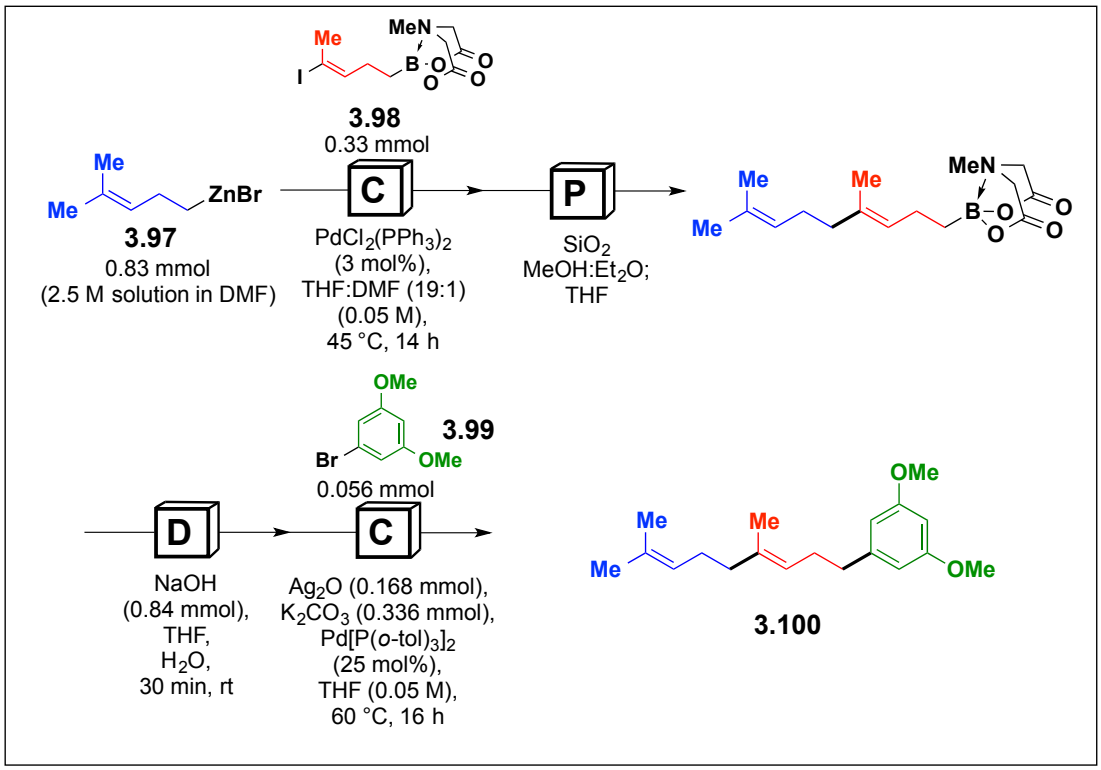

Polyterpene linear precursor 3.100. The general procedure was followed with the following modifications: In the first cross-coupling reaction, 0.33 mL of a freshly prepared solution of **3.97** in DMF (2.5 M) was added manually to the First Reaction Cartridge, the concentration was 0.05 M with respect to **3.98**, 3 mol% of $PdCl_2(PPh_3)_2$ was used, and the reaction was run at 45 °C for 14 hours. Furthermore, the Reaction Filtration Cartridge contained only 300 mg of Celite™ and after filtration, the crude reaction underwent an automated aqueous quench (6 mL saturated aqueous NH_4Cl + 1 mL water) followed by an automated drying process before being purified. In the second deprotection reaction, 0.84 mmol of NaOH were used and the reaction was run for 30 minutes. In the second cross-coupling reaction, the concentration was 0.05 M with respect to

3.99, 0.168 mmol of Ag_2O, 0.336 mmol of K_2CO_3, and 25 mol% of $Pd[P(o\text{-tol})_3]_2$ were used, the addition of the boronic acid was performed over 1 minute, and the reaction was run at 60 °C in a 7-mL glass vial. This automated cycle was performed 6 times to accumulate **3.100** as a slightly yellow residue (17.7 mg total; average of 3.0 mg, 0.010 mmol, 18% yield).

TLC (hexanes)

R_f = 0.31, visualized by UV, stained with $KMnO_4$

HPLC

tR = 19.9 min; flow rate = 25 mL/min, gradient of 50% → 95% MeCN in H_2O over 15 min followed by 95% MeCN in H_2O for 10 min. Detected at λ= 254 nm.

^{1}H-NMR (500 MHz, $CDCl_3$)

δ 6.38 (d, *J* = 2.3 Hz, 2H), 6.32 (t, *J* = 2.3 Hz, 1H), 5.20 (tq, *J* = 7.0, 1.3 Hz, 1H), 5.15 – 5.08 (m, 1H), 3.80 (s, 6H), 2.60 (dd, *J* = 9.0, 6.7 Hz, 2H), 2.35 – 2.28 (m, 2H), 2.11 – 2.04 (m, 2H), 2.00 (dd, *J* = 9.1, 5.9 Hz, 2H), 1.70 (d, *J* = 1.5 Hz, 3H), 1.63 – 1.59 (m, 6H).

^{13}C-NMR (125 MHz, $CDCl_3$)

δ 160.8, 145.0, 135.9, 131.5, 124.4, 123.7, 106.6, 97.8, 55.4, 39.9, 36.6, 29.9, 26.9, 25.8, 17.8, 16.2.

HRMS (ESI+)

Calculated for $C_{19}H_{29}O_2$:	289.2168
Found:	289.2175

X. REFERENCES

[1] Pangborn, A. B.; Giardello, M. A.; Grubbs, R. H.; Rosen, R. K.; Timmers, F. J. *Organometallics* **1996**, *15*, 1518-1520.

[2] Still, W. C.; Kahn, M.; Mitra, A. *J. Org. Chem.* **1978**, *43*, 2923-2925.

[3] For preliminary studies on the development of the small molecule synthesizer and details on the construction of the current synthesizer, see: (a) Gillis, E. P. Iterative Cross-Coupling with MIDA Boronates. PhD Dissertation, University of Illinois at Urbana-Champaign, 2011. (b) Ballmer, S. G. A Small Molecule Synthesizer. PhD Dissertation, University of Illinois at Urbana-Champaign, 2013.

[4] Details on the experimental procedure and characterization data, see: Ref 3b.

[5] Jung, M. E.; Duclos, B. A. *Tetrahedron* **2006**, *62*, 9321-9334.

[6] Fujii, S.; Chang, S. Y.; Burke, M. D. *Angew. Chem. Int. Ed.* **2011**, *50*, 7862-7864.

[7] Vaz, B.; Domínguez, M.; Alvarez, R.; de Lera, A. R. *Chem. Eur. J.* **2007**, *13*, 1273-1290.

[8] (a) Klubnick, J. A. Expansion of the Iterative Cross-Coupling Synthesis Strategy through Csp^3 Halide Cross-Coupling, Mida Boronate Synthesis, and Chan-Lam Couplings. Thesis, University of Illinois at Urbana-Champaign, 2011. (b) Burke, M. D.; Dick, G. R.; Knapp, D. M.; Gillis, E. P.; Klubnick, J. A. PCT/US2011/0201816, Aug 18, 2011.

[9] Aaroz, R.; Servent, D.; Molgó, J.; Iorga, B. I.; Fruchart-Gaillard, C.; Benoit, E.; Gu, Z.; Stivala, C.; Zakarian, A. *J. Am. Chem. Soc.* **2011**, *133*, 10499-10511.

[10] Lifchits, O.; Reisinger, C. M.; List, B. *J. Am. Chem. Soc.* **2010**, *132*, 10227-10229.

APPENDIX: ABBREVIATIONS

1st gen. SPhos palladacycle	chloro(2-dicyclohexylphosphino-2',6'-dimethoxy-1,1'-biphenyl)[2-(2-aminoethylphenyl)]palladium(II)	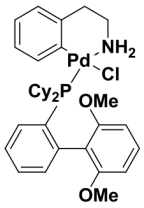
1st gen. XPhos palladacycle	chloro(2-dicyclohexylphosphino-2',4',6'-triisopropyl-1,1'-biphenyl)[2-(2-aminoethylphenyl)]palladium(II)	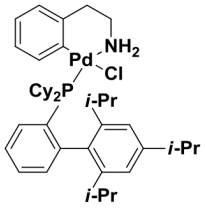
2nd gen. SPhos palladacycle	chloro(2-dicyclohexylphosphino-2',6'-dimethoxy-1,1'-biphenyl)[2-(2'-amino-1,1'-biphenyl)]palladium(II)	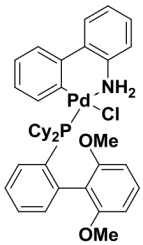
2nd gen. XPhos palladacycle	chloro(2-dicyclohexylphosphino-2',4',6'-triisopropyl-1,1'-biphenyl)[2-(2'-amino-1,1'-biphenyl)]palladium(II)	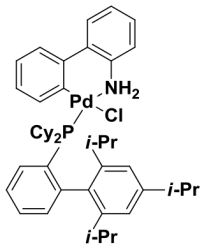
Boc	*t*-butoxycarbonyl	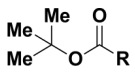
dba	dibenzylideneacetone	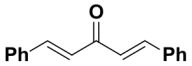
DCM	dichloromethane	
DMF	*N*,*N*-dimethylformamide	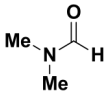
DMAP	4-(*N*,*N*-dimethylamino)-pyridine	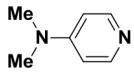

DMSO	dimethyl sulfoxide	
dppf	1,1’-bis(diphenylphosphino)ferrocene	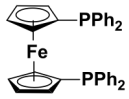
HPLC	high-performance liquid chromatography	
ICC	iterative cross-coupling	
LUV	large unilamellar vesicle	
MIDA	*N*-methyliminodiacetic acid	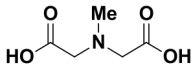
MOM	methoxymethyl	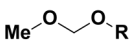
NMR	nuclear magnetic resonance	
SPhos	2-dicyclohexylphosphino-2’,6’-dimethoxybiphenyl	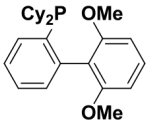
TBAF	tetra-*N*-butylammonium fluoride	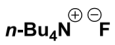
TBDPS	*t*-butyldiphenylsilyl	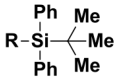
TBDPSE	2-(*t*-butyldiphenylsilyl)ethyl	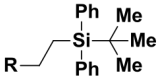
TBS	*t*-butyldimethylsilyl	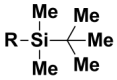
TIPS	triisopropylsilyl	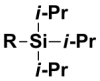

TMSE	2-(trimethylsilyl)ethyl	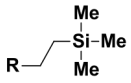
TLC	thin layer chromatography	
TMS	trimethylsilyl	
UV	ultraviolet	
XPhos	2-dicyclohexylphosphino-2',4',6'-triisopropylbiphenyl